The role of Trim71 in cell fate determination of embryonic stem cells and germline development

---

- DISSERTATION -

zur
Erlangung des Doktorgrades (Dr. rer. nat.)
der
Mathematisch-Naturwissenschaftlichen Fakultät
der
Rheinischen Friedrich-Wilhelms-Universität Bonn

vorgelegt von
Sibylle Mitschka

aus Berlin

Bonn, Juli 2015

Angefertigt mit Genehmigung der Mathematisch-Naturwissenschaftlichen Fakultät der Rheinischen Friedrich-Wilhelms-Universität Bonn

1. Gutachter: Prof. Dr. Waldemar Kolanus
2. Gutachter: Prof. Dr. Joachim L. Schultze

Tag der Promotion: 24.11.2015
Erscheinungsjahr: 2015

I hereby declare that I wrote the present thesis without sources other than indicated in the thesis and without help from third parties. On account of the common practice in English scientific writing, the present thesis is drafted using the first-person plural.

Parts of the data shown in the results part in chapters 3.1 to 3.2.4, as well as 3.3.1. have been published in the following publication with me as the first author:

- **Co-existence of intact stemness and priming of neural differentiation programs in mES cells lacking Trim71.**
  Sibylle Mitschka, Thomas Ulas, Tobias Goller, Karin Schneider, Angela Egert, Jérôme Mertens, Oliver Brüstle, Hubert Schorle, Marc Beyer, Kathrin Klee, Jia Xue, Patrick Günther, Kevin Bassler, Joachim L. Schultze, Waldemar Kolanus
  Sci Rep. 2015; 5: 11126.

Further publications

- **Rapid hierarchical assembly of medium-size DNA cassettes.**
  Jonathan Leo Schmid-Burgk, Zhen Xie, Stefan Frank, Sebastian Virreira Winter, Sibylle Mitschka, Waldemar Kolanus, Andrew Murray, Yaakov Benenson
  Nucleic Acids Res. 2012 July; 40(12): e92.

Conferences and posters

- **Trim71 and Lin28 cooperate to suppress let-7 maturation in stem cells and in cancer cells.** Sibylle Mitschka, Tobias Goller, Thomas Ulas, Angela Egert, Hubert Schorle, Joachim Schultze and Waldemar Kolanus (2014). Cell Symposium: Regulatory RNAs in Berkeley (USA); Poster

- **Trim71 regulates differentiation and suppresses let-7 maturation in mES cells.** Sibylle Mitschka, Tobias Goller, Angela Egert, Hubert Schorle and Waldemar Kolanus (2014). Annual meeting of the Bonner Forum Biomedizin (BFB) in Hennef; Poster awarded with a poster prize

- **Analysis of spatio-temporal regulation processes in ES cell differentiation.** Sibylle Mitschka, Tobias Goller, Karin Schneider, Waldemar Kolanus (2012) 11^{th} Joint Symposium of the Bonn University and the Waseda University in Tokyo (Japan); Poster awarded with a poster prize and oral presentation

- **Regulation of cell differentiation programming by Trim71 in mammalian development and in tumors.** Sibylle Mitschka, Karin Schneider, Tobias Goller, Waldemar Kolanus (2012). International Symposium of the SFB 832 in Bad Neuenahr; Poster

- **Trim71, a required protein for embryonic development and cell differentiation.** Karin Schneider, Sibylle Mitschka, Tobias Goller, Waldemar Kolanus (2011). Annual meeting of the Bonner Forum Biomedizin (BFB) in Bonn, Poster

Contents

List of abbreviations

A	adenine
ANOVA	analysis of variance
APS	ammonium persulfate
BCA	bicinchoninic acid
bp	base pairs
BSA	bovine serum albumin
C	cytosine
C. elegans	*Caenorhabditis elegans*, nematode
cDNA	complementary deoxyribonucleic acid
CSD	cold shock domain
D. melanogaster	*Drosophila melanogaster*, fruitfly
D. rerio	*Danio rerio*; zebrafish
DABCO	1,4-diazabicyclo[2.2.2]octane
DAPI	4',6-diamidino-2-phenylindole
ddH2O	double-distilled water
DE	differentially expressed
DMEM	Dulbecco's modified Eagle medium
DMSO	dimethyl sulfoxide
DNA	deoxyribonucleic acid
dNTP	deoxyribonucleiside triphosphate
dpc	days *post coitum*
DTT	dithiothreitol
E. coli	*Escherichia coli*, bacterium
EB	embryonic body
EDTA	ethylenediaminetetraacetic acid
EGF	epidermal growth factor
eGFP	enhanced green fluorescent protein
ESCC miRNAs	ESC-specific cell cycle regulating miRNAs.
et al.	et alia; and others

FACS	fluorescence-activated cell sorting
FBS	fetal bovine serum
FGF	fibroblast growth factor
fig.	figure
G	guanine
h	hour(s)
HEK	human embryonic kidney
HEPES	4-(2-hydroxyethyl)-1-piperazineethanesulfonic acid
HRP	horseradish peroxidase
ICM	inner cell mass
IG	immunoglobin
indel	Insertion/deletion of base pairs in the DNA
iPSCs	induced pluripotent stem cells
KO	knockout
LIC	ligation independent cloning
LIF	leukemia inhibitory factor
MACS	magnetic-activated cell sorting
MEFs	mouse embryonic fibroblasts
mESCs	mouse embryonic stem cells
min	minute(s)
miRNA	micro ribonucleic acid
MFI	mean fluorescence intensity
mRNA	messenger ribonucleic acid
NSC	neural stem cell
nt	nucleotides
PAGE	polyacrylamide gel electrophoresis
PBS	phosphate buffered saline
PFA	paraformaldehyde
PGC	primordial germ cell
PGCs	primordial germ cells
PMSF	phenylmethanesulfonylfluoride
RA	retinoic acid
RBP	RNA binding protein
RFP	red fluorescent protein
RISC	RNA-induced silencing complex
RNA	ribonucleic acid

rpm	rounds per minute
RPMI	Roswell Park Memorial Institute
RT	room temperature
SD	standard deviation
SDS	sodium dodecyl sulfate
sec	second(s)
SEM	standard error of the mean
siRNA	small interfering ribonucleic acid
SSCs	spermatogonial stem cells
SSEA	stage-specific early antigen
T	thymine
TALEN	Transcription activator-like effector nuclease
TEMED	tetramethylethylenediamine
TRIM	tripartite motif
U	uracil
UTR	untranslated region
WB	western blot
WT	wildtype

1 Introduction

1.1 What defines a stem cell?

More than 200 different cell types in the human body are generated by the tightly orchestrated differentiation of only one cell: the fertilized egg. In order to give rise to all specialized cell types, the fertilized egg undergoes several rounds of cell division thereby forming the zygote. The ability of cells to continuously divide while maintaining an undifferentiated state is called self-renewal and is a defining hallmark of stem cells. The zygotic cells are considered totipotent (*i.e.* having the whole power) because they will later on give rise to all embryonic and extraembryonic tissue cells. After some days, the morphology of the zygote changes. For the first time, different cell types are generated in the so called blastocyst, among them those which will later give rise to all cells of the embryo. The ability to differentiate, *i.e.* to generate at least one other specialized cell type, is defined as the second hallmark of stem cells. Thus, the whole organism is built up in a hierarchical fashion in which cells become more and more specified during development (figure 1.1). However, not all cells with stem cell character are lost after embryonic development. More restricted stem cells can persist throughout adulthood and are called multipotent, since they are able to generate a variety of cell types from a specific lineage. For example, multipotent hematopoietic stem cells can give rise to erythrocytes, platelets and leukocytes. While during development stem cells initially specify the different cell types and enable the growth of the organism, the purpose of adult stem cells is to replenish the pool of effector cells and to enable repair after tissue damage.

1.2 Embryonic stem cells

Embryonic stem cells (ESCs) are the *in vitro* equivalent of the cells from the inner cell mass (ICM) of a blastocyst which can be propagated in culture without losing their stemness. These cells correspond to a very early stage of embryonic devel-

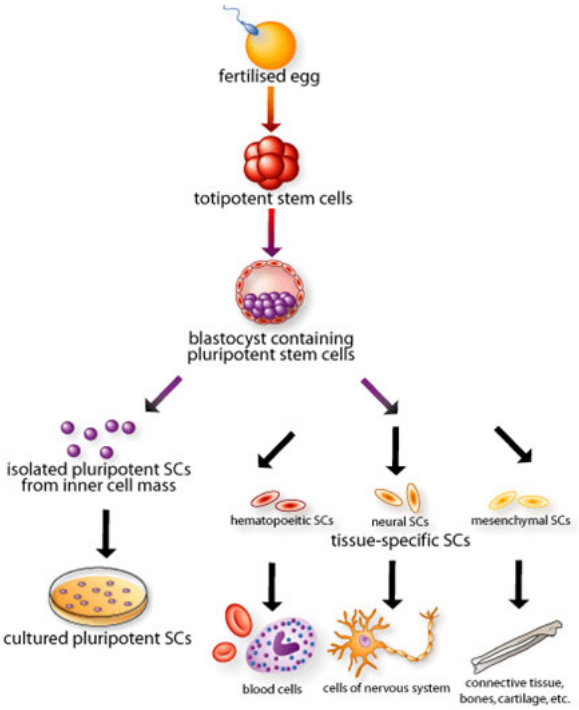

Figure 1.1: **The process of cell differentiation in mammalian development.** Image was taken from Chaudry (2004) [1]

opment and they retain the ability to differentiate into all cell types of the adult organism. Because of their enormous potential for clinical applications in the fields of organ transplantation and tissue engineering, ESCs are currently widely investigated. However, transplantation of cells generated from conventional ESC lines could elicit an immune reaction in the patient which limits their application. Moreover, due to the necessity of using human embryo material, ethical implications need to be considered. Both hurdles were overcome with the development of a technique which allows the generation of ESC-like cells from adult somatic cells of mice and humans [2, 3]. These so called induced pluripotent stem cells (iPSCs) are commonly produced by the overexpression of a set of ESC-typical transcription factors. However, alternative reprogramming cocktails have been put forward (reviewed in [4, 5]). The current clinical research is mainly focusing on the establishment of efficient differentiation protocols in order to generate specific cell types which can be transferred back to the patient without the threat of cancer formation.

Apart from this, there is a great interest to use ESCs as tools for the investigation of general cell biological processes. Interestingly, it was found that stem cells share certain features with cancer cells, *e.g.* their ability to proliferate constantly and the

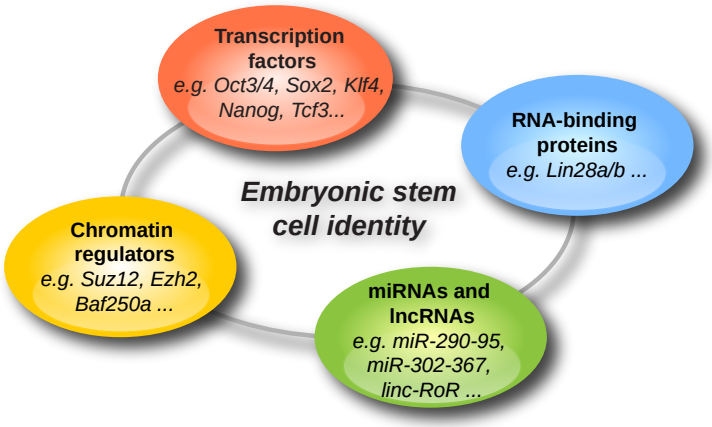

Figure 1.2: **The identity of ESCs is regulated and maintained on epigenetic, transcriptional and posttranscriptional levels.**

survival in hypoxic conditions (reviewed in [6, 7, 8]). Techniques which allowed ESC derivation from genetically modified mice or direct *in vitro* mutation have led to substantial advances in the understanding of principal mechanisms underlying cell identity, cell transformation and proliferation. This enabled the identification of a complex network governing ESC identity comprising transcription factors, miRNAs, RNA-binding proteins (RBPs) and epigenetic regulators (figure 1.2).

1.2.1 Transcription factors as master regulators of pluripotency

Transcription factors were the first components of the mESC network that were identified as pivotal regulators of pluripotency. There is a plethora of transcription factors that are constantly expressed in ESC, but only a handful of them were found to be acting as master regulators. The key to this finding was the development of iPSCs from murine somatic cells by overexpression of just four trasncription factors: Oct4, Sox2, Klf4 and c-Myc [2]. An independent study performed in human ESCs revealed a similar set of the transcription factors, namely Oct4, Sox2 and Nanog with the addition of the RNA-binding protein Lin28a [3]. These and other studies showed that Sox2 and Oct4 are indispensable for establishing pluripotency whereas other transcription factors such as Nanog, Esrrb, Klf4 and Tcf2l1 mainly support self-renewal [9, 10, 11]. They may bind to hundreds of genomic loci, leading to both activation and suppression of gene transcription [12, 13]. The efficient suppression of specific transcriptional programs is essential for the maintenance of pluripotency and should not be underestimated. This is the reason why the inhi-

bition of glycogen synthase kinase 3 (Gsk3) and mitogen-activated protein kinase kinase (Mek) signaling further promotes the derivation of mESCs [10, 14].

Master regulatory transcription factors in turn upregulate other transcriptions factors and this transcription factor hierarchy exerts far-reaching effects on the whole transcriptional landscape. Thereby, they stabilize the ground state of pluripotency and efficiently repress differentiation and somatic cell programs. A recent study found that a transcription factor set of just 12 components establishes the whole ESC network [15]. ESC transcription factors usually work cooperatively for efficient gene expression regulation and enforce their own transcription, thus establishing positive-feedback-loops [16, 17, 13, 12].

When ESCs start to differentiate some transcription factors are downregulated whereas others remain expressed depending on the stimulus. This creates an imbalance that will influence the germ layer formation. For example, it was found that during neuroectodermal cell commitment Sox2 remains highly expressed, while Oct4 becomes downregulated [18]. A similar mechanism was identified for Klf4 and Klf5 which differentially inhibit mesoderm and endoderm formation [19]. Accordingly, the reprogramming of adult stem cells to iPSCs usually requires less additional factors than are needed for fully differentiated cells [20] .

1.2.2 The chromatin landscape of the pluripotent genome is maintained by epigenetic regulators

While it is widely recognized that transcription factors play a major role in the global execution of specific gene programs, chromatin regulators are also essential for the organization of the genome and the stabilization of the uncommitted ESC state. The basic module of genome organization is the nucleosome; a 147 nucleotide stretch wrapped around an octamer protein complex consisting of two copies of H2A, H2B, H3 and H4 histones [21]. The modification of the nucleosomes can alter gene expression by making certain gene regions more or less accessible for DNA binding proteins. The nucleosome can be modified by site-specific incorporation of histone variants as well as histone-modifying enzymes and ATP-dependent remodeling complexes (reviewed in [22, 23, 24]). The best studied pathways leading to epigenetic regulation are histone modifications including acetylation, methylation, phosphorylation, ubiquitination, and ribosylation [25]. Indeed, it has been reported that the process of reprogramming adult tissue cells to iPSC is always accompanied by remodeling of the epigenome [2, 26, 27]. However the outcome of

specific modification patterns is context-dependent, hence the result of the same modification can be different depending on the gene and cell type.

Generally, it is thought that ESCs have a more open (meaning easily accessible) chromatin than differentiated cells [28]. Moreover, there is an unusually high prevalence of bivalent histone marks, allowing for pervasive gene transcription [29, 30]. Hence, many genes that are actually characteristic for differentiated cells are continuously expressed at low levels in ESCs, prompting the speculation that the expression of these developmental genes is maintained in a poised state in order to prime ESCs to rapidly induce differentiation. This may contribute to the general plasticity of the ESC genome. Induction of differentiation then leads to a dramatic reduction of the actively transcribed genome [31].

1.2.3 microRNAs regulate the balance between stemness and differentiation

microRNAs (miRNAs) constitute another level of protein expression regulation in cells downstream of gene transcription. miRNAs are short, about 22 nucleotide long, single-stranded RNA molecules which can repress protein expression of specific target genes by imperfect binding to the mRNA. Until today, more than 1,500 miRNAs have been identified in the human genome and it was estimated that about one third of all genes show conserved posttranscriptionally regulation by miRNAs [32].

The biogenesis of miRNAs is a multi-step process involving several protein complexes (figure 1.3). All miRNAs originate from Polymerase-II/III transcripts undergoing conventional capping and poly-A-tailing. In the canonical pathway from which most cellular miRNAs are produced, a stem loop structure within this primary transcript (pri-miRNA) is recognized by the so called microprocessor complex consisting of the proteins Dgcr8 and Drosha [34, 35]. The RNA-hairpin is cut out resulting in a pre-miRNA intermediate of about 70 nucleotides length, which is subsequently transported into the cytoplasm with the help of the shuttle protein Exportin-5 [36, 37]. There, the RNaseIII enzyme Dicer binds to the precursor and cleaves off the stem loop, generating an imperfect double strand RNA with a length of about 22 nucleotides [38, 39]. Usually only one of the two generated miRNAs is biologically active and loaded into the RNA-induced silencing complex (RISC), whereas the other one, known as the passenger strand, is rapidly degraded [40, 41]. A key component of the RISC is the protein Argonaute-2 (Ago2) which directly binds the miRNA and orients it for interaction with the target mRNA.

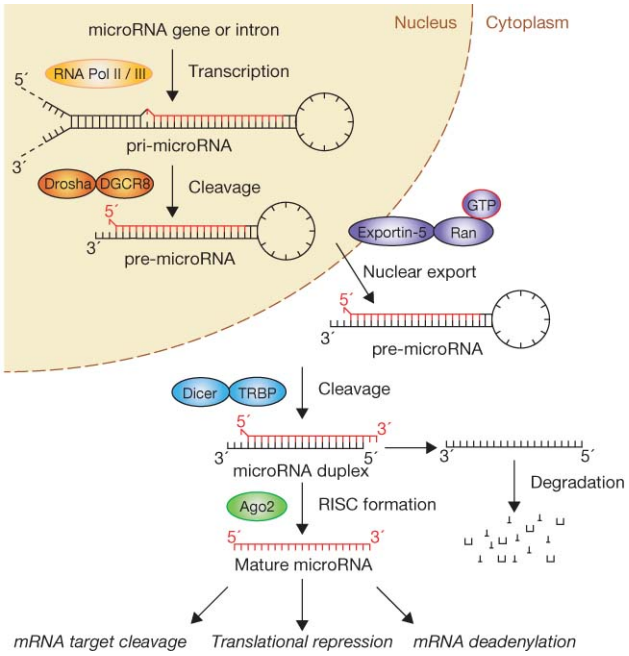

Figure 1.3: **The canonical miRNA processing pathway.** Figure taken from Winter *et al.* (2009)[33]

Upon binding of the miRISC, the initiation of translation is blocked [42]. Furthermore, miRNA induced deadenylation and decapping leads to decreased stability of the mRNA. However, other mechanims including mRNA sequestration, mRNA restriction and premature termination of translation were shown to contribute to miRNA-mediated effects (reviewed in [43]).

Essential for the miRNA activity on target mRNA regulation is the perfect pairing in the region of the nucleotides 2-8, also referred to as the seed sequence. This region is usually especially highly conserved and identical among the members of a miRNA family. The other parts of the miRNA confer further target specificity and stabilize the interaction [32, 44]. miRNAs are, like transcription factors, tightly regulated in their expression and the miRNome is very characteristic for a certain cell type. Hence, it is understandable that mESCs also have a unique expression pattern of miRNAs. The importance of miRNAs for governing ESC maintenance and differentiation has been demonstrated by the generation of Dgcr8 and Dicer KO mESCs which lack nearly all mature miRNAs. In the undifferentiated cell state, these cells exhibit a significantly prolonged cell cycle and G1 transit, which can be rescued by reintroduction of the stem-cell specific 290-miRNA family [45]. Moreover, upon induction of differentiation, Dicer and Dgcr8 knockout mESCs fail to

upregulate differentiation genes such as Hnf4a, Brachyury and Gata-1, which precludes the exit of the stem cell maintenance program [46, 47, 48]. However, overexpression of miRNAs of the let-7 family is able to overcome the inability to differentiate. These findings illustrate that the balance between miRNAs supporting stem cell maintenance and those promoting differentiation is critical for the full functionality of mESCs [49].

miRNAs that are important for the stem cell functions are summarized as ESC-specific cell cycle regulating (ESCC) miRNAs and comprise the related families of the miR-290 cluster, the miR-302/367 cluster and the miR-17/20/106 miRNAs which together constitute the majority of miRNAs expressed in the human and murine ESCs. These miRNAs support the unique ESC cycle as they lower the G1-S-checkpoint barrier by promoting both hyperphosphorylation of Rb proteins and suppression of miRNAs that antagonize rapid cell-cycling [50]. Furthermore, miRNAs indirectly promote the expression of factors and epigenetic modulators that enhance stem cell maintenance (*e.g.* Sall4, Lin28, Dnmt3a/b) [49, 51].

On the other hand, there are miRNAs which are functionally counteracting the ESCC miRNAs and which are upregulated upon induction of differentiation. Those miRNAs target the central ESC transcriptional network, help to stabilize the differentiated cell state and establish a somatic cell cycle. Those can be categorized as "pro-differentiation" miRNAs [52, 53, 54].

The let-7 miRNA, in particular, is a widely investigated miRNA since it has a central role in the regulation of differentiation and proliferation. let-7 was shown to be rapidly upregulated upon differentiation in different species [55, 56, 57, 58]. Furthermore, let-7 was one of the first miRNAs identified and let-7 target regulation is highly conserved during evolution [59]. Important target mRNAs of the let-7 miRNA family in mESCs are for example c-Myc Sall4, Lin28 and Trim71 [49]. In mouse and human there are 9 different let-7 members originating from 14 and 13 genes, respectively [60]. Surprisingly, the transcription of the let-7 primary transcript is already quite high in the undifferentiated state, although the mature let-7 miRNA is almost undetectable [61, 58]. This discrepancy could be explained by the discovery of a negative regulation exerted by the RNA binding protein Lin28 which recognizes a specific conserved sequence in the loop structure of pre-let-7 molecules. Binding of the precursor by the stemness factor Lin28a leads to sequestration from the Dicer complex and to the recruitment of the terminal-uridyl transferase Tut4 which tags the let-7 miRNA precursor for degradation by the exonuclease Dis3l2 [62, 63, 64, 65]. In addition, the Lin28b protein variant was shown

to induce pri-let-7 degradation already in the nucleus [66]. This mechanism enables fast upregulation of the mature miRNA upon differentiation since transcription must not be altered and posttranscriptional processing is directly linked to the expression of Lin28.

Transcription of miRNAs is majorly regulated by some master transcription factors like Oct4, Sox2, Nanog and Tcf3. They induce efficient expression of mESC specific miRNAs such as the miR-290 family. On the other hand, the promoter sites of pro-differentiation miRNAs are also bound by ESC transcription factors but they are at the same time repressed by Polycomb group complexes [67]. This indicates that these miRNAs are constantly kept in a poised state.

1.2.4 RNA binding proteins in stemness regulation

Like miRNAs, RNA-binding proteins (RBPs) act posttranscriptionally to regulate protein output. RBPs can regulate the localization, maturation, transport, stability and translational efficiency of specific coding and non-coding-RNAs. A recent estimation yielded a total of 1,500 RBPs in the human genome, equivalent to 7.5% of all human genes [68]. The largest class of them constitute the mRNA-binding proteins (mRBPs) with about 700 members. Concomitantly with extensive posttranscriptional mRNA regulation in higher eucaryotes, such as alternative splicing and polyadenylation, the class of mRBPs increased substantially during evolution. On the other hand, the actual binding units of RBPs seem to be highly conserved [68]. Especially the RBDs of ribosomal proteins show the highest conservation and can be structurally differentiated from mRBPs which mostly contain a limited set of RBDs such as an RNA recognition motif (RRM), a DEAD-motif, a K-homology (KH) domain or a zinc-finger domain. RBDs often occur in multiple repeats or in combination with other RBDs to increase sequence specificity and affinity [69]. Currently, the RNA target sequence cannot be predicted from the structure. Hence, the vast amount of RBPs need to be individually investigated to uncover their target spectrum and function. Moreover, the specificity of the interaction of an RBP with its target RNA can be sequence- as well as structure-mediated and regulatory posttranslational modifications of the RBP create an additional layer of complexity.

Recently, it was found that a number of RBPs are dynamically regulated in iPSC reprogramming and differentiation [70], suggesting an active contribution of these proteins in stem cell maintenance. In comparison to transcription factors our current understanding of RBPs in mESCs biology is limited. Some examples will be explained here in more detail.

Although they are not only expressed in stem cells, proteins of the PAZ (Piwi/ Argonaute/ Zwille) domain family are of significant importance to stem cells since they are majorly involved in post-transcriptional gene silencing. Argonaute proteins and Dicer are essential components of the RNA-silencing pathway. Argonaute proteins interact with miRNAs as well as their mRNA targets and they are important for both miRNA biogenesis and activity. Deficiency of all four Argonaute proteins was reported to induce apoptosis in mESC [71]. However, the single knockout of Argonaute-2 (the catalytic subunit of the RISC) in mESC leads to delayed differentiation and decreased proliferation [72], suggesting that the other Argonuate proteins may exert further functions that go beyond miRNA biogenesis and activity regulation.

A specific class of RBPs regulates alternative splicing of the primary mRNA transcript in the nucleus. Since more than half of the mouse and human genes have at least one alternative transcript, among them many pluripotency factors, RBPs are required for differential expression regulation of splicing variants. A couple of splicing factors have been identified to regulate the alternative expression of pluripotency factors. For example, in undifferentiated mESCs the Oct4a variant which supports self-renewal is primarily expressed at the expense of the Oct4b [73], a process that is regulated by Tip110 [74]. On the other hand, RBPs like Mbnl1 and Rbfox2 specifically induce the switch to differentiation promoting transcript variants and thus counteract stem cell maintenance [75, 76].

One of the best studied RBPs in ESC is Lin28. Lin28 was shown to bind to different classes of RNAs, namely let-7 pre-miRNA, mRNAs and snoRNAs [63, 77, 78]. Lin28 was first discovered as a heterochronic gene in the model organism *C. elegans* [79] where mutation of the *lin-28* gene leads to accelerated differentiation of the hypodermal seam cells. Its stem cell-specific expression pattern seems to be conserved in humans, where it was functionally associated with processes such as development, glucose metabolism, pluripotency and differentiation [3, 80, 81, 82, 83, 84, 85]. The overexpression of Lin28a together with Nanog, Oct4 and Sox2 was shown to reprogram human fibroblasts [27]. Moreover, some cancers were found to regain Lin28 protein expression. Lin28 overexpression in tumors was found to have a positive impact on tumor development and growth, for instance in germ cell tumors [86, 87], breast cancer [88], hepatocellular carcinoma [89] and Wilms tumor [84]. These findings further support the idea of a close relationship between stem cell biology and cancer.

In humans and mice, two isoforms of Lin28, called Lin28a and Lin28b, are expressed from two distinct genes. Structurally, both proteins are very similar. At the N-terminus there is a cold-shock domain (CSD) followed by a C-terminal Zinc-knuckle domain (ZKD) comprising two retroviral-type CHCC Zn-knuckles. Lin28b possesses a nuclear localization sequence allowing the protein to shuttle between cytoplasm and nucleus, whereas Lin28a can be mainly found in the cytoplasm, *i.e.* in P-bodies, ER-structures and stress granules [66, 90].

1.3 Germline stem cells

A specific type of adult stem cells are the germ stem cells. Germ cells give rise to gametes (sperm and eggs) in sexually reproducing species. While female mammals do not produce oocytes (precursors of eggs) after birth [91, 92, 93], a stem cell population constantly replenishes the sperm cell pool in males. The so called spermatogonial stem cells (SSCs) provide a *bona fide* example for the tightly regulated balance of stemness versus differentiation. Moreover, germ cells are unique in that their normal end product is again a totipotent zygote and they provide the enduring link between the generations [94]. It was found that embryonic germ cells (EGCs) when taken into culture, can reactivate cellular programs that closely resemble those of embryonic stem cells [95, 96]. Those cells can form tissues from all three germ layers when transferred into donor animals. Additionally, germ cell tumors have long been used as surrogate for embryonic stem cells for the investigation for stemness and differentiation [97].

The specification of primordial germ cells (PGCs) happens very early during embryonic development at around stage E6.5 by instructive signaling from neighboring yolk sac cells which secrete BMPs [98, 99] (see figure 1.4). This induces expression of early germ cell markers such as Blimp1/PRDM1 and Stella/Dppa3. In turn, Blimp-1 actively suppresses somatic cell fates (*i.e.* homeobox genes) [100]. In mice, a founder population of about 50 cells starts to migrate along the hindgut at E8.5 undergoing several rounds of mitosis before reaching the genital ridges. Upon arrival, the cells, about 5,000, start to express Vasa and germ cell nuclear antigen (Gcna). During germline development, an extensive remodeling of the epigenetic landscape occurs involving erasure of DNA methylation patterns and posttranslational histone modifications [101, 102]. PGCs are the only lineage that retains the expression of pluripotency-associated genes after gastrulation, such as Oct4, Nanog, Sall4 and Sox2. The Sry ((sex-determining region of Y)) gene is essential

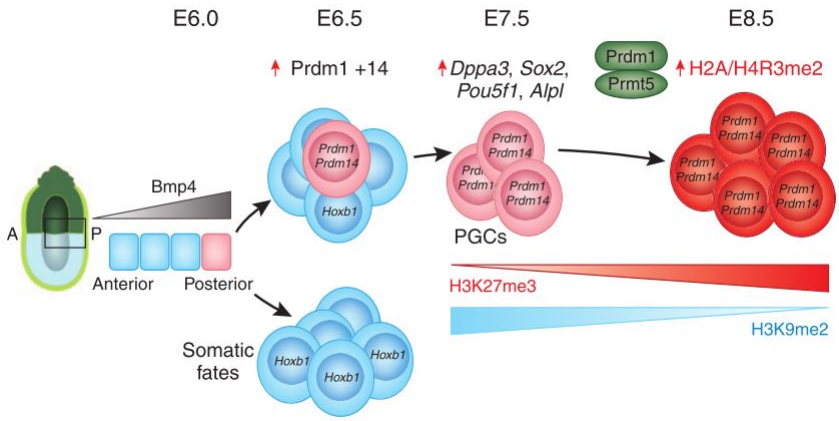

Figure 1.4: **The specification of the germ cell lineage during embryonic development.** Modified from Bikoff & Robertson (2008) [104].

for the sex-specific germ cell development starting at E10.5. In female embryos, meiosis starts already in the devolving embryo and arrests during Meiosis I. Meiosis II is then induced under the influence of hormones during puberty [103]. In contrast, in males meiosis is part of spermatogenesis which is actively suppressed until puberty.

1.4 The TRIM protein family

The TRIM protein family is characterized by the **tri**partite **m**otif consisting of an N-terminal RING finger domain in conjunction with one or two B-box motifs and a coiled-coil region [105, 106, 107]. The C-terminal domains following the tripartite motif can be diverse and define further subgroups within the TRIM protein family [108]. Two thirds of the human and mouse TRIM proteins contain a B30.2 domain at the C-terminus (also called PRY-SPRY-domain). This subfamily of TRIM proteins is evolutionary relatively young and mainly involved in immunological processes [109]. Other prevalent C-terminal domains are for instance the PHD-BROMO domain, the MATH domain or the Filamin-NHL domain [109] which show high conservation from invertebrates to humans (figure 1.5).

Due to their structural diversity, TRIM proteins are implicated in a plethora of processes including apoptosis regulation [111, 112, 113], autophagy [114], cell differentiation [115, 116, 117] and antiviral defense [118, 119]. Likewise, TRIM proteins are also playing a role in pathophysiological conditions, such as muscular dystro-

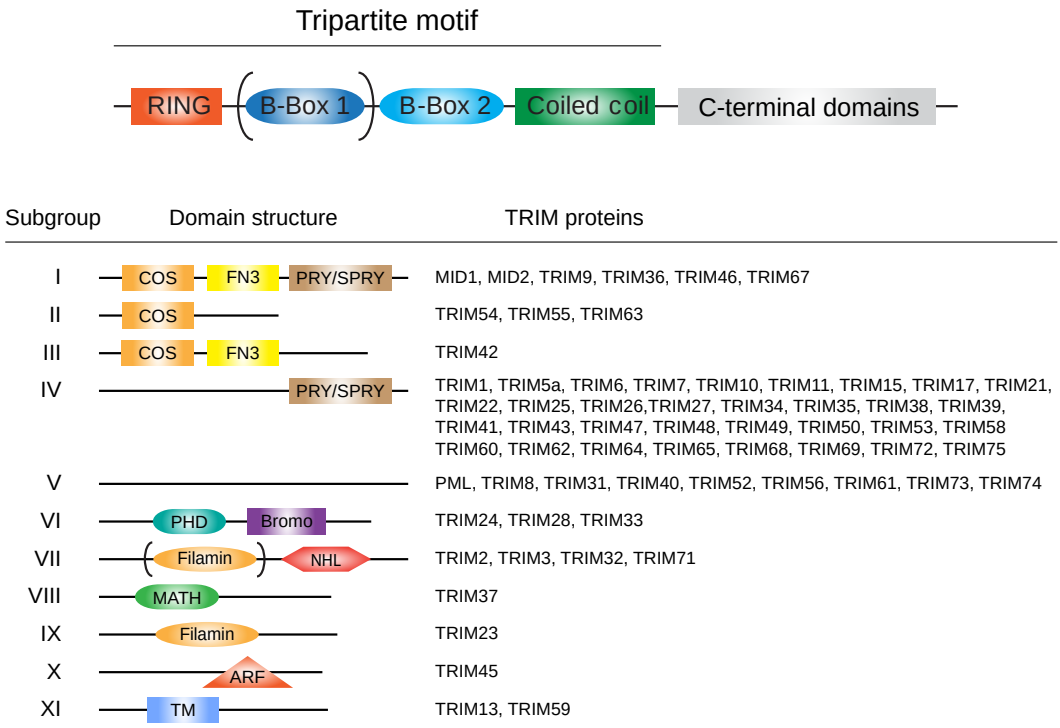

Figure 1.5: **Overview on the domain structure and composition of the TRIM protein family.** Definition of subgroups according to Ozato *et al.* (2008) [110] COS, C-terminal subgroup one signal; FN3, Fibronectin type 3; PHD, plant homeodomain, MATH, meprin and meprin and TRAF-homology domain; NHL, NCL1, HT2A and LIN41 domain; ARF, ADP-ribosylation factor-like; TM, transmembrane, PML, Promyelocytic leucemia; MID, midline

phy [115, 120], X-linked Opitz syndrome [121, 122], familial Mediterranean fever [123, 124] and also different types of cancers [113, 125, 126].

The RING finger domain is characterized by a series of cystedine and histidine residues forming a "cross-brace" to bind two zinc ions [127, 128]. RING domains are besides HECT domain-bearing proteins the largest class of E3-ubiquitin ligases. Many studies have shown that TRIM proteins can act as E3-ubiquitin ligases by adding ubiquitin residues to specific protein substrates (reviewed in [129]). The ubiquitination process begins with the ATP-dependent coupling of the 8.5 kDa Ubiquitin protein to the E1 ubiquitin-activating enzyme (see figure 1.6).. Next, the ubiquitin is transferred to one of several E2 ubiquitin-conjugating enzymes. Finally, E3 ubiquitin ligases mediate the transfer of the ubiquitin molecule from an E2 enzyme to a specific substrate. After attachment of a single ubiquitin moiety to a protein substrate, further ubiquitin molecules can be added to the first, yield-

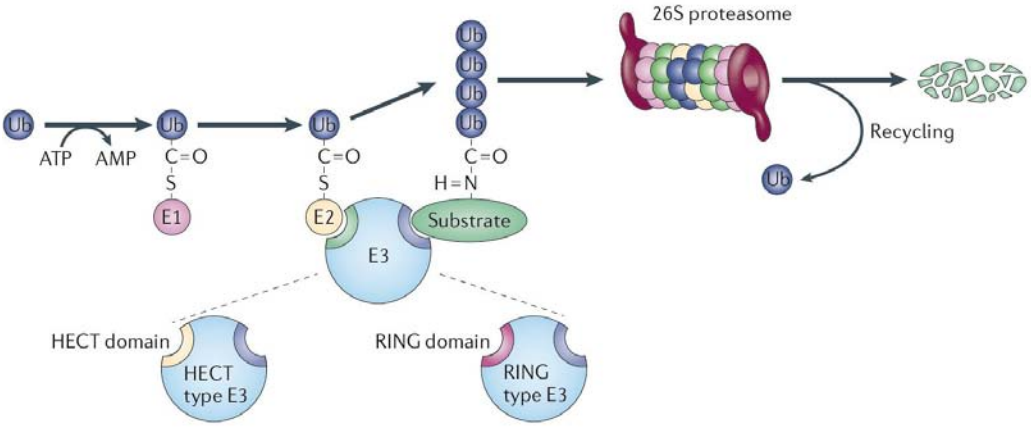

Figure 1.6: **Illustration showing the ubiquitination pathway leading to substrate degradation.** The figure was taken from Hatakeyama and Shigetsugu (2011)[135].

ing a poly-ubiquitin chain. In most cases ubiquitin-tagging induces degradation of the protein by the 26S proteasomal pathway. However, there are also examples in which ubiquitination plays a role as a signaling molecule for the activation or inactivation of a target protein (reviewed in [130]). It was found that ubiquitin modifications that are involved in signaling are mainly coupled via other than the classical Lys-48 bond [131] (*e.g.* Lys-63) and thus do not lead to formation of poly-ubiquitin chains. In addition, some TRIM proteins such as Trim27 or Trim40 were also found to catalyze the attachment of ubiquitin-like modifiers including SUMO proteins [132] IFN-stimulated gene 15 (ISG15) [133] and NEDD8 [134]. Hence, TRIM proteins are more than simple signaling mediators for protein degradation.

Less is known about the function of the B-boxes, which rarely appear outside of TRIM proteins. However, it is speculated that they contribute to E3-ligase activity [136, 137]. The coiled-coil domain on the other hand is a very generally occurring motif and is responsible for the ability of many TRIM proteins to form homo- and hetero-multimers with other TRIM proteins. In addition, the coiled-coil domain seems to be the guiding structure for proper intracellular TRIM protein localization [106].

1.4.1 The TRIM-NHL proteins

As mentioned before, the large family of TRIM proteins is further subdivided according to their C-terminal domains, one of them being the TRIM-NHL proteins. In mammals the TRIM-NHL family consists of four members: Trim2, Trim3, Trim32 and Trim71 [138], however TRIM-NHL proteins can also be found in invertebrates (see figure **??**). The name "NHL" was derived from the first three proteins identified in *C. elegans* harboring this domain feature: **N**CL-1, **H**T2A and **L**in-41 [107]. The NHL domain consists of 5-6 repeats of a 44 amino acid stretch, resembling WD40 repeats. Together the repeats form a tight beta-propeller structure which builds an interaction surface for other proteins as well as RNAs. The NHL repeat structure can also be found in a variety of prokaryotic proteins which can act as monooxygenases [139]. On the other hand, brat, a Trim-NHL protein from *D. melanogaster,* is a well characterized RNA binding protein which acts in concert with other post-transcriptional regulators to repress protein expression of target genes [140, 141]. The NHL domain may thus be able to interact with both proteins and RNA. In line with this it was found that the surface of those NHL proteins that interact with RNA is positively charged which enables more efficient interaction with negatively charged RNA molecules. This is particularly true for the human TRIM-NHL proteins TRIM71 and TRIM3 [141]. Nevertheless, the identification of concrete binding sites remains a challenging task. Surprisingly, several TRIM-NHL have furthermore been found to regulate the expression of miRNAs [142, 143, 144, 145]. Until now it is unclear whether they all use a common mechanism and if this is based on an interaction with the RNA itself or via regulation of proteins that regulate miRNA biogenesis and function.

1.4.2 Trim71 as a conserved regulator of embryonic development

Trim71 was first discovered as a heterochronic gene in the model organism *C. elegans* where it was named *lin-41* (lineage variant 41) [146]. In the same study, the authors found a reciprocal relationship between the protein expression of *lin-41* and the expression of a newly identified short non-coding RNA, named let-7 (lethal 7). Accordingly, LIN-41 is downregulated when let-7 miRNA is upregulated precisely at the switch between larval stages 3 and 4 [146]. Interestingly, mutation of the *lin-41* gene resulted in precocious differentiation of the hypodermal seam cells, a stem cell compartment at the lateral sites of the nematode. In contrast, overproduction of LIN-41 leads to reiteration of larval cell states instead of terminal dif-

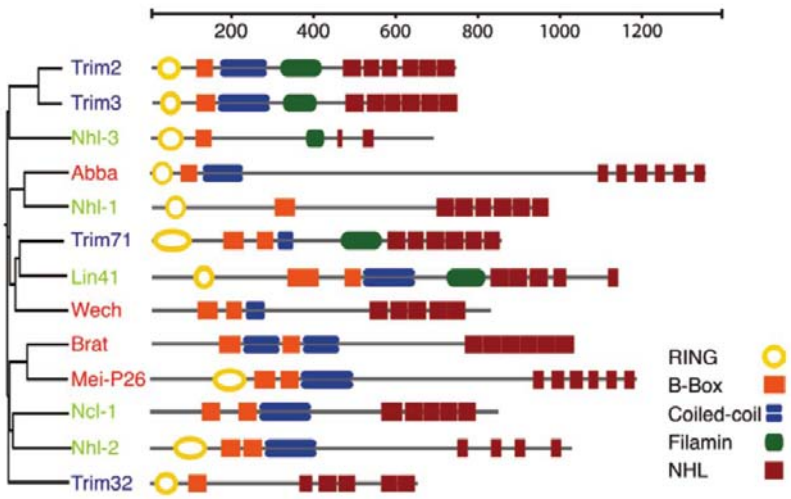

Figure 1.7: **Phylogenetic tree of TRIM-NHL proteins from mouse, fly and nematode shows high conservation of protein domain structures.** *C. elegans* proteins are in light green, *D. melanogaster* in red, *M. musculus* in blue type. The figure was taken from Wulczyn *et al.* (2010)[138].

ferentiation [147]. Thus, the *lin-41*-deficient mutants behaved exactly opposite to the mutants of the miRNA *let-7*. Indeed, the *lin-41* mRNA harbors two partially complementary let-7 binding sites which were later found to be conserved in many other Trim71/lin-41 homologs [57, 59]. miRNA-dependent gene regulation could also be shown for other heterochronic genes identified in *C. elegans* at the same time (*lin-14*, *lin-28*, *lin-42*) which established a new mechanism used for rapid cell fate changes as required during embryonic development [148]. Furthermore, the transcription factor *lin-29* was identified as major downstream target of *lin-41*, since the *lin-41* knockout phenotype could be reverted by simultaneous deletion of *lin-29* [147].

As in the nematode, the phenotype of the homozygous knockout of Trim71 in the mouse results in embryonic death at around midgestation. Most strikingly, the neural folds, precursor structures of the central nervous system, fail to fuse leading to an exencephalus phenotype [131]. However, the malformations in the central nervous system are likely not solely responsible for the embryonic death of the mutant animals, suggesting that other so far unknown phenotypes play a role during embryonic development. Interestingly, it was found that ablation of the last 24 amino acids was already enough to induce the exencephalous phenotype in the majority of the homozygous offspring. Independently of that, other studies in the

model organisms *D. melanogaster* and *D. rerio* showed that the respective Trim71 homologs are required for proper embryonic development [149, 150]. However, there still seem to be differences between the species with regards to Trim71-dependent cellular functions. For example, the lethal mutant phenotype of the *D. melanogaster* homolog of Trim71, *wech*, is caused by a general muscle detachment in the fly larvae. It was therefore postulated that the *wech* protein functions as an adapter protein for the cytoskeletal network and is a regulator of cell adhesion [150]. Until this day, there are no matching observations for other Trim71 homologs and it remains uncertain in how far this protein function is conserved in mammals.

On the molecular level, the mechanism of Trim71 functionalities are still poorly understood. Several studies have addressed the question whether Trim71 acts as a conventional E3-ligase and tried to identify putative protein substrates. Trim71 localizes to so called P-bodies where Ago2, the catalytic component of the RISC complex, can be found as well. Both proteins were shown to interact and it was postulated that Ago2 is a substrate for Trim71-mediated ubiquitination. This ubiquitination would result in the degradation of Ago2, thus influencing global miRNA-biogenesis and activity [145]. In line with this hypothesis, an altered expression of the miRNA let-7 was observed. However, other groups could not confirm this regulatory mechanism [151, 152, 153], whereas one study in the model organism *C. elegans* argues that Ago2 regulation only takes place in a timely restricted manner during development [154].

Another proposed substrate for Trim71-dependent ubiquitination was identified by Chen *et al.* [151]. This study links Trim71 to FGF signaling and postulated that Trim71 is a positive regulator of FGF signaling by the stabilization of the adapter protein Shcbp1 [151]. FGF signaling is very important during the formation of the central nervous system and could contribute to the morphological aberrations observed in Trim71-deficient embryos.

Finally, a very recent publication suggested that Trim71 could act as a negative regulator of LIN28b [155]. Interestingly, this again links Trim71 to the miRNA let-7, since Lin28a and Lin28b are the main posttranscriptional suppressors of let-7 expression. However, in contrast to other findings [145, 154], in this case an enhanced let-7 expression is expected when Trim71 is present.

Other studies mainly concentrated on the putative role of Trim71 as an RNA-binding protein (RBP). In a global screening approach, Trim71 was recently identified as an RBP in mESCs [70]. Moreover, when transfected together with Oct4, Sox2 and Klf4, Trim71 overexpression can enhance the reprogramming efficiency of

MEFs, presumably by suppression of pro-differentiation genes [156]. This suggests that there might be a specific role of Trim71 in the regulation of the balance between stemness and differentiation in ESCs. A couple of gene candidates have been proposed to be regulated in a Trim71-dependent fashion [152, 153, 156]. However, it is still unclear whether the NHL domain of Trim71 recognizes a specific sequence motif of a RNA structure. Accordingly, it is until now impossible to predict target genes.

1.5 Aim and objectives of this study

Trim71 is a highly conserved protein involved in the regulation of embryonic development, which was identified about 15 years ago in the nematode *C. elegans*. Since then, many studies have investigated the effect of Trim71 ablation in different model organisms, revealing striking effects on embryonic development in zebrafish, chicken, fruit fly and mouse. However, apart from these phenotypic analyses, very little mechanistic insight was gained regarding the function of Trim71. Instead, there are a variety of inconsistent reports describing a presumptive role of Trim71 in diverse processes such as ubiquitination, mRNA stability and miRNA expression regulation. Its stem cell restricted expression and the fact that Trim71 might be able to regulate target genes and proteins involved in various pathways, make this gene a putative master regulator for the balance between stemness and differentiation.

The aim of this study is to investigate the implications of Trim71 deficiency in a defined and relevant cell model. Since an early contribution of Trim71 in development was postulated, mESCs derived from conditional Trim71 knockout animals were used as a tool to investigate the effect of Trim71 on stemness and differentiation. In addition, this cell system could be used to validate proposed protein ubiquitination targets as well as Trim71-dependent regulation of mRNA and miRNA expression. Furthermore, we wanted to relate our findings to *in vivo* conditions for which a new conditional knockout mouse model was generated. A new conditional mouse line will overcome major drawbacks of all previous studies in mice using Trim71 knockout alleles for constitutive deletion. Until today, the relevance of Trim71 expression in adult tissues is completely unknown and a conditional knockout mouse might be used to analyze the effect of Trim71 deficiency in adult organs. Based on the finding that Trim71 expression can be detected in the testes of adult wildtype mice, and the fact that germ cells share some defining features with ESCs, we aim to investigate the role of Trim71 in the germ cell compartment in more detail. By crossing Trim71 conditional animals with a germ cell-specific Cre driver line we generated the first tissue specific Trim71 knockout and analyzed its phenotype with regards to fertility in males and females. In combination with *in vitro* data this might lead to better understanding of the principal biology of Trim71, potentially leading to valuable insights into the biology of stem cells, cell type specification and fertility.

2 Materials and Methods

2.1 Materials

2.1.1 Technical devices

Autoclave	135T, HP Medizintechnik (Oberschleißheim)
Automatic cell separator	Automacs pro, Miltenyi (Bergisch Gladbach)
Binocular	Wild Herrbrugg (Bad Dürkheim)
Blotting equipment	Mini Trans-Blot Cell, Bio-Rad Laboratories (Munich)
Centrifuge	5810R, Eppendorf (Hamburg)
Centrifuge	5415R, Eppendorf (Hamburg)
Centrifuge	Avanti J-20XP, Beckman Coulter (Munich)
CO_2 incubator	Labotect (Göttingen)
Developing machine	SRX-101A, Konica Minolta (Langenhagen)
Electropheresis chamber (agarose gels)	Polymehr (Paderborn)
Electropheresis chamber (SDS-PAGE)	Mini Trans-Blot Cell, Bio-Rad Laboratories (Munich)
Flow cytometer	Canto II, BD Bioscience (Heidelberg)
Gel documentation device	Gel Max, Intas (Göttingen)
Heat block	Thermomixer compact, Eppendorf (Hamburg)
Heating cabinet	EcoCell 55, MMM Medcenter (Munich)
Laminar flow hood	BioFlow, BDK (Sonnenbühl-Genkingen)
Luminometer	MicroLumat Plus LB96V, Berthold (Cologne)
Magnetic rack	DynaMag-2 magnet, Invitrogen/ Life Technologies (Carlsbad, USA)
Magnetic stirrer	Combimac RCT, IKA (Staufen)
Microplate reader	infinite M200, Tecan (Männedorf, Switzerland)

Microplate reader	Synergy HT, Biotek (Bad Friedrichshall)
Microscope	Axiovert 100, Zeiss (Jena)
Microscope	Digital sight ds-1, Nikon (Tokyo, Japan)
Microscope	LSM FV-1000, Olympus (Tokyo, Japan)
Orbital shaker	innova44, New Brunswick, Eppendorf (Hamburg)
PCR cycler	MyCycler, Bio-Rad Laboratories (Munich)
PH meter	MP220, Mettler Toledo (Greifensee,Switzerland)
Power supply	EV-243, Consort (Turnhout, Belgium)
Real-time PCR cycler	iCycler iQ5, Bio-Rad Laboratories (Munich)
Rocker	WS-10, Edmund Bühler (Hechingen)
Roller mixer	RS-TR05, Phoenix Instrument (Garbsen)
Rotation wheel	Neolab Rotator, Neolab (Heidelberg)
Scale	JB2002-G/FACT, Mettler Toledo (Greifensee, Switzerland)
Scanner	Scan Maker 8700, Mikrotek (Hsinchu, Taiwan)
Special accuracy weighing machine	AG285, Mettler Toledo (Greifensee, Switzerland)
Spectrophotometer	NanoDrop 2000, Thermo Scientific (Waltham, USA)
Suction pump	AC, HLC BioTech (Bovenden)
Ultracentrifuge	Optima LE-80K Ultracentrifuge, Beckman Coulter (Munich)
Vortex mixer	UNIMAG ZX3, VELP scientica (Milan, Italy)
Water bath	WNE, Memmert (Schwabach)

2.1.2 Chemicals and Reagents

1-Butanol	Merck (Darmstadt)
2-Mercaptoethanol	Carl Roth (Karlsruhe)
2-Propanol	Merck (Darmstadt)
Acetic acid	Carl Roth (Karlsruhe)
Aceton	Carl Roth (Karlsruhe)

Acrylamide/Bisacrylamide solution (30%)	Carl Roth (Karlsruhe)
Agar	BD (Heidelberg)
Agarose	Invitrogen/Life Technologies (Carlsbad, USA)
Ammonium acetate	Carl Roth (Karlsruhe)
Ammonium persulfate (APS)	Carl Roth (Karlsruhe)
Antipain	Sigma-Aldrich (St. Louis, USA)
Aprotinin	Sigma-Aldrich (St. Louis, USA)
Benzamidin	Carl Roth (Karlsruhe)
Bovine serum albumin (BSA)	Carl Roth (Karlsruhe)
Bromodeoxyuridine (BrdU) labeling reagent	Roche (Mannheim)
Bromphenolblau	Carl Roth (Karlsruhe)
Caesium chloride (CsCl)	Carl Roth (Karlsruhe)
Chloroform	Carl Roth (Karlsruhe)
collagenase (Type IV)	Sigma-Aldrich (St. Louis, USA)
Diazabicyclooctan (DABCO)	Sigma-Aldrich (St. Louis, USA)
Dimethyl sulfoxide (DMSO)	Carl Roth (Karlsruhe)
Disodium phosphate (Na_2HPO_4)	Carl Roth (Karlsruhe)
Dithiothreitol (DTT)	Applichem (Gatersleben)
DNA loading Dye (6x)	Fermentas (St. Leon-Rot)
Dynabeads Protein G	Invitrogen/Life Technologies (Carlsbad, USA)
Ethanol	VWR (France)
Ethidium bromide (EtBr)	Carl Roth (Karlsruhe)
Ethylenediaminetetraacetic acid	Carl Roth (Karlsruhe)
Gelatin, from porcine scin	Sigma-Aldrich (St. Louis, USA)
Glucose	Carl Roth (Karlsruhe)
Glycogen	Roche (Mannheim)
HEPES	Carl Roth (Karlsruhe)
Hydrochloric acid (HCl)	Carl Roth (Karlsruhe)
Hydrogen peroxide (H_2O_2)	Merck (Darmstadt)
Igepal CA-630	Sigma-Aldrich (St. Louis, USA)
LB-Agar	GIBCO/Life Technologies (Carlsbad, USA)
Leupeptin	Sigma-Aldrich (St. Louis, USA)
Magnesium chloride ($MgCl_2$)	Carl Roth (Karlsruhe)
Methanol	Carl Roth (Karlsruhe)

Milk powder	Carl Roth (Karlsruhe)
Mounting medium (IF), Fluoroshield	Immuno Bioscience (Burlington, USA)
Paraformaldehyde (PFA)	Merck (Darmstadt)
Phenol	Carl Roth (Karlsruhe)
Phenylmethanesulfonylfluoride (PMSF)	Sigma-Aldrich (St. Louis, USA)
Poly-L-lysine (PLL)	Sigma-Aldrich (St. Louis, USA)
Ponceau S	Carl Roth (Karlsruhe)
Potassium chloride (KCl)	Carl Roth (Karlsruhe)
Sodium azide (NaN3)	Carl Roth (Karlsruhe)
Sodium chloride (NaCl)	Carl Roth (Karlsruhe)
Sodium deoxycholate (SDS)	Sigma-Aldrich (St. Louis, USA)
Sodium fluoride (NaF)	Carl Roth (Karlsruhe)
Sodium hydroxide (NaOH)	Carl Roth (Karlsruhe)
Tetramethylethylenediamine (TEMED)	Sigma-Aldrich (St. Louis, USA)
Tris(hydroxymethyl)aminomethane) (TRIS)	Carl Roth (Karlsruhe)
Triton X-100	Carl Roth (Karlsruhe)
TRIzol Reagent	Invitrogen/ Life Technologies (Carlsbad, USA)
Trypsin, 2.5 %	GIBCO/ Life Technologies (Carlsbad, USA)
Tween 20	Carl Roth (Karlsruhe)

2.1.3 Kits

Anti-SSEA-1 MicroBeads	Miltenyi Biotec (Bergisch Gladbach)
BCA Protein Assay Reagent	Thermo Scientific (Waltham, USA)
Alkaline Phosphatase detection kit	Sigma-Aldrich (St. Louis, USA)
anti-FITC microbeads	Miltenyi Biotec (Bergisch Gladbach)
Anti-FITC MicroBeads	Miltenyi Biotec (Bergisch Gladbach)
anti-FLAG M2 Magnetic Beads	Sigma-Aldrich
DIG-RNA Labeling Mix	Roche (Mannheim)
DNase I (RNase-free)	Life Technologies (Carlsbad, USA)
Dual-Luciferase Reporter Assay System	Promega (Fitchburg, USA)
ECL Plus Western-Blotting Substrate	Thermo Scientific (Waltham, USA)
Fugene HD	Roche (Mannheim)
High-Capacity cDNA Reverse Transcription Kit	Applied Biosystems/ Life Technologies (Carlsbad, USA)
In-Fusion HD Cloning Kit	Clontech Laboratories (Mountain View, USA)
Kapa Sybr Fast qPCR Mastermix for Bio-Rad iCycler	Peqlab (Erlangen)
Lipofectamine 2000 Transfection Reagent	Invitrogen/Life Technologies (Carlsbad, USA)
Lipofectamine RNAiMAX Transfection Reagent	Life Technologies (Carlsbad, USA)
miScript II RT Kit	Quiagen (Hilden)
NucleoSpin Gel and PCR Clean-up kit	Macherey-Nagel (Düren)
PeqGold Hot Start Mix Real-Time	Peqlab (Erlangen)
Riboprobe® Combination System-SP6/T7 RNA Polymerase	Promega (Madison, USA)
Xfect mESC Transfection reagent	Clontech Laboratories (Mountain View, USA)

2.1.4 Antibodies

2.1.4.1 Primary antibodies

Target protein	Host species	Application	Supplier
CD90.2-FITC	mouse	FACS (0.25 µg/ $1x10^6$ cells)	BioLegend
Actin	rabbit	WB (1:2000)	Sigma-Aldrich
Ago2 (C34C6)	rabbit	WB (1:1000)	Cell Signaling
CD133-PE (13A4)	rat	FACS (0.4 µg/ $1x10^6$ cells)	eBiosciences
CD15 (SSEA-1) (MC-480) Alexa Fluor 647	mouse	FACS (0.2 µg/ $1x10^6$ cells)	BioLegend
c-Myc (9E10)	mouse	WB 1:400)	Santa Cruz Biotechnology
c-Myc (D84C12)	rabbit	WB 1:1000)	Cell Signaling
Digoxigenin-AP (Fab-fragments)	sheep	ISH (5 U/ml)	Roche
Flag	mouse	WB (1:1000)	Sigma-Aldrich
GFP (B-2)	mouse	WB (1:1000), IP (4 µg/mg)	Santa Cruz Biotechnology
Hmga2	rabbit	WB (1:1000)	Cell Signaling
Lin28a/LIN28A (D1A1A)	rabbit	WB (1:1000), FACS (1:200)	Cell Signaling
LIN28B human	rabbit	WB (1:1000)	Cell Signaling
Lin28b mouse	rabbit	WB (1:1000)	Cell Signaling
Oct4	rabbit	WB (1:1000)	Abcam
p21 (F-5)	mouse	WB (1:250)	Santa Cruz Biotechnology
p27	rabbit	WB (1:1000)	Cell Signaling
p53	rabbit	WB (1:1000)	Cell Signaling
PABP (H-300)	rabbit	WB (1:400)	Santa Cruz Biotechnology
Plexin B2 PE (3E7)	armenian hamster	FACS (0.8 µg/ $1x10^6$ cells)	Novus Biologicals

Target protein	Host species	Application	Supplier
Sall4 (6E3)	mouse	WB (1:500)	Sigma-Aldrich
Sox2	mouse	WB (1:500)	R&D Systems
Trim71	sheep	WB (1:1000)	R&D Systems
Trim71	rabbit	WB (1:1000)	Sigma-Aldrich
Tubulin	mouse	WB (1:1000)	Sigma-Aldrich
Vasa (N-14)	goat	WB (1:400)	Santa Cruz Biotechnology

2.1.4.2 Secondary antibodies

Target species	Modification	Host species	Application	Supplier
α-mouse	HRP	goat	WB (1:5000)	Santa Cruz
α-rabbit	HRP	goat	WB (1:5000)	Santa Cruz
α-rat	HRP	goat	WB (1:5000)	Santa Cruz
α-goat	HRP	donkey	WB (1:5000)	Santa Cruz
α-sheep	HRP	donkey	WB (1:5000)	Santa Cruz
α-mouse	Alexa-Fluor 647	goat	IF (1:400)	Jackson ImmunoResearch

2.2 Methods

2.2.1 Animal experiment techniques

2.2.1.1 The generation of a new conditional Trim71 targeting allele

At the beginning of this study only two Trim71 transgenic mouse lines have been described [131]. Both of them were based on gene trap insertions leading to a premature stop within the Trim71 gene. However, the lethal phenotype of the Trim71 full knockout is fatal for any investigations on the protein function that go beyond embryogenesis. Therefore, the new conditional Trim71 mouse allele with the name Trim71^{tm1695Arte} was created. The genetic engineering was planned and realized by the biotechnology company Taconic Artemis (Cologne).

The Trim71 gene has four exons gene which are located on Chromosome 9, about 15 kbp apart from the neighboring Ccr4 gene. According to the common databases, the coding sequence is spread over all four exons and there are no indications for alternative splicing products. For the targeting vector, the sequence of exon four from the Trim71 genomic locus, coding for the largest part of the protein, was flanked by unidirectional loxP sites (figure 1.5). Furthermore, two positive selection markers were inserted at both sites of the homology region in order to increase the chances for recombination events of both LoxP sites. These selection cassettes were flanked by FRT and F3-sites. A translational stop cassette was located downstream of the distal LoxP site and a mini-gene coding for thymidine kinase (Tk) was inserted in the targeting vector to ensure that the insertion into the genome is primarily facilitated via homologous recombination.

A first heterozygous mouse breeding pair containing the targeted Trim71 allele was crossed with a FLP-deleter strain to eliminate the neomycin and the puromycin resistance cassettes [157]. Subsequently, a constitutive Trim71 knockout allele mouse line was generated by crossing with PGK-Cre mice resulting in ubiquitious Cre activation [158]. Furthermore, in this study two additional mouse lines were generated with the floxed Trim71 allele allowing for temporally and spatially defined deletion of the gene. On the one hand, mice with the floxed allele were crossed with mice in which Cre expression is regulated by the germ cell specific Nanos3 gene resulting in a tissue specific knockout of Trim71 [159]. On the other hand, for the generation of inducible MEFs, ESCs and RG-like cells where the mutation can be induced by the application of the drug tamoxifen, conditional Trim71 mice were crossed with Rosa26-CreER^{T2} mice [160]. All mice used for the experiments had the C57BL/6J

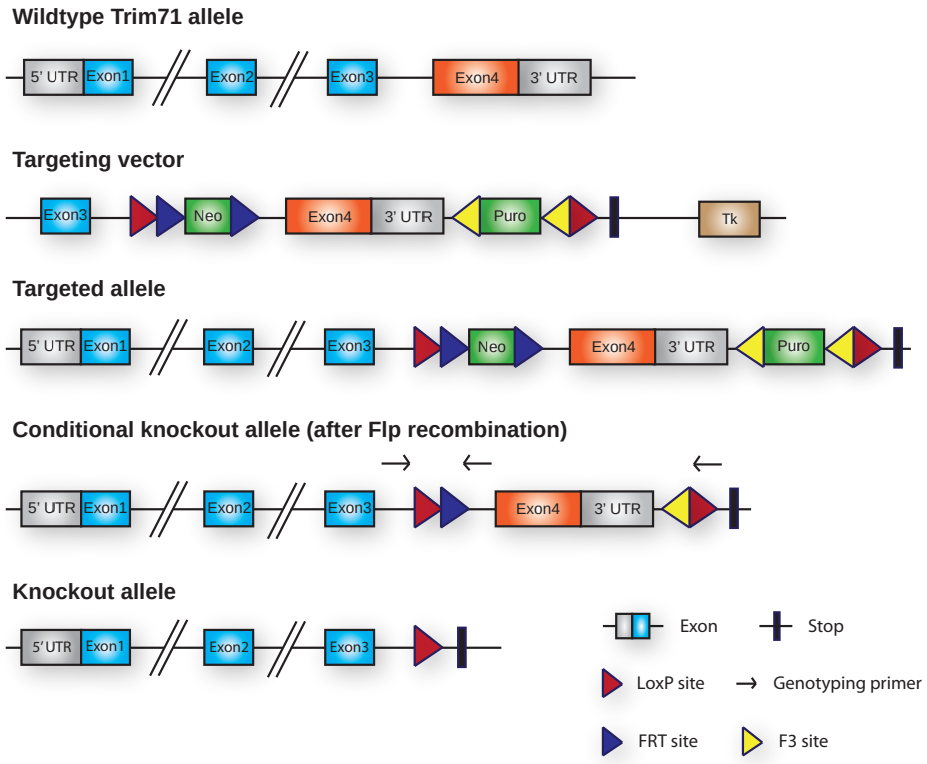

Figure 2.1: **Overview of the targeting strategy for the generation of a conditional Trim71 knockout allele in mice.** The last of four exons was flanked by unidirectional LoxP sites which allows for the excision of this exon after Cre activation.

genetic background. Breeding and maintaining of experimental animals was done in the LIMES Genetic Resources Center (GRC) as well as in the animal facility of the Department of Developmental Pathology in Bonn according to the German Animal Welfare Act.

2.2.1.2 Genotyping of mice

For genotyping of the mice, genomic DNA was extracted from tail tip biopsies. Therefore, the tail tips were cooked for 20 min at 95°C in 200 µl 50 mM NaOH solution. Afterwards, the solution was neutralized again by the addition of 50 µl 1M Tris (pH 8). 2 µl of the supernatant was used for the genotyping PCR. For the genotyping of cultured cells the DNA was extracted as described in section 2.2.2.7. Genotyping PCRs were performed with the DreamTaq polymerase (Thermo Scientific) according to the manufacturer's recommendations using 15 pmol of each

primer. For Trim71, Rosa26-Cre and Nanos3-Cre a three primer strategy was applied resulting in multiple possible bands (see below).

Trim71	Trim71-206	GAA AGG AGG CTA GCC AAA GG	WT 242 pb
	Trim71-207	ATG CTG TAC GGT AGG AGT CTT CC	KO 322 bp
	Trim71-209	CAC ACA AAA AAC CAA CAC ACA G	FL 361 bp
Rosa26-Cre	Rosa26 for	AAA GTC GCT CTG AGT TGT TAT C	WT 603 bp
	Rosa26 rev2	GGA GCG GGA GAA ATG GAT ATG	TG 397 bp
	Cre-rev	CAT CAC TCG TTG CAT CGA CC	
Nanos3-Cre	nos3-F1	CAG AGG CCA CTT GTG TAG CG	WT 220 bp
	nos3-R1	GGG ACT GAT AGA TGG CAC	TG 270 bp
	PGK-neo-R2a	CAG AGG CCA CTT GTG TAG CG	
Y-chromosome	Sry Mm for	TGG GAC TGG TGA CAA TTG TC	406 bp
	Sry Mm rev	GAG TAC AGG TGT GCA GCT CT	
X chromosome	Xist Mm for	GCT TTG TTT CAC TTT CTC TGG TGC	566 bp
	Xist Mm rev	ATT CTG GAC CTA TTG GGA AGG G	

2.2.1.3 Isolation of spermatogonia from mouse testes

Testes were isolated from male mice between 50-60 days of age. The cell isolation protocol was modified from Ogawa *et al.* (1997)[161]. First, the tunica albuginea was removed from the testis, thereby exposing the seminiferous tubules. The tubules of several organs were pooled and then incubated in approximately 10 volumes of HBSS with calcium and magnesium containing 1 mg/ml collagenase (Type IV) and DNAse I (200 to 500 µg/ml). The tissue was incubated at 37°C with gentle agitation for 15 min or until the tubules separated. Dispersion of the tubules can be hastened by careful dissection and spreading of the tubules. The testis tubules were then washed three times in 10 volumes of HBSS, followed by incubation at 37°C for 5 min in HBSS containing 0.25% trypsin and 150 µg/ml DNAse I with occasional gentle agitation. The trypsin treatment was terminated by adding 20% volume of FBS. Following digestion, the cell suspension is filtered through a nylon filter with 40 µm pore size to remove large clumps of cells. The filtrate was centrifuged at 1000 rpm for 5 min at 4°C and the supernatant carefully removed from the pellet. The cells were then resuspended in PBS for counting. Magnetic-activated cell sorting (MACS) for CD90 positive cells was used to enrich SSCs from the total cell population. Therefore, $1{\cdot}10^6$ cells were stained with 0.2 µg FITC anti-

CD90.2 antibody (BioLegend) for 15 min at 4°C. The cells were then washed in MACS-buffer and incubated in a 1:5 dilution of anti-FITC microbeads (Miltenyi) and incubated for another 15 min at 4°C before final washing in MACS buffer. The pellet was resuspended in 500 µl MACS buffer and loaded on AutoMACS device with the program setting positive selection. The efficiency of enrichment was later controlled by FACS.

MACS-buffer	2 mM	EDTA
	0.5% (v/v)	FBS
	ad 100% (v/v)	PBS

2.2.1.4 PGC detection in embryos by alkaline phosphatase

Embryos were obtained from pregnant females 8.5 with the first day of vaginal plug identification defined as 0.5 dpc. Embryos were dissected in PBS and the upper part of the embryo was cut off and used for genotyping. The lower parts were fixed in 4% PFA for 3 h, followed by washing in PBS. Embryos were placed in 70% ethanol at 4°C for 1 hour, then washed once in PBS and stained with Fast Red TR and α-naphthyl phosphate (Sigma) to detect alkaline phosphatase-positive cells.

2.2.2 Molecular biological methods

2.2.2.1 PCR for the amplification of cDNAs

In order to clone new cDNAs in a eukaryotic expression vector, a PCR was set up using sequence specific primers containing restriction sites for subsequent enzymatic digest. A mouse E19 embryonic library (Origene) and a homemade human NK cell library were used as template DNA pool for mouse and human cDNAs, respectively. The standard PCR reaction was set up as described below:

Standard PCR reaction	10 µl	5x Phusion GC buffer
	200 mM	10 mM dNTPs
	15 pmol	Forward primer
	15 pmol	Reverse primer
	100 ng	Template DNA
	0-2 µl	DMSO
	1 unit	Phusion DNA polymerase
	ad 50 µl	ddH_2O

Cycle number	Denature	Anneal	Extend	Hold
1	98°C, 2 min			
2-31	98°C, 30 s	55-62°C, 20 s	72°C, 30 s/kbp	
32			72°C, 3 min	4°C

2.2.2.2 Primers for the amplification of cDNAs

TRIM constructs	
Trim71 mm fo mlu	GCG GGG ACG CGT ATG GCT TCG TTC CCG GAG ACC GAC TT
Trim71 mm re not	GCG GGG GCG GCC GCT TAA GAT GAG GAT TCG ATT GTT GCC AAA
Trim71 C12L/C15A	GCG GGG ACG CGT ATG GCT TCG TTC CCG GAG ACC GAC TTC CAG ATA
mm/hs fo mlu	TTA CTG CTG GCC AAG GAG ATG TGC GGC T
Trim71 mm ΔRBCC fo mlu	GCG GGG ACG CGT TTC GGC AGT GAA GGT GAC GGG
Trim71 mm ΔNHL re not	GCG GGG GCG GCC GCT TTA GCT CTC CAG CTT GCT GAG ACT
Trim32 mm fo mlu	GCG CCC ACG CGT ATG GCT GCG GCT GCA GCA GCT TCT
Trim32 mm re not	GCG CCC GCG GCC GCT TAA GGG GTG GAA TAT CTT CTC
TRIM71 hs fo mlu	TCC ACA TCT ACC GGG ATG GCT TCG TTC CCC GAG
TRIM71 hs rev	CTC CTC CAC TCC CAA GGG AGA AGA CGA GGA TTC GAT TGT TGC
TRIM71 hs ΔRBCC fo mlu	GCG GGG GCG GCC GCT TTA GAT GTC TAG CGC TCT ACC CTC C
TRIM71 hs ΔNHL re not	TCC ACA TCT ACC GGG ATG AGC AGC GGG GCC TTT G
TRIM32 hs fo mlu	GCG GGG ACG CGT ATG GCT GCA GCA GCA GCT TC
TRIM32 hs re not	GCG GGG GCG GCC GC CTA TGG GGT GGA ATA TCT TCT CAG ATG G

Lin28 constructs	
Lin28a mm fo mlu	GCG CCC ACG CGT ATG GGC TCG GTG TCC AAC CAG CAG
Lin28a mm re not	GCG CCC GCG GCC GCT CAA TTC TGG GCT TCT GGG AGC AG
Lin28a mm ΔCHCC re not	GGG GCG GCG GCC GCT CCT TTG GAT CTT CGC TTC TGC
Lin28 mm ΔCSD fo mlu	GGG GCG ACG CGT GGT GGT GTG TTC TGT ATT GGG A
Lin28a mm H165A fo	GCT ATG GTG GCC TCG TGT CCA C
Lin28a mm H165A re	CGA GGC CAC CAT AGC GTT GAT GCT TTG GC
Lin28a mm H147A fo	CGC TCA TGC CAA GGA ATG C
Lin28a mmH147A re	GCA TTC CTT GGC ATG AGC GTC TAG CCC ACC GCA GTT GTA G
LIN28A hs fo mlu	GCG GGG ACG CGT ATG GGC TCC GTG TCC AAC C
LIN28A hs re not	GCG GGG GCG GCC GCT CAA TTC TGT GCC TCC GGG AG
LIN28B hs fo mlu	GGG GCG ACG CGT ATG GCC GAA GGC GGG GCT AG
LIN28B hs re not	GGG GCG GCG GCC GCT TAT GTC TTT TTC CTT TTT TGA ACT GAA GGC C

Luciferase constructs	
Foxj1 mm fo xho	GCG GGG CTC GAG AAG GTC AGG CCC CAC CCC ATC TCC
Foxj1 mm F1 xho	GCG GGG CTC GAG CAT ATC CAA GCC CAG AAG ACT GG
Foxj1 mm F2 xho	GCG GGG CTC GAG GCA CTC TGA GAG CTG AAG CCC
Foxj1 mm F3 xho	GCG GGG CTC GAG GAT GAT AAC AAA TTA ATT CCC AGG AGG C
Foxj1 mm F4 xho	GCG GGG CTC GAG CGA AAT GGT CTC TAA GCC CGC TAG
Foxj1 mm F5 xho	GCG GGG CTC GAG GTG AAT GTA GTT ATA GCT AAG ACT TAA CTG GG
Foxj1 mm re not	GCG GGG CGG CCG CCT TTA CAT GAA AAA GGT TAA ATT GCT CCA CG
Inhbb mm fo xho	GCG GGG CTC GAG CAG AGG CAA CGG GGG CGG AGC
Inhbb mm re not	GCG GGG CGG CCG CCC GTG GCA CTC CAT CTT TTA TTG TC
Mras mm fo xho	GCG GGG CTC GAG CAG CCT GAA GCC CTG GGC ATA GC
Mras mm re not	GCG GGG CGG CCG CCT CTG ATT GTT TCT TTA TTA ATA AGT AGA GAT ACA C
Nanos3 mm fo xho	GCG GGG CTC GAG GAG CTT GGA GTG GGG AGG AC
Nanos3 mm re not	GCG GGG CGG CCG CCC ACT CCT TAG CAT TTA TTG GAT GTT G
Obscn mm fo xho	GCG GGG CTC GAG TGC CAC ACA TTG GAG ATA AGG GTA AG
Obscn mm re not	GCG GGG CGG CCG CGA GGG TTT GGG ACT TGA TTT ATT GTT CTC ATC
Pou5f1 mm fo xho	GCG GGG CTC GAG CTG AGG CAC CAG CCC TCC

Pou5f1 mm re not	GCG GGG CGG CCG CAG CTA TCT ACT GTG TGT CCC AGT C
Prom1 mm fo xho	GCG GGG CTC GAG CAA CTG GAG TTG AAG CTG CTT GAA CAA C
Prom1 mm re not	GCG GGG CGG CCG CGT TCA TTC ATG CTT TAT TTT AAA TCT CAA CAT CAG G
Plxnb2 mm fo xho	GCG GGG CTC GAG CCG TCA ATG CCG CCT CAG GAT G
Plxnb2 mm F1 xho	GCG GGG CTC GAG CCT CTT GTA GAC TGT AGC GTC TTT CTC
Plxnb2 mm F2 xho	GCG GGG CTC GAG GGC GGT GGA GGC ATG GCC
Plxnb2 mm F3 xho	GCG GGG CTC GAG CAA TGC CTT CCT GAC CTC ACC
Plxnb2 mm F4 xho	GCG GGG CTC GAG AGG TCC TTG TCT CAG CTG TTA AAC
Plxnb2 mm re not	GCG GGG CGG CCG CCC AGA GAG TGA AAA AGA CAA CTG TAT TG
Plxnb2 mm F4a xho	CCT GAC TCG AGA CCC AGA AAA CTG AGG TCC TTG TCT CAG CT
Plxnb2 mm F4a not	GGA CTC GCC GGC GCC TGT TTA ACA GCT GAG ACA AGG ACC TCA G
Plxnb2 mm F4b xho	CCT GAC TCG AGC TGT CCT GGA GGC CCT GCC TGG ATC TGG GG
Plxnb2 mm F4b not	GGA CTC GCC GGC GGC TCC AGC ACC CCC AGA TCC AGG CAG GGC C
Plxnb2 mm F4c xho	CCT GAC TCG AGA GCA TCT CCC CCC AGG ACC ACC CAC CCT TT
Plxnb2 mm F4c not	GGA CTC GCC GGC GCG ATT TAC AAA AAG GGT GGG TGG TCC TGGG
Plxnb2 mm F4d xho	CCT GAC TCG AGT GAT TGT AAA TCC AAT ACA GTT GTC TTT TT
Plxnb2 mm F4d not	GGA CTC GCC GGC GCC AGA GAG TGA AAA AGA CAA CTG TAT TGG A
Tcf15 mm fo xho	GCG GGG CTC GAG ACC TGG ATC CCT GGT TTT CTC C
Tcf15 mm re not	GCG GGG CGG CCG CAT ACC TTT ATT TTG ACC CCC TCC C
Trim54 mm fo xho	GCG GGG CTC GAG CCC GAC TCT GAT CCA GAG CGC ACA C
Trim54 mm re not	GCG GGG CGG CCG CGG GAC ACT TGA GTC CTT TAT TGA GAA C

2.2.2.3 Enzymatic DNA digest and ligation

The PCR products were cleaned by phenol extraction and then precipitated using LiCl and 96% ethanol. The pellet was washed once and air-dried before resuspending in ddH_2O. The extracted DNA was then subjected to enzymatic digest with the appropriate buffer conditions (enzymes and buffers from Thermo Scientific). The restriction digest was incubated for 2 h at 37°C. Vector backbones were additionally treated with alkaline phosphatase for 10 min. Then, DNA loading buffer was added and the whole reaction was loaded on an agarose gel and run to separate the digestion products. The DNA gel bands of interest were cut out using a scalpel. The DNA was extracted from the gel using the NucleoSpin Gel and PCR Clean-up kit (Macherey-Nagel) according to the manufacturer's instructions. The concentra-

tions of the gel-purified DNA were measured and the ligation set up with a 1:3 molar ratio of vector to insert DNA in a final volume of 20 µl containing 2 µl ligase buffer and 0.5 units T4 DNA ligase. The ligation reaction was incubated either for 2 h at RT or at 16°C overnight.

2.2.2.4 Transformation of chemically competent *E. coli* bacteria

For transformation of plasmid DNA chemically competent *E. coli* bacteria of the strains DH5α, MC1061 and Stbl3 were used. The bacteria were thawed on ice and 60 µl of the cell suspension were mixed with either 7 µl of the ligation reaction (see above) or 50 ng of plasmid DNA for retransformation. After 10 min incubation on ice, the caps were placed in a 42°C water bath for 45 s and subsequently put back on ice 1 min. 1ml LB_0 medium was added to the bacteria which were then incubated on a shaker at 37°C for another 45 min. The cells were briefly centrifuged and resuspended in 150 µl LB_0 before plating on LB agar plates containing a selective antibiotic corresponding to the resistance cassette on the plasmid (30 µg/ml kanamycin or 100 µg/ml ampicillin). The plated bacteria were incubated overnight at 37°C.

2.2.2.5 Mini-preparation of plasmid DNA

After an overnight culture at 37°C, the colonies grown on the plate were individually picked using a pipet tip for inoculation of mini-preparation cultures. Picked bacteria were cultured in 4 ml LB medium with antibiotics overnight. The bacteria were spun down by centrifugation for 2 min at 5000 rpm. The pellet was resuspended in 200 µl solution I. 400 µl solution II was added to facilitate bacterial lysis and the solution was mixed by inversion of the caps and incubated for 3 min at RT. For neutralization, 300 µl solution III was added resulting in precipitation of bacterial proteins and genomic DNA. The crude precipitate was separated by centrifugation for 12 min at 13,000 rpm. The supernatant was transferred to a new cap and 400 µl phenol-chloroform (1:1) was added and the cap was shortly vortexed. After centrifugation for 5 min at 13,000 rpm, the upper aqueous phase containing the plasmid DNA was transferred to a new cap and 0.6 ml 2-propanol was added for DNA precipitation. The DNA was spun down for 12 min at 13,000 rpm and the pellet was washed once with 70% ethanol. The DNA was dried at 37°C and then resuspended in 50 µl water containing 5 µg RNAseA.

Solution I (pH 8)	**Solution II (pH 13)**	**Solution III (pH 5)**
10 mM EDTA	0.2 M NaOH	3 M KAc
25 mM Tris	1% SDS (w/v)	2 M HAc
50 mM Glucose		

2.2.2.6 Maxi-preparation of plasmid DNA

For maxi-preparations 1 l of an overnight bacterial culture was centrifuged for 20 min at 4,200 rpm. The resulting pellet was thoroughly resuspended in 40 ml solution I (see table in 2.2.2.5). Then, 80 ml of solution II was added to enable bacterial lysis. In order to neutralize the suspension another 40 ml of solution III was carefully mixed in resulting in precipitation of cellular material including genomic DNA. The mixture was spun down for 20 at 4,200 rpm and the supernatant transferred into a new vessel together with 100 ml of 2-propanol. The solutions were mixed and the plasmid-containing precipitate was spun down for 12 min at 5,000 rpm and the supernatant decanted. For further purification, the crude DNA was subjected to caesium chloride gradient-centrifugation according to Glisin *et al.* (1974) [162]. In short, the pellet was resuspended again in 3.5 ml solution I, then 5.5 g CsCl and 0.5 ml EtBr (2% solution) was added. The clear supernatant was filled in ultra-centrifugation tubes and sealed. the samples were centrifuged for 4 h at 80,000 rpm in which time a continuous gradient of salt density is build up. the plasmid DNA accumulates in the specific isopycnic layer. After centrifugation the visible EtBr-containing DNA layer can be collected using a syringe. The EtBr is subsequently removed by several washing steps with butanol. Finally, the plasmid-DNA was precipitated by adding 1 volume of sodium acetate (1M) and 3 volumes of 96% ethanol. The precipitate was pelleted by centrifugation (5 min; 5,000 rpm) and washed once with 70% ethanol before drying. The DNA was solved in sufficient ultra-pure water and the concentration was measured using a spectrophotometer.

2.2.2.7 Extraction of genomic DNA from cells

For preparation of genomic DNA, the cell pellet was dissolved in 200 µl of genomic DNA cell lysis buffer to which proteinase K was freshly added. The samples were incubated overnight at 56°C under constant agitation. Then 600 µl ethanol was added resulting in the precipitation of genomic DNA. The DNA was centrifuged and the pellet washed once with 75% ethanol. The pellet was dried and resus-

pended in 50 µl ddH_2O and further on stored at 4°C. The concentration of the DNA was measured using a spectrophotometer and about 100 ng DNA was used per PCR reaction (e.g. for genotyping). For large scale genomic DNA preparation in 96 well plates, cells were directly lysed in the plate with 50 µl lysis buffer applied per well. Accordingly, 100 µl ethanol was added for DNA precipitation and the supernatant was carefully tilted instead of centrifugation.

genomic DNA cell lysis buffer	10 mM	NaCl
pH 7.5	10 mM	Tris
	10 mM	EDTA
	0.5%	Sarkosyl
	80 units/ml	Proteinase K (freshly added)

2.2.2.8 RNA isolation

For RNA isolation from cells and tissues TRIzol reagent (Life Technologies) was used according to the manufacturer's instructions. In short, $1{\cdot}10^5$-$1{\cdot}10^7$ cells or 5-20 mg of ground tissue were resuspended in 1 ml of TRIzol reagent and either prepared directly or stored at -80°C for later preparation. 0.2 ml of chloroform was added and the sample thoroughly vortexed. To support phase separation, the samples were centrifuged at 10,000 rpm for 8 min at 4°C. The upper aqueous phase was transferred to a new cap and 0.5 ml 2-propanol was added. The RNA was precipitated by centrifugation at 13,000 rpm for 12 min at 4°C. The pellet was washed once with 70% ethanol and air-dried before resuspending in ddH_2O containing DNAseI (1 unit/25 µl). The DNA was digested for 30 min at 37°C and the enzyme then heat-inactivated for 30 min at 75°C.

2.2.2.9 cDNA synthesis for real-time PCR

The concentration of the RNA solution was measured using a spectrophotometer. Depending on the downstream application different protocols for reverse transcription were applied according to the manufacturer's recommendations.

Reverse Transcription	Application	Input	Method	Protocol
High-Capacity cDNA Reverse Transcription Kit (Applied Biosystems)	mRNA and pri-miRNA quantification	500 ng total RNA	random hexamer primers	37°C, 2 h 85°C, 5 min
TaqMan miRNA Assays plus TaqMan MicroRNA Reverse Transcription Kit (Applied Biosystems)	mature miRNAs and non-coding RNAs	100 ng total RNA	sequence-specific primers	16°C, 30 min 42°C, 30 min 85°C, 5 min
miScript II RT kit (Quiagen)	mature and pre-miRNAs	200 ng total RNA	oligo-ligation to all RNAs	37°C, 60 min 95°C, 5 min

2.2.2.10 Real-time qPCR

Two different 2x master mixes were used for the real-time analyses. On the one hand, gene specific TaqMan assays (Applied Biosystems) were used in combination with the Hot Start Mix Real-Time (Peqlab). This method works with a fluorescently labeled DNA probe which is binding to the amplified PCR product. With every amplification step more dye-molecules are degraded leading to increased light emission. The system has the advantage of high specificity since the light emission requires concurrent binding of both primers and the probe. For some experiments however, conventional primers in combination with a SYBR-green containing real time master-mix were used. SYBR-green induced fluorescence will occur as long as double stranded DNA is generated and does not require sequence specificity. Therefore, the PCR products were afterwards checked by gel electrophoresis and sequencing. For both applications the following PCR program was used:

Cycle number	Denature	Anneal	Extend	measure
1	95°C, 3 min			
2-46	95°C, 10 s	58°C, 30 s	72°C, 30 s	x

2.2.2.11 Preparation of RNA probes for i*n situ* hybridization

A part of the murine Trim71 cDNA referring to nt 1999-2970 (NM_001042503.2) was synthesized by PCR using a stage E19 whole embryo cDNA library (Origene). After PCR amplification, the cDNA fragment was cloned into the pGEM-T cloning vector (Promega). This plasmid was linearized with a restriction enzyme and used as a template for *in vitro* transcription. For *in vitro* transcription the linearized template DNA was incubated together with DIG-RNA Labeling Mix (Roche) and the Riboprobe® Combination System-SP6/T7 RNA Polymerase (Promega) according to the manufacturer's recommendations. The remaining plasmid DNA was digested with 1U DNAseI and the integrity of the RNA was controlled on an agarose gel.

2.2.2.12 Whole mount *in situ* hybridization

Whole-mount *in situ* hybridization procedures were performed according to Wilkinson (1992) [163] with some modifications. Briefly, after rehydration with a graduated MetOH/PBT series, embryos were bleached with 6% H_2O_2 in PBT for 15 min and treated with 10 μg/ml Protease K (Roche) for 8-15 min at RT depending on the stage, stopped with 0.2% glycine and the embryos were then re-fixed with 4% PFA, 0.2% glutaraldehyde in PBT for 20 min at RT. Pre- hybridization (in 5× SSC (pH 4.5), 50% formamide, 1% SDS, 50 μg/ml yeast tRNA (Roche), and 0.5 μg/ml heparin (Sigma-Aldrich)) was performed at 67 °C for 1 h, then a DIG-RNA probe (about 500 ng/ml) was added and hybridized for over 14 h at 70 °C. Subsequently, embryos were subjected to a series of post-hybridization washes in wash buffers containing formamide, SSC and SDS. After blocking with 10% sheep serum (Jackson ImmunoResearch) in TBS containing 0.1% Tween 20 (TBST) for 1 h at RT, embryos were incubated overnight with anti-DIG-AP Fab fragments antibody (Roche) and 1% sheep serum in TBST at 4 °C. After a series of washes with TBST, embryos were equilibrated with NTMT (5 M NaCl, 1 M Tris-HCl (pH 9.5), 1 M $MgCl_2$, and 0.1% Tween 20). Color reaction was performed at 4 °C or RT with nitro blue tetrazolium/5-bromo-4-chloro-3- indolyl phosphate (NBT/BCIP) (Roche), then embryos were stored in 4% PFA in PBT at 4 ° C. Stained samples were photographed with a SZX10 microscope and Colorview Soft Imaging system (Olympus).

2.2.3 The generation of homozygous Lin28a knockout mESC lines

In the course of the studies, Lin28a knockout mESCs were generated in the Trim71$^{fl/fl}$ #1 cell line. This would in principle allow the investigation of all combinations of Trim71 and Lin28a knockouts in the same cellular background. Whereas most conventional knockout cell lines are generated from homozygous mice we wanted to generate a homozygous Lin28a knockout directly in our *in vitro* cell system. However, using a targeting vector for homologous recombination does not result in homozygously targeted clone because the chances for such a event are very low. Recent advances in the field of reverse genetic engineering has offered new tools for the generation of genetically modified organisms. Both, zinc finger nucleases and Transcription activator-like effectors nucleases (TALENs) enable costum-designed DNA binding and restriction. For this approach, the TALENs are co-transfected with a partially homologous targeting plasmid which will be used during DNA repair by the cell intrinsic repair machinery.For the construction of the Lin28a knockout, a strategy was chosen that would insert a targeting cassette with a G-418 cassette with a transcriptional stop in close proximity of the translational start site of Lin28a. Due to this, the TALEN technique was combined with a Lin28a targeting vector which will allow the pre-selection with an antibiotic and thus increase the chance to yield homozygously targeted clones. The following sections will describe the specificities of the generation of the Lin28a KO cell lines, especially the cloning of the TALENs and the targeting construct. Both, the targeting construct and the TALENs require the assembly of several DNA fragments within one vector. Therefore, ligation independent cloning (LIC) techniques were applied to generate the constructs. LIC does not depend on the usage of unique restriction sites and is thus less limited in its application. Moreover, several DNA fragments can be assembled simultaneously. For the TALEN cloning the Golden Gate Assembly was used, whereas for the targeting vector the commercial In-Fusion system was used.

2.2.3.1 Construction of Lin28a-specific TALENs by hierarchical "Golden Gate Assembly"

The deciphering of the TALE code has enabled the generation of custom-designed binding domains[164]. TALEs are DNA bacterial binding proteins from *Xanthomonas sp.* consisting of 34 amino acid long tandem repeat modules which are binding to a specific DNA nucleotide[165, 166]. The repeats are highly conserved differing only in two amino acid positions, called the repeat variable diresidues (RVD), that

specify the targeted nucleotide. Via stringing together several monomers in a row, a target sequence from 5′ to 3′ can be defined (figure 2.2a). Linked to other effector domains TALEs can guide transcription activators or nucleases to a specific location in the genome[167, 168, 169]. For example, by pairwise binding of two TALE binding domains fused to the unspecific FokI endonuclease catalytic domain (TALENs) a molecular scissor can be build, generating a double strand break at a desired location in the genome (figure 2.2b). The error-prone DNA repair will eventually lead to insertion or deletions (indels) at the site of the strand break. If the targeted site is located within the coding region, there is a high chance to generate a frame sift mutation within the translational code. This will result in a premature stop of the translation. However, TALENs can also be used to facilitate the integration of a targeting construct. This method has the advantage that the mutation is clearly defined and moreover it allows the insertion of an antibiotic resistance cassette.

Two independent TALEN pairs were cloned, one of them cutting at 8 bp upstream, the other one 26 bp downstream of the start codon.

TALENs 1+2: Mus musculus lin-28 homolog A (C. elegans) (Lin28a), mRNA: ref | NM_145833.1 |

43 T GGGGCCCGGGGCCACGGGC tcagcagacgaccatg GGCTCGGTGTCCAACCAGC A 98

TALEN 1 NH NH NH NH HD HD HD NH NH NH NH HD HD NI HD NH NH NH HD

TALEN 2 NH HD NG NH NH NG NG NH NH NI HD NI HD HD NH NI NH HD HD

TALENs 3+4: Mouse DNA sequence from clone RP23-314D24 on chromosome 4, complete sequence

39499 T GGGCTCGGTGTCCAACCAG cagtttgcaggttcg AGCTTGCGATTCAGCGGGC A 39445

TALEN 3 NH NH NH HD NG HC NH NH NG NH NG HD HD NI NI HD HD NI NH

TALEN 4 NH HD HD HD NH HD NG NH NI NI NG HD NH HD NI NI NH HD NG

For the cloning of the TALEN vectors, a hierarchical ligation strategy as described by *Sanjana et al.* [170]was used. First, the TALE monomers were PCR-amplified with primers (please see ref. [170] for primer sequences) that will later on define the position of the TALE within the TALEN. For this step the primers were used as described in the protocol and the PCR was performed on TALE plasmids

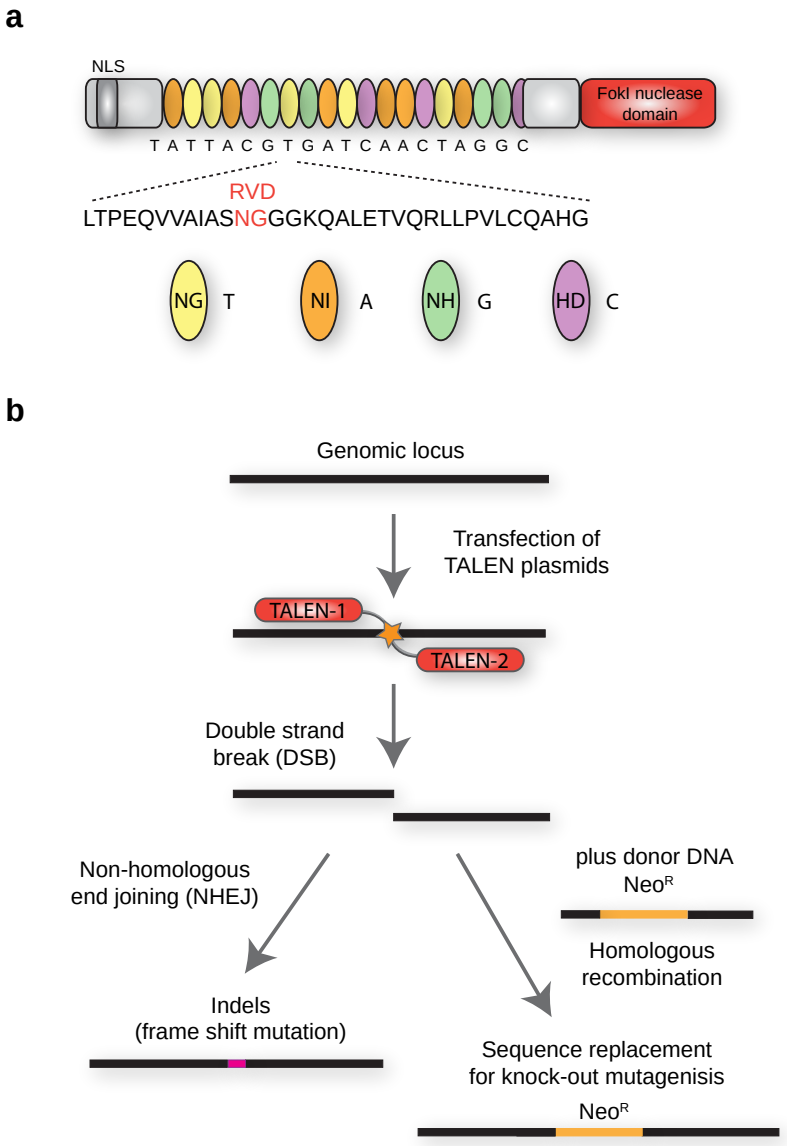

Figure 2.2: **Constructing customized TALENs for genome engineering (a)** The modular structure of the TALENs can be designed for binding a specific target sequence. Each monomer comprises 34 amino acids of which position 12 and 13, termed the repeat variable diresidues (RVD), specifies the bound nucleotide (NG=T, NI=A, NH=G, HD=C). In addition, a nuclear localization signal (NLS) and a FokI endonuclease catalytic domain are fused the N-terminus and C-terminus, respectively. **(b)** Pairwise binding of two TALENs at a target sequence will lead to a double strand break. Error-prone re-ligation of the two end will lead to indel mutations. However, co-transfection with a partially homologous donor DNA can be used to insert larger DNA fragments into the endogenous DNA locus by homologous recombination.

obtained as a gift from Feng Zheng (Addgene plasmids #32180, #32181, #32183, #37527[1]) In a first round, a combinatorial DNA assembly is used to generate 3 hexamers of TALE monomers (see figure 2.3). In this so called Golden Gate assembly PCR-products from a TALE monomer library are combined in a restriction ligation reaction. Thereby, the primers used for monomer PCRs code for the position of the different monomers within the hexamer, since they harbor restriction sites for type IIS endonucleases that will generate unique overhangs used for sequential ligation. Moreover, the last hexamer will ligate to the first one resulting in a circular DNA product that is protected against the following DNA digest. This reduces the occurrences of not completely assembled hexamers which can be isolated by gel extraction.

Golden Gate reaction I		
	1 µl	Tango buffer (10x)
	7.5 units	Esp3I (BsmBI)
	1 mM	DTT
	750 units	T7 ligase
	1 mM	ATP
	15-18 ng	6 different monomer PCR products (each)
	ad 10 µl	ddH_2O

Cycle number	**Digest**	**Ligate**	**hold**
1-15	37°C, 5 min	20°C, 5 min	4°C

DNA digest		
	1 µl	PlasmidSafe reaction buffer (10x)
	10 units	PlasmidSafe DNAse
	1 mM	ATP
	7 µl	Golden Gate reaction
	ad 10 µl	ddH_2O

The DNA digest was performed for 30 min at 37°C and the enzyme was subsequently heat-inactivated at 70°C for 30 min. In the following, the hexamers were again amplified by PCR.

[1]Please note that instead of the originally described NN-monomer binding to the nucleotides guanine and adenine, the improved NH-variant coding specifically for guanine was used.

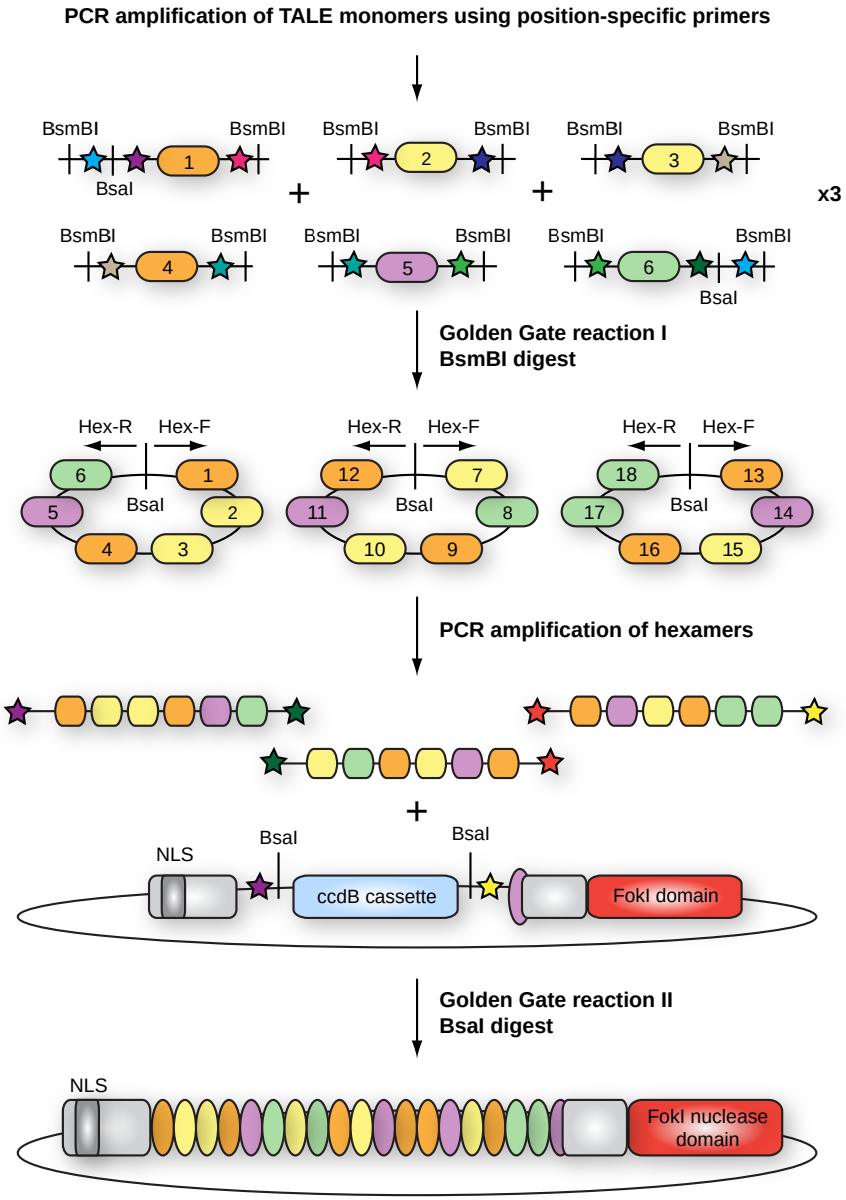

Figure 2.3: **Scheme showing the hierarchical assembly of TALEN monomers by ligation-independent cloning.**

Hexamer amplification		
	10 µl	Herculase II reaction buffer (5x)
	1 mM	dNTPs (each)
	200 mM	Hex-F and Hex-R primers (each)
	1 µl	PlasmidSafe reaction
	0.5 µl	Herculase II Fusion DNA polymerase
	ad 50 µl	ddH_2O

Cycle number	**Denature**	**Anneal**	**Extend**	**hold**
1	95°C, 2 min			
2-36	95°C, 20 s	60°C, 20 s	72°C, 30 s	
37			72°C, 3 min	4°C

The PCR reactions were completely loaded on a 2% gel and the corresponding band of 700 bps is cut out using a scalpel. The DNA was extracted using the NucleoSpin Gel and PCR Clean-up kit (Macherey-Nagel) according to the manufacturer's instructions. The concentration of the DNA was measured with a spectrophotometer.

Golden Gate reaction II		
	1 µl	NEBuffer 4 (10x)
	15 units	BsaI-HF
	1 µml	BSA (10x)
	1 mM	ATP
	750 units	T7 ligase
	100 ng	TALEN backbone [2]
	20 ng	3 different hexamers (each)[3]
	ad 10 µl	ddH_2O

Cycle number	**Digest**	**Ligate**	**Inactivate**	**Hold**
1-20	37°C, 5 min	20°C, 5 min	80°C, 20 min	4°C

. .

The product was used to transform Stbl3 *E.coli* bacteria according to the protocol described in section 2.2.2.4. The transformed bacteria were plated in three dilutions on LB plates with ampicillin. Single clones were picked and the plasmid was

[2]TALEN backbone vectors coding for the last bound nucleotide were a gift from Feng Zhang (Addgene plasmids 32190, 32191, 32192)

[3]replace with water for control reaction

isolated (see section 2.2.2.5) in order to preselect clones by enzymatic test digest with AfeI (3.3, 2.8, 2.1 and 0.2 kbp). Clones with the expected digestion pattern were sent for sequencing with the primers TALE-seq F1/F2/R1. Correct clones were further expanded and DNA was extracted by maxi-preparation as described insection 2.2.2.6.

2.2.3.2 Testing of TALENs with the T7 endonuclease I assay in NIH3T3 cells

In order to evaluate the ability of the TALENs to bind and cut the Lin28a locus in cells a test performed. Therefore, NIH3T3 fibroblasts were seeded in a 6 well and transfected with the TALEN vectors or a control plasmid using Lipofectamine2000 according to the manufacturer's recommendations. After 24 hours the cells were harvested and genomic DNA was extracted (section 2.2.2.7). The genomic region flanking the targeted Lin28a locus was amplified generating a product of about 650 bp (seesection 2.2.2.1). The PCR-products were purified by spin columns and the concentration was measured to set up the following hybridization reaction. 10 units of T7 endonuclease was added to the hybridized DNA and the reaction was further incubated for 1.5 h at 37°C. The samples were loaded on a 2% agarose gel for analysis. Since the T7 endonuclease recognizes non-perfectly matched DNA, the restriction will take place when indel (**in**sertion/**del**etion) mutations have occurred. Since the frequency of those kind of mutations should dramatically increase after several rounds of DNA breakage induced by TALENs, the appearance of two defined cleavage products is expected. Indeed, both TALEN pairs designed for Lin28a targeting resulted in indel mutations at the endogenous locus (2.4), suggesting that the TALENs can effectively bind and cut their target sequence in cells. Although both TALEN pairs showed similar activity in the T7 endonuclease assay, the derivation of Lin28a KO mESC was subsequently only tried with the TALEN pair 1+2 (see results figure 3.33).

Hybridization reaction	3 µl	NEBuffer 2 (10x)
	750 ng	PCR product
	ad 30 µl	ddH_2O

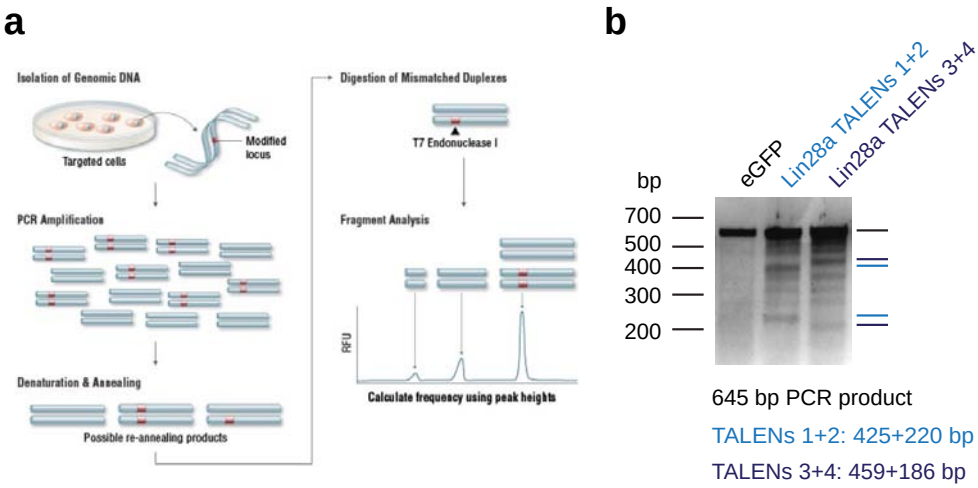

Figure 2.4: **The T7 endonuclease assay for the assessment of the restriction efficiency of TALENs (a)** Scheme showing the principle of this assay. Cells acquire indel mutations after transfection with TALENs. The genomic DNA is amplified, denatured and hybridized again. Hetero-duplex sites caused by the pairing of a WT strand with a DNA that acquired an indel mutation are recognized and cut by the T7 endonuclease. The image was retrieved from *www.neb.com* **(b)** T7 assay in NIH3T3 cells for 2 different Lin28a targeting TALEN pairs 24 hours after transfection. The agarose gel shows that restriction fragments of the expected size were generated using both TALEN pairs.

Cycle number	Annealing	ΔT/s	Hold
1	95°C, 3 min	3°C	
2	85°C, 1 min	0.1°C	
3	65°C, 1 min	0.1°C	
4	55°C, 1 min	0.1°C	
5	45°C, 1 min	0.1°C	
6	35°C, 1 min	0.1°C	
7	25°C, 1 min	2°C	8°C

2.2.3.3 Cloning of the Lin28a targeting construct

The targeting construct was generated for the insertion of a partially homologous DNA fragment at the site of TALEN-mediated DNA restriction. Therefore, two homology arms flanking the TALEN targeted site were amplified from genomic DNA

of mESCs. Both homology arms were designed to cover together about 5000 bp of the endogenous Lin28a locus, however one arm was significantly shorter than the other (1,500 vs. 3,500 bp) in order to facilitate the subsequent PCR screening which has to span at least one homology region (see figure 2.5). Cloning of large DNA fragments by classical step by step restriction and ligation reaction is very challenging due to the need of unique restriction sites and also very time consuming. Instead, ligation independent cloning (LIC) was used to assemble the four components of the targeting vector (5′ and 3′ homology region, Neo^R-cassette and vector backbone) in a single reaction without restriction endonucleases [171]. In this method, about 14 nucleotide long homologous overlapping DNA sequences were introduced into the PCR fragments via the primers. A exonuclease then chewed back one strand of the DNA generating compatible overhangs that will allow directional assembly of several DNA pieces simultaneously. The chew back and assembly was performed using the In-Fusion HD Cloning Kit from Clontech. After assembly, the reaction was not ligated but the nicked plasmid DNA was directly used to transform competent bacteria which will repair the DNA and amplify the plasmid.

5′ HR for	GGT ATC GAT AAG CTT GCT AGC GCT GAT GCC CCT GAA AGC AGG
5′ HR rev	CGT TTG TTC GGA TCC GGT CGT CTG CTG AGC CCG TGG
NeoR for	GGA TCC GAA CAA ACG ACC C
NeoR rev	AAG CTT ACT TAC CAT GTC AGA TCC
3′ HR for	ATG GTA AGT AAG CTT GTT CGA GCT TGC GAT TCA GC
3′ HR rev	TAG TGG ATC CCC CGG TGA TTC TGC CTC CCA AGG GAC ATT T

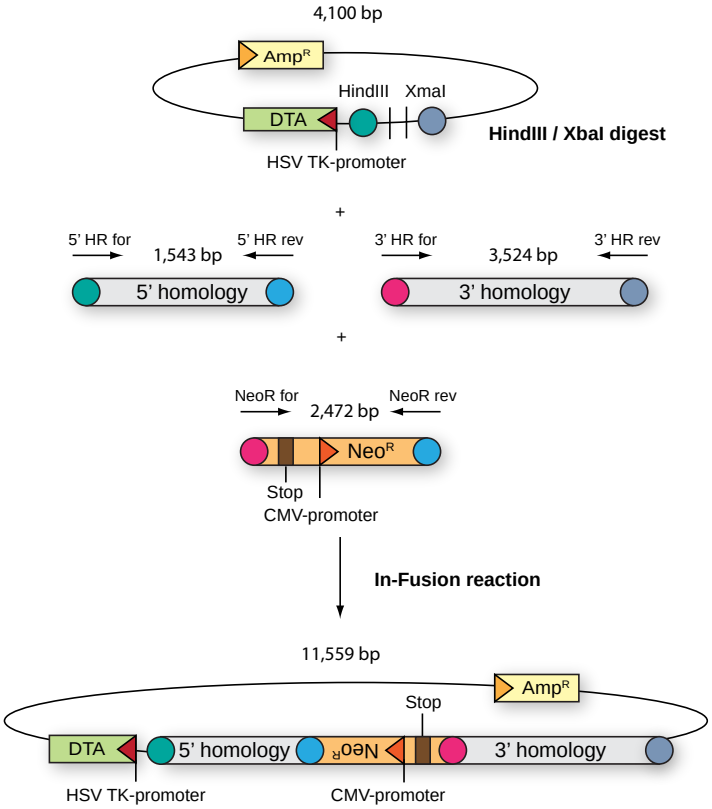

Figure 2.5: **Cloning strategy for the Lin28a targeting construct.** The linearized vector is combined in a so called In-Fusion reaction with the PCR-amplified 5′ and 3′ homology region from the Lin28a endogenous locus and a neomycin resistance cassette harboring an additional SV40 poly-A site. The partial overlaps of the fragments were introduced by the primers and guided the directionality of the ligation.

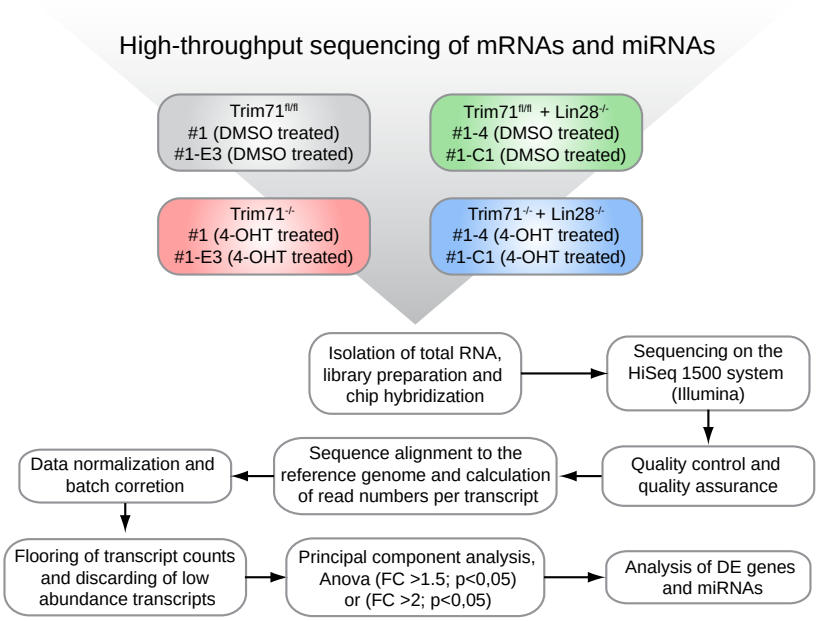

Figure 2.6: **Workflow for the high-throughput sequencing of mRNAs and miRNAs.**

2.2.4 Analysis of mRNA and miRNA expression changes in mESCs by high-throughput sequencing

For a broader analysis of changes on RNA level the different mESC lines were subjected to RNA and miRNA high-throughput sequencing (see figure 2.6). The technical execution as well as the bioinformatic data analysis was performed in collaboration with the lab of Prof. Joachim L. Schultze (Department for Genomics & Immunoregulation, LIMES institute, Bonn). An expanded analysis of the comparison of Trim71$^{fl/fl}$ and Trim71$^{-/-}$ mESC data sets was included in the publication from Mitschka *et al.*, 2015 [172]

2.2.4.1 Generation of cDNA libraries for high-throughput sequencing

TRIzol extracted total RNA from different mESC genotypes was converted into double stranded cDNA for subsequent high throughput sequencing the Illumina TruSeq RNA Sample Preparation Kit v2 was used according to the manufacturer's recommendations. Therefore, mRNA was purified from 100 ng total RNA by poly-T oligo coated magnetic beads with subsequent fragmentation using divalent cations under elevated temperature. The first cDNA strand was generated with annealing

of random hexamer primer in a SuperScriptII- guided RT reaction. Then, the second strand was complemented using DNA Polymerase I and RNase H.

The remaining overhangs were enzymatically removed and the 3'ends of the DNA adenylated to enable ligation of the Illumina PE adapter oligonucleotides. DNA fragments with ligated adapter molecules were selectively enriched and amplified using Illumina PCR primer PE1.0 and PE2.0 in a 15 cycle PCR reaction. cDNA fragments with about 200 bp in length were purified using SPRIBeads (Beckman-Coulter). Size-distribution of cDNA libraries was measured using the Agilent high sensitivity DNA assay on a Bioanalyzer 2100 system (Agilent). cDNA libraries were quantified using KAPA Library Quantification Kits (Kapa Biosystems). After cluster generation on a cBot, a 200 bp paired-end run was performed on a HiSeq1500.

2.2.4.2 RNA-seq preprocessing

After base calling and de-multipexing using CASAVA version 1.8 the 100 bp paired-end reads were aligned to the murine reference genome mm10 from UCSC by TopHat2 version v2.0.11 and Bowtie2 version 2.2.1 using the default parameters. This annotation included 32600 unique transcript entries with genomic coordinates. After mapping of the reads to the genome, we imported the data into Partek Genomics Suite V6.6 (PGS) to calculate the number of reads mapped to each transcript against the RefSeq mm10 annotation download on April 2014. These raw read counts were used as input to DESeq2 for calculation of normalized signal for each transcript [173] using the default parameters. Please note that, although all four analyzed mESC genotypes were sequenced simultaneously, in the subsequent data analyses two normalizations were done: one including all four genotypes and another one only comparing Trim71$^{fl/fl}$ with Trim71$^{-/-}$ mESC. This can lead to slightly different values in the expression count of genes. After DESeq2 normalization, the normalized read counts were imported back into PGS floored by setting all read counts to at least a read count of 1 after the batch-correction. Subsequent to flooring, all transcripts having a maximum over all group means lower than 10 were removed.

After dismissing the low expressed transcripts, the data with the normalization for the Trim71$^{fl/fl}$ and Trim71$^{-/-}$ mESC samples comprised 13,558 transcripts. For this analysis RNA-seq data can be accessed under GSE62398. On the other hand, expression data including all four genotypes yielded significant expression of 13,806 transcripts and data are not yet publicly available.

2.2.4.3 miRNA sequencing

Sequencing of miRNAs was done performed to the manufacturer's recommendations. In brief, 5x10 6 cells were harvested and total RNA including small RNAs was isolated. Small RNA libraries were generated from 500 ng total RNA with the NEBNext Multiplex Small RNA Library Prep Set (New England Biolabs). After successful ligation of the 3' adaptor to RNA molecules, the reverse transcription primer was added before ligation of the 5' adapter. Next, RNA was reverse - transcribed using ProtoScript II Reverse Transcriptase. cDNA was amplified by 15 PCR cycles with high - fidelity LongAmp Taq 2X Master Mix and the respective index primer. The indexed libraries with the size of miRNAs plus ligated adapters were quantified on the Roche LightCycler 480 II qPCR instrument using the KAPA Library Quantification Kit in triplicates, according to the manufacture's protocol (Kapa Biosystems, Woburn, MA, USA). After pooling of equimolar ratios of indexed libraries these were purified on a pre-cast 6% Tris/Borate/EDTA polyacrylamide electrophoresis gel (Invitrogen). Generation of clonal clusters from single molecules of the cDNA library was done with the TruSeq Cluster Kit (Illumina) on a CBot station. Sequencing by synthesis was performed by using the TruSeq SBS Kit on a HiSeq 1500 system (Illumina). Sequencing reads were retrieved as FASTQ files.

2.2.4.4 miRNA preprocessing

After base calling, de-multiplexing and trimming using CASAVA version 1.8 and FLICKR the 50 bp reads were aligned to the murine reference genome mm10 from mirBase v20 87 by Bowtie2 version 2.2.1 using the default parameters. SAMtools version 0.1.18 88 was then used to convert the SAM files into smaller BAM files. T he annotation included 24 . 521 unique transcript entries with genomic coordinates. After mapping of the reads to the genome, we imported them into Partek Genomics Suite V6.6 (PGS). To calculate the number of reads mapped to each transcript we generated a custom annotation file based on the BAM files using the integrated function in PGS. The normalization and post-processing of the data was performed the same way as described for RNA-seq processing. After dismissing the low expressed transcripts the data contained 592 miRNA transcripts. mi RNA-seq data can be accessed under GSE62509.

2.2.4.5 Statistical and descriptive bioinformatics of transcriptome data

A one - way A N alysis Of V A riance (ANOVA) model was performed to calculate the 1.000 most variable and the differentially expressed genes (transcripts) between Trim71$^{fl/fl}$ and Trim71$^{-/-}$ mESCs using PGS. Differentially expressed genes were defined by a fold change (FC) >1.5 or < - 1.5 and a p - value < 0.05. To visualize the structure within the data we performed Principle Component Analysis (PCA) on all genes and hierarchical clustering (HC) on the 1.000 most variable genes, with default settings in PGS, based on p - values according to the expression values of the samples across the conditions. In order to show whether the loss of Trim71 can be verified on the transcript level, read counts were visualized by IGV 89 mapping the aligned reads against the mouse genome (mm10). To identify the differences and similarities between Trim71$^{fl/fl}$ and Trim71$^{-/-}$ mESCs the differentially expressed genes were visualized with SigmaPlot version 12.0 (Systat Software, San Jose, CA) as a ratio - ranked (log_2) plot. The expression of known important ES transcription factors were visualized as a heatmap by Mayday 90. To link differentially expressed genes to known biological functions we used the 166 most differentially upregulated and 216 most downregulated genes in Trim71$^{-/-}$ compared to Trim71$^{fl/fl}$ mESCs in order to generate and visualize a network based on GO - enrichment analysis (GOEA) by using BiNGO [174], EnrichmentMap [175], and Word Cloud [176] in Cytoscape [177].

2.2.4.6 Descriptive bioinformatics of miRNome

A one - way ANalysis Of VAriance (ANOVA) model was performed to calculate the 100 most variable and the differentially expressed miRNAs between Trim71 $^{fl/fl}$ and Trim71$^{-/-}$ mESCs using PGS. Among the 592 miRNA differentially expressed miRNAs were defined by a fold change (FC) >1.5 or < - 1.5 and a p - value < 0.05. To visualize the structure within the data we performed PCA on all miRNAs and hierarchical clustering (HC) on the 100 most variable miRNAs, with default settings in PGS, based on p - values according to the expression values of the samples across the conditions. Me an ratios of differentially expressed miRNAs between Trim71$^{fl/fl}$ and Trim71$^{-/-}$ mESCs were plotted against the maximum abundance. Log_2-transformed read counts of differentially expressed miRNAs were visualized as a heatmap using MayDay. For tissue - related classification, we utilized miRNA-seq data by Chiang *et al .* (2010)[178] who measured the relative miRNA expression in various mouse tissues and developmental stages (ovary, testis, brain, newborn,

ESC, E7.5, E9.5, and E12.5 embryos). miRNAs were further categorized as proposed by Jouneau *et. al.* (2012) [179] by showing mainly expression (>50% of reads) in one of the following categories: mESCs, gonads (ovary and testis), brain, other somatic tissue (newborn, E12.5 , and E9.5). miRNAs not fulfilling these criteria *e.g.* miRNAs with similar expression in all categories, were classified as ubiquitous and not included in the analysis.

2.2.5 Eukaryotic cell culture and cell biological methods

2.2.5.1 Preparation and culture of mouse embryonic fibroblast (MEF) cells

MEFs were isolated from individually processed embryos at E12.5 to E14.5. After dissection from the uterus and placenta, the head and internal organs of the embryos were removed using forceps and the material was used for later genotyping. The remaining parts were washed in PBS and crudely cut into smaller pieces. The material was collected in a new falcon tube containing 5 ml trypsin/EDTA solution. The samples were incubated for 10-15 min at 37°C while occasional pipetting of the solution facilitated cell dissociation. By adding 2 ml FBS the digest was terminated. The mixture was let stand for additional 2 min to allow large pieces of tissue to settle down. The upper phase was transferred to a new tube and the cells were spun down for 5 min at 1,000 rpm. The supernatant was discarded and the cell pellet was resuspended in MEF medium (see below). MEF cells from one embryo were seeded on a 10 cm plates for further cultivation and expansion. When the cells reached confluence they were split in a 1:5 ratio using trypsin. MEFs were cultivated for 3-6 passages were frozen for long term storage when required. For *in vitro* mutagenesis of the floxed Trim71 allele, cells were treated with 500 nM 4-OHT or DMSO as vehicle control for 2 days. Conversion of the conditional allele was subsequently checked by genotyping.

MEF medium	10%	FBS
	1%	Non-Essential Amino Acid Solution (100x)
	1%	GlutaMAX (100x)
	1%	Penicillin-Streptomycin (100x)
	0.1%	2-Mercaptoethanol (50 mM)
	86.9%	DMEM

2.2.5.2 Generation of fetal radial glia-like neural stem cells

The isolation of fetal radial glia-like neural stem cells was performed according to the protocol described by Pollard *et al.* (2006) [180]. In short, a breeding of homozygously floxed Trim71 mice harboring the Rosa26-Cre-ER^{T2} allele was set up and pregnant mice were sacrificed at 14.5 dpc. Fetal forebrains were prepared in ice cold DMEM:F12 media and the cortices were subsequently pooled for centrifugation for 5 min at 1,000 rpm. The supernatant was aspirated and the tissue resuspended in 0.25% trypsin/0.53 mM EDTA in DMEM:F12 to enable tissue dissociation. The samples were incubated for 30 min at 37°C before stopping the digest by centrifugation. The cells were resuspended in NS-A medium (see below) in a density of $3 \cdot 10^6$ cells per 10 cm dish. The cells were incubated for another 5 days or until the cells were forming floating neurospheres. Those cells were collected and plated again on PO/Ln-coated dishes where they were further cultivated as adherent cells. The medium was changed every other day and the cells were regularly passaged by trypsin detachment and plated again on PO/Ln coated plastic dishes.

NS-A medium	80%	EuroMed-N
	18%	DMEM:F12
	1%	N-2 Supplement (100x)
	1%	Penicillin-Streptomycin (100x)

2.2.5.3 Transfection of HEK293T cells wit calcium phosphate

The calcium phosphate method is a well established method for cell transfection based on crystal formation of salt and DNA [181]. The HEK293T cells from an exponentially growing culture were seeded the day before transfection so that they would reach 40-60% confluence the next day. For a 10 cm plate 30 µg of plasmid DNA was solved in 0.5 ml 0.25 M $CaCl_2$ solution. While vortexing, 0.5 ml of HeBS solution (see below) was added. The mixture was then added dropwise to the cells and incubated for 6 hours at 37°C. Subsequently, the cells were washed once with PBS and fresh medium was added. 24 or 48 hours after begin of transfection the cells were harvested for further analysis.

HeBS	0.28 M	NaCl
pH 7.05	0.05 M	HEPES
	1.5 mM	Na_2HPO_4
	ad 50 ml	ddH2O

2.2.5.4 Transfection of TCam-2 cells with siRNA

One day before transfection, $5{\cdot}10^4$ cells were plated per 12-well in 1 ml growth medium. The next day, the medium was changed again and. 2 tubes per well containing each 25 µl Opti-MEM I were prepared. In one of them 5 pmol siRNA or miRNA mimic was solved, whereas in the second tube 1.5 µl Lipofectamine® RNAiMAX was added and mixed by pipetting. Both solutions were combined and after 15 min of incubation at RT, the transfection solution was added drop-wise to the well. The medium was changed again after 6 hours incubation at 37°C. Depending on the used oligos , the cells were further cultivated between 24 and 60 hours and then harvested for analysis.

Oligo name	**Targeted sequence**
Renilla siRNA	AAA CAT GCA GAA AAT GCT G
TRIM71 siRNA#1	CCG TGT GCG ACC AGA AAG TA
TRIM71 siRNA#2	CCA GAT CTG CTT GCT GTG CAA

2.2.5.5 mESC cultivation

Trim71 conditional mESCs were newly derived by crossing of animals homozygous for the floxed Trim71 allele and the Rosa26-Cre-ER^{T2} allele. Blastocysts at stage E3.5 were washed out of the oviducts of pregnant females and digested with trypsin in order to isolate the inner cell mass. The cells were freshly seeded and expanded on irradiated MEFs in mESC medium with the addition of MEK inhibitor PD0325901 (1 µM). Different clones were cultivated individually. After further expansion, the cells were weaned off the MEF cultivation. mESCs were cultivated feeder-free in mESC cultivation medium (see below). The cells were seeded on gelatin-coated plasticware (0.1% gelatin for 20 min). The medium was changed daily and cells were split every other day. In order to induce the conversion of the floxed allele to the knockout allele, cells were treated with 500 nM 4-hydroxytamoxifen or DMSO as a solvent control for 48 hours. If not indicated differently the cells were further cultivated for five days before performing experiments in order to rule out side effects of drug treatment as reported elsewhere[182].

mESC cultivation medium	15%	FBS
	1%	Non-Essential Amino Acid Solution (100x)
	1%	GlutaMAX (100x)
	1%	Penicillin-Streptomycin (100x)
	0.1%	2-Mercaptoethanol (50 mM)
	0.2%	LIF (homemade supernatant)
	81.7%	KnockOut DMEM

2.2.5.6 mESC differentiation procedures

Unbiased EB differentiation of mESCs For unbiased differentiation either the EB model or the monolayer model was used. In the first approach, mESC were detached from the dish using Accutase, washed in PBS and then seeded in a density of 0.5-1·10^6 cells/ml in differentiation medium on non-adherent plastic. This leads to the formation of so called embryoid bodies (EBs) which are spherical ESC aggregates in suspension. The cells in the EB will differentiate into all three germ layers (*i.e.* ectoderm, mesoderm, endoderm). The progress of differentiation depends on the time span of incubation. Samples were taken at the indicated time points and the EB were spun down and washed once in PBS before continuing with RNA or protein extraction.

mESC differentiation medium	10%	FBS
	1%	Non-Essential Amino Acid Solution (100x)
	1%	GlutaMAX (100x)
	1%	Penicillin-Streptomycin (100x)
	0.1%	2-Mercaptoethanol (50 mM)
	86.9%	KnockOut DMEM

Because cells grown as EB are not easily dissociated, for some FACS experiments cells were differentiated by seeding 1·10^5cells in mESC medium on an uncoated 6 cm dish. Next day the medium was replaced with mESC differentiation medium which marks the time point 0. Afterwards the medium changed every other day. Samples were taken by detachment of cells with Accutase®.

Neuroectodermal differentiation of mESCs stimulated by retinoic acid For increasing the efficiency of the derivation of neuroectodermally committed cells mESCs

were first cultivated as EBs for 4 days (see above). Then, cells were dissociated using 2 mM EDTA in HBSS (plus 200 units DNAseI/ml). The cells were centrifuged for 3 min at 1,000 rpm before plating them on poly-L-ornithin /laminin (PLO/LN) coated plastic dishes in differentiation medium additionally containing 0.1 µM retinoic acid (RA). The medium was changed every other day. The cells were harvested after another 4 days of incubation (in total day 8).

Neuroectodermal differentiation by monolayer culture in N2B27 medium As an alternative protocol for neural differentiation, $1x10^4$ cell/cm^2 were seeded on gelatin-coated tissue culture plastic in mESC cultivation medium. The next morning the medium was substituted for N2B27 medium (see below). The medium was changed daily and cells were harvested at the indicated time points for subsequent analysis.

N2B27 medium	0.5%	GlutaMAX (100x)
	1%	N2 Supplement (100x)
	2%	B27 Supplement (50x)
	50 mg/ml	BSA (fraction V)
	1%	Penicillin-Streptomycin (100x)
	47.5%	Neurobasal medium
	47.5%	DMEM/F12

2.2.5.7 mESC transfection

For transfection of plasmid DNA Xfect mES reagent from ClonTech was used according to the manufacturer's instructions. In short, cells were seeded on gelatinized plasticware ($5{\cdot}10^5$-$1{\cdot}10^6$ per 6-well in 1 ml mES culture medium) and let adhere for 5 hours. For each 6 well 5 µg plasmid was solved in 100 µl reaction buffer and mixed with 2,5 µl transfection reagent in 100 µl reaction buffer. After incubating the mix for 10 min at RT the lipid-DNA complexes were added to the cells. Medium was changed again after 4 hours. Depending on the experiment cells were harvested 24-48 hours after transfection.

For experiments performed with siRNAs as well as miRNA analogs and inhibitors, transfections were performed with Lipofectamine® RNAiMAX reagent (Invitrogen). For this purpose, $2\text{-}5{\cdot}10^5$ cells were seeded in a gelatinized 12-well the day before transfection. The next day, 10 pmol of RNA was solved in 50 µl Opti-MEM I. A second solution containing 3 µl Lipofectamine® RNAiMAX in 50 µl Opti-MEM

I was prepared and incubated for 5 min at RT before mixing both solutions. After further incubation for 20 min at RT, the mixture was added to the cells. The medium was changed again after 6 hours. Cells were harvested for analysis about 48 hours post transfection.

2.2.5.8 Luciferase reporter assay

For the 3'UTR activity assays the psiCHECK^{TM}-2 vector system from Promega was used inserting the 3'UTR sequences of murine Tcf15 (NM_009328.2), Plxnb2 (NM_-001159521.2), Foxj1 (NM_008240.3), Inhbb (NM_008381.3), Mras (NM_008624.3), Nanos3 (NM_194059.2), Obscn (NM_199152.3), Prom1 (NM_008935.2) and Trim54 (NM_021447.2) using the restriction sites for XhoI and NotI (see section 2.2.2.2 for primer sequences). Dual-luciferase reporter constructs were transfected into mESCs together with a Trim71 construct or a control plasmid, respectively. Transfection was carried out using Xfect mES reagent from ClonTech in a 24-well plate scale. The amount of total plasmid DNA per well was 750 ng that included 250 ng of firefly reporter DNA and 500 ng of Flag-Trim71 or eGFP as a control. For the analysis of let-7 miRNA activity in mESCs the psiCHECK2-let-7 8x was used which was a gift from Yukihide Tomari (Addgene plasmid # 20931) [183]. Luciferase activities were measured 24 hours after transfection using the Dual Luciferase Assay System (Promega) and the MicroLumatPlus LB96V (Berthold Technologies) according to the manufacturer's instructions. Results are mean ratios of Renilla to Firefly activity normalized to the respective control condition. For some candidate RNAs an effect ratio was determined as the normalized reporter signal without Trim71 and with maximal Trim71 expression (Trim71 knockout versus Trim71 overexpression).

$$RLU_{(x)} = \frac{Renilla_{(x)}}{Firefly_{(x)}}$$

$$norm.\,RLU_{(x)} = \frac{RLU_{(x)}}{RLU_{(vehicle(WT))}}$$

$$effect\,ratio_{(x)} = \frac{norm.\,RLU_{(x(vehicle(KO))}}{norm.\,RLU_{(x(Trim71(KO))}}$$

2.2.5.9 Immunofluorescence staining

For immunofluorescence staining, cells were seeded on poly-l-lysine coated (100 µg/ml) cover slips the day before. The cells were fixed with 4% PFA for 15 min and then carefully washed three times. Subsequently, the cells were permeabilized

to enable antibody penetration using 0.2 Triton X-100/PBS for exactly 10 min. After further washing the cover slips were incubated with 3% BSA/ PBS for 30 min at RT in order to block unspecific epitopes. The primary antibodies were diluted in blocking solution and incubated on the cover slips for either one hour at RT or at 4°C overnight. The cover slips were washed with PBS before adding the fluorescently labeled secondary antibodies corresponding to the species of the primary antibodies. For visualization of the cell nuclei, DAPI (1 µg/ml) was added during secondary antibody incubation. The cover slips were washed again and then mounted on microscope slides using Fluoroshield to which DABCO (0.25% w/v) was freshly added.

2.2.5.10 FACS staining

For staining of surface molecules, 1.10^6 cells were detached using Accutase® and incubated with the fluorescently labeled antibody in FACS buffer (2% FCS in PBS) for 20 min at 4°C. Subsequently, the cells were washed twice in PBS and directly analyzed by flow cytometry.

In contrast, for FACS analysis of intracellular antigens the cells were beforehand permeabilized using the fixation and permeabilization/wash buffers from BioLegend according to the product protocol. All following incubation and washing steps were also performed in permeabilization/wash buffer. The cells were incubated with the primary antibody for 30 min at 4°C and then washed twice before incubation with the fluorescently labeled secondary antibody (30 min 4°C).

2.2.6 Protein biochemistry

2.2.6.1 Preparation of cell lysates and protein quantification

In order to perform protein extraction cells were detached and washed once in PBS. The dry cell pellet was either frozen at -80°C or used for immediate protein preparation. Therefore, the pellet was resuspended in a small volume (20-100 µl) lysis buffer (see below) containing freshly added protease inhibitors. The lysate was incubate for 20 min on ice to ensure complete dissociation of protein complexes. Then, the samples were centrifuged for 5 min at 13,000 rpm to separate the insoluble cellular components. The supernatant was transferred to a new cap and the protein concentration was measured using the BCA assay. This method relies on the change in color of Cu^{2+}-complexes in the presence of cysteine residues. Using a

standard dilution range of known protein content, the measured sample absorption at a wavelength of 562 nm can be related to absolute protein concentrations.

Lysis buffer	10 mM	HEPES
	150 mM	NaCl
	10 mM	KCl
	2 mM	$MgCl_2$
	0.5 mM	EDTA
	0.5% (v/v)	Triton X-100
Protease inhibitors	20 µg/ml	Antipain
	10 µg/m	Aprotinin
	20 µg/ml	Benzamidine
	10 µg/m	Leupeptin
	1:1000	PMSF (saturated solution)

2.2.6.2 SDS-PAGE

SDS-PAGE is a method top separate proteins according to their molecular weight. The use of SDS is essential for this technique since it eliminates the factors of protein structure and charge which might otherwise influence the migration behavior of the proteins. A discontinuous SDS gel was used for all the studies. Thereby the upper stacking gel with a low acrylamide concentration (5%) helps to congregate the proteins in a precise band before reaching the lower phase, the separation gel, where the actual size separation takes place. Depending on the size of the analyzed proteins different acrylamide concentrations ranging from 8-12% were used for the separation gel in order to optimize the resolution. For standard western blot analysis 20 µg of protein were mixed with Laemmli sample buffer and cooked for 5 min at 95°C before loading onto a SDS-PAGE gel. The gel was run in Tris-glycine running buffer for 20 min at 80V and for another 80 min at 120V before proceeding with the blotting.

	Stacking gel (5%)	**Resolving gel (8-12%)**		
	4%	**8%**	**10%**	**12%**
Bidest. water	3.4 ml	2.3 ml	1.9 ml	1.6 ml
1.5 M Tris HCl (pH 8.8)	-	1.3 ml	1.3 ml	1.3 ml
1 M Tris HCl (pH 6.8)	0.63 ml	-	-	-
Acrylamide mix (30%)	0.83 ml	1.3 ml	1.7 ml	2.0 ml
SDS (10%)	50 µl	50 µl	50 µl	50 µl
APS (10%)	50 µl	50 µl	50 µl	50 µl
TEMED	5 µl	3 µl	2 µl	2 µl

Laemmli sample buffer (5x)	100 mM	Tris HCl (pH 6.8)
	20%	Glycerol
	4% (w/v)	SDS
	200 mM	DTT
	1 mg/ml	Bromophenol blue
Tris-glycine running buffer (1x)	25 mM	Tris
pH 8.3	192 mM	Glycine
	0.1% (w/v)	SDS

2.2.6.3 Western blotting and immunodetection of proteins

Using the wet electroblotting technique, the size-separated proteins were transferred from the SDS gel to a nitrocellulose membrane on which immunodetection of specific proteins can be performed. Therefore the gel was placed together with the membrane in a sandwich of Whatman filter papers and sponge pads which was pressed together by a support grid. This was put vertically in a transfer chamber filled with transfer buffer (see below). The transfer was performed under constant voltage of 80 V for 2 hours at 7°C. The nitrocellulose membrane was shortly washed with water and then incubated for 1 hour in 3% BSA/TBST for blocking of unspecific epitopes. The primary antibody was diluted in blocking buffer and incubated for 2 hours at RT or at 4°C overnight. Subsequently, the blot was washed three times for 5 min with TBST before incubation with the HRP-coupled secondary antibody matching to the species of the primary antibody. The membrane was washed again three times. Then the ECL-substrate was pipetted on the membrane and a chemoluminescence film was placed on top for signal detection. The exposure time

typically ranged between 0.5 to 30 min depending on the signal intensity. For regeneration (stripping) of the membrane, the blot was incubated in stripping buffer for 15 min at 150°C. Afterwards, the membrane was extensively washed, before beginning again with blocking.

Transfer buffer (1x)	192 mM	Glycine
	25 mM	Tris
	20% (w/v)	Methanol
	0.002% (w/v)	SDS
TBST (1x)	50 mM	Tris
pH 7.6	150 mM	NaCl
	0.05%	Tween-20
Stripping buffer (1x)	62.5 mM	Tris HCl (pH 6.8)
	2% (w/v)	SDS
	100 mM	2-Mercaptoethanol

2.2.6.4 Co-immunoprecipitation

Co-immunoprecipitation was performed in mESCs and HEK293T cells after overexpression of tagged proteins. The cells were harvested 24 h after transfection and protein lysates were prepared according to the description in 2.2.6.1. A BCA assay was performed to measure protein concentration and the samples were adjusted to final protein concentration of 1-2 µg/µl. 20 µg of the sample was used as input control. Equal amounts of protein was mixed with equilibrated Protein A coupled Dynabeads® (Life Technologies) for capturing IgG-fusion proteins, or with Anti-FLAG® M2 Magnetic Beads (Sigma) for FLAG-tagged proteins, respectively. The lysate-bead mixture was incubated for 2 h on a rotating wheel at 4°C. Then the beads were washed five times with lysis buffer using a magnetic stand to separate the beads from the liquid. For some experiments, lysates were additionally treated with RNaseA. For RNA digest 200 µg/ml RNaseA was added to the first washing solution and the lysates were incubated for 20 min at 37°C. After the final washing step, the beads were resuspended in 1.5 x concentrated protein loading buffer and cooked for 5 min at 95°C.

3 Results

3.1 The generation of a new conditional mouse model for Trim71

The role of Trim71 has been mostly investigated in the context of embryonic development. Therefore, we used the characterization of Trim71 expression and function during mouse embryonic development as a starting point for our investigation before exploring other systems. We analyzed the expression pattern of Trim71 mRNA at different time points in wildtype embryos using whole mount *in situ* hybridization staining. At the earliest investigated stage, E7.5, Trim71 was found to be ubiquitously expressed (figure 3.1) in the whole embryo. At E8.5, Trim71 expression became more restricted and was found to be especially high in the neural folds which constitute the precursor structure of the central nervous system. At E9.5 and E10.5, Trim71 expression was mainly found in the facial prominence, the neuroepitheleum, the branchial arches and the developing limb buds. Starting from E11.5 Trim71 expression generally decreased except for the mid-hindbrain region and the limb buds. Taken together, Trim71 was abundantly expressed in early embryonic development but became more restricted at later stages with longer lasting expression in the central nervous system and the developing limbs.

For the investigation of the full Trim71 knockout phenotype, mice bearing the new Trim71 conditional allele were crossed with mice expressing the Cre recombinase under the control of the ubiquitously active PGK promoter [158], thereby generating a Trim71 knockout allele (figure 3.2a). Trim71 heterozygous animals were subsequently used for further breeding. The average number of born pubs per litter was smaller in heterozygous intercrosses than in matings of the parental strain (figure 3.2b). In addition, genotyping of the adult offspring revealed that 63% of animals were again heterozygous for the mutated Trim71 allele and 37 % were wildtype. We never found any living homozygous Trim71 mutant mice which led us to conclude that homozygous Trim71 knockout animals did not survive until birth. Therefore, embryos of heterozygous intercrosses were prepared and geno-

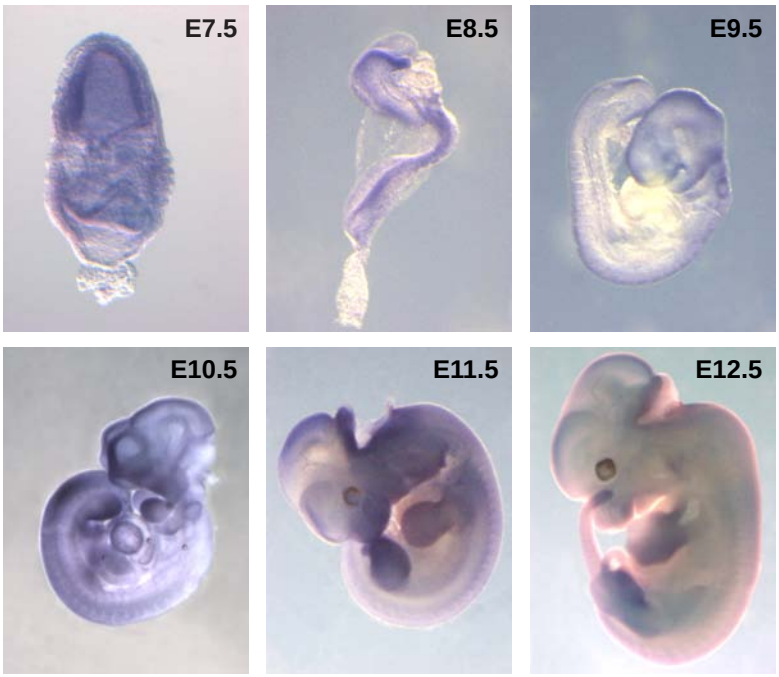

Figure 3.1: **Trim71 is prominently expressed in the developing central nervous system and the limb buds.** Whole mount *in situ* hybridization analysis of wildtype embryos at the indicated embryonic stages using a probe complementary to the Trim71 mRNA.

typed at several developmental stages. While at E7.5 Trim71 knockout embryos were still found at the expected Mendelian ratio (about 25%), the number of homozygous Trim71 mutant embryos started to decrease from stage E9.5 (figure 3.2b). We never found living embryos after E13.5, indicating that Trim71 deficiency led to lethality during embryonic development with 100% penetrance. The morphological analysis of embryos performed by Tobias Goller revealed that in E9.5 Trim71 mutant embryos the anterior neural tube did not close (figure 3.2d). Also at later stages of development the neural folds failed to fuse resulting in an exencephalus phenotype in all investigated Trim71 mutant embryos (figure 3.2d). In contrast, the posterior neural tube closed properly. Furthermore, starting from E10.5 Trim71 mutant embryos additionally exhibited a general and severe growth retardation. Notably, heterozygous Trim71 embryos did not display any visible abnormalities during development (data not shown).

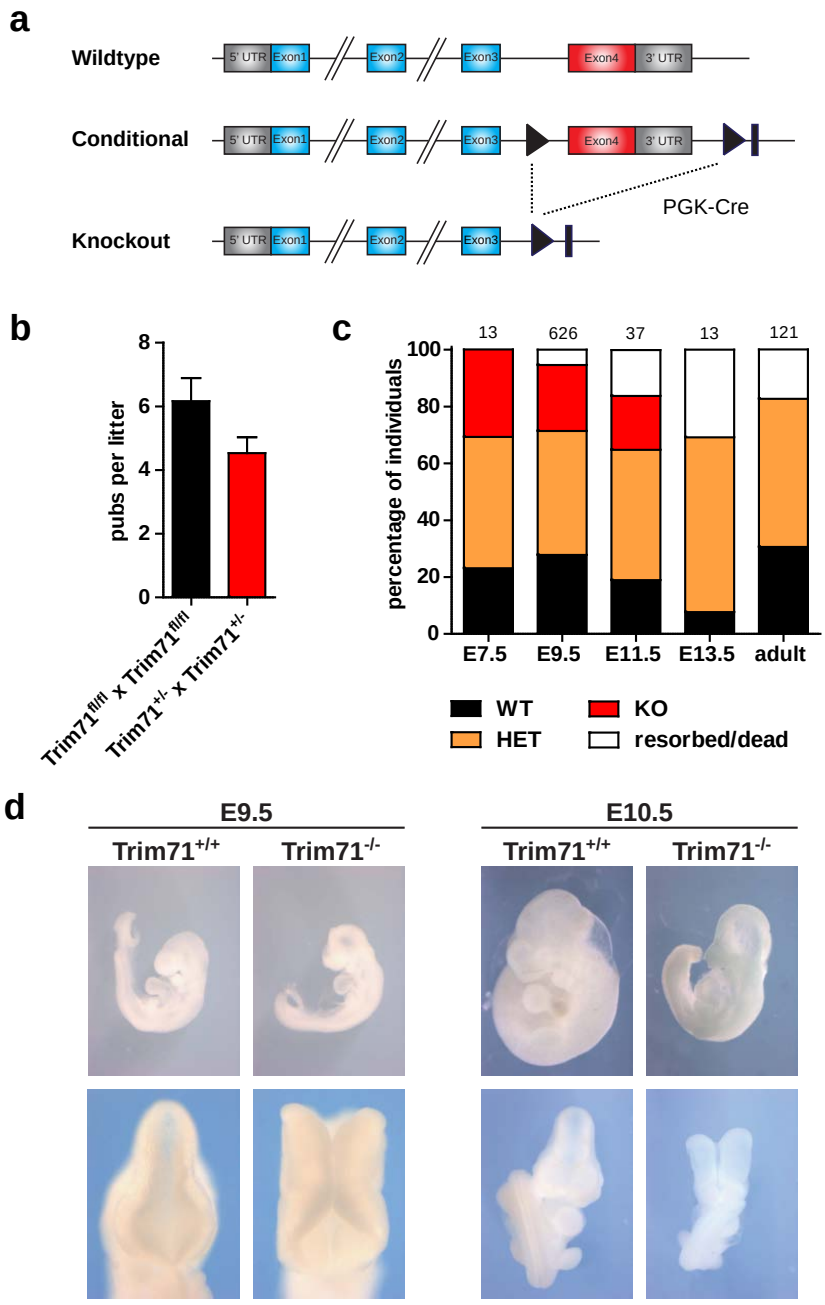

Figure 3.2: **Homozygous mutation of Trim71 leads to embryonic lethality in mice. (a)** Scheme of the Trim71 locus in wildtype, conditional and knockout state. **(b)** Average litter size of heterozygous intercrosses is smaller than in control mouse breedings (mean+SEM; n=10). **(c)** Genotyping statistics of embryos from heterozygous intercrosses. Numbers above the bars indicate the number of analyzed animals. **(d)** Comparison of wildtype and knockout Trim71 embryos at developmental stages E9.5 and E10.5. Homozygous Trim71 mutant embryos exhibit a neural tube closure defect and growth retardation. Upper panel lateral view, lower panel dorsal view on headfolds (30 and 75 x magnification, respectively). Embryos were dissected and pictures were taken by Tobias Goller. Figure modified from Mitschka *et al.*, 2015[172].

Considering the severe phenotype of homozygous Trim71 knockout in mice leading to embryonic lethality, the question arose whether also heterozygously targeted Trim71 mice display phenotypes. Indeed, we found that both adult male and female heterozygous mice weighed significantly less than their wildtype littermates (figure 3.3a-b). The lower body weight correlated with a significant reduction of the nose-rump-length of heterozygously targeted Trim71 mice (figure 3.3c). In order to investigate the course of postnatal development, we monitored the weight gain of newborn wildtype and heterozygous mice from week 4 to 15. Again, Trim71 heterozygous individuals from both sexes were in average 15% lighter than their wildtype littermates at any given time point (figure 3.3d). This difference in weight was also not restored in older mice, however this did not result in a reduced viability of heterozygous mice in the course of one year (data not shown).

Next, we measured the weight of several organs relative to the body weight of adult wildtype and heterozygous Trim71 mutant mice. The results for heart, kidney and testis obtained from 10-14 week old male mice are depicted in figure 3.3e. Whereas kidney and heart showed a normal organ weight in relation to the reduced body weight, the testes of male mice were significantly smaller in Trim71 heterozygous males in comparison to their wildtype littermates. In parallel, samples from the different organs of adult wildtype and heterozygous mice were taken to examine Trim71 mRNA expression by RT-qPCR. This analysis revealed that Trim71 expression was undetectable in kidney and heart while there were significant amounts of Trim71 mRNA in whole testes samples (figure 3.3f). The amount of Trim71 mRNA detected in testes of Trim71 heterozygous males was half of the amount found in wildtype animals, suggesting that both alleles need to be functional to yield normal Trim71 mRNA expression. These finding supported the notion that the reduced testis size observed in Trim71 heterozygous male mice was indeed caused by organ intrinsic mechanisms.

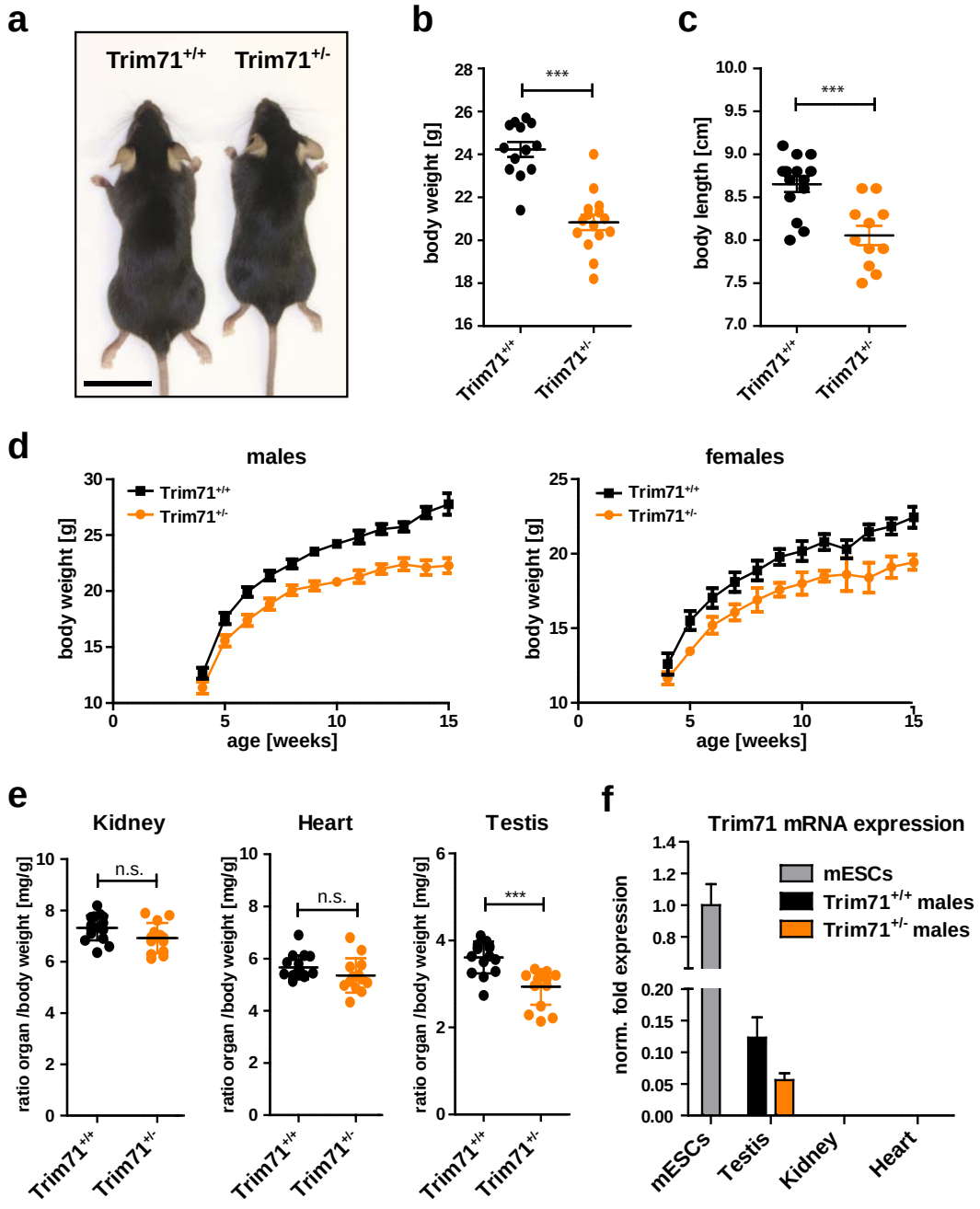

Figure 3.3: **Heterozygous deletion of Trim71 leads to persistent growth retardation and male Trim71 exhibit a reduced testis size. (b)** Representative images of an adult male wildtype mouse and its Trim71 heterozygous littermate (bar = 2 cm). Body weight **(b)** and body length **(c)** of 10 week old males (mean+SEM; Student's t-test; n=11-15; *** p<0.001). Error bars represent SEM. **(d)** Growth curves for Trim71 wildtype (black) versus heterozygous (orange) mice. Both male (left) and female (right) mice show a reduced body weight (mean+SEM; n=3-15; *** p<0.001). **(e)** Relative organ weights of kidney, heart and testis in Trim71 wildtype (black) versus heterozygous (orange) mice (Student's t-test; n=15-16) **(f)** Trim71 mRNA expression levels in testis, kidney and heart normalized to wildtype mESCs (mean +SEM; n=3).

3.2 *In vitro* mutagenesis of Trim71 as a versatile tool for investigating protein functions

We and others have shown that Trim71 is abundantly expressed during embryonic development with a temporally and spatially restricted expression pattern. However, the investigation of protein functions in the embryonic organism is difficult and a complementary *in vitro* system is needed to answer basic cell biological questions. Mouse embryonic stem cells (mESCs) are the *in vitro* equivalent of the inner cell mass (ICM) of an early blastocyst and they were shown to endogenously express high amounts of Trim71 [153, 152, 156]. Cultured mESCs retain the capacity to form all cell types of the adult organism and are thus a very versatile tool for the investigation of lineage determination and differentiation. To ascertain the importance of Trim71 for mESC functions and to identify key biological processes that are controlled by Trim71, we established a genetic model for inducible Trim71 ablation by generating mice carrying floxed Trim71 alleles plus the Cre-recombinase-oestrogen-receptor-T2 (Rosa26 CreER^{T2}) allele. Mice, homozygous for both alleles were crossed and the blastocysts were extracted from the oviducts of pregnant female mice at embryonic stage E3.5. The blastocysts were digested with trypsin to isolate the ICM (see figure 3.4a). These cells were propagated on feeder cells and further expanded. The derived mESC clones were later on weaned off the feeder culture and cultured on gelatinized plastic dishes.

The expression of the CreER^{T2}transgene in Trim71$^{fl/fl}$ mESCs allowed the mutation of the Trim71 allele *in vitro.* In this system, the treatment with the hormone-like drug hydroxy-tamoxifen (4-OHT) induces the shuttling of the Cre recombinase to the nucleus leading to the looping out of the loxP flanked exon four of the Trim71 gene (figure 3.4b). The success of the deletion was subsequently monitored by genotyping of the Trim71 genetic locus, revealing an efficient conversion of the floxed allele to the knockout allele already after 48 hours of 4-OHT treatment (figure 3.4c). Accordingly, the expression of Trim71 mRNA was almost completely lost when using a primer pair binding to exon four (figure 3.4d). Notably, we also observed a reduction of the remaining 5′ mRNA by about 50% in comparison to DMSO-treated control cells. This indicated a destabilization of the Trim71 mRNA after deletion of exon four containing a part of the coding sequence as well as the entire 3'UTR. In line with this, the Trim71 protein content decreased following 4-OHT-treatment as assessed by western blot analysis and almost no Trim71 protein could be detected after 48 hours of 4-OHT treatment (figure 3.4e).

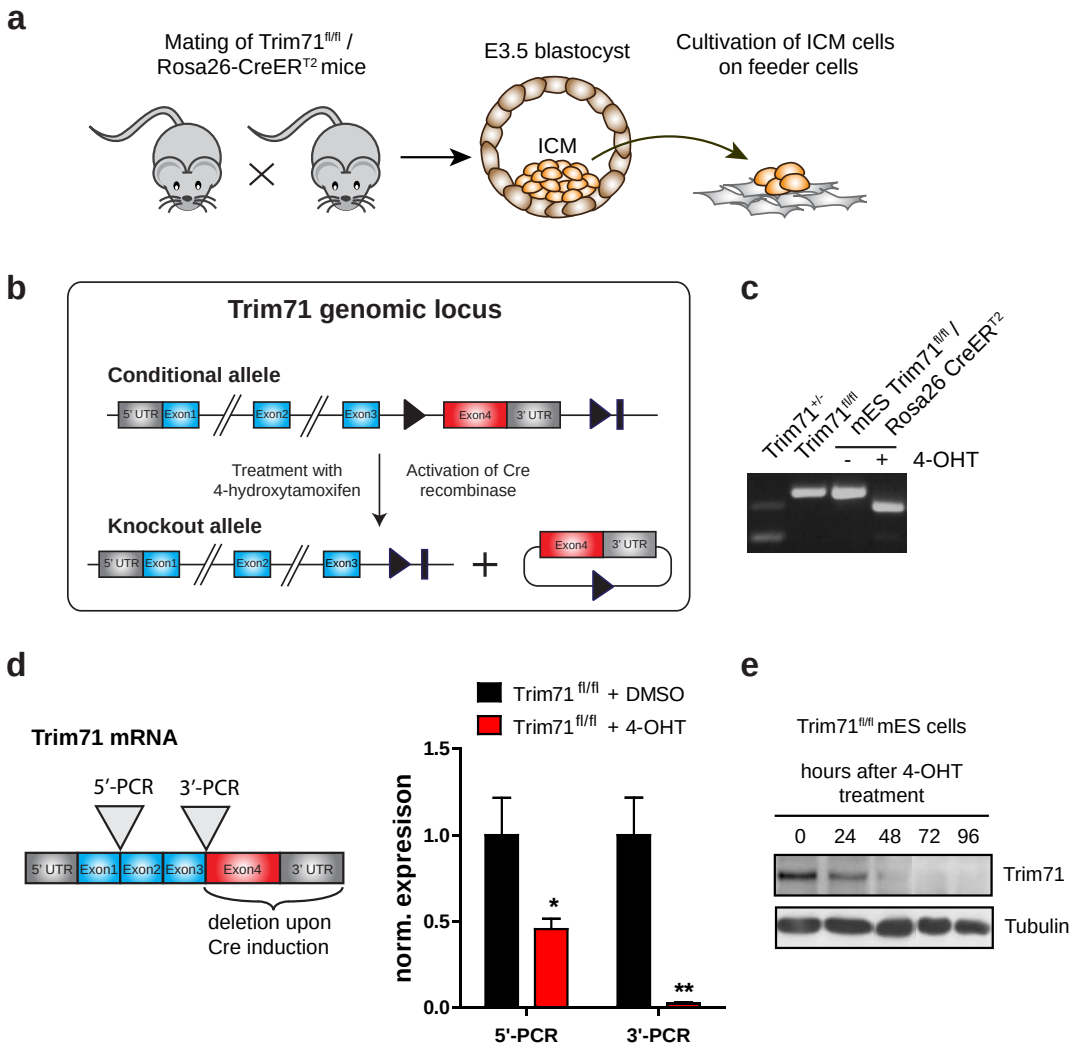

Figure 3.4: **Derivation of conditional Trim71 mESCs from mouse blastocysts. (a)** Mice with homozygously floxed Trim71 alleles and the Rosa26 CreER^{T2} locus were crossed and the inner cell mass of E3.5 blastocysts was taken into culture. **(b)** Application of the drug tamoxifen (4-OHT) induces Cre recombinase activation and deletion of the loxP flanked fourth exon of Trim71. **(c)** The efficiency of recombination was evaluated by genotyping PCR. **(d)** Analysis of knockout efficiency and stability of the remaining mRNA after 4-OHT treatment by RT-qPCR. Values are means +SEM normalized to the respective DMSO treated sample (Student's t-test; n=6-9; * $p<0.05$; ** $p<0.01$) **(e)** WB analysis of Trim71 expression at different time points after beginning with 4-OHT treatment reveals fast protein turnover and high knockout efficiency of Trim71 in mESCs. Figure modified from Mitschka *et al.* 2015 [172]

This rapid loss of protein expression indicated a high Trim71 protein turnover in undifferentiated mESCs. Taken together, our conditional mESCs system proved to be suitable for fast and efficient *in vitro* deletion mutagenesis of the Trim71 gene.

3.2.1 Trim71 is not required for the maintenance of stemness and proliferation in undifferentiated mESCs

When comparing undifferentiated Trim71$^{fl/fl}$ and Trim71$^{-/-}$ mESCs, no differences were observed concerning the morphology in steady-state culture. Cells of both genotypes were similarly able to form characteristic mESC colonies when grown on gelatin-coated plastic dishes (see figure 3.5b). In order to further investigate the stem cell qualities of Trim71-deficient cells, a SSEA-1 surface staining was performed to measure the proportion of undifferentiated cells. We found that the frequency of SSEA-1-positive cells was not significantly different in Trim71-deficient mESCs and control cells (figure 3.5c). Furthermore, a RT-qPCR analysis of a set of well-established stem cell transcription factors revealed equal marker expression in Trim71$^{fl/fl}$ and Trim71$^{-/-}$ mESCs (figure 3.5d). Since another study had reported that mESCs exhibit a decreased proliferation rate after Trim71 knockdown [153], we also monitored the increase in cell number over time. However, in contrast to the previously mentioned study, we did not detect an altered steady-state proliferation of Trim71$^{-/-}$ mESCs in comparison to control cells (figure 3.5e). Thus, we concluded that the maintenance of stemness including the proliferation capacity was not impaired in Trim71$^{-/-}$ mESCs.

3.2.2 Trim71 deficiency enhances neural differentiation

As shown above, Trim71 is highly expressed in early stages of embryonic development, however, Trim71 knockout phenotypes are only apparent at later stages of development and defined regions. This suggests that Trim71 deficiency mostly affects differentiation decisions in specific tissues. It was shown that Trim71 knockout leads to premature differentiation of neural progenitor cells *in vivo* which is accompanied by a decreased proliferation [151]. Therefore, we hypothesized that Trim71 might likewise regulate the timing of differentiation after stimulation *in vitro*.

To test this assumption, cells were seeded in low density on gelatin-coated plastic and subsequently the medium was substituted with serum-free N2B27 medium without LIF to initiate neural differentiation in a monolayer culture. Samples were taken for RT-qPCR analysis at regular intervals to monitor differentiation kinetics.

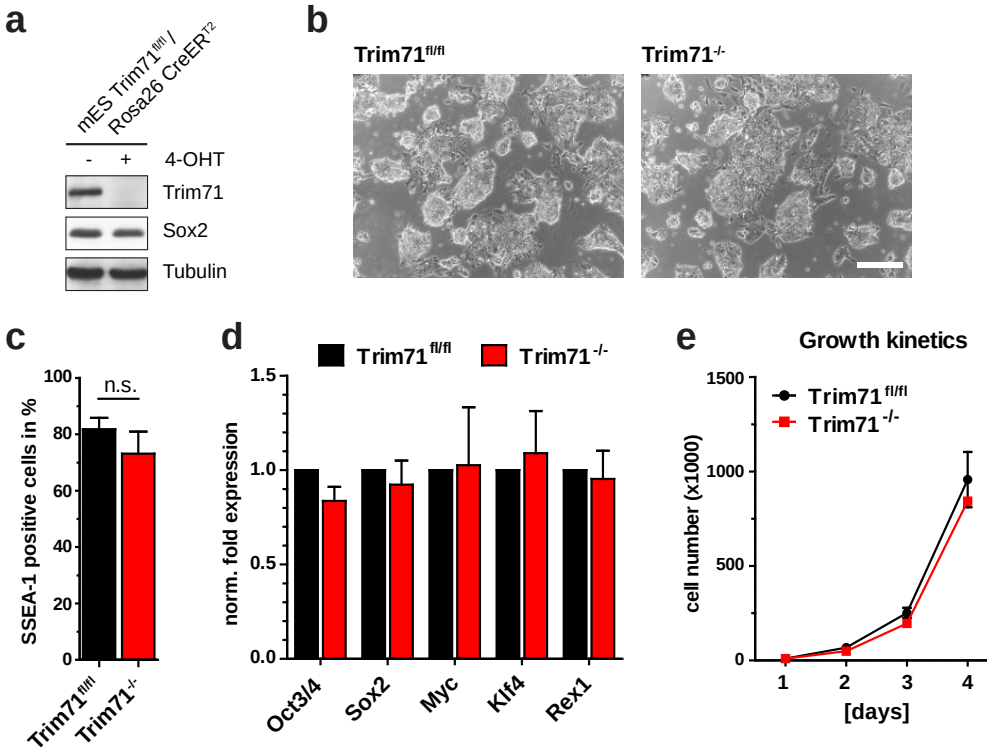

Figure 3.5: **Trim71-deficient cells were able to maintain stemness. (a)** WB showing complete absence of Trim71 protein in 4-OHT treated cells which were still retaining expression of the stem cell marker Sox2. **(b)** Trim71-deficient cells exhibited a mESC-typical morphology (scale bar represents 200 µm).**(c)** Surface expression of the SSEA-1 was not significantly altered upon Trim71 knockout (mean +SEM; Student's t-test; n=5; n.s not significant). **(d)** The mRNA expression of stemness factors was not altered in Trim71 knockout mESCs in comparison to control cells. Values are normalized mean +SEM (n=3). **(e)** Analysis of proliferation in $Trim71^{fl/fl}$ and $Trim71^{-/-}$ cells during four days of culture (representative experiment with three technical replicates). The figure was modified from Mitschka *et al.* 2015 [172]

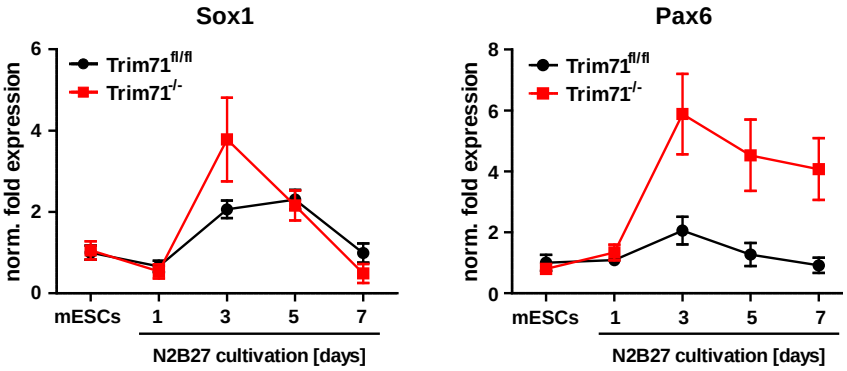

Figure 3.6: **Trim71 deficiency enhanced neuroectodermal marker gene expression upon N2B27 stimulation.** Trim71$^{fl/fl}$ and Trim71$^{-/-}$ mESCs were differentiated for 7 days in N2B27 medium and analyzed for Sox1 and Pax6 expression at different time points by RT-qPCR. Data were normalized to marker levels in Trim71$^{fl/fl}$ cells in undifferentiated state (mESCs) and represent mean +SEM of 4 independent experiments. Figure modified from Mitschka *et al.* 2015 [172]

We analyzed the expression of the transcription factors Sox1 and Pax6, which are the earliest markers expressed in mouse and human neuroectoderm, respectively [184, 185, 186]. Notably, the basal expression levels of both markers were comparable in undifferentiated Trim71-deficient compared to control mESCs figure 3.6. In control cells, both marker genes displayed a characteristic increase of expression after induction of differentiation with a peak expression at day 3. However, we found that the peak expression of Sox1 was higher in Trim71$^{-/-}$ cells than in control cells, while the expression kinetics were similar in both cell types at later time points. Also for Pax6 the peak expression at day 3 was found to be elevated, but in contrast to Sox1, the expression was steadily elevated and failed to decrease afterwards. These results indicated that the differentiation into the neuro-ectodermal lineage was enhanced in Trim71-dificient mESCs

We also tested an alternative approach for induction of neural differentiation. This time, cells were cultured for 4 days as embryonic bodies (EB) in the absence of LIF and subsequently plated on poly-l-ornithine/laminin coated plastic in medium supplemented with 0.1 µM retinoic acid (RA). After 8 days of differentiation the cells were harvested and subjected to marker expression analysis by RT-qPCR. In the panel of investigated neuroectodermal marker genes, Sox2 was the only gene that showed equal expression in Trim71-deficient and control cells 3.7. Of note, Sox2 is known to be continuously expressed from the undifferentiated ESC-state to neuroectodermal differentiating cells, whereas it is downregulated in non-

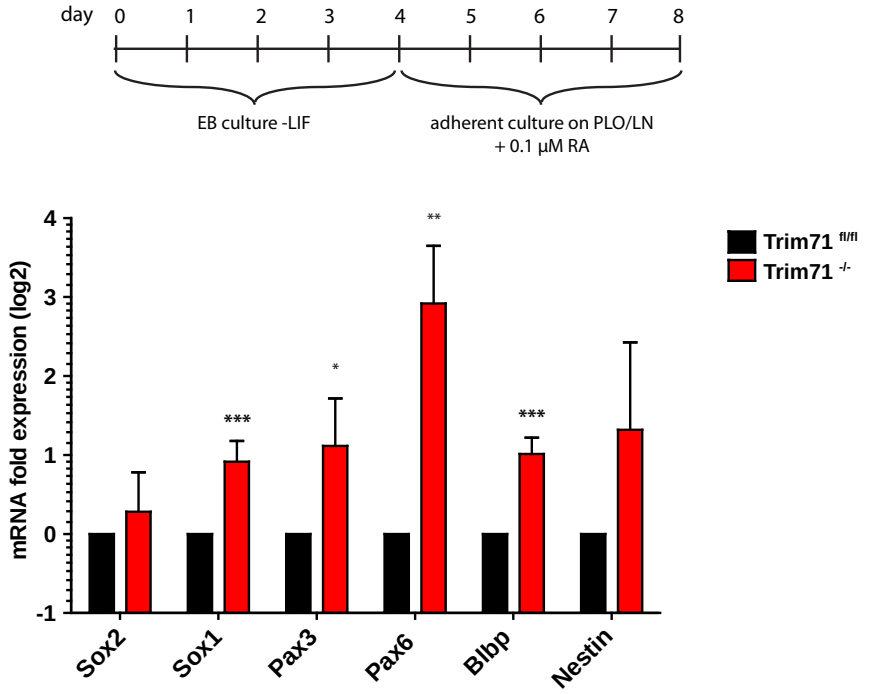

Figure 3.7: **Trim71 deficiency enhances neuroectodermal marker gene expression after stimulation with RA.** Time course of RA-stimulated neural differentiation of Trim71$^{fl/fl}$ and Trim71$^{-/-}$ mESCs. Data were normalized to respective marker gene expression levels in Trim71$^{fl/fl}$ cells and represent mean +SEM of 4 independent experiments (Student's t-test with * p<0.05, ** p<0.01, *** p<0.001). Figure modified from Mitschka *et al.* 2015 [172]

ectodermal differentiating cells [187, 188]. In contrast, the other markers were specifically upregulated in neuro-ectodermally differentiating Trim71$^{-/-}$ cells. Also the early markers Sox1 and Pax6 were significantly upregulated. The same holds true for the transcription factor Pax3 and the metabolic protein BLBP of which the expression was enhanced in Trim71-deficient cells. With respect to the neuro-specific filament protein Nestin we have encountered the highest inter-assay variability of all tested markers. Nevertheless, a tendency for a higher expression in Trim71-deficient cells was clearly detected.

It must be taken into account that differentiation protocols are usually not efficient enough to differentiate all cells of a sample preparation into the designated cell lineage. Hence, working with these dynamic cell systems remains challenging. Because it was proposed that Trim71 would help to maintain neural progenitor cells *in vivo* [151], we next aimed to extract a late neural stem cell population from conditional Trim71animals for propagation *in vitro*. Radial glia (RG)-like stem cells from the neocortex of E14.5 embryos were extracted and further cultured *in vitro* with addition of FGF2 and EGF. Due to the advanced differentiation state of these cells, the expression of the Trim71 upstream-regulating miRNA let-7 was increased in RG-like cells in comparison to undifferentiated mESCs (figure 3.8a). The opposite was true for the expression of the ESC-specific cell cycle regulating (ESCC) miRNAs miR-294 and miR-302. The treatment of conditional Trim71 RG-like neural stem cells with 4-OHT resulted in efficient conversion of the Trim71 floxed allele to the knockout allele (figure 3.8b). RG-like stem cells of both genotypes were morphologically indistinguishable (figure 3.8c). However, WB analysis of Trim71 revealed that neither floxed nor knockout RG-like cells expressed detectable amounts of Trim71 protein (figure 3.8d). In line with this, the mRNA expression of Trim71 was only about 5% of the level detected in wildtype mESCs. Accordingly, Trim71$^{-/-}$ RG-like cells were not affected by loss of Trim71 and protein expression of the neural marker genes Tuj-1 and Sox2 was unaltered.

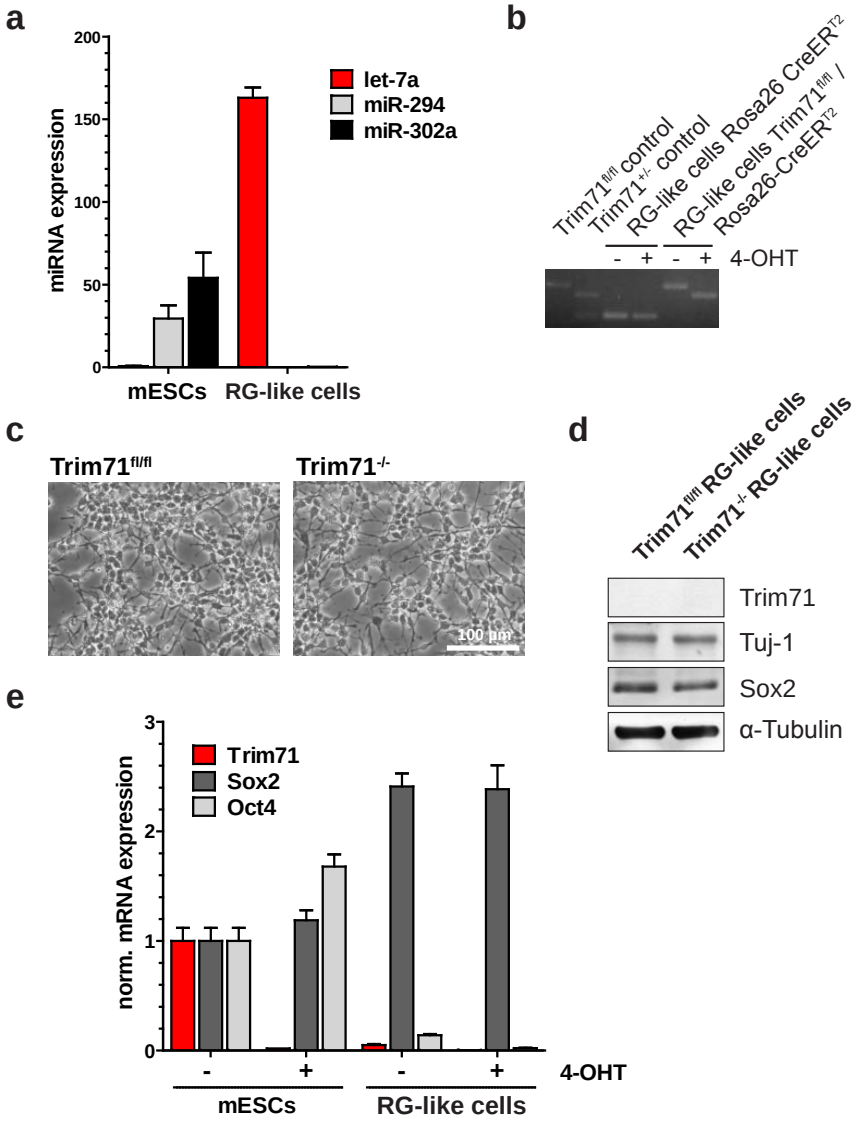

Figure 3.8: **The expression of Trim71 is lost at later stages of embryonic neurodevelopment. (a)** Primary RG-like stem cells were isolated from Trim71$^{fl/fl}$ /Cre-ER^{T2} embryos at stage E14.5. The expression of let-7a as well as cells the expression of ESCC miRNAs miR-294 and miR-302a was analyzed in comparison to mESCs. **(b)** Genotyping PCR showing the conversion of the floxed Trim71 allele to the deleted allele in RG-like stem cells after 48 hour treatment with 250 nM 4-OHT. DMSO treated cells and wild-type Trim71 cells with Rosa26-CreER^{T2} background served as a control. Upper band: floxed allele; middle band: knockout allele; lower band: wild-type allele. **(c)** No morphological changes were observed after 4-OHT treatment. Scale bar represents 100 µm. **(d)** RG-like neural stem cells do not express the Trim71 protein any longer, therefore the deletion has no effect on the protein expression of typical neural stem cell markers such as Sox2, Tuj-1. **(e)** RT-qPCR confirming massive downregulation of Trim71 mRNA in RG-like stem cells in comparison to mESCs (mean+SEM, n=3). Figure modified from Mitschka *et al.* 2015 [172]

3.2.3 Loss of Trim71 in undifferentiated mESCs leads to changes in gene expression

Although we did not detect any impairments regarding the principal stem cell characteristics of Trim71-deficient undifferentiated mESCs, we observed enhanced neural differentiation after stimulation. Hence, we were interested whether mESCs could be predisposed for neural differentiation. Two recently published studies found that Trim71 might act as an RNA-binding protein (RBP) in mESCs [152, 70], suggesting that Trim71 is directly or indirectly involved in expression regulation of specific target genes. In order to obtain an overview of the changes in gene expression in Trim71-deficient mESCs in comparison to the parental cell line, we performed a global transcriptome analysis in collaboration with the lab of J. L. Schultze at the LIMES institute. For this purpose, Trim71 $^{fl/fl}$ and Trim71$^{-/-}$ were sorted for the surface expression of the stemness marker SSEA-1 to remove any spontaneously differentiating cells in culture. The extracted total RNA was subjected to cDNA synthesis with subsequent high-throughput sequencing. After alignment of the sequences to the reference genome and data normalization 13,558 different gene transcripts were found to be expressed above background level. A principal component analysis (PCA) showed that the biological replicate samples of each genotype clustered together, whereas the Trim71-deficient and control mESCs showed a clearly distinguishable global gene expression profile (figure 3.9a and b). Furthermore, alignment of sequence reads from Trim71$^{-/-}$ mESCs to the genomic locus of Trim71 verified the absence of transcripts originating from exon four (see figure 3.9c). Although there was remaining expression detected originating from the other exons, the total Trim71 signal was reduced by almost 80% in comparison to control cells. Thus, Trim71 was among the top five downregulated genes in our data set, proving the accuracy and reliability of the RNA-seq analysis. By using one-way ANOVA, we next identified differentially expressed (DE) genes with a calculated fold change (FC) of $\leq$1.5 or $\geq$-1.5 and a p-value of p$\leq$0.05. Applying these criteria, we determined 166 up- and 216 downregulated genes in undifferentiated Trim71 $^{-/-}$ mESCs, respectively (figure 3.9d and Appendix).

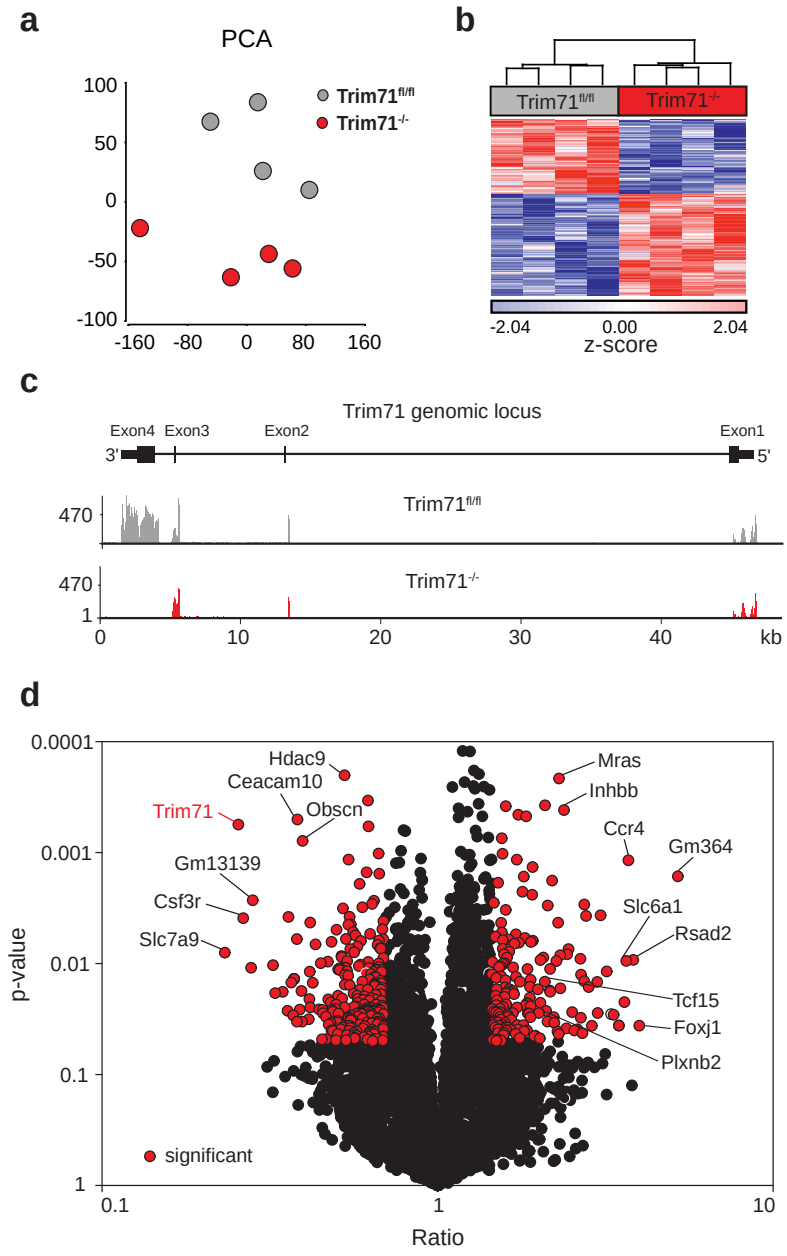

Figure 3.9: **Transcriptome analysis of Trim71$^{fl/fl}$ and Trim71$^{-/-}$ cells reveals changes in the mRNA expression landscape.** **(a)** Principal component analysis (PCA) of replicate samples from Trim71$^{fl/fl}$ and Trim71$^{-/-}$ mESCs. **(b)** Dendrogram depicting the hierarchical clustering of the top 1,000 differential z-transformed expression values. **(c)** Distribution of sequencing reads across the genomic locus of Trim71 in one Trim71$^{fl/fl}$ and one Trim71$^{-/-}$ mESC sample verified deletion of the fourth exon in 4-OHT treated cells. **(d)** Volcano plot showing expression ratio and p-value of all analyzed genes. Red dots mark DE genes with $|FC| \leq 1.5$ and $p \leq 0.05$. Data analysis and figures were done by Thomas Ulas (AG Schultze). Figure modified from Mitschka *et al.* 2015 [172]

In order to predict which biological functions were majorly affected by the gene expression changes observed in Trim71$^{-/-}$ mESCs, DE genes were subjected to gene ontology - enrichment analysis (GOEA). This analysis lists the biological terms (GO terms) used to describe a given selection of genes and identifies overrepresented GO terms in comparison to the statistically expected outcome. The data were visualized by connecting gene hubs according to their functional relation using different Cytoscape plug-ins [174, 175, 176, 177], thus creating a network of Trim71 regulated genes (figure 3.10). In this network map two clusters of upregulated genes that were implicated in ectodermal differentiation/development in general and the central nervous system development in particular. Furthermore, a number of regulated genes was associated with general cellular metabolism or negative regulation of cell proliferation and survival. Finally, and in agreement with the observation of reduced testis size in Trim71 heterozygous knockout mice, there was a cluster of downregulated genes that was implicated in reproductive processes. Notably, there were no gene annotations related to stem cell regulation or maintenance, which corroborated our finding that stemness networks were intact in Trim71-deficient mESCs.

In the following, the features of Trim71-mediated gene regulation were investigated in more detail focusing on potential posttranscriptional mRNA regulation by Trim71. In order to validate the RNA-seq results, the expression of some predicted DE genes was independently analyzed by RT-qPCR. For this purpose, a selection of representative up- and downregulated genes was chosen for further analysis (see table 3.1). The selected candidate genes coded for proteins implied in diverse biological functions ranging from transcription factors to membrane receptors and signaling proteins. Furthermore, the mRNA candidates also differed regarding their 3'UTR length and the presence or absence of putative miRNA target sites that were predicted using the TargetScan 6.2 tool [32, 44, 189]. As a negative control, we also included the Pou5f1 gene in our analysis which codes for the stemness-related transcription factor Oct4 and was found to be unaltered in Trim71-defient mESCs.

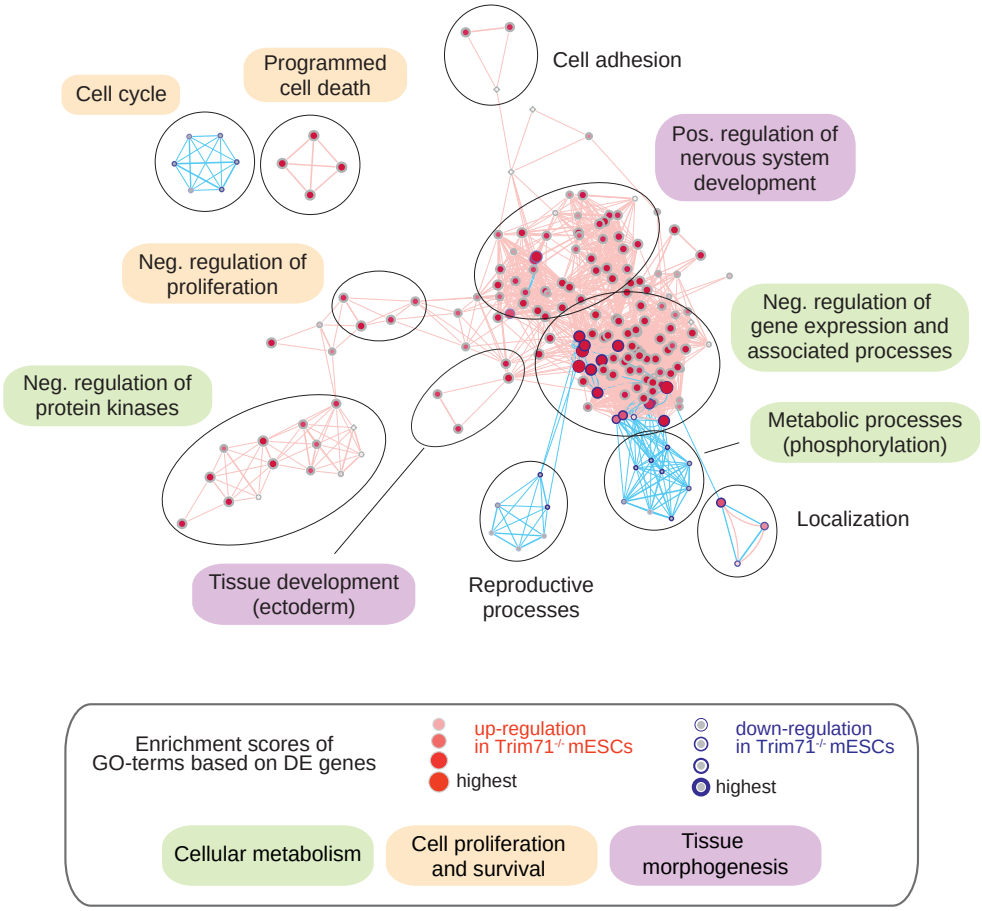

Figure 3.10: **DE genes of Trim71-deficient mESCs were primarily implicated in tissue morphogenesis, cellular metabolism and proliferation regulation.** Visual representation of gene ontology- enrichment analysis (GOEA) performed with DE genes from Trim71$^{-/-}$ mESCs using BiNGO and EnrichmentMap. Red nodes and blue nodes mark up- and down-regulated genes of enriched GO-terms, respectively. Color and size represent the corresponding FDR-adjusted enrichment p-value (q-value). Overlap of genes between nodes is indicated by edge thickness. Furthermore, clusters of similar biological functions were marked in colored boxes (see legend). Data analysis and visualization was performed by Thomas Ulas (AG Schultze). Figure modified from Mitschka *et al.* 2015 [172]

Gene	Function	3'UTR[1]	Broadly conserved miRNA target sites[2]
Pou5f1	Transcription factor essential for early embryogenesis [190] and embryonic stem cell pluripotency [12]	264 bp	none
Tcf15	Early transcriptional regulator of (mesodermal) differentiation [191]	344 bp	none
Plxnb2	Transmembrane receptor required for normal differentiation and migration of neuronal cells during brain corticogenesis and for normal embryonic brain development [192, 193]	754 bp	miR-124ab/506 miR-137ab miR-138ab miR-192/215
Foxj1	Transcription factor that is involved in the formation of motile cilia [194, 195], lung development [196], postnatal neurogenesis [197]	1027 bp	miR-141/200a
Inhbb	Protein subunit of inhibins and activins which act as both a growth/differentiation factor and a hormone, especially in the gonads [198]	1857 bp	>5 sites
Mras	Membrane-anchored, intracellular signal transducer regulating various processes [199, 200]	3266 bp	>5 sites
Nanos3	RNA-binding protein regulating germ cell maintenance[201, 159]	215 bp	none
Obscn	Signaling and anchor protein involved in the organization of myofibrils in striated muscle [202, 203]	495 bp	let-7/98/4458/4500
Prom1	Pentaspan transmembrane glycoprotein expressed in adult stem cells and cancer cells; suppressor of differentiation [204, 205]	1167 bp	miR30a-f/384 miR-203
Trim54	E3-ubiquitin ligase regulating titin kinase and microtubule-dependent signaling pathways in striated muscles [206]	149 bp	none [3]

Table 3.1: **List of selected candidate genes which were unchanged, upregulated or downregulated in Trim71$^{-/-}$mESCs.** [1] Data were obtained from the respective reference transcripts deposited on NCBI. [2] Indications according to annotations in TargetScan Release 6.2. [3] This 3'UTR was differently annotated in NCBI and TargetScan 6.2 [32, 44, 189]. Besides, there were no references for miRNA binding sites.

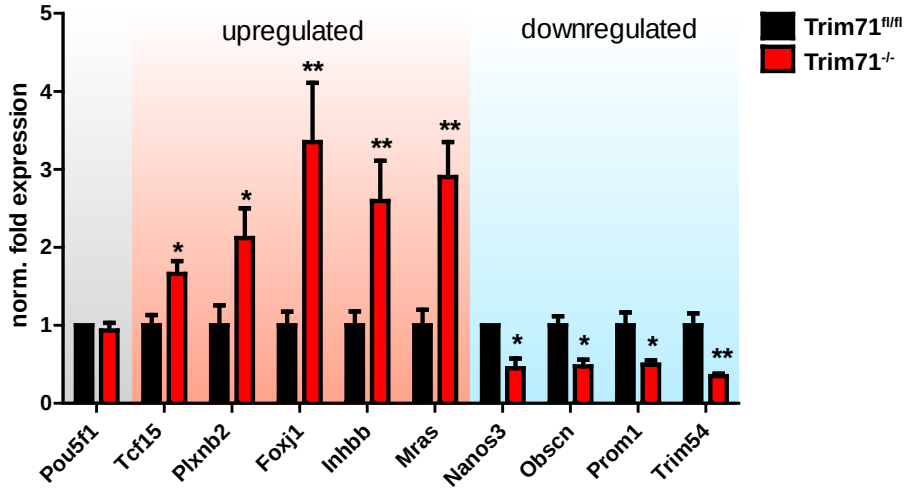

Figure 3.11: **Validation of differentially expressed genes identified by RNA-seq analysis**. The mRNA expression of one unaltered, five up- and four downregulated genes were measured by qRT-PCR relative to Gapdh. Expression levels were normalized to Trim71$^{fl/fl}$ samples. Values are mean+SEM (Student's t-test, n=4-11; * p<0.05, ** p<0.01). Figure modified from Mitschka *et al.* 2015 [172]

First, we could independently confirm differential gene expression in Trim71$^{-/-}$ mESCs of all selected up- or downregulated candidate genes by RT-qPCR (figure 3.11). As previously mentioned, all DE genes were functionally unrelated to mESC maintenance regulation but rather to embryonic development and differentiation. Therefore, we asked the question whether the observed changes in gene expression were indeed inherent to the entire stem cell population or if they reflect a tendency towards spontaneous differentiation within the analyzed cell pool. To answer this question, the protein products of one up- and one downregulated candidate gene were analyzed by FACS allowing for simultaneous staining of undifferentiated cells via the marker protein SSEA-1. In this setting, Plexin-B2, which had from all upregulated genes the highest basal mRNA expression in wildtype cells (data not shown), showed homogenous staining on all SSEA-1 expressing cells. In Trim71$^{-/-}$ mESCs, the MFI of Plexin-B2 was elevated in the entire cell population, resulting in a right-shifted histogram peak (figure 3.12a). In contrast, CD133, the protein product of the Prom1 gene, showed very low basal expression in wildtype cells. This was even further decreased in Trim71$^{-/-}$ mESCs (figure 3.12a). Again, there was no correlation between SSEA-1 surface expression and the expression of CD133, suggesting that the observed effects were not due to spontaneously occur-

ring cell differentiation of sub-populations within the mESCs culture. Moreover, these analyses illustrated that the measured differences in mRNA expression led to significant changes in protein output in intact undifferentiated Trim71$^{-/-}$ mESCs (figure 3.12b).

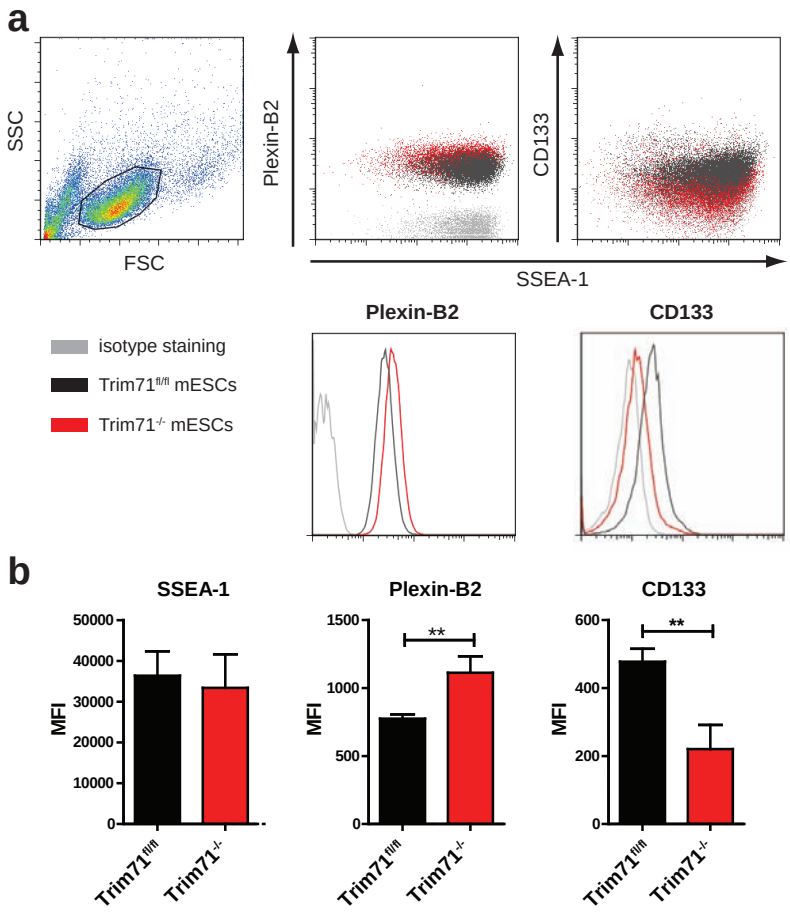

Figure 3.12: **Altered gene expression in Trim71$^{-/-}$ mESCs was not restricted to differentiated cells (a)** FACS analysis of Plexin-B2 or CD133 together with SSEA-1 revealed altered protein expression in the entire stem cell population. **(b)** MFI for SSEA-1, Plexin-B2 and CD133 in Trim71$^{fl/fl}$ and Trim71$^{-/-}$ mESCs from four independent experiments. Values are mean +SD (Student's t-test, n=4, ** p<0.01). Figure modified from Mitschka *et al.* 2015 [172]

3.2.4 The repression of mRNA targets is mediated by Trim71 response elements in the 3'UTR

Since we were further interested in the mechanism of Trim71-mediated gene regulation, we tried to elucidate how Trim71 modulates the expression of the selected candidate genes. Typically, RBPs regulate the expression of their target genes via binding motifs in the 3'UTR of the mRNAs [68, 207]. However, the existence and the characteristics of a putative Trim71 binding motif are not clarified yet. In order to test whether the 3'UTR is necessary and sufficient to mediate Trim71 expression regulation, the respective 3'UTRs of the selected candidate genes were cloned in a reporter vector, downstream of the coding sequence of the Renilla luciferase enzyme. Thereby, the Renilla luciferase expression, which can be easily quantified by light emission, reports about the regulation by RBPs and miRNAs binding to the respective 3'UTR. The system can be internally normalized to the activity of the Firefly luciferase, which is constitutively transcribed from the same plasmid (figure 3.13a).

From the five upregulated genes three genes also showed a significantly enhanced reporter activity in Trim71-deficient mESCs (figure 3.13b), namely Plxnb2, Foxj1 and Inhbb. Notably, the relative expression changes of the reporter constructs and the endogenous mRNA expression were not directly proportionate (compare to 3.11). For instance, Plxnb2 showed consistently the highest de-repression in the reporter system but not the highest relative fold change on endogenous level in Trim71$^{-/-}$ mESCs. On the other hand, neither the 3'UTR of the unaltered gene Pou5f1 nor the four downregulated genes displayed any differences in reporter expression between Trim71$^{-/-}$ and control cells, arguing that Trim71-mediated downregulation was not mediated on posttranscriptional level.

Next, we wanted to explore the characteristics of Trim71-mediated mRNA suppression in more detail. Therefore, we asked whether the enhanced reporter activity of target 3'UTR in Trim71$^{-/-}$ mESCs can be restored upon reintroduction of Trim71 cDNA. We transfected the reporter plasmids containing the different 3'UTRs together with flag-tagged Trim71 WT cDNA or a control plasmid in Trim71-deficient and wildtype mESCs (figure 3.14a). Indeed, we found that the luciferase reporter expression containing the 3'UTRs of Plxnb2, Foxj1 and Inhbb was decreased again upon Trim71 WT cDNA transfection in Trim71$^{-/-}$ mESCs. Moreover, overexpression of Trim71 WT together with the Foxj1 or Inhbb 3'UTR reporters further decreased reporter activity below basal control levels in wildtype mESCs (figure 3.14a). This was not the case for the Plxnb2 3'UTR where Trim71 WT over-

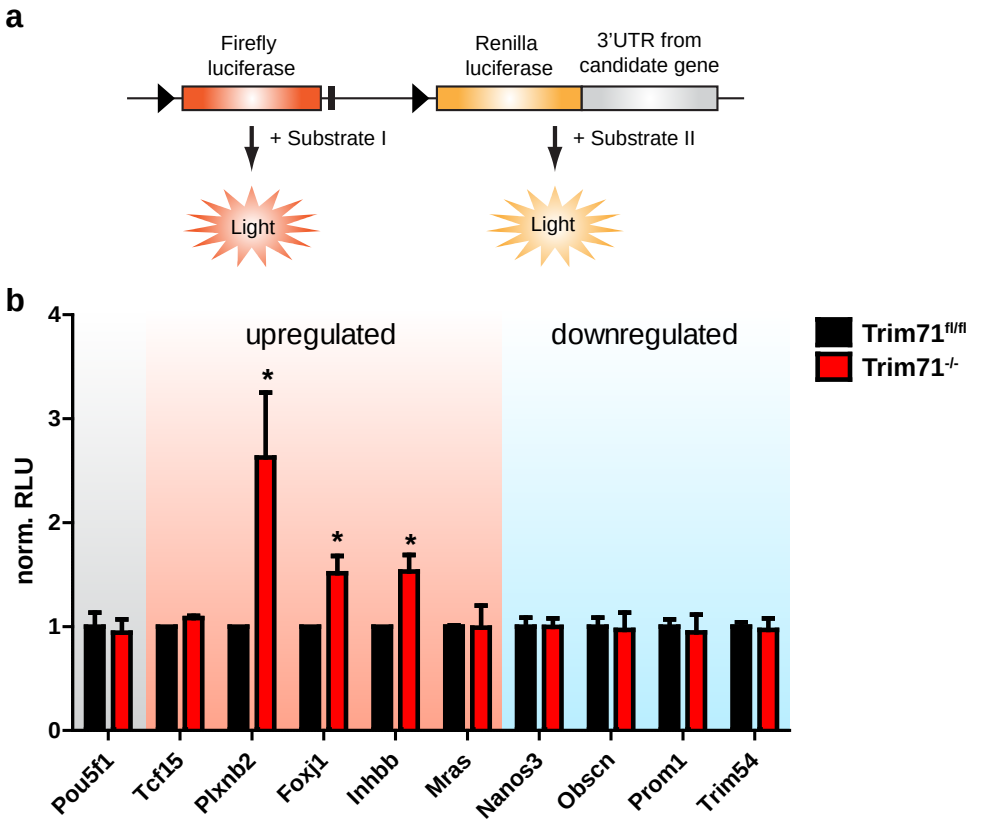

Figure 3.13: **Trim71 regulated target genes via response elements located in the 3'UTR. (a)** Illustration showing the strategy of Renilla luciferase expression regulated by candidate mRNA 3'UTR. **(b)** Normalized RLU values of ten different candidate 3'UTRs (see figure 3.11) relative to $Trim71^{fl/fl}$ levels. Values are depicted as mean+SEM normalized to control cell level of 3 independent experiments (Student's t-test with * $p<0.05$). Figure modified from Mitschka *et al.* 2015 [172]

expression could not further repress Luciferase reporter expression. To account for the full regulatory capacity of Trim71 on a specific candidate RNA, we established the parameter of the effect ratio, which is calculated as the quotient of normalized RLU values in $Trim71^{-/-}$ mESCs (no Trim71 present in the cell) and $Trim71^{-/-}$ mESCs plus Trim71 WT overexpression (maximal Trim71 amount). A quotient of 1 means that both values are equal and Trim71 does not influence target gene expression. Values >1 indicate a Trim71-dependent repression and values <1 an enhancement of reporter gene expression in the presence of Trim71. The plotted effect ratios shown in figure 3.14b illustrate that the three 3'UTRs of Plxnb2, Foxj1 and Inhbb are Trim71-dependently regulated, whereas this is not the case for Tcf15.

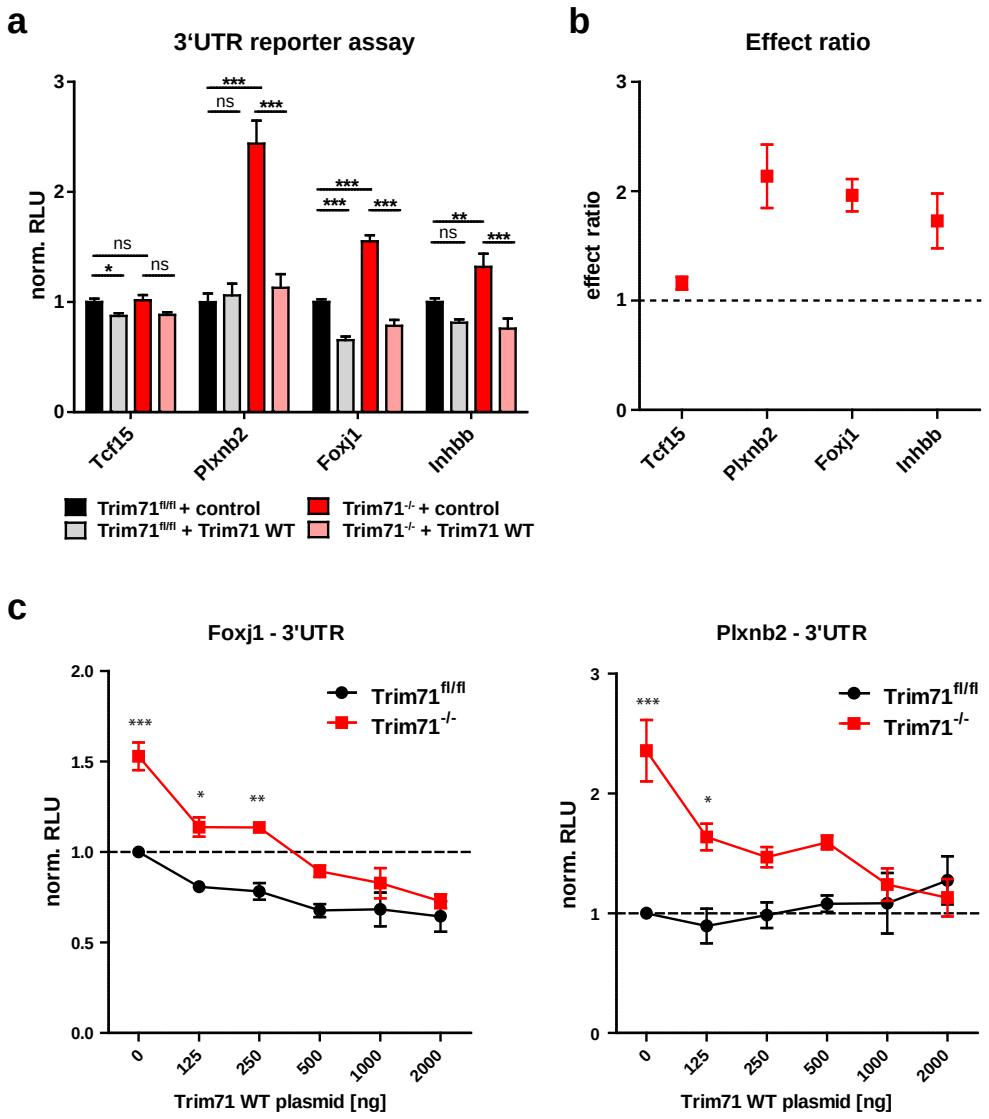

Figure 3.14: **Trim71 overexpression rescued reporter gene expression phenotype in Trim71$^{-/-}$ mESCs. (a)** Normalized RLU after transfection of reporter plasmids containing different candidate gene 3'UTRs together with and without Trim71 WT cDNA in Trim71-deficient and control cells. **(b)** Plotted effect ratios calculated from (a). **(c)** Measurement of Foxj1 and Plxnb2 3'UTR-dependent reporter expression in correlation with increasing amounts of transfected Trim71 WT cDNA. The amount of co-transfected reporter plasmid was constant (0.5 µg).Values are means +SEM (ANOVA, Tukey's test, n=3-6; n.s. not significant, * p<0.05, ** p<0.01, *** p<0.001).

Next, we wanted to know whether the inhibitory function of Trim71 is correlated with the amount of Trim71 protein present in the cell. Therefore, Trim71-deficient and control cells were transfected with the Foxj1 or the Plxnb2 reporter constructs together with increasing amounts of Trim71 WT cDNA. In both cases, small amounts of transfected Trim71 cDNA led already to a substantial reduction of reporter gene expression (figure 3.14c). Starting from 1 µg of transfected Trim71 plasmid per 0.5 µg of reporter plasmid, reporter expression was equal in $Trim71^{fl/fl}$ and $Trim71^{-/-}$ mESCs, suggesting that the repression effect is maximal. Hence, reporter repression could not be further enhanced by increasing amounts of Trim71 plasmid in the cell (figure 3.14c). Moreover, this experiment recapitulated the previous finding that, whereas the Foxj1-3'UTR can be further repressed in wildtype cells transfected with Trim71, this is not the case for Plxnb2. Taken together, we confirmed a clear dose-response relationship between the expression levels of Trim71 and its regulated target 3'UTRs.

3.2.5 Several protein domains of Trim71 are required for optimal target binding and repression

Since there is very little known about the functional relevance of different Trim71 protein domains, we tried to establish which parts of Trim71 are required for target gene repression. Therefore, we generated different Trim71 deletion constructs either lacking the putative RNA binding domain, the NHL domain, or the RBCC domain. Furthermore, a double point mutation of the RING domain (C12L/C15A) which was shown to disable the ubiquitin ligase activity [145] was included in the analysis (figure **??**a). For both tested 3'UTR reporter constructs only the transfection of Trim71 WT cDNA was able to rescue the relieve of reporter expression in $Trim71^{-/-}$ mESCs (figure **??**b). This suggested that more than one protein domain of Trim71 was actively involved in mRNA target repression. It was especially surprising to find that the double point mutant of Trim71 was also not able to rescue the $Trim71^{-/-}$ phenotype since the E3-ubiquitin ligase activity of Trim71 has not been implicated in RBP function so far. Finally, the structurally related Trim-NHL protein Trim32 was not able to compensate for Trim71 deficiency, most likely due to different binding specificities of its respective NHL domain.

All overexpression experiments shown so far were performed using N-terminally flag-tagged Trim71 constructs. However, it was surprising to find that the overexpression of the same constructs tagged with a more bulky eGFP-tag showed partially adverse effects on reporter gene expression. Figure 3.16 shows a compari-

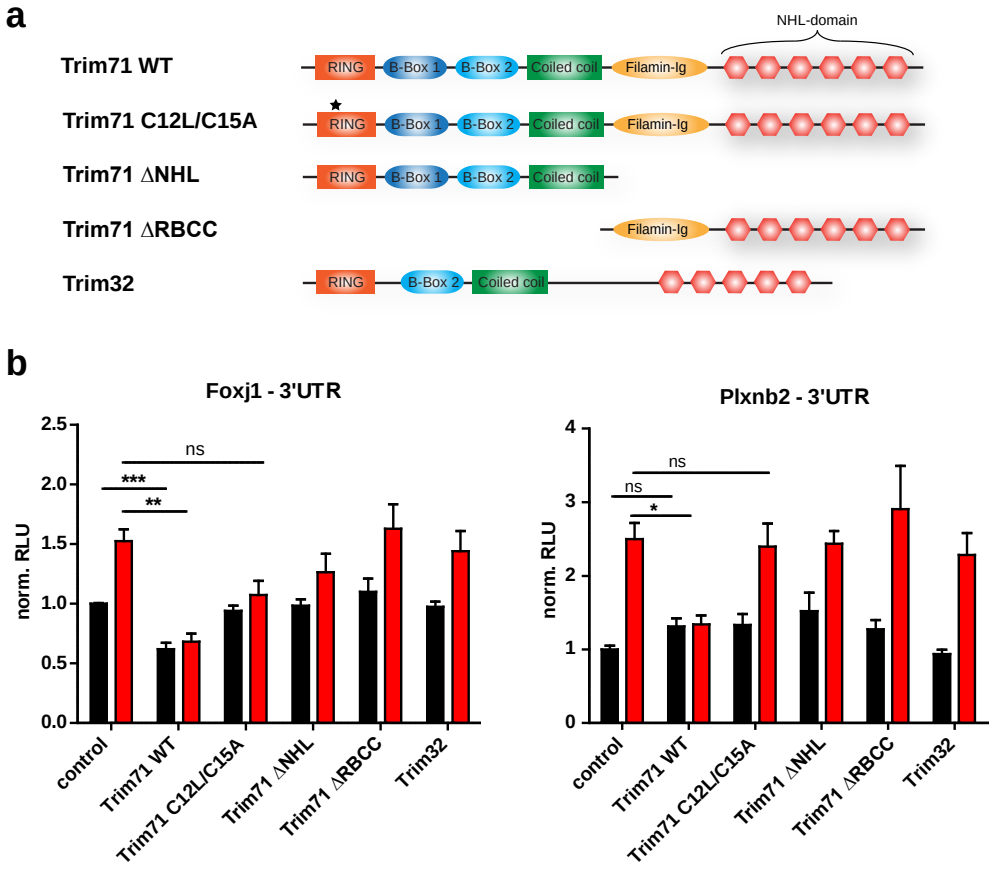

Figure 3.15: **An intact Trim domain and the NHL domain of Trim71 were both required for target gene repression. (a)** Overview on different Trim71 constructs and Trim32 used in this study. **(b)** Reporter gene assay using Trim71 wildtype (WT) and different Trim71 deletion mutants as well as Trim32 in Trim71$^{fl/fl}$ and Trim71$^{-/-}$ mESCs. Values are mean +SEM (ANOVA, Tukey's test; n=3-6; n.s. not significa* p<0.05, ** p<0.01, *** p<0.001)

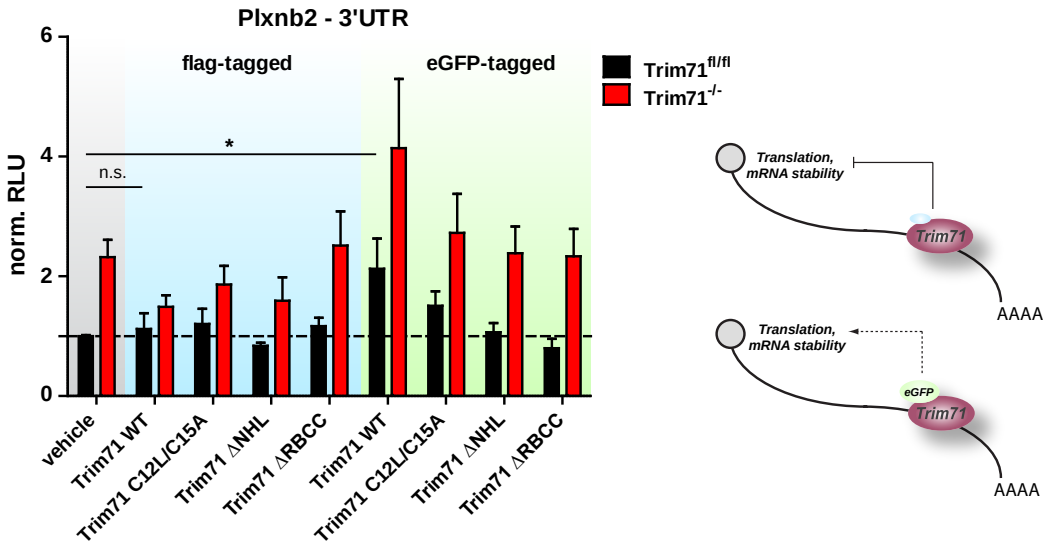

Figure 3.16: **Both N- and C-terminus of Trim71 were important for the mRNA repressor function.** Luciferase assay performed in Trim71$^{-/-}$ and control mESCs after overexpression of different Trim71 constructs N-terminally fused with a small flag- or a bulky eGFP-tag. Values are mean +SEM (n=3-4).

son of different constructs either tagged with a short flag-tag (1 kDa) or a bulky eGFP-tag (27 kDa) regarding Plxnb2 reporter gene expression. As shown before, the overexpression of flag-tagged Trim71 WT normalizes reporter gene expression in Trim71-deficient cells, whereas it remains unaltered in control cells. In contrast, we found that the overexpression of eGFP-tagged Trim71 in control cells actually de-repressed the Plxnb2 3'UTR reporter to a similar extent as the absence of Trim71 in mESCs. In Trim71$^{-/-}$ mESCs, the overexpression of eGFP-Trim71 WT even further enhanced reporter expression. This was not the case after overexpression of the RING domain mutant of Trim71 (3.16). The fact, that the eGFP-masked N-terminus which is unlikely to directly interact with the target mRNA had such adverse effect on reporter gene expression suggests that the N-terminus is important for the recruitment of effector proteins. Together with the previously shown experiment, these results confirm that several protein domains of Trim71 are required for target mRNA repression.

All experiments presented so far did not exclude the possibility that miRNAs are directly or indirectly involved in Trim71-dependent posttranscriptional expression regulation. All three verified targets (Inhbb, Plxnb2 and Foxj1) also contain predicted miRNA binding sites. Hence, it is conceivable that Trim71 cooperates with or modulates miRNA binding and function. To exclude the involvement of miRNAs in Trim71 target gene regulation and to identify putative Trim71 binding sites within the candidate genes, 5'-end deleted fragments of the Plxnb2 and Foxj1 test-3'UTRs were generated (figure 3.17a). According to the TargetScan 6.2 database [32], the murine Foxj1 3'UTR does contain only one broadly conserved miRNA binding site for the miR-200a/141 which is located at the 5'end of the mRNA and therefore only included in the full length Foxj1 3'UTR and in fragment F1 (figure 3.17a left panel). In contrast, the Foxj1 3'UTR fragments F2 to F5 did not contain any miRNA binding sites. By testing all deletion constructs of the Foxj1 3'UTR, we found that the fragments F1 to F4 showed Trim71-dependent regulatory effects. Whereas fragments F1 and F2 were as effectively repressed by Trim71 as the Foxj1 full length 3'UTR construct, the effect of the fragments F3 and F4 was reduced to about half (figure 3.17c). The last fragment F5 showed no differential expression in wildtype and Trim71-deficient mESCs. The step-wise decrease of the effect ratios could indicate that several Trim71 response elements might be located within the Foxj1 3'UTR.

We also investigated the Plxnb2 3'UTR which contains five predicted miRNA binding sites, present in all but 3'-end located fragment F4 (figure 3.17a right panel). We tested the different fragments in the luciferase reporter system and observed that all deletion fragments showed enhanced luciferase expression in the Trim71$^{-/-}$ mESCs in comparison to control cells. The effect could be rescued again upon overexpression of Trim71 WT cDNA. Notably, there was even a decrease below wildtype control level upon Trim71 overexpression in the last two fragments (figure 3.17b). However, the calculated effect ratios were similar for all deletion constructs and the full length Plxnb2 3'UTR (figure 3.17c).

This experiment allows the conclusion that miRNA binding was not to a prerequisite for Trim71-mediated expression regulation. Moreover, in the case of Plxnb2 we could locate the Trim71 response element within the last 150 nt of the 3'UTR which constitutes the shortest Trim71-regulated RNA identified so far.

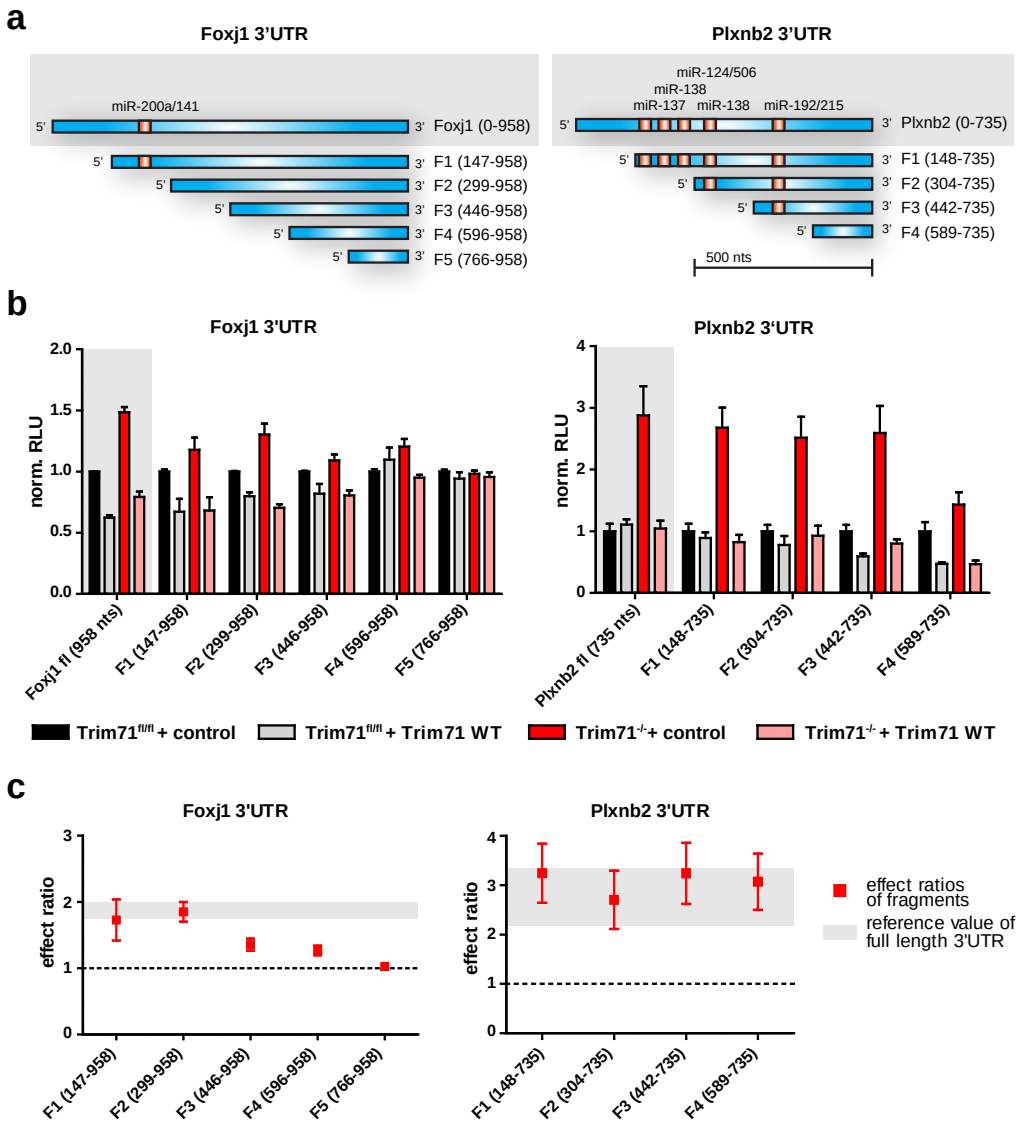

Figure 3.17: **The repression of target 3′UTRs by Trim71 is independent from miRNA binding. (a)** Schematic of the full length and shorter fragments of the Foxj1 and Plxnb2 3′UTRs showing the location of predicted miRNA binding sites. **(b)** Reporter assay and plotted effect ratios **(c)** with full length (grey shading) and fragments of the Foxj1 and Plxnb2 3′UTRs. Values are mean+SEM (n=3-6).

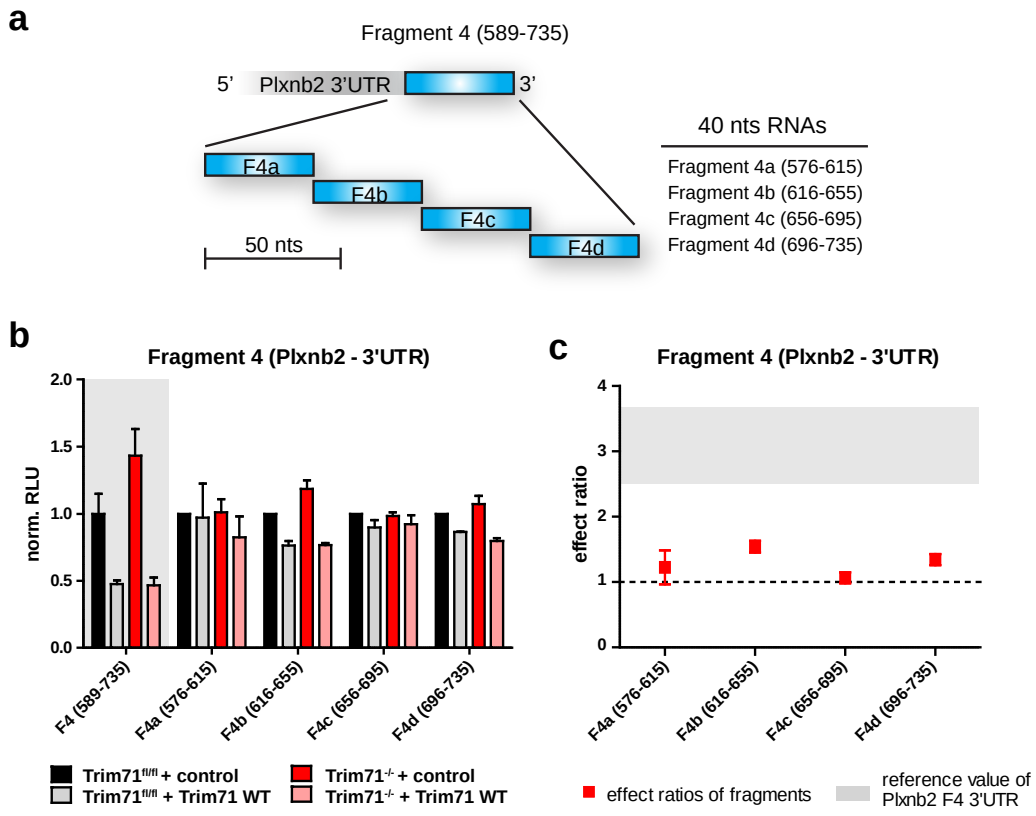

Figure 3.18: **Trim71 dependent repression of the Plxnb2 mRNA required spatially separated binding elements. (a)** Schematic showing the generation of four 40 nts fragments from the 3'-end of the Plxnb2 3'UTR **(b)** Reporter assay and plotted effect ratios **(c)** of fragment F4 (gray shading) and 40 nts subfragments. Values are mean+SEM (n=3-6).

We further subdivided the most '3-end of the Plxnb2 mRNA into 4 40-mer fragments (figure 3.18a) in order to localize the putative Trim71 response element more precisely. However, none of the sub-fragments showed a comparable efficiency for reporter expression regulation as the 150 nt F4 fragment (figure 3.18b). Surprisingly, two non-adjacent fragments, F4b and F4d, showed a higher effect ratio than 1, however this was still considerably lower than for the whole F4 fragment (figure 3.18c). This indicated, that, as in the case with the Foxj1 3'UTR, different spatially separated motif elements might be involved in the Trim71-mediated mRNA repression.

3.3 The role of Trim71 in miRNA biogenesis and expression regulation

Next to the RBPs, miRNAs constitute a second option for posttranscriptional expression regulation. It is long since known that Trim71 itself is a conserved target of miRNA regulation, especially by the miRNAs miR-125 and let-7 [59, 147, 208]. In order to test the correlation of Trim71 expression with let-7 miRNA abundance, we performed expression analysis by RT-qPCR in different human cell lines. We observed a strong inverse correlation between the expression of the miRNA let-7a and the mRNA expression of Trim71 (figure 3.19a). This relationship was not linear but exponential with a correlation coefficient of 0.92. In contrast, there was no relationship between the expression of the miRNA let-7a and the mRNA expression of the structurally related Trim-NHL protein Trim32 which has no predicted let-7a binding sites [32](figure 3.19b).

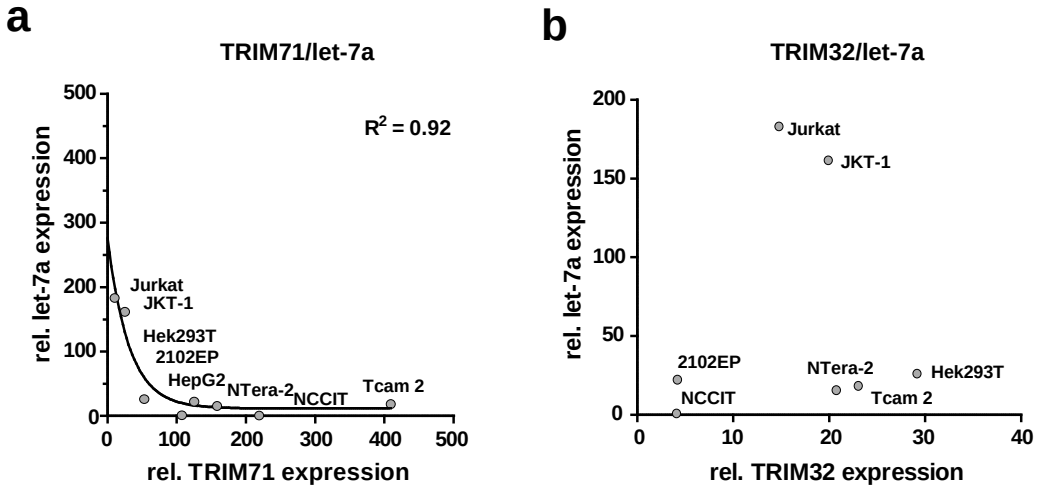

Figure 3.19: **The expression of Trim71 and the miRNA let-7 is inversely correlated.** The relative expression of the miRNA let-7a and the Trim-NHL proteins Trim71 and Trim32 were measured relative to 18S rRNA in eight different human cell lines. The relative expression values of Trim71 **(b)** and Trim32 **(c)** were plotted against the expression of the miRNA let-7a. For the Trim71-let-7 plot, an exponential decay regression curve was calculated with a correlation coefficient of 0.92.

However, there is also accumulating evidence suggesting that Trim71 might not only be a target of miRNA-mediated repression. A study published by Rybak *et al.* demonstrated that Trim71 acts as a ubiquitin ligase for Ago proteins [145], thereby decreasing the amount of available Ago proteins in the cell. Since Ago proteins represent a bottleneck in the miRNA biogenesis pathway, the downregulation of Ago proteins would have severe consequences for the whole miRNA expression landscape in the cell. However, other studies did not confirm this observation [151, 153].

We tried to recapitulate some major findings supporting the idea of an involvement of Trim71 in miRNA biogenesis. Trim71 was found to be localized in so called P-bodies which are sites of mRNA storage and miRNA-mediated repression. All proteins that take part in miRNA-mediated mRNA repression are present in P-bodies, such as Ago proteins, GW182, decapping proteins and RNA helicases (reviewed in [209]). Indeed, after overexpression in human HEK293T cells, we found TRIM71 to be exclusively localized to a series of discrete spots at the nuclear periphery which is characteristic for P-bodies (figure 3.20a). In order to specifically prove the previously reported interaction of TRIM71 with AGO2, we overexpresed flag-tagged TRIM71 constructs in HEK293T cells. Notably, we did not observe a change in AGO2 protein content when Trim71 was present. However, we could detect endogenous AGO2 protein in the IP-fraction which was co-purified together with TRIM71 WT protein (figure 3.20b). The interaction with AGO2 was abrogated when the E3 ubiquitin ligase mutant of Trim71 or a construct lacking the NHL domain was overexpressed. This suggested that at least two different structural features located at the N- as well as the C-terminus of TRIM71 were influencing the ability to bind Ago2.

Although we and others have obtained similar results regarding the molecular interaction of Trim71 with Ago2 [145, 151, 152, 153, 154], the involvement of Trim71 in Ago2 degradation is still controversially discussed. Using our Trim71 conditional mESC lines we had for the first time the chance to analyze the impact of endogenously expressed Trim71 protein in a defined cell system. We have performed WB analysis and observed similar Ago2 protein expression levels in Trim71-deficient mESCs and control cells (figure 3.21a). However, we wanted to exclude the possibility that a constitutive deficiency of Trim71 in mESCs initiated compensatory transcriptional upregulation of Ago2 expression. Therefore, we also performed RT-qPCR analysis, but again we found no difference in the Ago2 mRNA expression levels between both mESC types (figure 3.21b). This led us to conclude

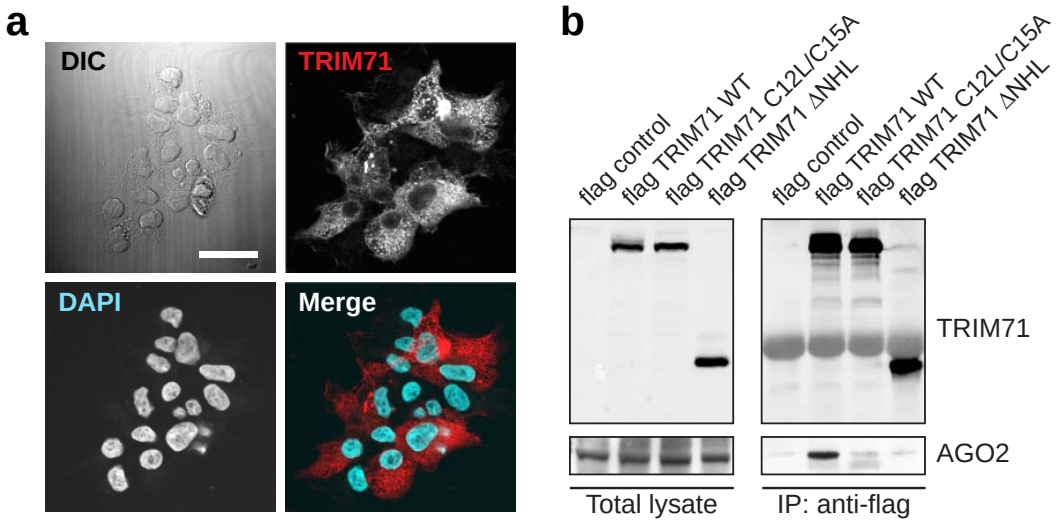

Figure 3.20: **Interaction of Trim71 with the RISC protein AGO2. (a)** Immunofluorescence staining of overexpressed flag-TRIM71 (red) and nuclear stain with DAPI (blue) in HEK293T cells. Scale bar represents 30 µm. **(b)** Representative AGO2 co-immunoprecipiation experiment performed in HEK293T cells using overexpression of flag-tagged TRIM71 WT and mutants.

that in undifferentiated mESCs Ago2 stability and turnover were not subject to expression regulation by Trim71.

3.3.1 Trim71 deficiency induces changes in the miRNA expression landscape of mESCs

Nevertheless, we were still interested whether Trim71 might affect miRNA expression by other means than by Ago2 stability regulation. For this purpose, we performed high-throughput sequencing of small RNAs and mapped the sequences to all known miRNAs. Overall, 590 miRNAs were found to be expressed above background level in at least one of the two cell types. In total, we detected about 20% more miRNA sequence counts in Trim71$^{-/-}$ mESCs in comparison to control cells. Evidently, Trim71$^{-/-}$ mESCs did not have any general defects in the Ago2-controlled miRNA biogenesis pathway. The PCA revealed that Trim71$^{-/-}$cell samples clustered together and they could be distinguished from Trim71$^{fl/fl}$ control samples (figure 3.22a) DE miRNAs showed low inter-replicate variability (figure 3.22b). Several members of the let-7 family as well as miR-21a were found among the miRNAs that showed the highest mean upregulation. On the other hand several miRNAs were found to be downregulated in Trim71 deficient mESCs in compar-

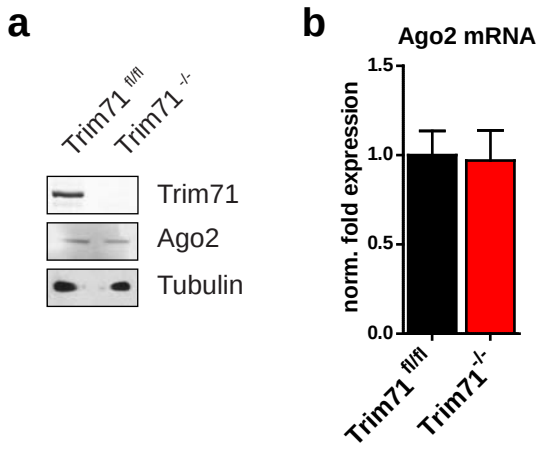

Figure 3.21: **Ago2 expression is not affected by Trim71 knockout in mESCs. (a)** WB analysis of Ago2 in Trim71$^{fl/fl}$ and Trim71$^{-/-}$ mESCs. **(b)** Likewise, the mRNA expression of Ago2 was not significantly altered (mean +SEM; n=5).

ison to control cells *e.g.* miR-127, miR-410 and miR-136. When plotting the mean expression of all miRNAs in wildtype cells against their respective fold change in Trim71$^{-/-}$ mESCs, we could prove that expression regulation was not only occurring in low abundant miRNAs (figure 3.22c). When also taking the p-value into account there were in total 31 DE miRNAs in Trim71$^{-/-}$ mESCs with a $\left|FC\right| \geq 1.5$ and $p \leq 0.05$, 24 of which were downregulated and 7 upregulated (see Appendix).

In order to link the observed changes in miRNA expression to certain functionalities, we grouped all expressed miRNAs as proposed by Chiang and colleagues according to their dominant expression in certain developmental stages or tissues [178] . We then counted the number of miRNAs that showed a higher expression in either Trim71$^{fl/fl}$ or Trim71$^{-/-}$ mESCs and evaluated the relative differences in the miRNA subgroups (figure 3.23). Indeed, most ESC-specific miRNAs were higher expressed in Trim71$^{fl/fl}$ cells. Although the individual effects of specific miRNAs were usually not very pronounced this might indicate a decreased stability of stem cell maintenance in Trim71$^{-/-}$mESCs. On the other hand, brain-specific miRNAs were in average higher expressed in Trim71$^{-/-}$ mESCs going in line with the upregulation of mRNAs involved in neural development (figure 3.10). Most strikingly, the vast majority of gonadal miRNAs, *i.e.* those species which were annotated to be characteristic for ovaries and testes, were also higher expressed in Trim71-deficient mESCs. The table in figure 3.23 shows some examples of miRNAs belonging to the different categories and a brief description of their described functions.

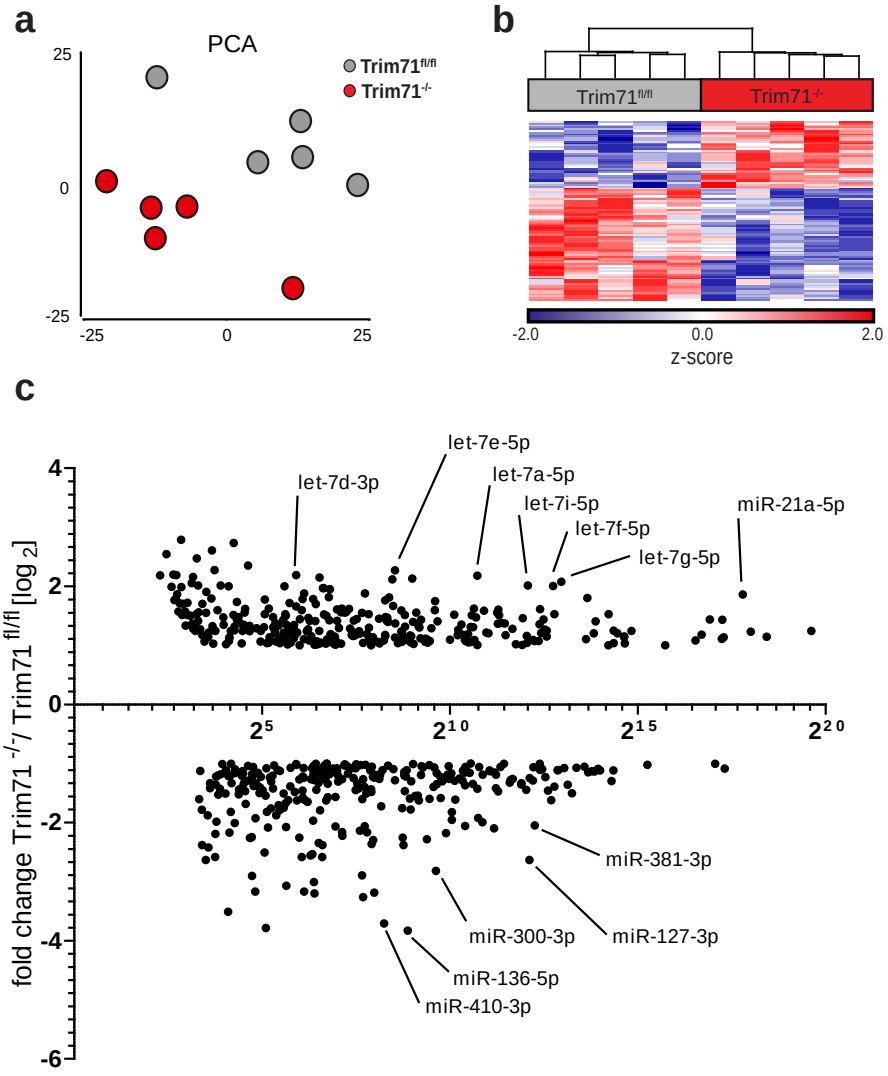

Figure 3.22: **Differential expression of miRNAs in Trim71$^{fl/fl}$ and Trim71$^{-/-}$ mESCs. (a)** Principal component analysis (PCA) of technical replicates from Trim71-deficient and control mESCs revealed genotype specific changes in the miRNA profile. **(b)** Trim71$^{fl/fl}$ and Trim71$^{-/-}$replicate samples were clustered according to the expression profiles of the top 100 differentially expressed miRNAs. **(c)** Expression values of miRNAs in Trim71$^{fl/fl}$ control cells were plotted against their respective fold changes in Trim71$^{-/-}$ mESCs, demonstrating that not only low abundance miRNAs show an altered expression. The data analysis was performed by Thomas Ulas (AG Schultze). Figure modified from Mitschka *et al.* 2015 [172]

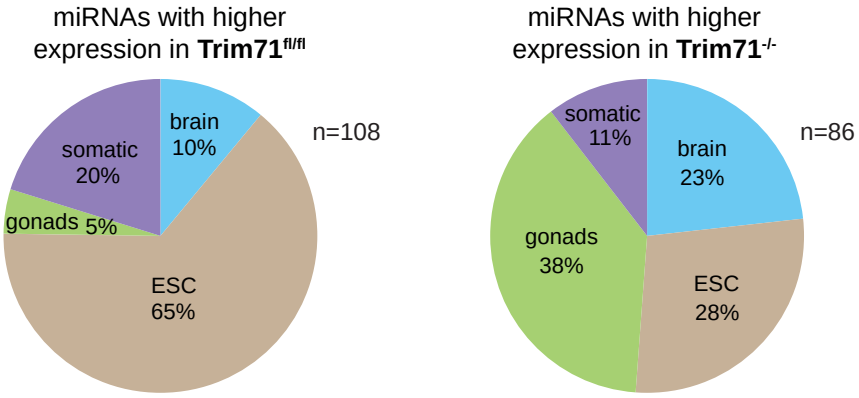

Tissue	miRNA	FC	Functions
ESC	miR-20b	-1.28	promotes breast cancer, modulates ERK, STAT3 and BMP signaling [210, 211, 212]
	miR-18b	-1,51	inhibits melanoma cell proliferation by targeting the p53 regulator Mdm2 [213], expression correlates with malignancy of HCC [214]
Gonads	miR-881	1.53	no information available
	miR-184	1.86	highly expressed in testis (function unknown) and brain, governs NPC proliferation and differentiation [215, 216]
	miR-743a miR-743b	2.40 1.83	downregulated by oxidative stress in the brain [217]
Somatic	miR-410	-4.88	overexpressed in gliomas and neuroblastomas, positive regulator of proliferation via MET [218, 219]
	miR-136	-4.15	tumor suppressor in glioma [220], tumor promoter in lung cancer [221], positive regulator of keratinocyte proliferation [222]
	miR-127	-3.04	regulates proliferation, upregulated in senescent fibroblasts [223], modulates fetal lung development [224]
	miR-9	1.56	regulation of neural differentiation [225] downregulated in breast cancer [226]and renal cancer [227]
Neural	miR-200a	1.41	establishment of epithelial phenotype via regulation of adhesion molecules [228], regulates cell cycle exit in NPCs [229], downregulated in different cancers [228, 230]
	miR-128	1.54	drives differentiating neural progenitors to neuronal cell fate [231]
	miR-132-5p	1.79	regulates neurite outgrowth [232] and dendritic plasticity [233]

Figure 3.23: **Loss of Trim71 increased expression of tissue-specific miRNA at the expense of ESC miRNAs.** Based on the miRNA annotation by Chiang *et al.* (2010) [178] ESC, gonadal, somatic and brain-specific miRNAs were grouped to the genotype which exhibits higher expression and results were depicted in a pie chart. N indicates the total number of miRNAs that showed higher expression in the respective group. Data analysis was performed by Thomas Ulas (AG Schultze). Figure modified from Mitschka *et al.* (2015) [172]. Table with representative miRNAs belonging to the different categories depicted above with their functional associations.

3.3.2 Trim71 deficiency leads to elevated let-7 miRNA expression

As shown in 3.22c, several members of the let-7 miRNA family were found to be upregulated in Trim71-deficeint mESCs. In contrast to the miRNAs analyzed in figure 3.23, let-7 miRNAs are not tissue-specifically expressed but their expression is generally considered to be restricted to all differentiated cell types [234, 58]. Previous studies have analyzed let-7 expression in the context with Trim71 [145, 153, 154], however no consistent hypothesis has been developed so far and we decided to analyze this miRNA in more detail.

10 highly similar miRNAs belong to the let-7 miRNA family (let-7a-g, let-7i, miR-98 and miR-202) originating from 13 and 14 genes in humans and mice, respectively [60]. Using the RNA-seq data we compared the expression of the individual let-7 members in wildtype and Trim71-deficient undifferentiated mESCs (figure 3.24a). We noticed that the basal expression of individual let-7 miRNAs strongly varied already in control cells: let-7f, let-7g and let-7i showed the highest basal expression whereas let-7b,-7d and -7e exhibited a very low expression and miR-202 was not detectable. Despite very different baseline expression levels, we observed a substantial increase of expression across all let-7 members in Trim71$^{-/-}$ mESCs which was in average 2.06 ($\mp$0.23) fold in comparison to control cell levels. Hence, the total let-7 content was doubled in Trim71$^{-/-}$ mESCs figure 3.24a). Since it has been proposed that ESCC miRNAs of the miR-290 family can partially counteract let-7 in mESCs [49], we were examining the relative abundance of those miRNAs as well. In contrast to let-7, the basal expression levels of the ESC-specific miR-290 miRNAs were very high. However, we found that Trim71 deficiency did not affect the expression of single miR-290 members or overall expression (figure 3.24b). This illustrated that Trim71-deficiency specifically led to an upregulation of let-7 miRNAs.

In order to independently confirm the upregulation of mature let-7 miRNAs, we performed RT-qPCR analysis of different miRNAs in Trim71$^{-/-}$ and control mESCs. Again we found a significantly elevated expression of the let-7 family members let-7a and let-7g, but not for miR-294, miR-302a and miR-125a, which were investigated as well (figure 3.25a). Next, we measured the levels of mature let-7a, Trim71 mRNA and Trim71 protein at different time points after begin of 4-OHT treatment. Because of the high Trim71 turnover we observed a substantial reduction of both Trim71 mRNA and protein after 24 hours of 4-OHT treatment (figure 3.25b). At this early time point, let-7a was already found to be upregulated, which speaks for a direct involvement of Trim71 in let-7 expression regulation rather than for indi-

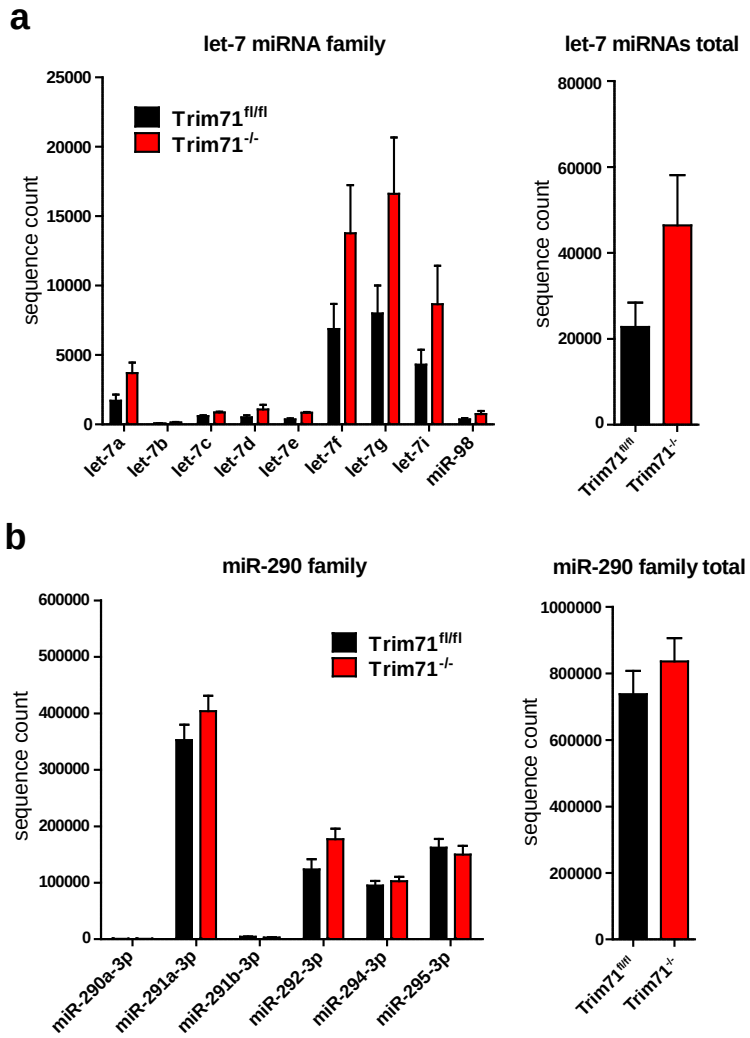

Figure 3.24: **High-throughput sequencing of miRNAs confirmed a selective upregulation of let-7 miRNAs but not of ESCC miRNAs in Trim71$^{-/-}$ mESCs.** Sequence counts in Trim71 knockout and control mESCs attributed to the family members of the let-7 family **(a)** and the miR-290 family **(b)**. Values are mean +SEM (n=5-6).

rect effects caused by other targets. Last, we could show that let-7a and let-7g levels could be restored again after reintroduction of Trim71 WT cDNA. Moreover, overexpression of Trim71 WT in wildytpe cells further reduced let-7 expression below baseline level (figure 3.25c), highlighting that Trim71 levels influenced let-7 expression already in steady-state in undifferentiated mESCs.

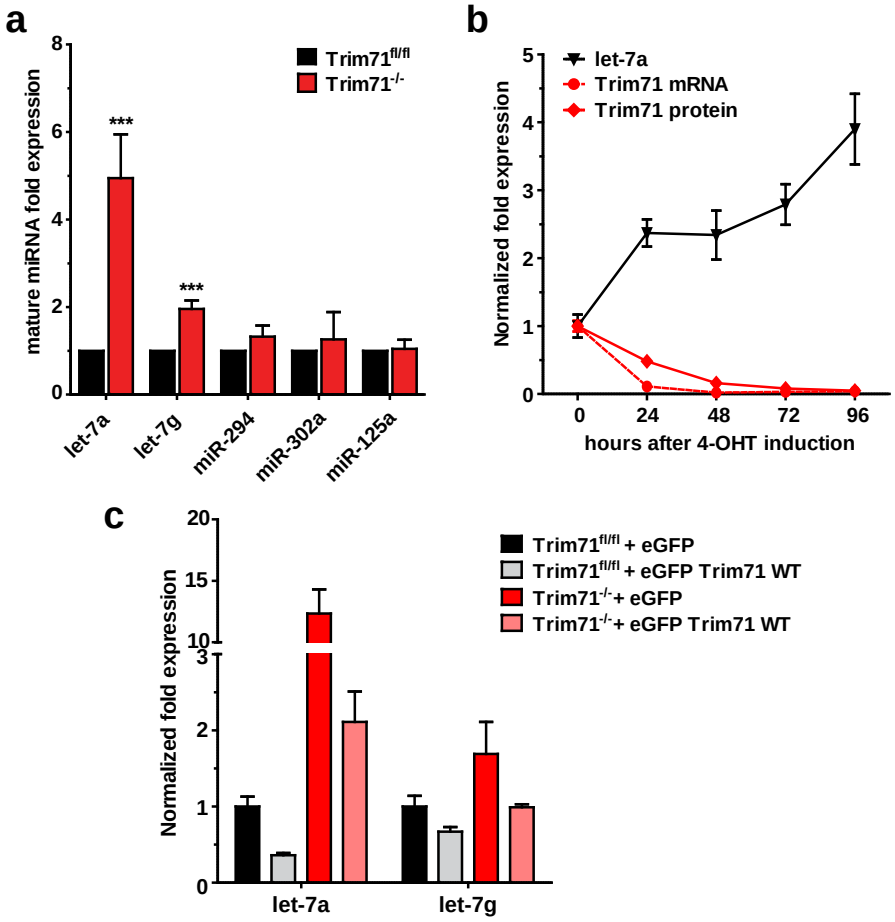

Figure 3.25: **Trim71 deficiency in undifferentiated mESCs leads to higher let-7 expression in steady-state culture. (a)** RT-qPCR analysis of the expression of different miRNAs in Trim71$^{fl/fl}$ and Trim71$^{-/-}$ mESCs**. (b)** Reduction of Trim71 mRNA and protein immediately gradually leads to increased expression of let-7. Values are depicted as mean +SEM (Student's t-test; n=3; *** p<0.001). **(c)** Trim71 overexpression in Trim71$^{-/-}$ and control mESCs reduced the expression of let-7a and let-7g (mean +SEM, n=3).

3.3.3 Let-7 miRNA processing is affected by Trim71 deficiency in mESCs

The maturation of miRNAs to the final 21 nt single stranded RNA is a multi-step process involving many different processing enzymes and regulatory proteins (figure 3.26a). Hence, any impacts on let-7 processing could lead to an elevated mature miRNA expression. In order to identify at which level Trim71 might regulate let-7 expression, we comparatively measured the levels of pri-, pre- and mature miRNAs for the miRNA let-7a-1 by RT-qPCR. It was found that only the mature let-7a miRNA but not its pri- and pre- form were significantly elevated (figure 3.26b). Thus, we could exclude that the Trim71 repression effect on let-7 miRNAs was mediated by transcriptional regulation. Furthermore, the primary processing of the pri-let-7 transcript by the Dgcr8/Drosha enzyme complex was also unaffected (figure 3.26b). Taken together, this finding suggested that Trim71 could be either involved in a late step of precursor miRNA processing, or could decrease the stability of the mature let-7 miRNAs.

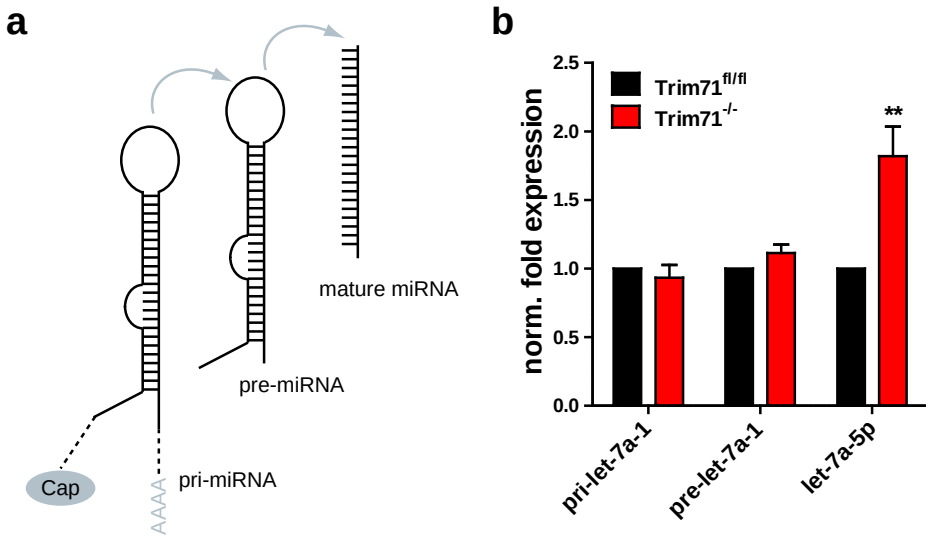

Figure 3.26: **Unaltered transcription and primary processing of let-7 miRNAs in Trim71$^{-/-}$ mESCs. (a)** Schematic showing miRNA biogenesis from the primary transcript to precursor and mature miRNA. **(b)** RT-qPCR of pri-,pre- and mature let-7a-1. Values are mean + SEM (Student's t-test; n=3-10; ** p<0.01).

For distinguishing between miRNA processing and stability regulation, we took advantage of the RNA-seq data which record expression of all 21-mers independent of their functional relevance. Naturally, all mature miRNAs have a by-product, a second less conserved 21 nt RNA strand which is also referred to as the passenger strand. This passenger strand is the partial complement of the mature miRNA and is separated from the active guide strand during loading into the RISC complex. The passenger strand is usually rapidly degraded after strand separation [235]. If Trim71 were to decrease the stability of mature let-7 miRNAs, this would require a direct or indirect recognition of the mature (guide strand) sequences which are indeed very similar between the different let-7 family members. On the other hand, the passenger strands are very different to the guide strand and also show more variability among the let-7 members. Hence, it is unlikely that miRNA stability regulation would also affect the passenger strand, too. In contrast, any impact on the prior processing step from the pre-miRNA would equally affect both RNA strands.

In order to investigate this aspect, we picked the two let-7 family member let-7a and let-7f to investigate their guide and passenger strand expression. Both miRNAs are coded by two distinct genes resulting in an identical 5p strand (guide) miRNA, but different 3′ (passenger) miRNAs. The pre-miRNAs with the annotated 5p and 3p strand as well as the terminal loop sequence is depicted in figure 3.27a. As expected, the sequence counts for the respective 5p guide strand were dramatically higher than for the corresponding 3p passenger strands. However, for both miRNAs we observed a similar upregulation of guide and passenger strand counts in Trim71$^{-/-}$ mESCs (figure 3.27b). This experiment led us to conclude that Trim71 affects pre-miRNA processing instead of let-7 miRNA stability.

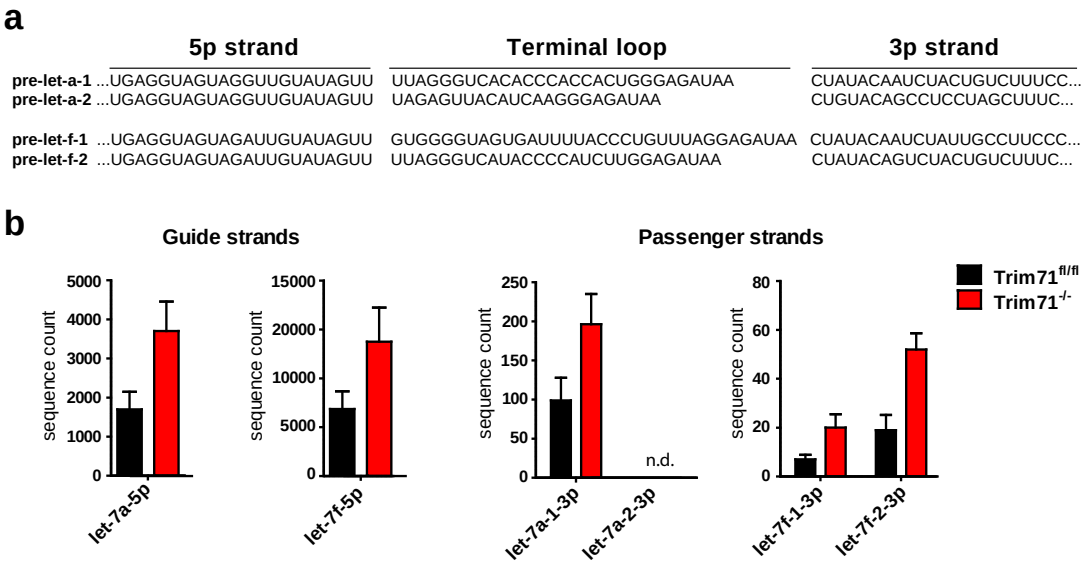

Figure 3.27: **Trim71 deficiency led to an equal increase of guide and passenger strands of let-7 miRNAs. (a)** let-7a and let-7f can be generated from two different precursor miRNAs that differ in their respective loop sequence and the 3p-strand. **(b)** miRNA-seq of wild-type and Trim71-deficient cells revealed a comparable increase in both the functional guide strands as well as the passenger strands. n.d. not detectable.

3.3.4 Trim71 interacts with the let-7 regulatory protein Lin28

The functional analysis of Trim71-dependent let-7 expression regulation revealed a striking resemblance to the effects described for another developmental regulatory protein: lin-28/Lin28/LIN28 (lineage abnormal 28). In the model organism *C. elegans* it acts upstream of the miRNA let-7 in the heterochronic pathway and this regulatory relationship is highly conserved across species [146, 59]. In mammals, two different Lin28 paralogs, Lin28a and Lin28b, which have different expression patterns but share similar molecular functionality, have been identified [63, 89, 236, 237]. Lin28 binds to the let-7 pre-miRNAs and sequesters them from the Dicer complex and also indirectly mediates their degradation. In this role, Lin28 is an established posttranscriptional regulator of let-7 expression in stem cells [62, 63, 66, 238].

In order to explore the molecular connection between Trim71-dependent let-7 regulation and Lin28 protein function, we first investigated whether these proteins physically interact in mESCs. For this purpose, flag-tagged Lin28a was overexpressed in wildtype mESCs. 24 hours post transfection the cells were lysed and flag-tagged proteins were enriched by immunoprecipitation using magnetic beads coated with antibodies raised against the flag-tag. This resulted in an enrichment of flag-tagged Lin28a in the IP fraction (figure 3.28a). Indeed, we found that Trim71 was co-purified in the IP-fraction together with Lin28a. As a positive control we stained for the poly(A)-binding protein (PABP) which was previously shown to co-precipitate together with Lin28a [90]. However, as both Lin28a and Trim71 are RBPs, a co-precipitation could be the result of coincidental binding to common mRNA targets. In order to exclude this possibility, we treated a part of the lysates with RNaseA to degrade any RNAs that might act as molecular linker. After RNaseA treatment, PABP binding to Lin28a was abolished, whereas Trim71 was equally detected in RNaseA-treated and untreated fractions (figure 3.28b). This suggested that Trim71 binding to Lin28a was protein-mediated and that RNA binding was not a prerequisite for the protein interaction.

Lin28 possesses two RNA-binding domains (RBDs): an N-terminal cold-shock domain (CSD) followed by two tandem Cys-Cys-His-Cys -type zinc-binding motifs (CCHCx2) which are connected by a flexible linker sequence. Several studies had shown that both RBDs are required for efficient pre-let-7 binding and suppression [64, 66, 239]. In order to identify the interaction site of Trim71 with Lin28a, different constructs were cloned lacking specific protein domains. Furthermore, we also included a Lin28a cDNA introducing two point mutations which were shown

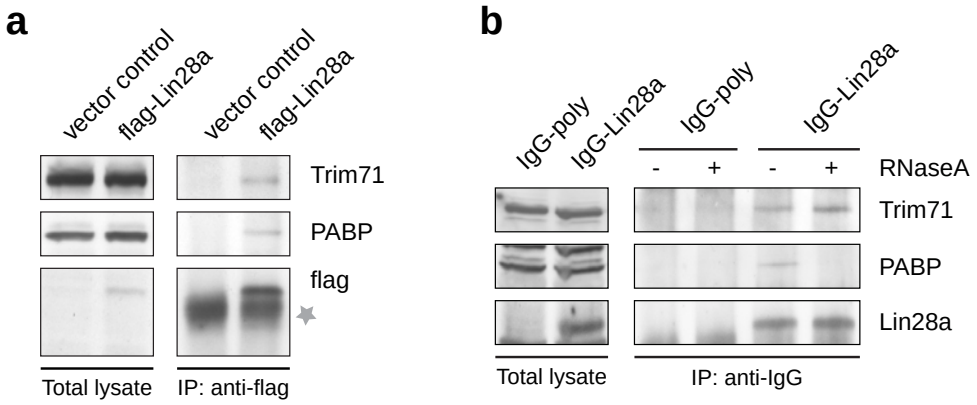

Figure 3.28: **RNA-independent protein interaction of Trim71 with Lin28a. (a)** Flag-tagged Lin28a was overexpressed in wildtype mESCs and immunoprecipated from the total lysate. Trim71 as well as the known interactor PABP were specifically found in the Lin28a enriched sample. The grey star marks the antibody light chain. **(b)** Similar procedure as in (a) but IP-fractions were additionally treated with or without RNaseA to eliminate RNA-mediated binding of proteins.

to impede let-7 suppressive activity [90]. Trim71 interacted with similar efficiency with the Lin28a WT protein as well as with a Lin28a construct lacking the CCHC domains and the double point mutant which is able to bind but not suppress pre-let-7 miRNAs (figure 3.29a). However, Trim71 binding was nearly completely abolished upon deletion of the CSD of Lin28a. A similar binding pattern was observed for the known interactor PABP (figure 3.29a). Thus we concluded that the 74 amino acid long CSD of Lin28a is required and sufficient for the interaction with Trim71.

Lin28 is a multifunctional protein as it was proposed to likewise interact with mRNAs as well as miRNA precursors (reviewed in [240]). Likewise, Lin28a was described to be localized to various subcellular compartments [90]. In order to further strengthen the claim of a relevant interaction of Trim71 and Lin28a we performed microscopic co-localization analysis. Since ESCs have a very low cytoplasm to nucleus ratio which hinders the discrimination of specific cytoplasmic compartments, the colocalization analysis was performed in HEK293T cells. Flag-tagged Trim71 and mRFP-tagged Lin28a were co-overexpressed and cells were subsequently subjected to immunofluorescence staining. Indeed, we found a rather broad subcellular localization pattern of Lin28a in both nucleus and cytoplasm. On the other hand, Trim71 was majorly found in precise perinuclear speckles formerly identified as P-bodies [145] (compare also 3.20). We found overlapping fluorescence signals

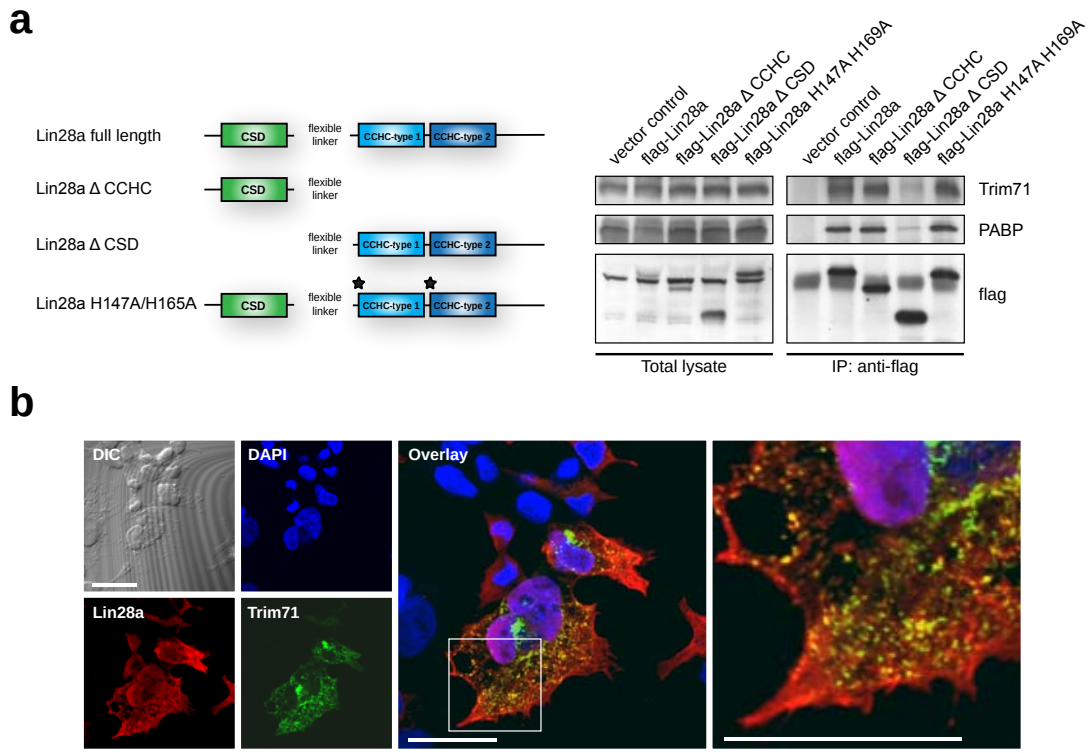

Figure 3.29: **The interaction of Trim71 with Lin28a is mediated by the cold-shock domain of Lin28a. (a)** Different Lin28a deletion and mutation constructs were overexpressed in wildtype mESCs. Trim71 could be co-precipitated with any construct containing an intact cold shock domain (CSD). PABP was used as a positive control and showed similar binding characteristics. **(b)** Co-localization of Trim71 and Lin28a in perinuclear P-bodies. Immunofluorescence staining of overexpressed mRFP-Lin28a (red) and flag-Trim71 (green) together with DAPI nuclear stain (blue) in HEK293T cells. Scale bar represents 20 µm.

of both proteins in these structures, which might be part of the interaction platform for Trim71 and Lin28 (figure 3.29b)..

In our analysis of the mRNA repression activity of Trim71 we found that the E3-ligase mutant of Trim71 was not able to repress specific target genes. Therefore, we wondered whether the activity of Trim71 to regulate let-7 miRNA expression is similarly dependent on this enzymatic function. To answer this question, we overexpressed Trim71 WT, the double point mutant of the RING domain (C12L/C15A) or a control plasmid in wildtype mESCs. We found that 48 hours post transfection the levels of mature let-7a and let-7g were decreased in both Trim71 WT and Trim71 E3-ligase mutant overexpressing cells in comparison to the control transfected cells (figure 3.30a).

In order to show that protein binding of LIN28A to TRIM71 is also not impaired when using the E3-ligase mutant we performed a co-precipitation experiment in HEK293T cells. Surprisingly, quantification of the relative protein enrichment of TRIM71 WT and E3-ligase mutant revealed that the binding to LIN28A was even stronger for the Trim71 E3-ligase mutant in comparison to TRIM71 WT protein (figure 3.30b). Accordingly, we found that mostly the lower-running, non-ubiquitinated, pool of the overexpressed TRIM71 WT protein was bound to LIN28A in the IP-fraction. Conversely, TRIM71 binding with AGO2 was decreased by mutation of the RING domain (figure 3.30c and figure 3.20b). This result implied that the pool of Trim71 protein that is regulating mRNAs is distinct from the Trim71 pool regulating let-7 miRNA expression and that the balance between both functions is regulated by auto-ubiquitination of Trim71/TRIM71.

3.3.5 Trim71 cooperates with both Lin28 paralogs in mice and humans

As mentioned earlier the genome of mammals codes for two highly similar Lin28 paralogs. all analyses so far have been performed using the Lin28a isoform because it is the predominantly expressed variant in mESCs. However, depending on the cell type, the Lin28b variant can substitute its function. Therefore, we were interested whether Trim71 is likewise able to cooperate with the Lin28b variant when present. Figure 3.31a shows a comparative structural overview of the Lin28a and Lin28b isoforms in mice and humans which share 97 and 87 % identity on amino acid level, respectively. In contrast to Lin28a, Lin28b possesses an additional C-terminal extension which harbors an additional nuclear localization signal (NLS) [66]. Notably, it was found that both paralogs are able to shuttle between nucleus and cytoplasm, indicating that other sequences, presumably in the linker region, can also serve as NLS [66].

First, we screened a panel of different human cell lines for their endogenous expression levels of TRIM71, LIN28A and LIN28B by RT-qPCR and WB. We found that a number of embryonic carcinoma cell lines, *i.e.* NCCIT, 2102EP and NTera-2, indeed co-expressed all three proteins (figure 3.31b and c). Furthermore, the hepatocellular carcinoma cell line HepG2 as well as the seminoma cell line TCam-2 were found to express TRIM71 together with LIN28B. Notably, there were two cell lines, JKT-1 and Jurkat T-cells which did not express significant levels of any of the investigated proteins (figure 3.31b and c). Taken together, we concluded that Trim71 expression always coincides with expression of at least one Lin28 isoform, thus enabling a functional cooperation of both proteins in these cell types.

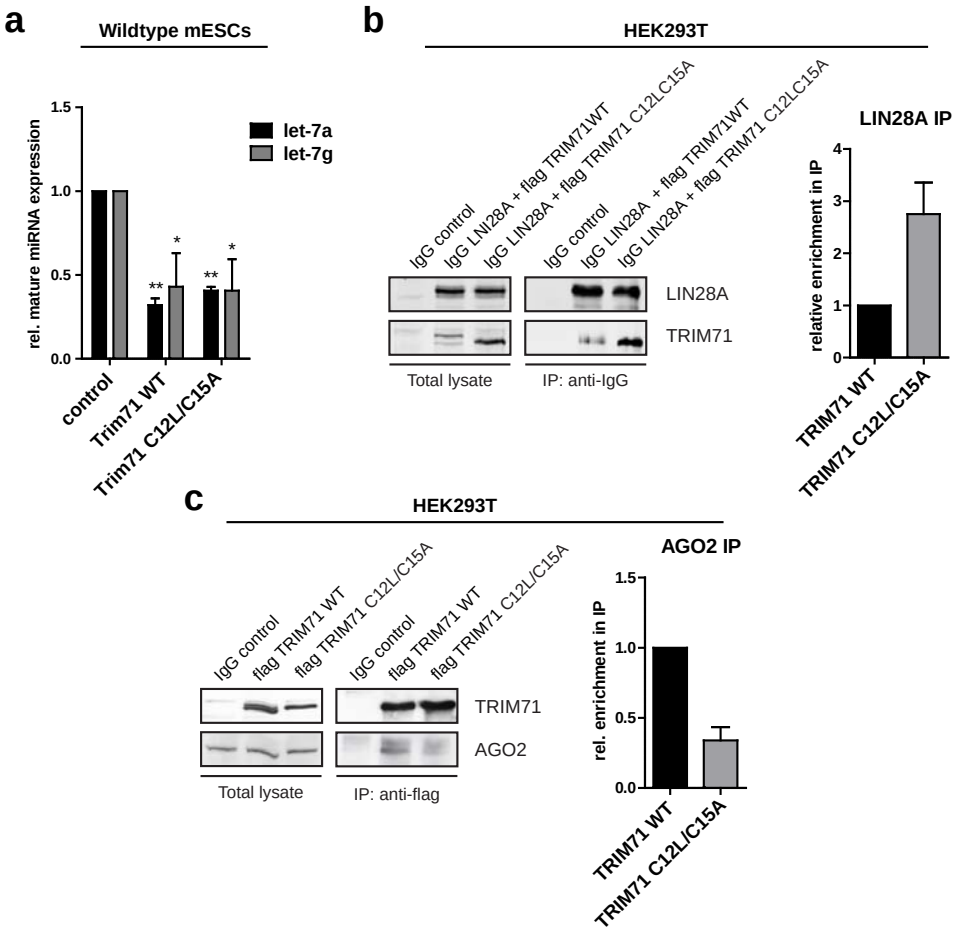

Figure 3.30: **Lin28a preferentially associates with non-ubiquitinated Trim71. (a)** Overexpression of Trim71 WT or the point mutant of Trim71 in wildtype mESCs and measurement of let-7a and let-7g levels 48 hours post transfection by RT-qPCR (ANOVA, Tukey's test; n=3; * p<0.05, ** p<0.01). **(b)** Representative WB of Lin28-IP with Trim71 in HEK293T cells and quantification of relative enrichment relative to Trim71 WT construct (n=2). **(c)** Same as in (b) with AGO2-IP in HEK293T cells (n=2).

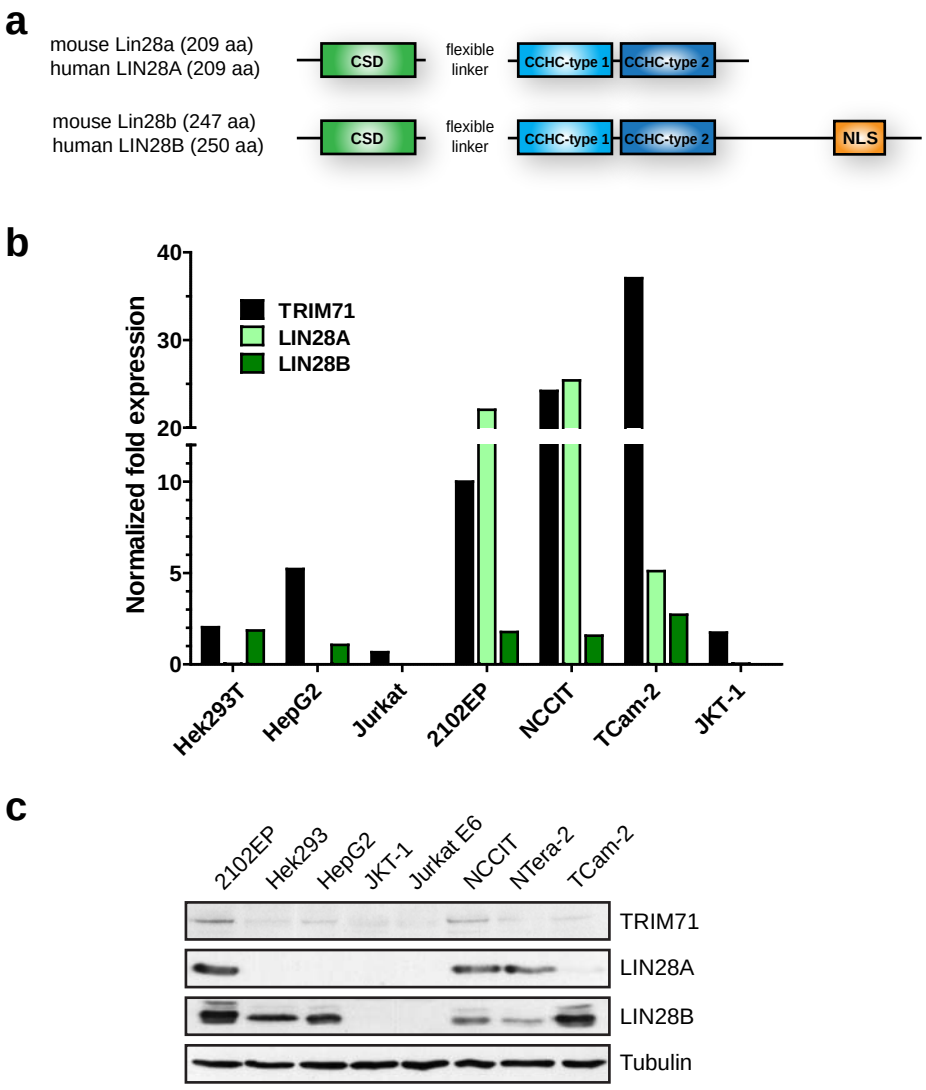

Figure 3.31: **TRIM71 is frequently co-expressed with LIN28A or LIN28B in human cell lines (a)** Overview of the domain structure of mouse and human Lin28a/LIN28A and Lin28b/LIN28B. **(b)** Expression analysis in human cell lines shows differential expression of both Lin28 isoforms. **(c)** WB analysis in the same cell lines.

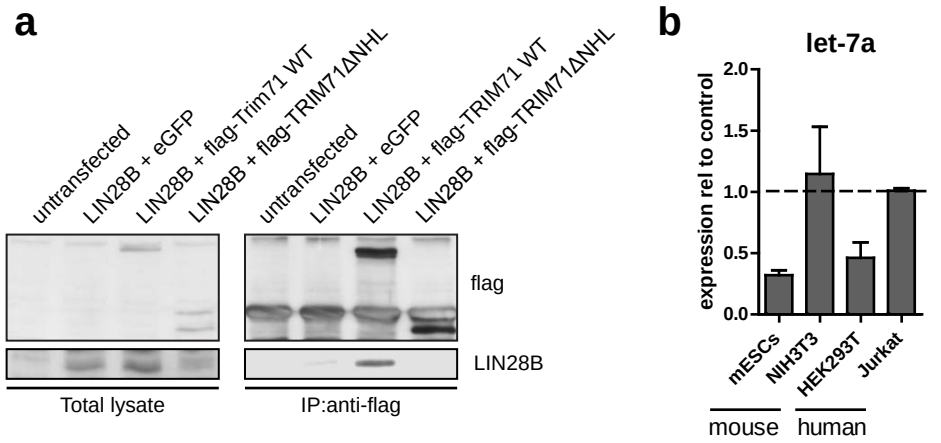

Figure 3.32: **Interaction of Trim71 and Lin28b contributes to Trim71 dependent let-7 regulation. (a)** Representative WB showing co-immunoprecipitation of TRIM71 with LIN28B in HEK293T. **(b)** Diagram showing relative expression of mature let-7a in different human and murine cell lines after overexpression of TRIM71/Trim71 (n=2-7).

To further investigate into cooperativity of TRIM71 with LIN28B, we performed immunoprecipitation of TRIM71 and LIN28B in HEK293T cells. After overexpression and precipitation flag-tagged Trim71 constructs, we could specifically enrich LIN28B together with Trim71 WT protein (figure 3.32a). However, when we instead used a TRIM71 variant lacking the NHL domain the interaction was abolished. This proved that Lin28b/LIN28B is like Lin28a/LIN28A able to interact with Trim71. For a functional validation of the cooperativity, we overexpressed either Trim71/TRIM71 WT or a control vector into two human and two murine cell lines and measured let-7a levels by RT-qPCR. Whereas overexpression of Trim71 led to a relative reduction of mature let-7a in mESCs and in HEK293T cells this was not the case for the NIH3T3 fibroblasts and the Jurkat T cell lines (figure 3.32b). In contrast to Hek293T cells, which are positive or LIN28B, Jurkat T-cells do not express any LIN28 isoform (see 3.31). The same holds true for the NIH3T3 fibroblasts [241] which did also not display a decrease in let-7 content upon Trim71 overexpression. In contrast, let-7a was reduced after overexpression in mESCs which express Lin28a and to a lesser extent Lin28b. This experiment unambiguously showed that the ability of Trim71 to regulate let-7 levels is mediated by Lin28a proteins which need to be co-expressed in the same cell.

3.3.6 Homozygous gene targeting of the Lin28a locus assisted by TALENs in mESCs

In order to further support the hypothesis of cooperativity between Trim71 and Lin28a with regard to let-7 expression regulation in mESCs, we wanted to test whether Trim71 can still regulate let-7 in the absence of Lin28a. Therefore, we generated a double mutant mESC line which was deficient in both Trim71 and Lin28a. This required the mutation of both Lin28a alleles in the background of the Trim71 conditional allele mESCs. The Lin28a gene is located on chromosome 4 and consists of four exons, all of which contain coding sequences (see figure 3.33a). The classical strategy of homologous recombination is very suitable to introduce defined mutations but has very low success rate. Instead, we performed an approach of *in vitro* mutagenesis using transcription activator-like effector nucleases (TALENs) for site-specific genome editing. We transfected a Lin28a-specific TALEN pair together with a targeting construct introducing a stop site and a neomycin resistance cassette flanked by homology regions (figure 3.33b). The insertion of the neomycin resistance cassette increased the number of positive clones after positive selection and also facilitates screening by PCR, since wildtype and targeted alleles were easily distinguishable.

The transfection of the Lin28a targeting construct alone yielded about double as many mESC clones as the transfection of the TALEN pair which can be considered as the background level (figure 3.34a). The number of G-418-resistant clones was again doubled when cotransfecting the targeting vector together with the TALEN pair, showing that the efficiency of genome integration was increased. Individual G-418-resistant mESC clones were picked and screened by PCR (figure 3.34b). Out of 48 picked mESC clones, the genotypes of 36 could be determined by PCR screening. Of those, more than 50% showed the expected band for the targeted allele which indicated that there was at least one site-specific integration event (figure 3.34c). Moreover, 17% of all analyzed mESC clones did not show a corresponding wildtype allele signal, indicating that both alleles underwent homozygous recombination. Thus, TALEN-assisted mutagenesis dramatically increased the efficiency and accuracy of gene targeting. As a proof for the success of the Lin28a targeting mutagenesis, three clones identified as $Lin28^{WT/WT}$ (wildtype), $Lin28^{WT/KO}$ (heterozygous) and $Lin28^{KO/KO}$ (knockout) were analyzed by WB for Lin28a protein expression. As expected, the Lin28a knockout cell clone exhibited no Lin28a protein signal, while the heterozygous clone had a slightly reduced Lin28a amount in comparison to the wildtype clone (figure 3.34d).

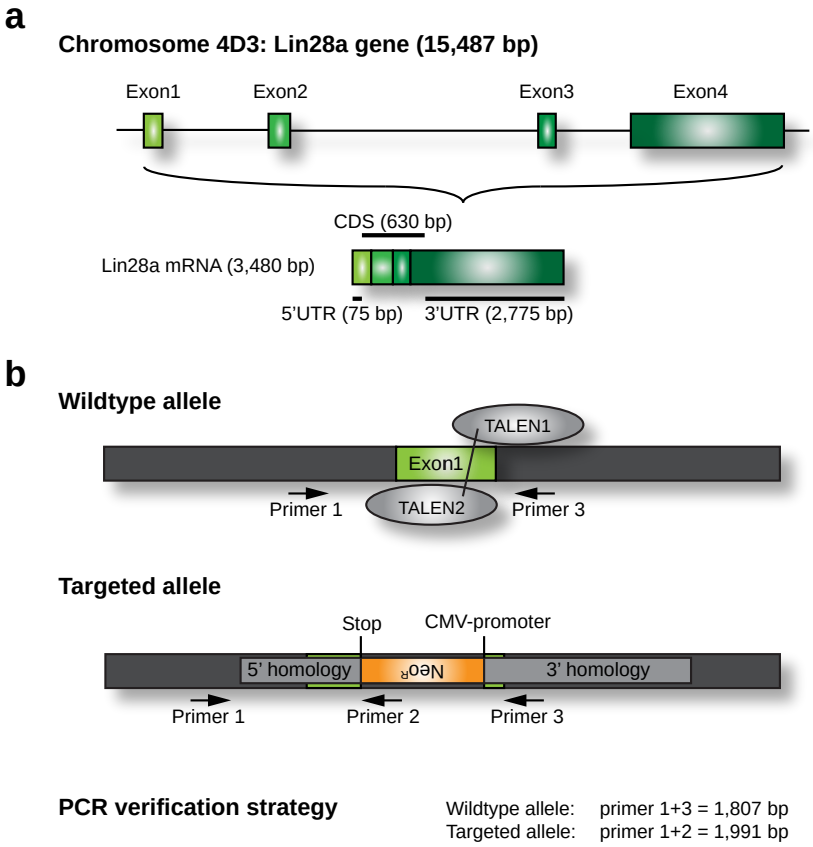

Figure 3.33: **Strategy for the generation of TALEN-assisted mutagenesis of the Lin28a genomic locus. (a)** Genome organization and mRNA splicing of Lin28a. **(b)** A TALEN pair was designed to bind to sequence within the first exon of Lin28a in close proximity of the start codon. Integration of the targeting construct via homologous recombination will disrupt translation and furthermore lead to the expression of an antibiotic resistance gene. The screening for recombined clones was done with a PCR using a set of three primers generating PCR products of different lengths.

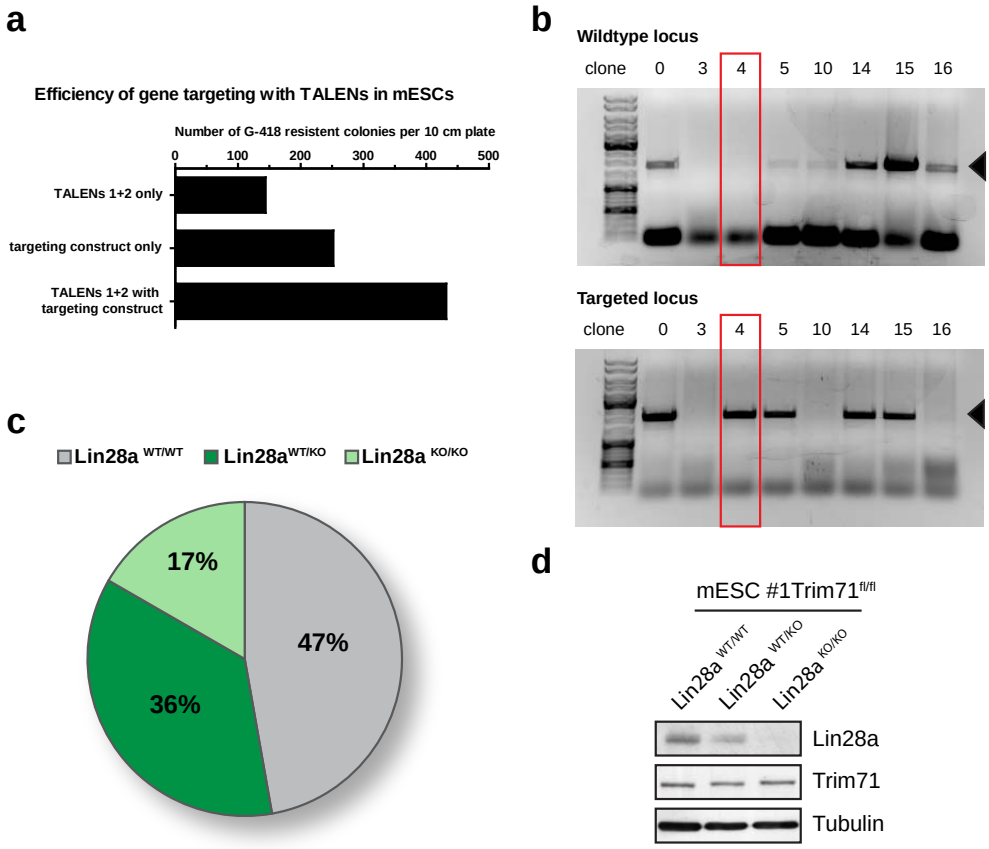

Figure 3.34: **Generation of Lin28a knockout mESC lines by TALEN-assisted mutagenesis.** **(a)** Co-transfection of TALENs together with the targeting construct markedly increases the number of G-418 resistant clones. **(b)** Representative genotyping PCR on Lin28a wildtype and targeted locus. Red box marks a homozygously targeted clone. **(c)** Statistical analysis of targeting efficiency showing that more than 50% of the clones had integrated at least one copy of the partially homologous donor DNA (n=36). **(d)** WB analysis verifies the absence of Lin28a protein in a homozygously targeted mESC clone.

For all further analyses we used one Lin28a homozygously targeted mESC clone and compared it the parental Trim71$^{fl/fl}$ clone. Additional Cre activation by 4-OHT treatment allowed the generation of four different mESCs genotypes originating from just one parental Trim71$^{fl/fl}$ mESC line (figure 3.35a). For convenience, the different mESC genotypes are in the following just called wildtype (Trim71$^{fl/fl}$, Lin28a$^{+/+}$), Lin28a KO (Trim71$^{fl/fl}$, Lin28a$^{-/-}$), Trim71 KO (Trim71$^{-/-}$, Lin28a$^{+/+}$) and Trim71/Lin28a dKO ((Trim71$^{-/-}$, Lin28a$^{-/-}$). Figure 3.35b illustrates that the conversion of the Trim71 allele after 4-OHT treatment works very efficiently also in the Lin28a-deficient mESC background. Whereas we could detect remaining Lin28a mRNA, there was no evidence for intact Lin28a protein in Lin28a KO mESCs (figure 3.35b and c). Interestingly, we found that the mRNA expression of Trim71 in Lin28a KO mESCs was significantly increased in comparison to wildtype cells (figure 3.35c). However, this increase did not yield changes in Trim71 protein expression. Because we were furthermore interested whether the Lin28a paralog, Lin28b, would be affected by compensatory feedback regulation, we also monitored Lin28b protein expression by WB analysis. However, in contrast to previous publications, neither Trim71 nor Lin28a deficiency resulted in increased expression of Lin28b [78, 155] (figure 3.35b and c).

As there are until now no data available describing complete Lin28a deficiency in mESCs, we first had to verify that stemness was not impaired of Lin28a deficient mESCs. All knockout mESC lines were morphologically indistinguishable from the parental mESC line (figure 3.36a). Furthermore, we measured the mRNA expression of Oct4 and Nanog by RT-qPCR and found no significant differences between the different mESC lines. Taken together, we did not observe any impairments in stem cell maintenance, arguing that, like Trim71, Lin28a is not an essential component of the mESC-regulating network.

Next, we measured the levels of pre- and mature let-7a and let-7g in the different knockout mESC lines. We found that the pre-let-7 levels were unaltered in all knockout cells (figure 3.37a and b). In contrst to that, the levels of mature let-7a and let-7g were dramatically increased in Lin28a KO cells in about the range that has been previously reported after efficient Lin28a knockdown in mESCs [242]. This increase was more pronounced than the relative let-7 increase observed in Trim71 KO cells, indicating that Trim71 is mostly a modulating Lin28a function. Also the Trim71/Lin28a dKO cell line had significantly more mature let-7 than wildtype control cells. However, in comparison to Lin28a single KO cells, there was no additional effect on let-7 expression in Trim71/Lin28a dKO mESCs (figure 3.37a and

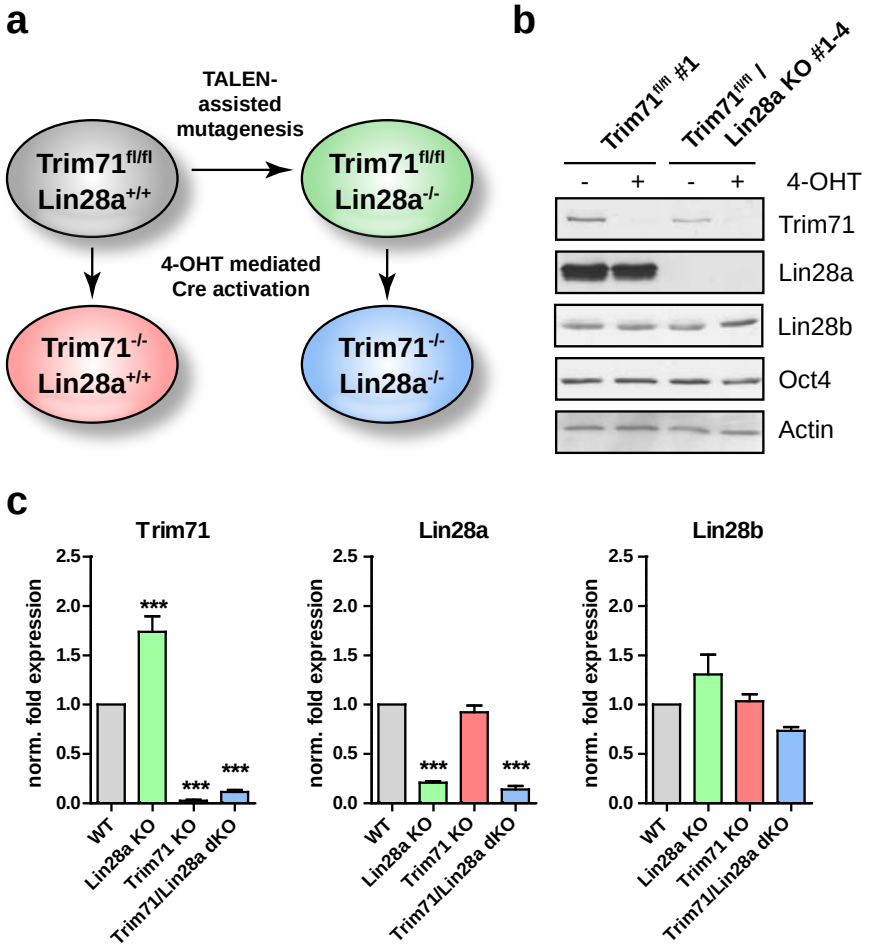

Figure 3.35: **The generation of Trim71/Lin28 double knockout mESCs. (a)** Scheme showing the derivation of different knockout mESC lines. WB **(b)** and RT-qPCR analysis **(c)** confirming Trim71 deletion in the background of Lin28a knockout mESCs after application of tamoxifen. In contrast, Lin28b expression is not significantly affected. Expression was calculated relative to Gapdh and values are depicted as means +SEM (ANOVA, Tukey's test; n=3-9; *** p<0.001).

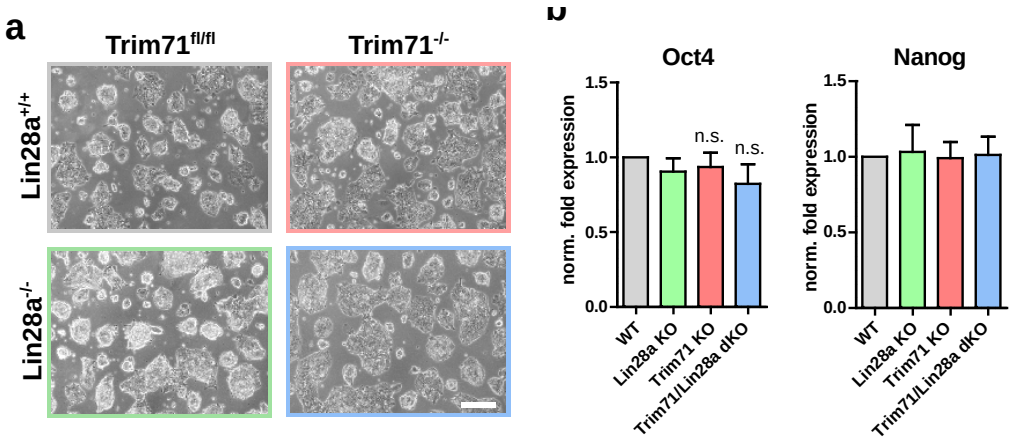

Figure 3.36: **Lin28 and Trim71-deficient mESCs shown no deficiency in the maintenance of stemness. (a)** Bright field microscopic images of different stem cells grown on gelatin. Scale bar represents 200 µm. **(b)** mRNA expression of the stemness genes Oct4 and Nanog relative to WT cell levels. Values are depicted as means +SEM (ANOVA, Tukey's test; n=5-6; n.s. not significant).

b). In order to analyze the impact of the knockout-induced let-7 overexpression on potential target genes, we performed a reporter assay with a Renilla luciferase construct containing 8 let-7 binding sites in its 3'UTR [183] (figure 3.37c). In Trim71 KO mESCs the let-7 responsive reporter gene was slightly, but nevertheless significantly, repressed in comparison to wildtype control cells (figure 3.37d). However, in accordance with the stronger increase of let-7 expression, the reporter repression was more pronounced in Lin28a KO cells. In comparison to the Lin28a single KO, the downregulation of the let-7-reporter was similar in Trim71/Lin28a dKO mESCs, again highlighting that Trim71 effects are mdiated by Lin28a function in mESCs.

The binding of Lin28a to let-7 precursors is mediated by two critical structural characteristics of the pre-miRNA. On the one hand, Lin28 proteins can recognize and bind to a GGAG RNA motif in the pre-let-7 loop [243, 239]. On the other hand, a guanine-rich bulge in the dsRNA adjacent to the Dicer cleavage site was proposed to play a role in target specificity [243]. The GGAG RNA sequence was also identified as a consensus motif for mRNA binding and is majorly depending on the CSD of Lin28a [77, 78]. Other miRNAs also have conserved GGAG motifs in their terminal loop sequence *e.g.* miR-107, -143, -200c, -324 and -363. These miRNA were proposed to respond to Lin28a knockdown in a similar fashion like let-7 [64]. Thus, we tested two of those miRNAs (miR-107 and miR-143) and one

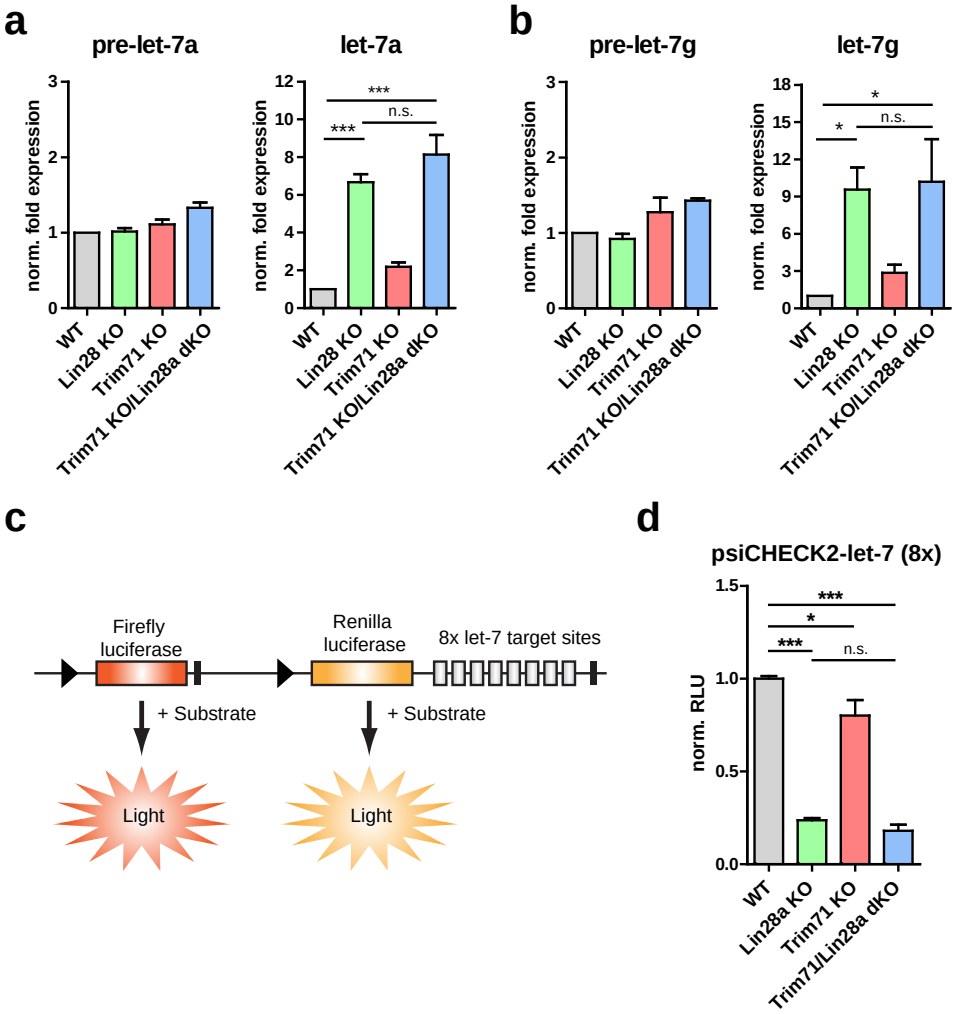

Figure 3.37: **Both Trim71 and Lin28a deficiency result in de-repression of let-7 target genes in mESCs.** RT-qPCR analysis of precursor and mature let-7a **(a)** and let-7g **(b)** relative to the reference U6 snRNA. Values are means +SEM, n=2-7. **(c)** Principle of reporter assay with 8 let-7 response elements in the 3'UTR of a Renilla luciferase cDNA. **(d)** Relative repression of a let-7 responsive reporter construct as shown in (c) which was transfected in different knockout mESC lines. Results are mean +SEM of 4 independent experiments (ANOVA, Tukey's test; n.s. not significant, * $p<0.05$, ** $p< 0.001$).

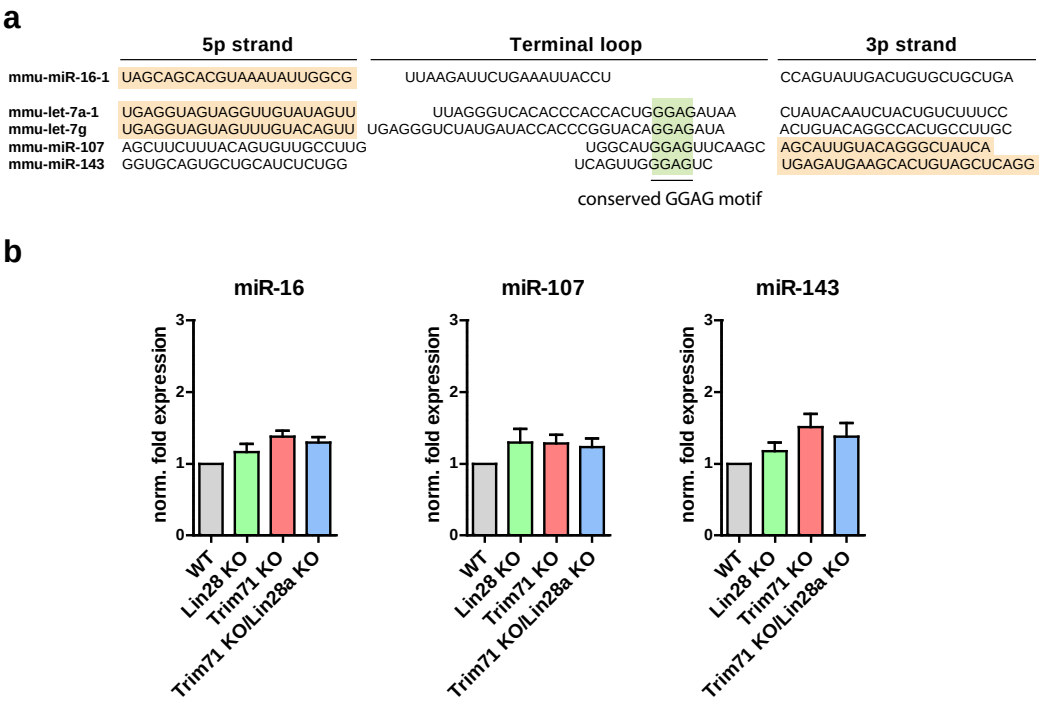

Figure 3.38: **The GGAG sequence in the stem loop of miRNA precursors alone is not sufficient for Lin28a and Trim71-dependent repression. (a)** Several miRNAs share a conserved GGAG sequence in their terminal loop (highlighted in green) of the miRNA precursor. The respective mature miRNAs are marked in orange. **(b)**The expression levels of GGAG-containing miRNAs miR-107 and miR-143 as well as the unrelated miR-16 were unaltered in Trim71 and Lin28a knockout conditions. Values are relative expression to U6 snRNA and are depicted as means +SEM, n=4-11 (ANOVA, Tukey's test).

control miRNA lacking the GGAG motif (miR-16) for changes in expression in the different knockout mESC lines (figure 3.38a). However, none of the investigated miRNAs were significantly elevated in Trim71 or Lin28a KO cell lines (figure 3.38b), indicating that miRNA regulation is not only dependent on the sequence motif located at terminal loop but that other structural features also play an important role.

To obtain a complete overview of the global mRNA expression changes in the different knockout mESC lines, we performed another RNA-seq analysis of all four genotypes in collaboration with the group of J. L. Schultze (LIMES institute, Bonn). In comparison to the Trim71 knockout mESCs, the amount of DE genes was substantially higher in Lin28a KO and in Trim71/Lin28a dKO mESCs (2.5% in comparison to 12.9% and 10.5% of all genes, respectively) (figure 3.39a). This suggested that Lin28a has a broader target mRNA spectrum. However, we were most of all interested whether Trim71 and Lin28a also cooperate in mRNA target regulation. Figure 3.39b illustrates the overlap of DE genes that were either significantly upregulated or downregulated in the different KO mESC lines. In general, there was a striking overlap of DE genes between Lin28a KO and Trim71/Lin28a dKO mESC lines. For further analysis we concentrated on the DE genes in Trim71 KO mESCs and evaluated those in the context of the other mutant mESC lines. We found that among the significantly downregulated genes in Trim71 KO mESCs very few genes showed concomitant regulation in Lin28a KO cells (figure 3.39c). In contrast, when analyzing the genes that were identified as upregulated in the Trim71 KO mESCs, we found that the majority of those (52%) were actually also upregulated in the Lin28a KO mESCs. From those about 90% were likewise significantly overexpressed in the Trim71/Lin28a dKO mESCs. In contrast, fewer than expected genes were counterregulated in this group (figure 3.39c). This suggested that Trim71 specifically cooperated with Lin28a in target gene suppression, whereas the upregulation of target genes was specific to Trim71 and Lin28a, respectively.

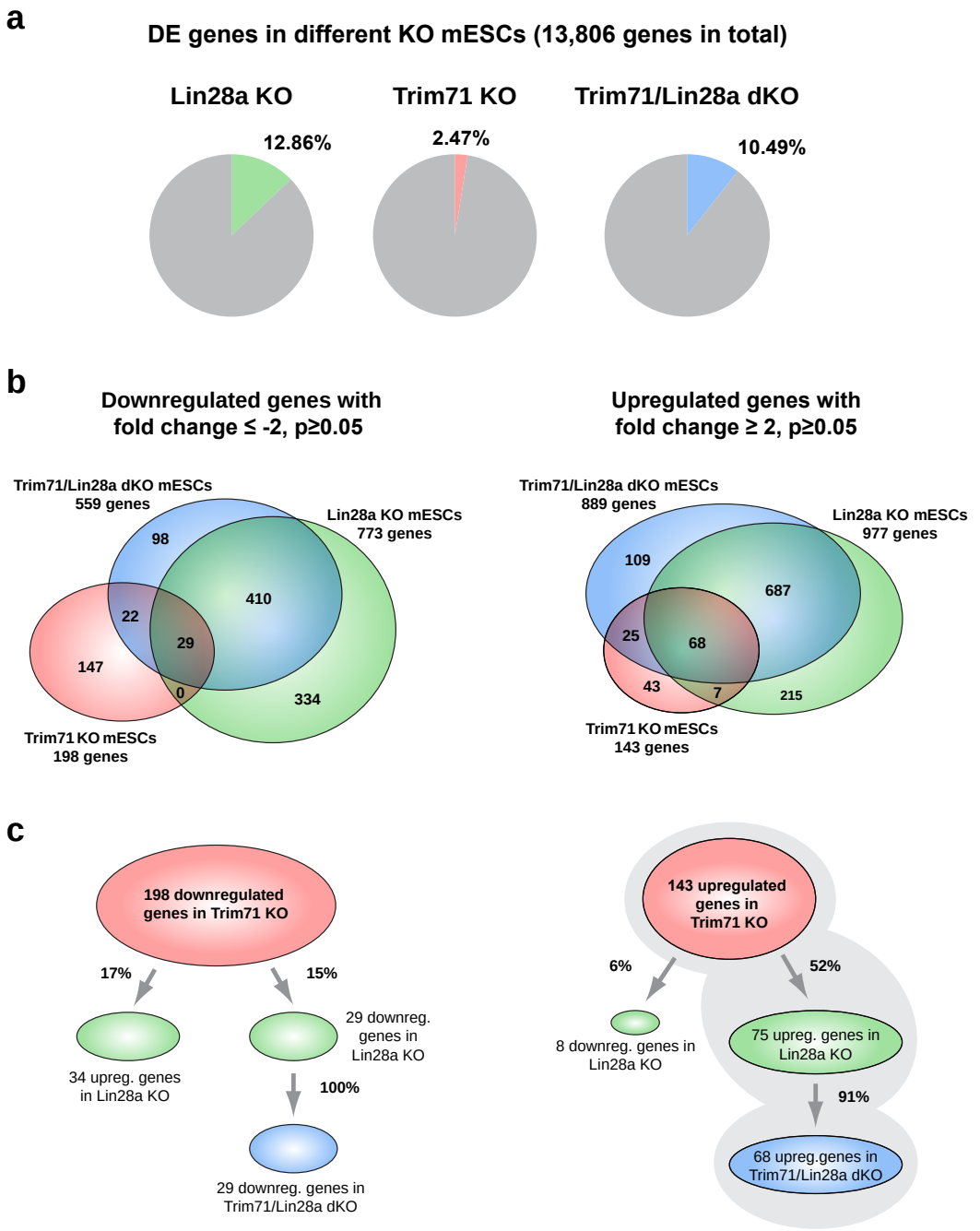

Figure 3.39: **Cooperativity of Lin28a and Trim71 in the repression of specific target genes in undifferentiated mESCs. (a)** Pie charts indicating the percentage of DE genes with $|FC| \geq 2$ and $p \leq 0.05$ in the genome of different KO cell lines. **(b)** Overlap of down- (left) and upregulated (right) genes from (a) visualized in Venn diagrams. **(c)** Tree diagrams focusing on up- and downregulated DE genes in Trim71 KO cells. Grey background highlights majorly overlapping path.

3.4 The role of Trim71 in germ cell development

3.4.1 Trim71 expression is restricted to spermatogonial stem cells (SSCs) in testes

The role of Trim71 in adult tissues and organs is still unknown, however, several studies have shown endogenous expression of Trim71 in mESCs. Intriguingly, there is a significant overlap of proteins which are important for ESCs as well as for gonadal stem cells [244, 245]. In fact, one study has shown that Trim71 is expressed in the testes of adult mice [145]. We wanted to validate theses findings and hypothesized that Trim71 expression could originate from the stem cell niche in mouse testis - the spermatogonial stem cells (SSCs). In order to prove this, we dissected the testes of 12 week old mice and prepared a cell suspension of the seminiferous tubules. SSCs were enriched by CD90.2 (also known as Thy1.2)-FITC antibody staining with subsequent magnetic activated cell sorting (MACS) using anti-FITC antibody coupled microbeads. Both positive and negative fractions were collected. Using this method we could enrich the fraction of CD90.2 positive cells about fivefold (from 2.4 % to 13.2 %) (figure 3.40a and b). We performed RT-qPCR and WB with the whole cell population as well as with positive and negatively enriched cell populations. We found that the Trim71 mRNA signal was increased about fourfold in the CD90.2 enriched population in relation to the whole cell population (figure 3.40c). This reflects quite accurately the increase in the amount of SSCs in comparison to the initial cell pool. As a positive control, we also measured Lin28a and Sall4 mRNA expression which are established marker genes for SSCs [86, 246, 247]. Both genes were elevated to a similar extent as Trim71 in the enriched cell population. In contrast, Lin28b mRNA which was reported to be transiently expressed in postmitotic spermatids as well as in interstitial Leydig cells was slightly decreased in CD90.2-positive SSCs [248]. In accordance with the mRNA expression data, we found that Trim71 and Lin28a protein signals were higher in CD90.2 positively selected cells whereas this was not the case for Lin28b (figure 3.40d).

In order to further prove that Trim71 must be primarily originate from undifferentiated spermatogonia we recorded the expression of SSC marker genes during postnatal development and early spermatogonia differentiation. The pool of adult SSCs is established after birth by the transient population of gonocytes. In the male germline, the gonocytes are quiescent until shortly after birth when they start to migrate into the seminiferous tubule basement membrane (figure 3.41a). From this point they are referred to as SSCs. Concomitantly, the cell pool is expanded by

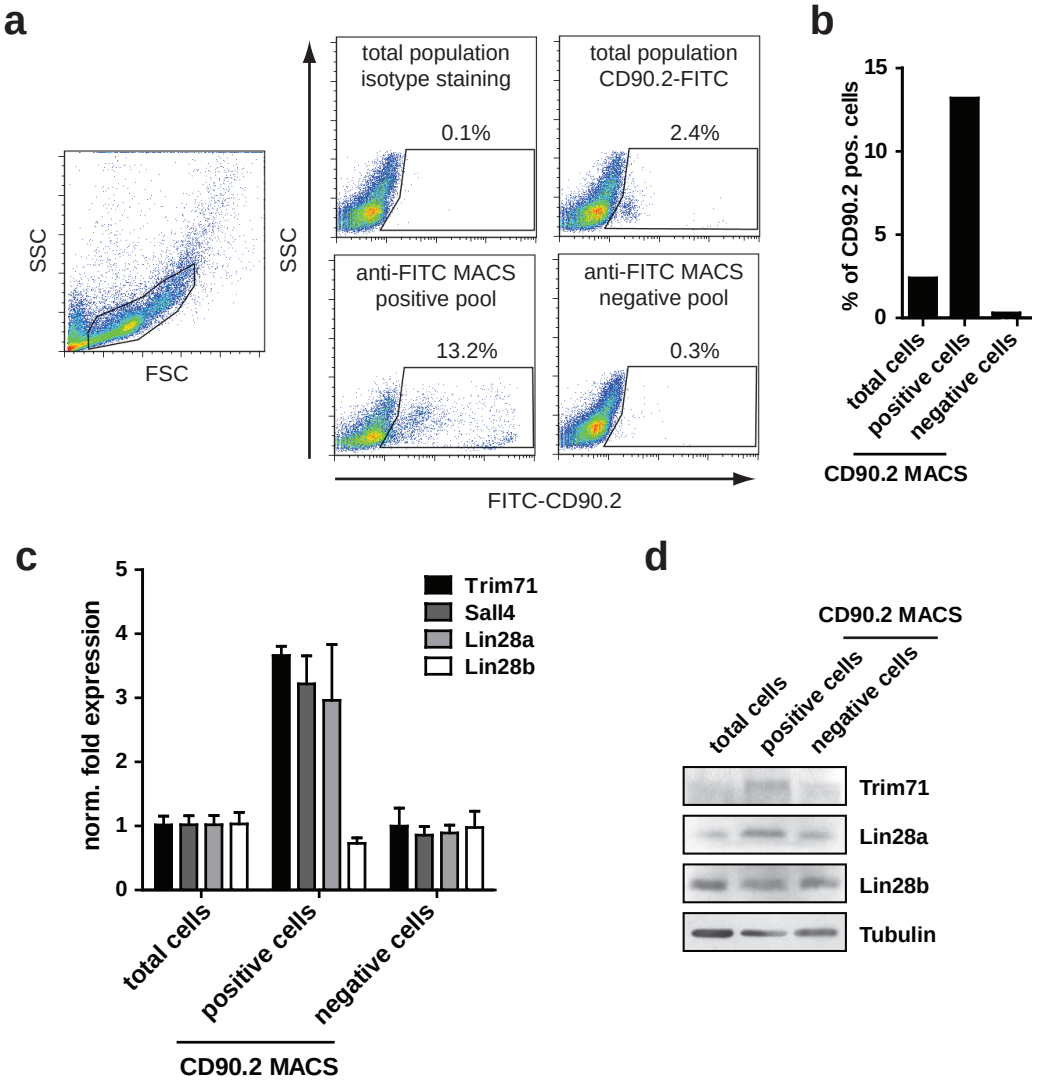

Figure 3.40: **CD90.2 positive spermatogonia express Trim71. (a)** CD90.2-positive cells were enriched from testicular cells using MACS, resulting in a 4-fold enrichment of CD90.2 positive cells **(b)**. **(c)** RT-qPCR analysis of Trim71 and spermatogonial marker genes before and after CD90.2 MACS. **(d)** WB analysis confirms Trim71 expression in positively-selected cells.

re-entering of the cell cycle. This expansion of the SSCs results in a characteristic increase of SSC marker expression at around 1 to 2 weeks after birth. At this time the first SSCs start to differentiate to give rise to the first wave of spermatogenesis. Therefore, the number of undifferentiated SSCs decreases again and is stabilized thereafter to maintain a stem cell pool throughout life. In order to analyze Trim71 expression during postnatal development we took samples of testes of wildtype mice from day 0 (day of birth) to 8 weeks (adult). We analyzed the tissue samples for expression of Trim71, Lin28a and Lin28b as well as Sall4 (figure 3.41b-e). We found a peak expression of Trim71 between days 7 and 14. This was similar for the SSC markers Lin28a and Sall4. In comparison, Lin28b peak expression was delayed, with its peak expression between days 14 and 21 (figure 3.41d) with the beginning of spermatogonia differentiation. These results were confirmed on protein level using WB (figure 3.41f). Taken together, these results strengthened the hypothesis that Trim71 expression in testes originates from undifferentiated SSCs.

3.4.2 Trim71 deficiency results in infertility in male and female mice

In order to analyze the requirement of Trim71 expression in the gonads, Trim71 conditional mice were used to generate germline-specific adult Trim71 knockout mice. For this purpose homozygously floxed Trim71 females were crossed with Trim71 heterozygous males which additionally expressed the Cre recombinase under the control of the endogenous Nanos3 promoter (figure 3.42a). Endogenous Nanos3 expression is restricted to primordial germ cells (PGCs) as early as E7.25 and and remains expressed throughout spermatogenesis [159, 201, 250]. This crossing scheme yielded 25% germ-line-specific Trim71 knockout animals which are at the same time heterozygous for Trim71 in all other tissues (figure 3.42a). For a first functional evaluation of the Trim71 effect, adult $Trim71^{fl/-}$/Nanos3 Cre mice were crossed with wildtype mice. However, neither homozygously targeted males nor females were able produce offspring in the course of several weeks. This suggested that Trim71 deficiency results in complete infertility in both sexes. The mice were sacrificed and the reproductive organs were prepared. Macroscopic analysis revealed that both ovaries and testes were drastically reduced in size indicating severe defects in the germline of Trim71-deficient mice (figure 3.42b and c).

As the weight of the testis correlates with sperm count in mice and thus has a predictive value for fertility [251, 252] we measured the testis weight of adult mice also including mice with additional genotypes of the parental strains. Whereas all the wildtypic allele combinations (wildtype and floxed alleles) had similar testes to

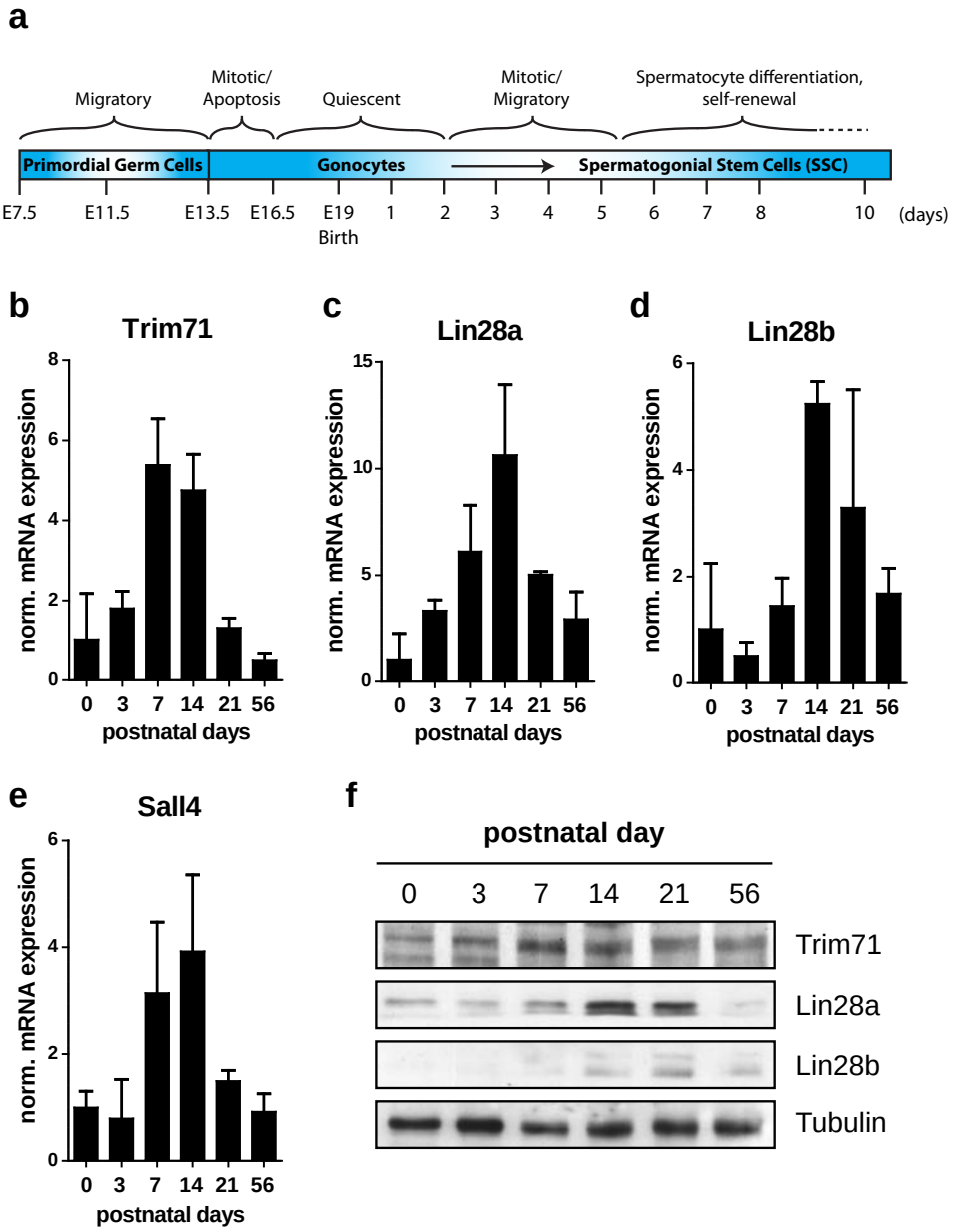

Figure 3.41: **Trim71 expression in mouse testis during postnatal development. (a)** Schematic overview of pre- and postnatal development of male germ cells. Modified from Culty *et al.* (2009) [249]. RT-qPCR analysis of Trim71 **(b)** as well as Lin28a **(c)**, Lin28b **(d)** and Sall4 **(e)** at indicated time points after birth. Data are means +SD normalized to day 0 (n=3). **(f)** WB showing peak expression of Trim71 between days 7 to 14 after birth.

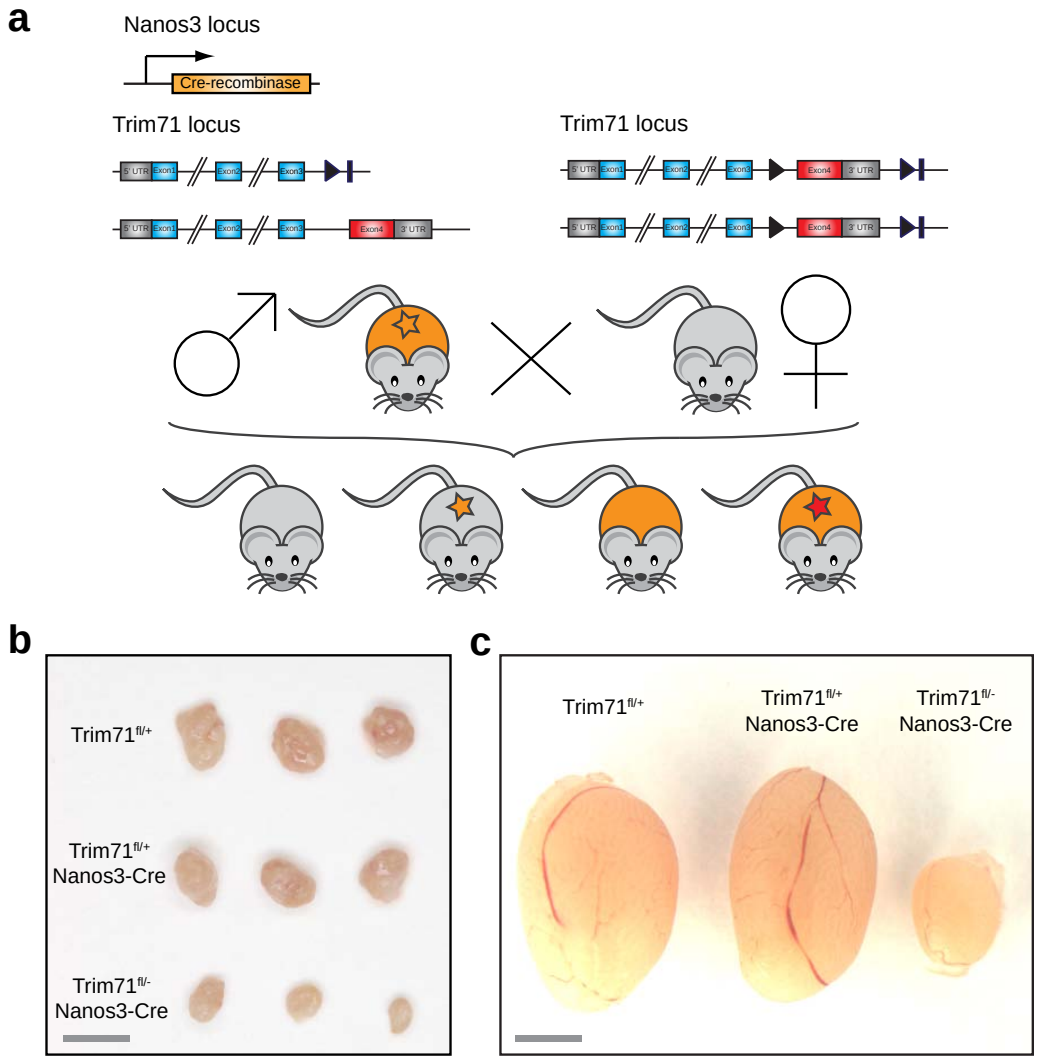

Figure 3.42: **Mouse breeding strategy for the generation of germline-specific Trim71 knockout mice. (a)** Heterozygous males additionally carrying the Nanos3 Cre allele were crossed with homozygously floxed Trim71 females. Grey indicates WT (wildtype and floxed), orange heterozygous and red homozygous Trim71 mutation. The star represents the germline (ovary and testis) in adult males and females. **(b-c)** Representative images of Trim71 ovaries (b) and testes (c) of Trim71/Nanos3-Cre animals. Scale bar represents 2 mm.

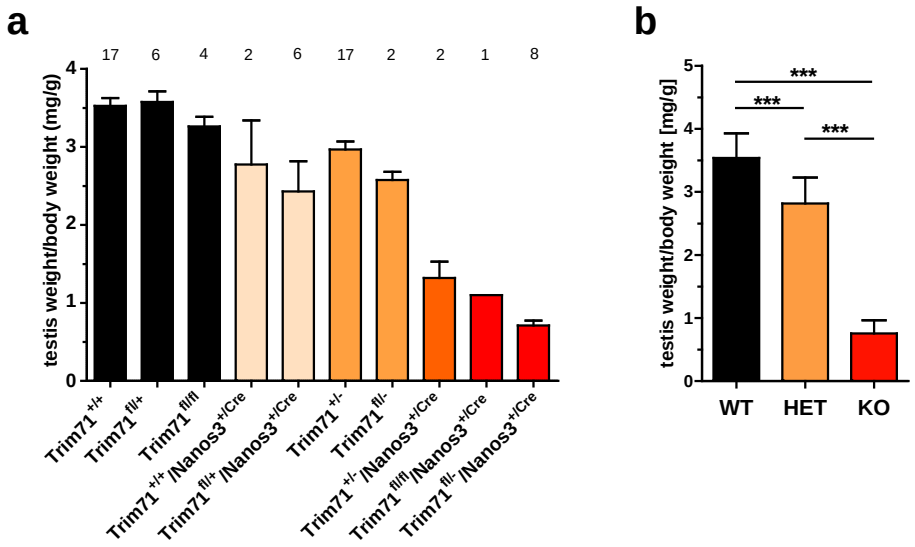

Figure 3.43: **Trim71 expression levels are critical for normal testis development. (a)** Testis weight ratios of different genotypes of Trim71/Nanso3 intercrosses. Values are mean +SEM. Numbers above columns indicate the number of analyzed individuals.**(b)** Summary of (a) and statistical analysis testis size from animals wildtype (WT), heterozygous (HET) and knockout (KO) for Trim71 (ANOVA, Tukey's test; n=9-27; *** p<0.001).

body weight ratios, the Nanos3-Cre-containing mice displayed a tendency towards smaller testes (figure 3.43a). This might be explained by the fact that the Cre cDNA substitutes the endogenous Nanos3 cDNA and thus the Cre-positive mice are by definition heterozygous for Nanos3. Notably, this effect was in the range of Trim71 heterozygous testes which is in congruence with the general observations made in heterozygous Trim71 males (see figure 3.43b). Surprisingly, we found that the combined effect of Trim71 and Nanos3 heterozygocity had a remarkable effect on testes size leading to a weight reduction of more than 50%. Complete knockout of Trim71 led to drastically reduced testis size (figure 3.43a and b). We also found one male mouse that had transferred a floxed allele from a Nanos3 carrying parental mouse. This is only possible when Trim71 recombination rates were not 100%. Taken together, this analysis showed that Trim71 is essential for a proper development of the mouse testis.

For further analysis of the male germ cell compartment, the expression of SSC markers was analyzed by RT-qPCR and WB. For this purpose, the before mentioned categories of wildtype (WT), heterozygous (HET) and knockout (KO) animals were analyzed. In germ cell KO animals the expression of Trim71 was reduced by about 90%, arguing that the recombination rates were generally high,

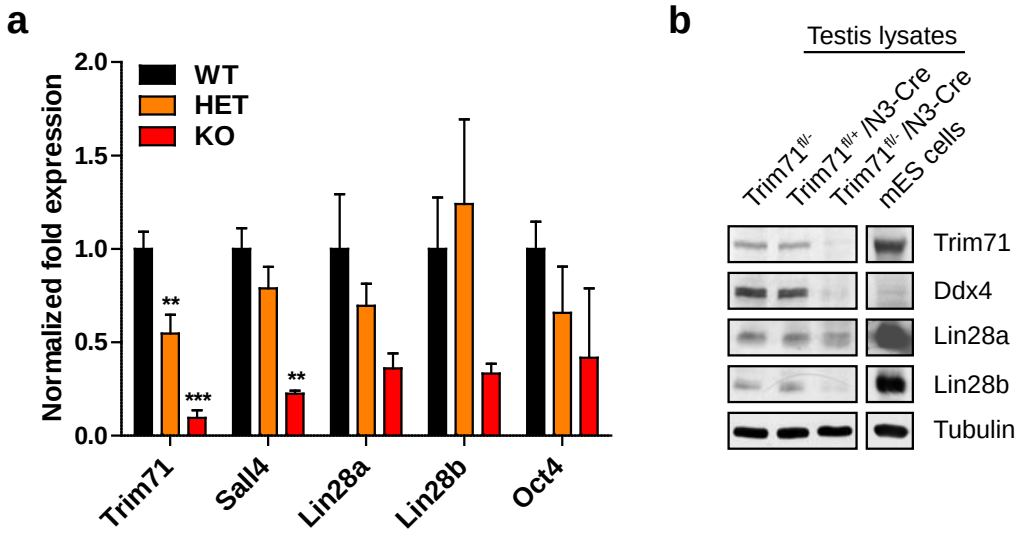

Figure 3.44: **Trim71-deficient adult testes lack SSCs. (a)** RT-qPCR analysis of wildtype (WT) heterozygous (HET) and knockout (KO) testis for markers genes of spermatogenesis. Values are mean +SEM (ANOVA, Tukey's test; n=3-7; ** $p<0.05$, *** $p<0.001$) **(b)** WB analysis reveals absence of SSC marker expression in Trim71-deficient testes.

but not complete (figure 3.44a). Nevertheless, there was a strong downregulation of the analyzed SSC marker genes Sall4, Lin28a and Oct4. Furthermore, in Trim71 heterozygous animals there was also a tendency for downregulation of the same SSC markers, coinciding with the already reduced testis size in heterozygous males. The marker gene Lin28b which is expressed in both Leydig cells and maturing spermatocytes showed a downregulation in the knockout but no alteration in the heterozygous animals arguing that organ integrity is generally still preserved in testes of heterozygous animals. These results were highly congruent with the protein analyses from testis tissue that revealed strong downregulation of Lin28a, Lin28b and the germ cell marker Ddx4 in Trim71 deficient testes (figure 3.44b).

Next, we wanted to investigate if Trim71 expression is required for initial PGC specification during embryonic development. In order to exclude that at the beginning of germ cell specification the expression of the Nanos3-driven Cre expression is not yet sufficient for Trim71 deletion, Trim71 heterozygous animals were mated to yield complete Trim71 knockout embryos. Embryos at stages E8.5 and E8.75 were dissected and the alkaline phosphatase (AP)-positive PGCs were stained. At stage E8.5 PGCs were detected in close proximity to the allantois in both Trim71-deficient and wildytpe embryos (figure 3.45). We found similar numbers of AP-positive PGCs in Trim71-deficient and control embryos and in both groups PGCs

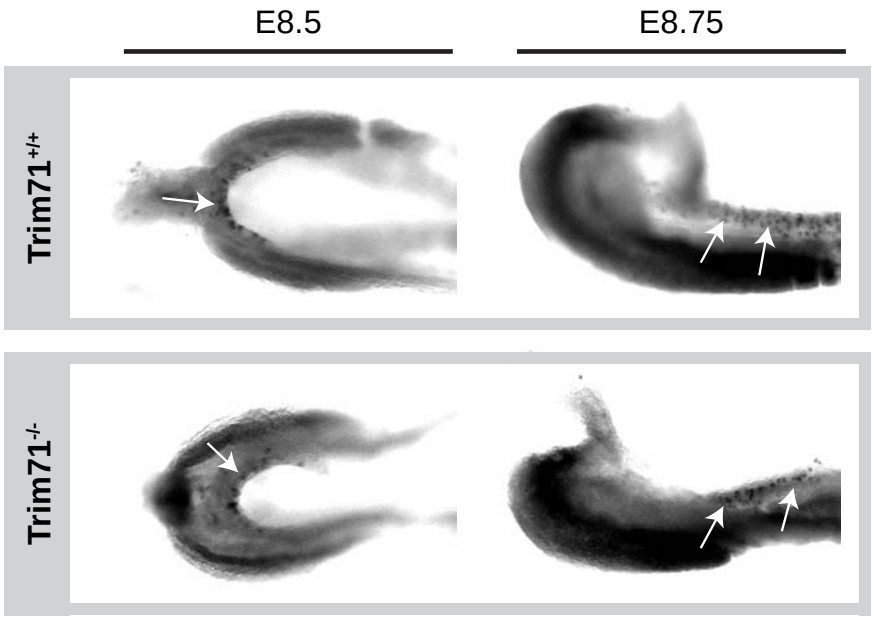

Figure 3.45: **Trim71 deficiency does not impair PGC specification during embryogenesis.** Alkaline phosphatase staining in Trim71 wildtype and knockout embryos. Alkaline phosphatase-positive PGCs (white arrows) in posterior hindgut pieces from E8.5 (dorsal view) and E8.75 (lateral view) sibling embryos from a Trim71$^{+/-}$ mating.

started to migrate along the hindgut at E8.75. These results suggested that Trim71 deficiency elicited the loss of PGCs at later stages of germ cell development.

During the migration and after the arrival of the PGCs at the genital ridges, the germ cell founder population strongly increases in numbers. Because proliferation is an important process in PGC development and Trim71 has been formerly implicated in proliferation regulation, we wanted to investigate this specific aspect in more detail. However, the assessment of absolute cell numbers is difficult *in vivo*. Hence, we used an *in vitro* cell model to analyze the impact of Trim71 knockdown on proliferation. We could show before that the human seminoma cell line TCam-2 endogenously expresses Trim71 (figure 3.31). Knockdown of Trim71 using two different siRNA oligos resulted in a long lasting decrease of cell proliferation (figure 3.46a and b). Concomitantly, we observed an increase in expression of the negative regulators of cell proliferation p53, p27 and p21 (figure 3.46c). Therefore, it can be assumed that Trim71 might be also important for the expansion of the germ cell pool during embryogenesis.

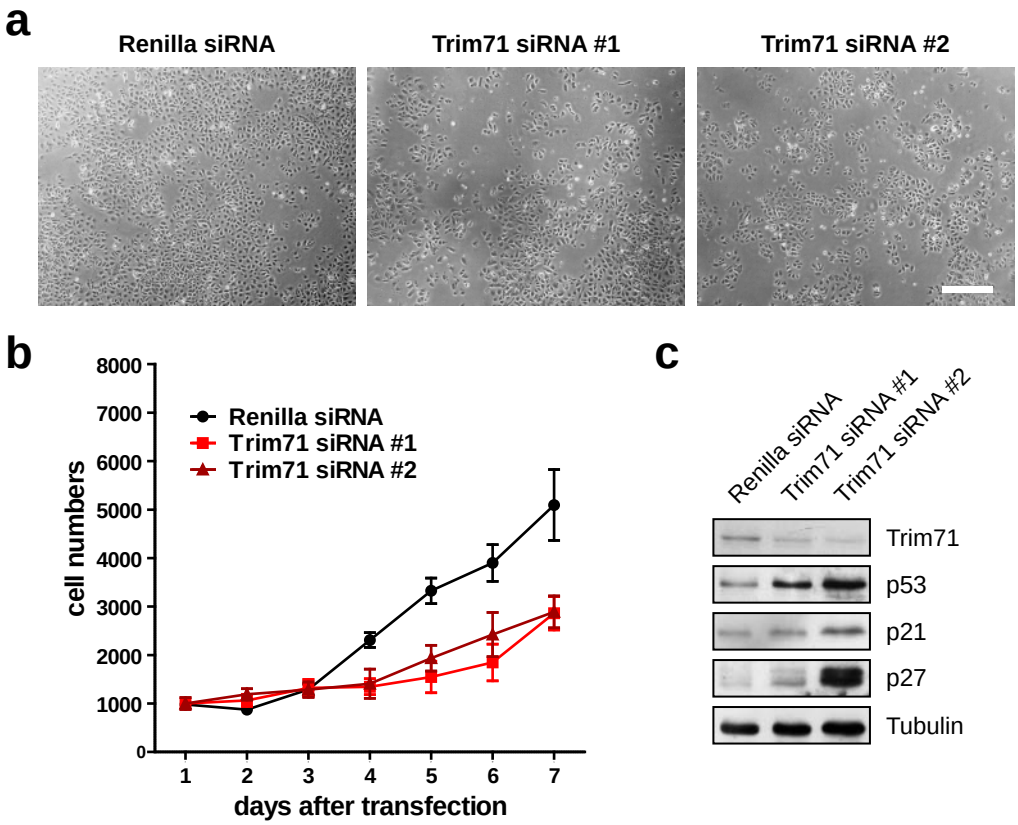

Figure 3.46: **Trim71 is a positive regulator of proliferation in the seminoma cell line TCam-2. (a)** Bright field microscopy of Trim71 and control siRNA treated TCam-2 cells four days after transfection. Scale bar represents 200 µm. **(b)** Normalized cell numbers in the time course of 7 days post transfection. The graph shows one representative experiment with three technical replicates. **(c)** Expression analysis of proliferation regulators seven days after siRNA treatment by WB.

4 Discussion

Developmental biology has tremendously profited from extensive studies that were performed using simple model organisms. The reason for this is the high degree of conservation of genes involved in developmental processes. Despite the undeniably large differences regarding morphology, complexity and environmental adaptation of the investigated organisms, numerous studies have pointed out that key developmental regulators are consistently maintained during evolution from the nematode to human [253]. While the investigation of developmental phenotypes were often the key for elucidating gene functions, most of these genes have later on been shown to be likewise involved in other biological contexts and conditions. Trim71 is a prime example for genetic conservation, since homologs of this gene can be found in all common animal model systems, including the nematode, fruitfly, zebrafish and the mouse. Human Trim71 shares more than 90% identity on protein level with its mouse homolog, and 41.2% identity with the nematode homolog *lin-41* [254].

In the year 2000, the nematode homolog of Trim71, *lin-41*, was identified as a downstream target of the miRNA let-7 and an essential component of the heterochronic pathway [147]. 15 years after the initial discovery of *lin-41*/Trim71 we are now introducing the first Trim71 conditional mouse line which allows advanced analysis of Trim71 functions both *in vivo* and *in vitro*.

We started with the phenotypic analysis of the Trim71 full knockout mouse which was generated with the help of a new conditional targeting allele. We found that homozygous deletion of Trim71 caused the death of all homozygous animals before E13.5 [131, 255, 151]. Furthermore, starting at day E9.5, the mutant embryos displayed severe growth deficits. We could show that Trim71 plays an essential role in embryonic neurodevelopment because Trim71 deficient mice exhibit a neural tube closure defect leading to an exencephalus phenotype. The gathered information suggest that Trim71 is essential for normal embryonic development and in particular for the development of the central nervous system. Taken together, our phenotypic analysis of Trim71 deficiency using the new Trim71 conditional

mouse line further supports published data using other Trim71 knockout alleles [131, 151, 255]. This is remarkable considering the different structure of Trim71 targeting constructs used. While our new Trim71 conditional allele enables the deletion of the last of four exons, coding for a part of the coiled coil region and the NHL domain of Trim71, other gene trap insertion mutations disrupt the Trim71 gene already after the first exon [131, 255]. This suggests that the NHL domain, which is affected in all reported mouse alleles, is essential for Trim71 protein function.

Apart from the embryonic phenotype of Trim71 mutant mice, we noticed that also Trim71 heterozygously targeted adult mice displayed specific defects, which has not been reported so far. Usually heterozygous deletion phenotypes are comparatively rare, because reduction of the mRNA/protein amount by half is usually well tolerable. However, in Trim71 heterozygous mice both male and female mice displayed a growth retardation resulting in a reduced body weight and length. This is very characteristic for metabolic defects and cannot be sufficiently explained with the currently known expression pattern of Trim71 in the adult organism [131]. Database studies have shown that both the haploinsufficency phenotype in mice as well as the functional association of a gene with early development morphogenesis predisposes a gene to be haploinsufficient in humans, too [256, 257]. Whereas it is quite likely that homozygous mutations of Trim71 would lead to the death of the embryo during early development also in humans, single loss-of-function mutation carriers might exist. Currently, there are only 13 haploinsufficient genes known that cause growth retardation in humans [256] and thus Trim71 might be a so far unknown disease gene.

4.1 Trim71 negatively regulates differentiation in mESCs by suppression of pro-differentiation mRNAs and miRNAs

In comparison to the description of the embryonic Trim71 knockout phenotype, the data concerning the molecular function of Trim71 are less consistent. The NHL domain of Trim71 has been proposed to act as an RNA-binding domain (RBD) which enables the protein to function as a posttranscriptional regulator of target gene expression [152, 70, 156]. Independently of that, Trim71 has also been implicated in miRNA biology [145, 155].

All available studies so far either worked with RNAi-mediated knockdown or overexpression of Trim71 but both methods are very prone to generate artifacts. Therefore, there was a strong demand for establishing a defined knockout cell sys-

tem for Trim71, in order to solve fundamental issues raised in the last years of research on Trim71. Mouse embryonic stem cells (mESCs) are especially suitable as a model system because Trim71 is endogenously expressed in mESCs, where it was shown to belong to a pool of stem cell-specific RNA-binding proteins (RBPs) [70, 153, 152, 156]. Moreover, there have been controversial discussions whether or not Tim71 is actually required for mESC maintenance [153, 156].

Therefore, we derived mESC lines form Trim71$^{fl/fl}$- Rosa26-Cre-ER^{T2} mice to control Trim71 allele conversion *in vitro*. The major advantage of this *in vitro* mutagenesis system in comparison to individual knockout mESC clones is that it enables the comparison of Trim71 knockout mESCs with their cognate parental cell line. This is specifically important in the light of recent evidence for substantial inter-clone differences of human and mouse ESCs, for example regarding epigenetic marks [258, 259].

Notably, the mutagenesis of Trim71 in undifferentiated mESCs did not result in spontaneous differentiation and cell proliferation was not impaired. In order to obtain an unbiased overview on the mRNA and miRNA expression profile of Trim71-deficient and control cells, we performed high-throughput sequencing in collaboration with the group of J. L. Schultze (LIMES Institute, Bonn). Significantly, there were very few differentially expressed (DE) genes known to be involved in stemness regulation, which corroborates our evaluation of a normal stemness phenotype in Trim71$^{-/-}$ mESCs (see also the extended analysis in Mitschka *et al.* [172]). While the RNA-seq analysis revealed that some of the DE genes in TRim71-deficient mESCs were functionally associated with the regulation of proliferation and apoptosis, this seems not to be the primary function of Trim71 in mESCs, which proliferated normally in the absence of Trim71. In contrast, we clearly found diminished proliferation in the cancer cell line TCam-2 after Trim71 knockdown. Similar effects might play a role once differentiation is initiated and the levels of ESC-specific cell cycle regulating (ESCC) miRNAs decrease which were shown to actively support proliferation in mESCs [50]. In summary, Trim71 is not essential for mESC proliferation but this does not exclude the involvement of Trim71 in proliferation regulation in other contexts.

While the stemness network was clearly intact in Trim71-deficient mESCs, we found that many pro-differentiation genes were deregulated. Especially genes associated with neurodevelopment were affected. In addition, we could demonstrate that the measured changes in gene expression were not due to spontaneous differentiation but instead inherent in the whole cell population. Using two different

approaches, we could show that neural differentiation was enhanced in Trim71-deficient cells when mESCs were stimulated *in vitro*. This is very much in line with the prevalent phenotype in the mouse embryo lacking Trim71 expression, where a premature differentiation of neural precursor cells has been observed ([151] and Tobias Goller, unpublished data). It is tempting to speculate that an accelerated differentiation of neural precursor cells might be the cause of the malformations in Trim71 knockout embryos. Although there are studies performed on other genetic mutations that imply a connection between the neural differentiation behavior of mESCs *in vitro* and a neural tube closure defect *in vivo* [260, 261, 262], this needs to be further investigated in the case of Trim71.

The neuroectodermal priming of Trim71$^{-/-}$ mESCs clearly suggests that Trim71 might in general control neural differentiation. We found that Trim71 expression in the neuroepitheleum is steadily decreasing *in vivo* and this might be necessary to limit differentiation until the appropriate time point. Pro-differentiation mRNAs are constantly transcribed at low and medium levels in undifferentiated mESCs and RBPs like Trim71 are needed to suppress their protein expression posttranscriptionally. In line with this, an interesting study which had employed *C. elegans* as a model system has shown that Trim71 overexpression enhances the ability of neurons to regenerate axons [154]. Although we and others have not found Trim71 expression in neuronal stem cells, a very recent publication found that Trim71 becomes re-expressed in the postnatal brain in the ependymal stem cell niche [255]. Therefore, the controlled manipulation of Trim71 expression levels might help to increase the plasticity and connectivity of neuronal circuits after brain injury.

Concomitantly with the de-repression of pro-differentiation mRNAs in Trim71-deficient mESCs, we also found that the expression of neuro-specific miRNAs was enhanced in Trim71-deficient mESCs in comparison to wildtype cells. Among the upregulated miRNAs were the brain-specific miRNAs miR-9 and miR-124 which were shown to affect the neural lineage differentiation *in vitro* [263]. Furthermore, miR-9 target genes were have been shown to regulate neural progenitor proliferation, migration and differentiation also *in vivo* [264, 265]. Overexpression of miR-9 has been demonstrated to reduce the number of proliferating neural precursor cells in zebrafish [266], chicken [267] and mouse [268] embryos. In addition, Lim *et al.* showed that the overexpression of miR-124 in Hela cells shifts the mRNA expression profile towards that of brain [269]. The relevance of these two miRNAs for the instructive fate determination is further highlighted by the study of Yoo and colleagues who found that overexpression of these two miRNAs can convert human

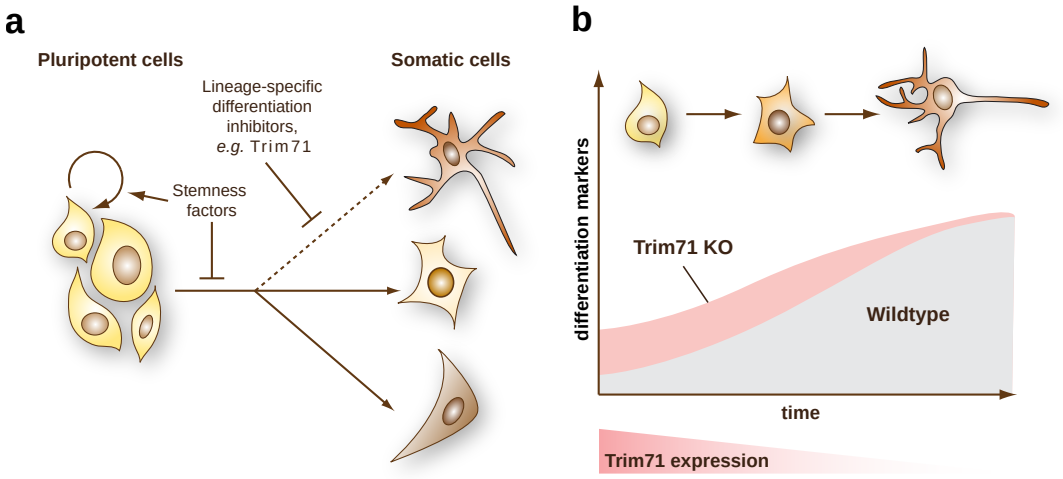

Figure 4.1: **Spatio-temporal control of cell fate differentiation by Trim71 (a)** Stemness-maintaining and differentiation-regulating factors guide lineage-specific mESC differentiation. **(b)** Enhanced neural differentiation in Trim71-deficeint mESC is casued by premature de-repression of pro-differentiation mRNAs and miRNAs.

fibroblasts into neuronal cells, a process that can be further facilitated by the addition of neuro-specific transcription factors [267]. Therefore, we speculate that the overexpresison of miRNAs that are relevant for neural commitment and differentiation might contribute to the functional phenotype seen in Trim71-deficient mESCs upon induction of differentiation.

Our analysis of undifferentiated mESCs showed that stemness-supporting and differentiation-limiting factors constitute distinct regulatory levels of stem cell maintenance (figure 4.1a). Therefore, activation of pro-differentiation mRNAs and miRNAs alone is not sufficient to induce differentiation. Furthermore, Trim71 seems to be a lineage specific differentiation inhibitor, which implies that several such regulators are acting together to guide lineage-specific cell fate determination. Although it cannot be excluded that those safeguards might additionally help to stabilize the undifferentiated cell state in mESCs, their actual importance becomes only apparent after downregulation of the stemness maintaining factors upon differentiation-inducing signaling (figure 4.1b). Further unraveling this second line of control will certainly help to understand the dynamics of cell commitment and is likely essential for the clinical application of stem cell therapy.

4.2 Trim71 decreases the stability of target mRNAs

Our unbiased mRNA sequencing identified both significantly down- and upregulated genes in Trim71$^{-/-}$ mESCs, together accounting for about 2.5-2.8% of the mESC transcriptome (depending on data normalization). Independent verification of the RNA-seq results performed on a group of candidate genes showed that the screening was highly reliable in identifying Trim71-mediated gene regulation targets. However, only some of the significantly upregulated genes in Trim71$^{-/-}$ mESCs were indeed targeted on posttranscriptional level in a Trim71-dependent manner. Hence, the other differentially regulated genes, especially the downregulated genes in Trim71$^{-/-}$ mESCs, must be the result of alternative Trim71-dependent mechanisms and indirect effects. Although the number of investigated genes needs to be further increased, these results support the notion that Trim71 primarily acts as a suppressor of mRNA stability. Trim71 might thus act as an adapter between specifically bound mRNAs and the mRNA-degrading machinery. Whether Trim71 might additionally influence mRNA translation efficiency of target mRNAs needs to be further investigated.

The characteristics of target repression were investigated in more detail using the 3'UTRs of two responsive genes: Plxnb2 and Foxj1. Significantly, both genes are also implicated in developmental processes. As a transcriptional regulator of motile cilia, Foxj1 regulates the commitment of cileated cells via modulation of cellular responses to Sonic hedgehog signaling in different tissues *e.g.* the airway epithelium [196] and the neural tube [270]. Foxj1 deficient mice exhibit defects in postnatal neurogenesis due to alterations in proliferation and differentiation of neural progenitor cells [197, 271]. Furthermore, Foxj1 was shown to be differentially regulated in different types of cancer [272, 273]. Plxnb2, on the other hand, is a transmembrane receptor for semaphorins that participates in axon guidance and cell migration. During development, Plxnb2 is expressed in the central nervous system but its mRNA expression becomes restricted to the subventricular zone of the brain and the vascular system in adults [192, 274].

By investigating these two candidate genes, we could gain valuable insights into the mechanism of Trim71-dependent mRNA repression. The NHL domain of Trim71 serves as the RNA-binding element [152] and seems to confer binding specificity, since overexpression of the structurally related Trim32 did not yield repression of Trim71 target genes. However, we found that the NHL domain alone is not sufficient for target gene repression. The N-terminal domains of Trim71 reg-

ulate target gene repression as well, either by modulating the binding of Trim71 to target mRNAs or by coupling these to downstream effector molecules. In addition, we found that the N-terminal coupling of a bulky eGFP-tag altered Trim71 protein functions, as cells overexpressing this N-terminally-masked Trim71 behave like Trim71$^{-/-}$ mESCs regarding mRNA suppression. This N-terminally-masked Trim71 protein is likely to compete with the endogenously expressed functional Trim71 for binding to response elements located in the 3'UTR of target mRNAs which results in de-repression.

We also identified a function of the intrinsic E3-ligase activity for target gene repression, since a RING domain mutant of Trim71 did not result in target mRNA regulation. Since it was shown that Trim71 can modify itself by auto-ubiquitination [145, 151] this suggests that the enzymatic activity of Trim71 intrinsically regulates its own function, *e.g.* target mRNA binding. Significantly, none of the currently proposed ubiquitination targets could be independently verified by others [145, 151, 155] which raises the question if the E3-ligase activity of Trim71 is rather a mean of self-regulation instead of needed for classical protein degradation. A similar mechanism has been identified for the TRIM-NHL protein Trim32, where it was found that exogenous signaling causes phosphorylation of Trim32, which in turn induces auto-ubiquitination. Ubiquitinated and non-modified Trim32 were shown to preferentially associate with separate protein complexes and also localize differently within the cells [275]. In line with this, unbiased mass spectrometric analysis performed in steady state mESCs and embryonic carcinoma cells has already provided evidence for both conserved phosphorylation and ubiquitination of Trim71 [276].

We could exclude the necessity of miRNA binding sites within the 3'UTRs for Trim71-dependent repression. However, it needs to be further investigated whether the entire miRNA protein machinery is likewise dispensable for the repression. For both analyzed candidate genes, Plxnb2 and Foxj1, several spatially separated Trim71 response elements were located apart from each other in the 3'UTR. By consecutive shortening of the 3'UTR we detected a step-wise decrease of reporter gene repression. This result is compatible with several interpretations: First, a number of short Trim71 binding sequences could be located within the 3'UTR and only the cooperative binding yields the full repression effect. Second, other mRBPs could be involved, which either function in a complex together with Trim71 or act in cis on binding to the mRNA. A similar mechanism has been recently proposed by Loedige and colleagues who found that the Trim-NHL protein Brat associates together with

Pumilio and Nanos, each of them binding to distinct sequence elements within the target mRNAs [141].

Until today the precise sequence requirements for Trim71 are still unknown and thus the identification of the consensus binding site will be a main research topic for the future. It must be highlighted that most mRBPs have very short binding sites which can also be degenerated and are thus difficult to identify. Methods like PAR-CLIP offer the possibility to catch RPBs in action and identify the bound mRNAs by subsequent sequencing.

4.3 Trim71 as a new regulator of let-7 biogenesis in mESCs

Apart from RBPs, miRNAs represent a second common cellular mechanism for posttranscriptional expression regulation. Several Trim-NHL proteins across different species have been proposed to regulate miRNA activity and biogenesis, *i.e.* NHL-2 [144], Mei-P26 [142] and Trim32 [143]. Trim71 was first associated with miRNA biology in a study which proposed Trim71 to be the mediator of Ago2 degradation, the bottleneck-protein of miRNA biogenesis and function [145]. In order to prove their hypothesis, the authors chose let-7 as a candidate miRNA and could show that let-7 expression was inversely proportional to Trim71 levels. However, several studies trying to recapitulate these results could not find Trim71-dependent downregulation of Ago2 [151, 152, 153]. In parallel with the present study another publication came out which identified Lin28b as a binding partner and ubiquitination substrate of Trim71. In line with this, they stated that Trim71 would actually be inducing let-7 expression [155]. Taken together, there has been an inconclusive debate on whether Trim71 affects miRNA expression and function, and if so, by which mechanism.

The studies published so far were either performing transient overexpression of Trim71 likely generating an unphysiological excess of protein in the cell, or siRNA-mediated knockdown, which on the other hand largely depends on Ago2 functionality. Both methodologies could thus produce undesired side effects which might not reflect the behavior of Trim71 in a normal cellular environment. Taking advantage of the new genetic mESC model for conditional Trim71 mutagenesis as well as by acquiring additional cell line data, we were able to shed light on this issue. We found that Trim71 deficiency leads to partial de-repression of mature let-7 miRNAs in mESCs. In congruence with others, we found that Trim71 associates with the RISC protein Ago2 in P-bodies [145, 151, 152, 153]. However, Ago2 protein

levels were completely unaffected in Trim71-deficient cells, arguing that Trim71 is not regulating Ago2 stability or turnover in mESCs. Nevertheless, some miRNAs still showed differential expression in Trim71 knockout mESCs, but this might be mostly due to an altered transcriptional regulation. However, in the specific case of let-7 miRNAs, we could find an increase of let-7 abundance in Trim71-deficient mESCs while let-7 transcription was unaffected.

As an alternative mechanism to Ago2 protein regulation, we propose the functional cooperation of Trim71 with Lin28 proteins for the efficient repression of let-7 maturation. The mechanism of let-7 miRNA repression by the stem cell protein Lin28 is a well accepted and thoroughly investigated aspect of miRNA research [236, 238, 239, 277]. Lin28 proteins have a high affinity for the conserved loop region of pre- and pri-let-7 miRNAs which allows Lin28 to compete with Dicer for pre-let-7 binding [238, 239]. Apart from sequestration, Lin28 can furthermore actively reduce the pool of available pre-let-7 miRNA by recruitment of the endonucleases Tut-4 and Tut-7, which modify precursor miRNAs by attaching several uridine residues [64, 238]. Poly-uridylated pre-miRNAs are then recognized and degraded by the endonuclease Dis3l2 [65, 242]. The Lin28b isoform might additionally sequester pri-let-7 in the nucleus [66]. The discovery of this mechanism solved an apparent paradox in stem cell research: The transcription rate of let-7 sequences is permanently high in undifferentiated ESCs while at the same time the levels of mature let-7 miRNAs are relatively low. Therefore, we identified Trim71 as a new modulator of the bistable switch of let-7 and Lin28 which regulates the balance between stemness and differentiation (figure 4.2).

We have mapped the region of interaction with Trim71 to cold-shock domain (CSD) of Lin28a which exhibits 84% identity at the amino acid level (Uniprot [278]) to closely related paralog Lin28b. Therefore, we were not surprised to also find an interaction between Trim71 and Lin28b. Both paralogs are found in the cytoplasm and the nucleus and the repertoire of bound mRNAs and miRNAs is in great part overlapping [63, 77, 89, 236, 237]. Because Trim71 is a strictly cytoplasmatic protein, the association of Trim71 is restricted to the cytoplasmic fraction of Lin28 proteins. In congruence with other studies we find that the expression of the Lin28 paralogs is cell type-dependent.

We found a striking pattern of coexpression of Trim71 with either Lin28a or Lin28b.This is likely the result of common transcriptional and posttranscriptional expression regulation. For instance, it was found that the transcription of both genes is majorly regulated by the transcription factor c-Myc [279, 280, 281]. Fur-

thermore, both genes are subject to posttranscriptional regulation by the miRNAs let-7 and miR-125 [208, 277]. Hence, there is a abundant expression of Trim71 and Lin28 in undifferentiated mESCs which declines upon induction of differentiation [70]. Both proteins are also strongly expressed during embryonic development [131, 151, 237, 282, 283]. The same applies for germline cells, which are positive for both Trim71 and Lin28a [86, 145, 248, 284].

Lin28a knockout results in postnatal death of the majority of homozygous offspring and the surviving animals display severe dwarfism [82]. Furthermore, also Lin28b was shown to be important for pre- and postnatal growth [81] similarly to Trim71 heterozygous knockout mice. Interestingly, a combined knockout of Lin28a and Lin28b results in embryonic death of all animals by E12.5. The affected animals also exhibit a retardation in growth and some additionally display a neural tube closure defect [81]. Very recently, Lin28a deficiency was also found to reduce neural progenitor proliferation in the developing brain [285]. Taken together, the described Lin28a/b deficiency phenotypes show striking similarities to the phenotype of Trim71 mutant mice and further corroborate a functional cooperation of Trim71 and Lin28 proteins.

Nevertheless, the question arises as to why there would be the need for an additional regulator of the let-7 biogenesis pathway apart from Lin28. The concept of Lin28 mediated let-7 repression still lacks an essential component: the switch that deactivates Lin28a repression once differentiation is induced. Up to this day, there is no mechanism known that would modulate the ability of Lin28 to bind to pre-let-7 or to deliver it to the degradation pathway. Our data indicate that the release of the interaction of Trim71 and Lin28a does partially release this repression of let-7 maturation, yet without inducing differentiation. In undifferentiated mESCs, opposing miR-290 miRNAs were shown to keep let-7 function in check [49]. As mentioned before, Trim71, as an E3-ubiquitin ligase, is able to mediate auto-ubiquitination. Again we found a relationship between the modification-state of Trim71 and its activity regulation. Whereas the E3-ligase mutant of Trim71 was not able to efficiently repress target mRNAs, the opposite was the case for Lin28 binding. The relative abundance of the modified versus the non-modified Trim71 could be decisive for let-7 repression activity and thereby the timing of differentiation (figure 4.2).

In the future, it will be of great interest to investigate by which mechanism Trim71 enhances the Lin28-dependent let-7 repression. One plausible option would be that the binding of Trim71 directly increases the affinity of Lin28a for the let-7 precur-

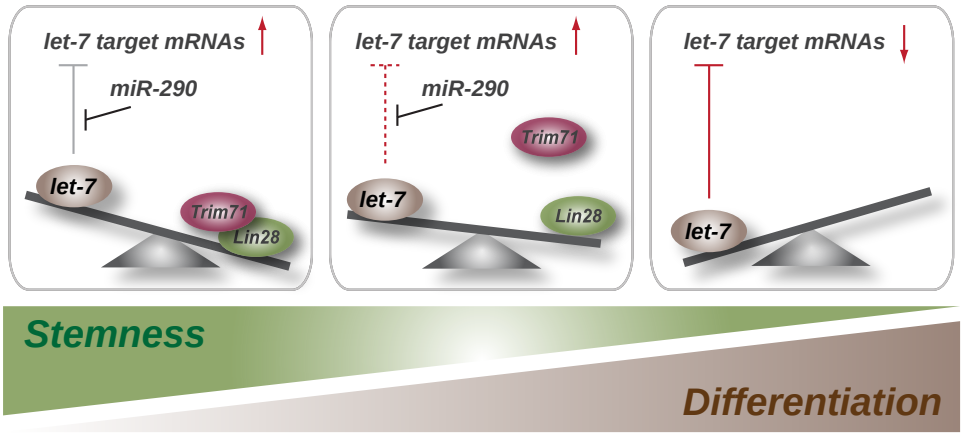

Figure 4.2: **Trim71 fine-tunes the balance between let-7 and Lin28 for the regulation of stem cell differentiation.**

sors. However, Lin28a was shown to bind to pre-let-7 *in vitro* with high affinity in the absence of Trim71 [62, 64, 286] which refutes this theory of affinity regulation. Alternatively, Trim71 could facilitate the recruitment of the TUTase to the pre-let-7/Lin28a complex. Finally, there is the possibility that Trim71 majorly affects the protein localization of Lin28 by acting as a molecular anchor to the P-bodies. Lin28 proteins can potentially localize to ER complexes, P-bodies, stress granules and the nucleus [77, 90]. Since the pool of available Lin28 protein is limited, a factor that influences the localization would have tremendous influence on target repression. Further evidence supporting this argument may lie in the finding that also the mRNA target spectrum of Trim71 and Lin28a partially overlap. In line with this, the overlapping targets would not be *bona fide* Trim71 targets but rather Lin28 responsive targets that are less occupied in the absence of Trim71. It is still unknown how cells balance the various effector functions of miRNA and mRNA regulation by Lin28. The investigation of the precise mechanism will be important to the field and will contribute to the understanding of both let-7 biogenesis regulation and mRNA suppression.

Along with certain transcription factors, overexpression of Lin28a can induce reprogramming of fibroblasts to iPSCs. This phenomenon was explained by the ability of Lin28a to suppress let-7 biogenesis [3] since the molecular inhibition of let-7 had a similar effect as Lin28a overexpression and both strongly enhanced reprogramming efficiencies [49, 156]. A study from Worringer and colleagues aiming to identify the major let-7 target proteins (apart from Lin28) that would mediate

this effect, found that the RBP Trim71 alone was able to enhance reprogramming efficiency to a similar extent as let-7 inhibition [156]. The authors attributed this effect to the ability of Trim71 to regulate other downstream mRNA targets by post-transcriptional mechanism. However, in the light of the present study, it seems worthwhile to speculate that Trim71 also directly helps to overcome the let-7 barrier to facilitate reprogramming. Because Trim71 and Lin28a are endogenous let-7 target genes, this would further shift the balance towards more efficient let-7 repression. As a consequence, Trim71 reprogramming effects would be mediated both upstream and downstream of let-7.

It will be of specific importance to investigate into processes that were already known to be modulated by the Lin28/let-7 axis in the context of Trim71. One of them is the role of Trim71 in cancer. Many cancers were shown to downregulate let-7 miRNAs which is generally linked to phenotypic de-differentiation. Among the tumors that have shown responsiveness to let-7 and Lin28a expression levels are lung cancer [287], breast cancer [288], ovarian cancer [289] and hepatocellular carcinoma [89], the latter being the first tumor model where Trim71 was already being correlated with tumor-promoting function [280].

4.4 Germ cell development critically depends on Trim71 protein expression

Trim71 is receiving more and more attention in the scientific community in recent years, but there is still a large backlog concerning the role of Trim71 in adult tissues or organs. Until now only two studies have described Trim71 expression in adult tissues or organs in mammals, namely in ependymal cells of the brain and in testes of mice [145, 255]. However, these previous studies had only descriptive and generic character and did not contribute any functional data.

Using the new conditional Trim71 knockout allele, we were now able to generate a tissue-specific adult Trim71 knockout mouse. In a first approach, we decided to target the germ cell niche which seemed a promising candidate for several reasons: First, Rybak *et al.* had detected Trim71 mRNA in adult testes of mice [145] - a finding that we could recapitulate. We found Trim71 expression in the small population of spermatogonial stem cells (SSCs) which represent the stem cell niche of the male reproductive organ in which self-renewal and differentiation is tightly controlled. Second, we noticed that Trim71 heterozygous male mice had already 20% smaller testes than wildtype littermates. This led us to conclude that the level

of Trim71 expression might be critical for proper organ development. Furthermore, germ cells show striking similarities to ESCs, the model in which most functional research on Trim71 has been performed so far. We and others have investigated the role of Trim71 with regard to pluripotency regulation in mESCs [152, 153]. By definition, pluripotency marks the ability of cells to give rise to all cells of the adult body. Sperm and egg cells are the precursor cells of a new organism and can thus be considered as the real biological equivalent of generation-spanning pluripotency. The similarity is further illustrated by the finding that primordial germ cell (PGC)-derived embryonic germ cells are the only cells apart from ESCs that can proliferate indefinitely in culture without undergoing malignant transformation. After re-transplantation into a blastocyst, embryonic germ cells can also contribute to all embryonic tissues [290, 291, 292]. Last, several marker genes are unique for both undifferentiated ESCs and PGCs, such as Oct4[293], Nanog [294], Lin28a [86, 247], Sall4 [295], Dppa3 [296] and Iftm3 [296].

By crossing conditional Trim71 mice with mice carrying the Cre recombinase under the control of the Nanos3 promoter, we could generate adult germline-specific Trim71 knockout mice. Nanos3 is an RBP that is exclusively expressed in PGCs as early as E7.25 and throughout spermatogenesis [159, 201, 250]. We found that homozygous deletion of Trim71 in the germline leads to infertility of male and female mice. Both ovaries and testes were drastically reduced in size and SSC marker expression analysis in Trim71 knockout testes revealed the absence of germ cells in adult mice. The fact that both sexes were equally affected in germline-specific Trim71 knockout mice suggests that Trim71 expression might be relevant in an early step of germ cell development. Divergent gene expression in PGCs of male and female embryos can be first observed at E10.5 and the cell fate is considered irreversible at E13.5 (reviewed in [297]). At this time point, female germ cells start entering meiosis while male germ cells do not undergo meiosis until after birth. Due to the lack of adult germ cells we tested whether PGCs are actually specified in the embryo. The fact that we found similar numbers of PGCs in wildtype and Trim71 knockout animals at E8.5 suggests that initial PGC specification does not require Trim71. Moreover, we have observed directed cell migration to the genital ridges, which excludes that the migration behavior or chemokine sensing are the primary cause of the defect. Thus it seems likely that Trim71 knockout PGCs would subsequently arrive at the genital ridge at around E10.5. The evidence presented here would therefore suggest that Trim71 deficiency leads to the loss of PGCs in

the time frame between E10.5 and E13.5. However, this hypothesis requires further experimental validation.

Right before and after arrival at the genital ridges, the population of PGCs increases drastically from about 250 to 25,000 cells in wildtype embryos [298]. It has preciously been proposed that siRNA-mediated downregulation of Trim71 could lead to decreased proliferation by upregulation of the gene Cdkn1a [153]. The protein product of Cdkn1a, p21, is a negative regulator of cell proliferation. Indeed, we found that Trim71 knockdown in TCam-2 cells, a germ cell derived seminoma cell line, reduced proliferation and likewise elevated the protein expression of the cell cycle regulators p21, p27 and p53. This is contrast to the Trim71$^{-/-}$ mESCs which do not a exhibit deficits in proliferation, suggesting that this function of Trim71 is cell context-dependent. It was shown that Dicer mutants of the germline also exhibit deficits in PGC proliferation, however this does not ablate the whole pool of germ cells [299]. Hence, it seems worthwhile to speculate that PGC proliferation regulation alone would not sufficiently explain the drastic phenotype of Trim71 mutation. Last, we found that a great part of differentially expressed miRNAs in Trim71-deficient mESCs are considered as germ cell-specific. Throughout germ cell development, factors are required that actively suppress the somatic cell fate. The most prominent is the Prdm1 protein that is involved in the suppression of somatic program by repressing the expression of Hox genes [100, 300] at the transcriptional level. Germ cell-specific RBPs like Nanos3 further assist the suppression of somatic genes at the posttranscriptional level. In fact, the evidence gathered so far regarding the Trim71 deficiency phenotype shows striking resemblance to Nanos3 deficiency in mice. Moreover, we found Nanos3 among the significantly downregulated genes in undifferentiated Trim71$^{-/-}$ mESCs. In Nanos3 knockout mice, the PGC population progressively shrinks due to somatic differentiation as well as apoptosis [159]. Furthermore, the Trim71 homolog in drosophila, Brat, was found to cooperatively bind and repress target mRNAs together with the RBPs Nanos and Pumilio [141]. Both Pumilio and Nanos proteins are highly conserved and are also involved in germline development [301, 302, 303]. In the transgenic Nanos3 Cre mouse line that we used for germline targeting of Trim71, the Nanos3 coding sequence is substituted with the Cre gene on one allele. Due to this, Cre-positive mice are concurrently heterozygous for Nanos3. Like for Trim71, Nanos3 heterozygocity already slightly reduced testis size in comparison to wildtype animals. However, when both genes were present in the heterozygous state, the size of testes was dramatically reduced, speaking for a functional cooperation of both proteins in a

common pathway. Besides Nanos3, also the RBPs Tiar and Dnd1 have also been shown to cause loss of PGCs during development [304, 305]. Our global expression analysis performed in mESCs showed that Trim71 is actively involved in the suppression of somatic neural cell fates and Trim71 knockout led to the upregulation of pro-differentiation genes. The resulting overexpression of neural lineage determining genes might very well interfere with proper germ cell identity. Moreover, we found that some of the significantly downregulated genes in Trim71 deficient mESCs were functionally associated with reproductive processes and fertility.

In parallel with the present study, two independent studies found that the nematode homolog of Trim71, *lin-41*, is required for normal oocyte maturation [306, 307]. In *lin-41* deficient nematodes, oocytes precursor cells spontaneously differentiated and the authors proposed that this might be due to insufficient suppression of somatic lineage-specific markers such as Hox genes [306]. However, in stark contrast to our own observations in Trim71 germline knockout mice, the male germline was not affected in Trim71 mutant nematodes.

In addition, the expression regulation of the miRNA let-7 also plays an important role in gem cell development because germ cell specifiers such as Prdm1 are direct targets of let-7 miRNA-mediated suppression [284]. Hence, deficiency in the let-7 master regulator, Lin28a, reduces the germ cell pool, however, the phenotype is not as drastic as seen for Trim71 knockout animals [86].

To improve the understanding of the processes governing germ cell biology is generally of great interest since it might pave the way for new therapeutic applications in the fields of reproductive medicine and cancer treatment. Testicular cancer, which in the majority of cases has a germ cell origin, is the most common cancer in men between 20 and 39 years of age [308]. Although the chances of successful treatment for this type of cancer have greatly improved in the last years, this achievement is partially overshadowed by a drastically rising overall prevalence of germ cell tumors, especially in the western world [309, 310]. The reasons for this are still unknown. In the present study, we found that a number of human embryonic carcinoma and a seminoma cell lines (both germ cell-derived) were positive for Trim71 expression and it seems likely that many clinical tumors are likewise expressing Trim71. As mentioned before, the knockdown of Trim71 caused a decrease in cell proliferation of the seminoma cell line TCam-2. The development of a compound that acts as an inhibitor for Trim71 could thus be of great therapeutic value. A major drawback of most applied chemotherapies is that they directly target very central components of common pro-proliferation pathways. The fact that Trim71

has a very restricted expression pattern in the adult organism can be considered as an advantage, since it minimizes the expected side effects caused by the treatment with a Trim71 inhibitory drug.

On the other hand, infertility is a worldwide problem, affecting up to 15% of the reproductive-aged couples [311]. It is estimated that 40% of the cases can be attributed to the man, 40% to the woman and the remaining 20% might be caused by combined problems of both partners or are unexplained [312]. In most cases the genetic causes of the infertility are unknown. Trim71 may be considered as a relevant gene that might help to understand cases of genetically caused infertility. In addition, changes in lifestyle, especially in the western world, have delayed family planing resulting in reduced fecundity due to the increase in age. This is why there is an increasing demand to fight age-related decline of natural fertility, and in the same line to further improve assisted reproductive technologies. Hence, it is important to catalog genes that directly affect fertility. The fact that testis size in mice was already affected in Trim71 heterozygous mice suggests that also humans with heterozygous mutations in the Trim71 gene might be categorized as subfertile. Only when the mechanisms underlying the maintenance and differentiation regulation of germ cells are sufficiently understood, effective treatment can be developed.

In summary, this study unraveled important aspects of Trim71 functions in the regulation of cell fate determination in both embryonic stem cells and the developing germline. Trim71 could be established as a suppressor of alternative gene expression states which is not essential for stem cell maintenance but for proper spatio-temporal control of cell lineage differentiation.

5 Summary

The formation of complex tissues and organs from a limited set of stem and progenitor cells requires precise regulation of the balance between stem cell maintenance and differentiation. In the present study we introduce Trim71 as a novel regulator of this balance. Trim71 heterozygous mice exhibit lifelong growth retardation, while complete deficiency of Trim71 causes defects in neural tube closure and embryonic lethality. To unravel the molecular processes regulated by Trim71, we derived mESC lines in which the Trim71 gene can be conditionally mutated *in vitro*. Interestingly, Trim71 knockout mESCs display no deficits in the maintenance of stemness in steady-state conditions. However, upon induction of differentiation a premature upregulation of neural marker gene expression can be observed, which is in accordance with the already described phenotype of the Trim71 knockout mice [151]. High-throughput sequencing of mRNAs and miRNAs in Trim71-deficient and control mESCs revealed that neuroectodermal priming already occurred in undifferentiated mESCs. While genes associated with stemness regulation were majorly unaffected, Trim71 deficiency led to an upregulation of both mRNAs and miRNAs involved in neuroectodermal development. We could show that Trim71 reduces the stability of specific target mRNAs via response elements located in their respective 3'UTRs.

Furthermore, we found that Trim71 is involved in a feedback mechanism regulating the expression of the pro-differentiation miRNA let-7. We propose that Trim71 cooperates with the stem cell protein Lin28 to facilitate repression of let-7 miRNA maturation in undifferentiated mESCs. We observed co-localization and physical interaction of Trim71 with Lin28 and found functional cooperation of both proteins in different cell types which led to the repression of let-7 maturation. These results suggested that Lin28 was necessary and sufficient for the function of the Trim71 protein as a let-7 repressor, and this was confirmed by ablating the Lin28 gene in mESCs using TALEN-based genome engineering. Importantly, Trim71 and Lin28 are both relevant targets of let-7 and are downregulated once differentiation is in-

duced. Therefore, our data establish a role of Trim71 as an important regulator of the bistable let-7/Lin28 switch in mESCs.

Last, we were interested to investigate the role of Trim71 in the adult organism. For this purpose, we used the conditional Trim71 allele to generate a germ cell-specific Trim71 knockout mouse. Deletion of Trim71 in the germline leads to infertility of both male and female mice. Whereas initial germ cell fate determination seems not to be impaired in Trim71 knockout mice, we found that Trim71 is essential for the survival of these cells during embryonic development. Moreover, we showed that Trim71 expression is retained in the spermatogonial stem cell population of the testis in adult mice.

Taken together, the acquired data reveal important aspects of Trim71 functionality that might further the understanding of cell fate programming and maintenance in both normal and pathophysiological conditions.

Bibliography

[1] Chaudry, A. STEM CELL BIOENGINEERING (2004). URL `http://www.scq.ubc.ca/stem-cell-bioengineering/`.

[2] Takahashi, K. & Yamanaka, S. Induction of pluripotent stem cells from mouse embryonic and adult fibroblast cultures by defined factors. *Cell* **126**, 663–676 (2006).

[3] Yu, J. *et al.* Induced pluripotent stem cell lines derived from human somatic cells. *Science* **318**, 1917–1920 (2007).

[4] Inoue, H., Nagata, N., Kurokawa, H. & Yamanaka, S. iPS cells: a game changer for future medicine. *EMBO J.* **33**, 409–17 (2014).

[5] Amabile, G. & Meissner, A. Induced pluripotent stem cells: current progress and potential for regenerative medicine. *Trends Mol. Med.* **15**, 59–68 (2009).

[6] Reya, T., Morrison, S. J., Clarke, M. F. & Weissman, I. L. Stem cells, cancer, and cancer stem cells. *Nature* **414**, 105–11 (2001).

[7] Beck, B. & Blanpain, C. Unravelling cancer stem cell potential. *Nat. Rev. Cancer* **13**, 727–38 (2013).

[8] Kreso, A. & Dick, J. E. Evolution of the cancer stem cell model. *Cell Stem Cell* **14**, 275–91 (2014).

[9] Chambers, I. *et al.* Nanog safeguards pluripotency and mediates germline development. *Nature* **450**, 1230–4 (2007).

[10] Martello, G. *et al.* Esrrb is a pivotal target of the Gsk3/Tcf3 axis regulating embryonic stem cell self-renewal. *Cell Stem Cell* **11**, 491–504 (2012).

[11] Martello, G., Bertone, P. & Smith, A. Identification of the missing pluripotency mediator downstream of leukaemia inhibitory factor. *EMBO J.* **32**, 2561–74 (2013).

[12] Loh, Y.-H. *et al.* The Oct4 and Nanog transcription network regulates pluripotency in mouse embryonic stem cells. *Nat. Genet.* **38**, 431–40 (2006).

[13] Boyer, L. A. *et al.* Core Transcriptional Regulatory Circuitry in Human Embryonic Stem Cells. *Cell* **122**, 947–956 (2005).

[14] Ying, Q.-L. *et al.* The ground state of embryonic stem cell self-renewal. *Nature* **453**, 519–523 (2008).

[15] Dunn, S.-J. J., Martello, G., Yordanov, B., Emmott, S. & Smith, A. G. Defining an essential transcription factor program for naïve pluripotency. *Science* **344**, 1156–1160 (2014).

[16] Kim, J., Chu, J., Shen, X., Wang, J. & Orkin, S. H. An extended transcriptional network for pluripotency of embryonic stem cells. *Cell* **132**, 1049–61 (2008).

[17] Chickarmane, V., Troein, C., Nuber, U. A., Sauro, H. M. & Peterson, C. Transcriptional dynamics of the embryonic stem cell switch. *PLoS Comput. Biol.* **2**, e123 (2006).

[18] Thomson, M. *et al.* Pluripotency Factors in Embryonic Stem Cells Regulate Differentiation into Germ Layers. *Cell* **145**, 875–889 (2011).

[19] Aksoy, I. *et al.* Klf4 and Klf5 differentially inhibit mesoderm and endoderm differentiation in embryonic stem cells. *Nat. Commun.* **5**, 3719 (2014).

[20] Kim, J. B. *et al.* Pluripotent stem cells induced from adult neural stem cells by reprogramming with two factors. *Nature* **454**, 646–50 (2008).

[21] Luger, K., Mäder, A. W., Richmond, R. K., Sargent, D. F. & Richmond, T. J. Crystal structure of the nucleosome core particle at 2.8 A resolution. *Nature* **389**, 251–60 (1997).

[22] Becker, P. B. & Hörz, W. ATP-dependent nucleosome remodeling. *Annu. Rev. Biochem.* **71**, 247–73 (2002).

[23] Henikoff, S. Nucleosome destabilization in the epigenetic regulation of gene expression. *Nat. Rev. Genet.* **9**, 15–26 (2008).

[24] Margueron, R., Trojer, P. & Reinberg, D. The key to development: interpreting the histone code? *Curr. Opin. Genet. Dev.* **15**, 163–76 (2005).

[25] Tessarz, P. & Kouzarides, T. Histone core modifications regulating nucleosome structure and dynamics. *Nat. Rev. Mol. Cell Biol.* **15**, 703–8 (2014).

[26] Mikkelsen, T. S. *et al.* Genome-wide maps of chromatin state in pluripotent and lineage-committed cells. *Nature* **448**, 553–60 (2007).

[27] Park, I.-H. *et al.* Reprogramming of human somatic cells to pluripotency with defined factors. *Nature* **451**, 141–6 (2008).

[28] Pijnappel, W. W. M. P. *et al.* A central role for TFIID in the pluripotent transcription circuitry. *Nature* **495**, 516–9 (2013).

[29] Efroni, S. *et al.* Global transcription in pluripotent embryonic stem cells. *Cell Stem Cell* **2**, 437–47 (2008).

[30] Bernstein, B. E. *et al.* A bivalent chromatin structure marks key developmental genes in embryonic stem cells. *Cell* **125**, 315–26 (2006).

[31] Park, S.-H. *et al.* Ultrastructure of human embryonic stem cells and spontaneous and retinoic acid-induced differentiating cells. *Ultrastruct. Pathol.* **28**, 229–38 (2004). URL `http://www.ncbi.nlm.nih.gov/pubmed/15693634`.

[32] Lewis, B. P., Burge, C. B. & Bartel, D. P. Conserved seed pairing, often flanked by adenosines, indicates that thousands of human genes are microRNA targets. *Cell* **120**, 15–20 (2005).

[33] Winter, J., Jung, S., Keller, S., Gregory, R. I. & Diederichs, S. Many roads to maturity: microRNA biogenesis pathways and their regulation. *Nat. Cell Biol.* **11**, 228–234 (2009).

[34] Gregory, R. I. *et al.* The Microprocessor complex mediates the genesis of microRNAs. *Nature* **432**, 235–240 (2004).

[35] Denli, A. M., Tops, B. B. J., Plasterk, R. H. A., Ketting, R. F. & Hannon, G. J. Processing of primary microRNAs by the Microprocessor complex. *Nature* **432**, 231–235 (2004).

[36] Lund, E., Güttinger, S., Calado, A., Dahlberg, J. E. & Kutay, U. Nuclear export of microRNA precursors. *Science* **303**, 95–8 (2004).

[37] Yi, R., Qin, Y., Macara, I. G. & Cullen, B. R. Exportin-5 mediates the nuclear export of pre-microRNAs and short hairpin RNAs. *Genes Dev.* **17**, 3011–6 (2003).

[38] Bernstein, E., Caudy, A. A., Hammond, S. M. & Hannon, G. J. Role for a bidentate ribonuclease in the initiation step of RNA interference. *Nature* **409**, 363–366 (2001).

[39] Hutvágner, G. *et al.* A cellular function for the RNA-interference enzyme Dicer in the maturation of the let-7 small temporal RNA. *Science* **293**, 834–8 (2001).

[40] Khvorova, A., Reynolds, A. & Jayasena, S. D. Functional siRNAs and miRNAs exhibit strand bias. *Cell* **115**, 209–16 (2003).

[41] Schwarz, D. S. *et al.* Asymmetry in the assembly of the RNAi enzyme complex. *Cell* **115**, 199–208 (2003).

[42] Meijer, H. A. *et al.* Translational repression and eIF4A2 activity are critical for microRNA-mediated gene regulation. *Science* **340**, 82–85 (2013).

[43] Filipowicz, W., Bhattacharyya, S. N. & Sonenberg, N. Mechanisms of post-transcriptional regulation by microRNAs: are the answers in sight? *Nat. Rev. Genet.* **9**, 102–114 (2008).

[44] Grimson, A. *et al.* MicroRNA Targeting Specificity in Mammals: Determinants beyond Seed Pairing. *Mol. Cell* **27**, 91–105 (2007).

[45] Wang, Y. *et al.* Embryonic stem cell-specific microRNAs regulate the G1-S transition and promote rapid proliferation. *Nat. Genet.* **40**, 1478–1483 (2008).

[46] Castellano, L. & Stebbing, J. Deep sequencing of small RNAs identifies canonical and non-canonical miRNA and endogenous siRNAs in mammalian somatic tissues. *Nucleic Acids Res.* **41**, 3339–51 (2013).

[47] Kanellopoulou, C. *et al.* Dicer-deficient mouse embryonic stem cells are defective in differentiation and centromeric silencing. *Genes Dev.* **19**, 489–501 (2005).

[48] Wang, Y., Medvid, R., Melton, C., Jaenisch, R. & Blelloch, R. DGCR8 is essential for microRNA biogenesis and silencing of embryonic stem cell self-renewal. *Nat. Genet.* **39**, 380–5 (2007).

[49] Melton, C., Judson, R. L. & Blelloch, R. Opposing microRNA families regulate self- renewal in mouse embryonic stem cells. *Nature* **463**, 621–626 (2010).

[50] Wang, Y. *et al.* miR-294/miR-302 promotes proliferation, suppresses G1-S restriction point, and inhibits ESC differentiation through separable mechanisms. *Cell Rep.* **4**, 99–109 (2013).

[51] Benetti, R. *et al.* A mammalian microRNA cluster controls DNA methylation and telomere recombination via Rbl2-dependent regulation of DNA methyltransferases. *Nat. Struct. Mol. Biol.* **15**, 998 (2008).

[52] Tay, Y., Zhang, J., Thomson, A. M., Lim, B. & Rigoutsos, I. MicroRNAs to Nanog, Oct4 and Sox2 coding regions modulate embryonic stem cell differentiation. *Nature* **455**, 1124–8 (2008).

[53] Xu, N., Papagiannakopoulos, T., Pan, G., Thomson, J. A. & Kosik, K. S. MicroRNA-145 regulates OCT4, SOX2, and KLF4 and represses pluripotency in human embryonic stem cells. *Cell* **137**, 647–58 (2009).

[54] Johnson, C. D. *et al.* The let-7 microRNA represses cell proliferation pathways in human cells. *Cancer Res.* **67**, 7713–22 (2007).

[55] Sempere, L. F., Dubrovsky, E. B., Dubrovskaya, V. A., Berger, E. M. & Ambros, V. The expression of the let-7 small regulatory RNA is controlled by ecdysone during metamorphosis in Drosophila melanogaster. *Dev. Biol.* **244**, 170–179 (2002).

[56] Liu, S. *et al.* Characterization and expression patterns of let-7 microRNA in the silkworm (Bombyx mori). *BMC Dev Biol* **7**, 88 (2007).

[57] Lancman, J. J. *et al.* Analysis of the regulation of lin-41 during chick and mouse limb development. *Dev. Dyn.* **234**, 948 –960 (2005).

[58] Wulczyn, F. G. *et al.* Post-transcriptional regulation of the let-7 microRNA during neural cell specification. *FASEB J.* **21**, 415–426 (2007).

[59] Pasquinelli, A. E. *et al.* Conservation of the sequence and temporal expression of let-7 heterochronic regulatory RNA. *Nature* **408**, 86–9 (2000).

[60] Roush, S. & Slack, F. J. The let-7 family of microRNAs. *Trends Cell Biol.* **18**, 505–516 (2008).

[61] Thomson, J. M. *et al.* Extensive post-transcriptional regulation of microRNAs and its implications for cancer. *Genes Dev.* **20**, 2202–2207 (2006).

[62] Hagan, J. P., Piskounova, E. & Gregory, R. I. Lin28 recruits the TUTase Zcchc11 to inhibit let-7 maturation in mouse embryonic stem cells. *Nat. Struct. Mol. Biol.* **16**, 1021–1025 (2009).

[63] Heo, I. *et al.* Lin28 mediates the terminal uridylation of let-7 precursor microRNA. *Mol. Cell* **32**, 276–284 (2008).

[64] Heo, I. *et al.* TUT4 in concert with Lin28 suppresses microRNA biogenesis through pre-microRNA uridylation. *Cell* **138**, 696–708 (2009).

[65] Ustianenko, D. *et al.* Mammalian DIS3L2 exoribonuclease targets the uridylated precursors of let-7 miRNAs. *RNA* **19**, 1632–1638 (2013).

[66] Piskounova, E. *et al.* Lin28A and Lin28B inhibit let-7 microRNA biogenesis by distinct mechanisms. *Cell* **147**, 730–0748 (2011).

[67] Marson, A. *et al.* Connecting microRNA genes to the core transcriptional regulatory circuitry of embryonic stem cells. *Cell* **134**, 521–33 (2008).

[68] Gerstberger, S., Hafner, M. & Tuschl, T. A census of human RNA-binding proteins. *Nat. Rev. Genet.* **15**, 829–845 (2014).

[69] Lunde, B. M., Moore, C. & Varani, G. RNA-binding proteins: modular design for efficient function. *Nat. Rev. Mol. Cell Biol.* **8**, 479–490 (2007).

[70] Kwon, S. C. *et al.* The RNA-binding protein repertoire of embryonic stem cells. *Nat. Struct. Mol. Biol.* **20**, 1122–1130 (2013).

[71] Su, H., Trombly, M. I., Chen, J. & Wang, X. Essential and overlapping functions for mammalian argonautes in microRNA silencing. *Genes Dev.* **23**, 304–317 (2009).

[72] Shekar, P. C., Naim, A., Sarathi, D. P. & Kumar, S. Argonaute-2-null embryonic stem cells are retarded in self-renewal and differentiation. *J. Biosci.* **36**, 649–57 (2011).

[73] Lee, J., Kim, H. K., Rho, J. Y., Han, Y. M. & Kim, J. The human OCT-4 isoforms differ in their ability to confer self-renewal. *J. Biol. Chem.* **281**, 33554–33565 (2006).

[74] Liu, Y., Timani, K., Ou, X., Broxmeyer, H. E. & He, J. J. C-MYC controlled TIP110 protein expression regulates OCT4 mRNA splicing in human embryonic stem cells. *Stem Cells Dev.* **22**, 689–94 (2013).

[75] Venables, J. P. *et al.* MBNL1 and RBFOX2 cooperate to establish a splicing programme involved in pluripotent stem cell differentiation. *Nat. Commun.* **4**, 2480 (2013).

[76] Han, H. *et al.* MBNL proteins repress ES-cell-specific alternative splicing and reprogramming. *Nature* **498**, 241–5 (2013).

[77] Hafner, M. *et al.* Identification of mRNAs bound and regulated by human LIN28 proteins and molecular requirements for RNA recognition. *RNA* **19**, 613–626 (2013).

[78] Wilbert, M. L. *et al.* LIN28 binds messenger RNAs at GGAGA motifs and regulates splicing factor abundance. *Mol. Cell* **48**, 195–206 (2012).

[79] Moss, E. G., Lee, R. C. & Ambros, V. The cold shock domain protein LIN-28 controls developmental timing in C. elegans and is regulated by the lin-4 RNA. *Cell* **88**, 637–46 (1997).

[80] Shinoda, G. *et al.* The Lin28/let-7 axis regulates glucose metabolism. *Cell* **147**, 81–94 (2011).

[81] Shinoda, G. *et al.* Fetal deficiency of Lin28 programs life-long aberrations in growth and glucose metabolism. *Stem Cells* **31**, 1563–1573 (2013).

[82] Zhu, H. *et al.* Lin28a transgenic mice manifest size and puberty phenotypes identified in human genetic association studies. *Nat. Genet.* **42**, 626–630 (2010).

[83] Shyh-Chang, N. *et al.* Lin28 enhances tissue repair by reprogramming cellular metabolism. *Cell* **155**, 778–792 (2013).

[84] Urbach, A. *et al.* Lin28 sustains early renal progenitors and induces Wilms tumor. *Genes Dev.* **28**, 971–82 (2014).

[85] Papaioannou, G., Inloes, J. B., Nakamura, Y., Paltrinieri, E. & Kobayashi, T. let-7 and miR-140 microRNAs coordinately regulate skeletal development. *Proc. Natl. Acad. Sci. U. S. A.* **110**, E3291–300 (2013).

[86] West, J. A. *et al.* A role for Lin28 in primordial germ-cell development and germ-cell malignancy. *Nature* **460**, 909–913 (2009).

[87] Murray, M. J., Saini, H. K. & Siegler, C. A. LIN28 expression in malignant germ cell tumors downregulates let-7 and increases oncogene levels. *Cancer Res.* **73**, 4872–4884 (2013).

[88] Feng, C. *et al.* Lin28 regulates HER2 and promotes malignancy through multiple mechanisms. *Cell Cycle* **11**, 2486–94 (2012).

[89] Guo, Y. *et al.* Identification and characterization of lin-28 homolog B (LIN28B) in human hepatocellular carcinoma. *Gene* **384**, 51 – 61 (2006).

[90] Balzer, E. & Moss, E. G. Localization of the developmental timing regulator Lin28 to mRNP complexes, P-bodies and stress granules. *RNA Biol.* **4**, 16–25 (2007).

[91] Zuckerman, S. The number of oocytes in the mature ovary. *Recent Prog Horm Res* **6**, 63–108 (1951).

[92] Rudkin, G. T. & Griech, H. A. On the persistence of oocyte nuclei from fetus to maturity in the laboratory mouse. *J. Cell Biol.* **12**, 169–75 (1962).

[93] Begum, S., Papaioannou, V. E. & Gosden, R. G. The oocyte population is not renewed in transplanted or irradiated adult ovaries. *Hum. Reprod.* **23**, 2326–2330 (2008).

[94] Surani, M. A., Hayashi, K. & Hajkova, P. Genetic and Epigenetic Regulators of Pluripotency. *Cell* **128**, 747–762 (2007).

[95] Kanatsu-Shinohara, M. *et al.* Genetic and epigenetic properties of mouse male germline stem cells during long-term culture. *Development* **132**, 4155–4163 (2005).

[96] Guan, K. *et al.* Pluripotency of spermatogonial stem cells from adult mouse testis. *Nature* **440**, 1199–203 (2006).

[97] Kleinsmitsch, L. J. & Pierce, G. B. Multipotentiality of single embryonal carcinoma cells. *Cancer Res.* **24**, 1544–1551 (1964).

[98] Lawson, K. A. & Hage, W. J. Clonal analysis of the origin of primordial germ cells in the mouse. *Ciba Found. Symp.* **182**, 68–84; discussion 84–91 (1994).

[99] Lawson, K. A. *et al.* Bmp4 is required for the generation of primordial germ cells in the mouse embryo (1999).

[100] Ohinata, Y. *et al.* Blimp1 is a critical determinant of the germ cell lineage in mice. *Nature* **436**, 207–213 (2005).

[101] Seisenberger, S. *et al.* The Dynamics of Genome-wide DNA Methylation Reprogramming in Mouse Primordial Germ Cells. *Mol. Cell* **48**, 849–862 (2012).

[102] Sasaki, H. & Matsui, Y. Epigenetic events in mammalian germ-cell development: reprogramming and beyond. *Nat. Rev. Genet.* **9**, 129–140 (2008).

[103] Peters, H. Migration of gonocytes into the mammalian gonad and their differentiation. *Philos. Trans. R. Soc. Lond. B. Biol. Sci.* **259**, 91–101 (1970).

[104] Bikoff, E. E. K. & Robertson, E. E. J. One PRDM is not enough for germ cell development. *Nat. Genet.* **40**, 934–935 (2008).

[105] Torok, M. & Etkin, L. D. Two B or not two B? Overview of the rapidly expanding B-box family of proteins. *Differentiation* **67**, 63–71 (2001).

[106] Reymond, A. *et al.* The tripartite motif family identifies cell compartments. *EMBO J.* **20**, 2140–2151 (2001).

[107] Slack, F. J. & Ruvkun, G. A novel repeat domain that is often associated with RING finger and B-box motifs. *Trends Biochem. Sci.* **23**, 474–475 (1998).

[108] Meroni, G. & Diez-Roux, G. TRIM/RBCC, a novel class of single protein RING finger E3 ubiquitin ligases. *BioEssays* **27**, 1147–1157 (2005).

[109] Sardiello, M., Cairo, S., Fontanella, B., Ballabio, A. & Meroni, G. Genomic analysis of the TRIM family reveals two groups of genes with distinct evolutionary properties. *BMC Evol. Biol.* **8**, 225 (2008).

[110] Ozato, K., Shin, D.-M., Chang, T.-H. & Morse, H. C. TRIM family proteins and their emerging roles in innate immunity. *Nat. Rev. Immunol.* **8**, 849–60 (2008).

[111] Chae, J. J. *et al.* Targeted disruption of pyrin, the FMF protein, causes heightened sensitivity to endotoxin and a defect in macrophage apoptosis. *Mol. Cell* **11**, 591–604 (2003).

[112] Kimura, F. *et al.* Cloning and characterization of a novel RING-B-box-coiled-coil protein with apoptotic function. *J. Biol. Chem.* **278**, 25046–25054 (2003).

[113] Pearson, M. & Pelicci, P. G. PML interaction with p53 and its role in apoptosis and replicative senescence. *Oncogene* **20**, 7250–7256 (2001).

[114] Mandell, M. A. *et al.* TRIM proteins regulate autophagy and can target autophagic substrates by direct recognition. *Dev. Cell* **30**, 394–409 (2014).

[115] Bodine, S. C. *et al.* Identification of ubiquitin ligases required for skeletal muscle atrophy. *Science* **294**, 1704–1708 (2001).

[116] Harada, H. *et al.* HERF1, a novel hematopoiesis-specific RING finger protein, is required for terminal differentiation of erythroid cells. *Mol. Cell. Biol.* **19**, 3808–3815 (1999).

[117] Beer, H.-D. *et al.* The estrogen-responsive B box protein: a novel regulator of keratinocyte differentiation. *J. Biol. Chem.* **277**, 20740–20749 (2002).

[118] Patarca, R. *et al.* rpt-1, an intracellular protein from helper/inducer T cells that regulates gene expression of interleukin 2 receptor and human immunodeficiency virus type 1. *Proc. Natl. Acad. Sci. U. S. A.* **85**, 2733–2737 (1988).

[119] Tissot, C. & Mechti, N. Molecular cloning of a new interferon-induced factor that represses human immunodeficiency virus type 1 long terminal repeat expression. *J. Biol. Chem.* **270**, 14891–14898 (1995).

[120] Frosk, P. *et al.* Limb-girdle muscular dystrophy type 2H associated with mutation in TRIM32, a putative E3-ubiquitin-ligase gene. *Am. J. Hum. Genet.* **70**, 663–672 (2002).

[121] Trockenbacher, A. *et al.* MID1, mutated in Opitz syndrome, encodes an ubiquitin ligase that targets phosphatase 2A for degradation. *Nat. Genet.* **29**, 287–294 (2001).

[122] Quaderi, N. A. *et al.* Opitz G/BBB syndrome, a defect of midline development, is due to mutations in a new RING finger gene on Xp22. *Nat. Genet.* **17**, 285–291 (1997).

[123] French FMF Consortium. A candidate gene for familial Mediterranean fever. *Nat. Genet.* **17**, 25–31 (1997).

[124] International FMF Consortium. Ancient missense mutations in a new member of the RoRet gene family are likely to cause familial Mediterranean fever. The International FMF Consortium. *Cell* **90**, 797–807 (1997).

[125] Urano, T. *et al.* Efp targets 14-3-3 sigma for proteolysis and promotes breast tumour growth. *Nature* **417**, 871–875 (2002).

[126] Salomoni, P. & Pandolfi, P. P. The role of PML in tumor suppression. *Cell* **108**, 165–170 (2002).

[127] Borden, K. L. *et al.* The solution structure of the RING finger domain from the acute promyelocytic leukaemia proto-oncoprotein PML. *EMBO J.* **14**, 1532–41 (1995).

[128] Barlow, P. N., Luisi, B., Milner, A., Elliott, M. & Everett, R. Structure of the C3HC4 domain by 1H-nuclear magnetic resonance spectroscopy. A new structural class of zinc-finger. *J. Mol. Biol.* **237**, 201–11 (1994).

[129] Ikeda, K. & Inoue, S. TRIM proteins as RING finger E3 ubiquitin ligases. *Adv. Exp. Med. Biol.* **770**, 27–37 (2000).

[130] Komander, D. & Rape, M. The Ubiquitin Code (2012).

[131] Maller Schulman, B. R., Liang, X., Stahlhut, C., DelConte, C. & Slack, F. J. The let-7 microRNA target gene, Mlin41/Trim71 is required for mouse embryonic survival and neural tube closure. *Cell Cycle* **7**, 3935–3942 (2008).

[132] Chu, Y. & Yang, X. SUMO E3 ligase activity of TRIM proteins. *Oncogene* **30**, 1108–1116 (2010).

[133] Nakasato, N. *et al.* A ubiquitin E3 ligase Efp is up-regulated by interferons and conjugated with ISG15. *Biochem. Biophys. Res. Commun.* **351**, 540–6 (2006).

[134] Noguchi, K. *et al.* TRIM40 promotes neddylation of IKKγ and is downregulated in gastrointestinal cancers. *Carcinogenesis* **32**, 995–1004 (2011).

[135] Hatakeyama, S. TRIM proteins and cancer. *Nat. Rev. Cancer* **11**, 792–804 (2011).

[136] Massiah, M. A., Simmons, B. N., Short, K. M. & Cox, T. C. Solution structure of the RBCC/TRIM B-box1 domain of human MID1: B-box with a RING. *J. Mol. Biol.* **358**, 532–45 (2006).

[137] Tao, H. *et al.* Structure of the MID1 tandem B-boxes reveals an interaction reminiscent of intermolecular ring heterodimers. *Biochemistry* **47**, 2450–7 (2008).

[138] Wulczyn, F. G., Cuevas, E., Franzoni, E. & Rybak, A. miRNAs need a TRIM: Regulation of miRNA activity by Trim-NHL proteins. In *Regul. MicroRNAs*, 1–21 (2010).

[139] Husten, E. J. & Eipper, B. A. The membrane-bound bifunctional peptidylglycine alpha-amidating monooxygenase protein. Exploration of its domain structure through limited proteolysis. *J. Bol. Chem.* **266**, 17004–10 (1991).

[140] Edwards, T. A., Pyle, S. E., Wharton, R. P. & Aggarwal, A. K. Structure of Pumilio reveals similarity between RNA and peptide binding motifs. *Cell* **105**, 281–9 (2001).

[141] Loedige, I. *et al.* The NHL domain of BRAT is an RNA- binding domain that directly contacts the hunchback mRNA for regulation. *Genes Dev.* **28**, 749–764 (2014).

[142] Neumüller, R. A. *et al.* Mei-P26 regulates microRNAs and cell growth in the Drosophila ovarian stem cell lineage. *Nature* **454**, 241–246 (2008).

[143] Schwamborn, J. C., Berezikov, E. & Knoblich, J. A. The TRIM-NHL protein TRIM32 activates microRNAs and prevents self-renewal in mouse neural progenitors. *Cell* **136**, 913–925 (2009).

[144] Hammell, C. M., Lubin, I., Boag, P. R., Blackwell, T. K. & Ambros, V. nhl-2 modulates microRNA activity in Caenorhabditis elegans. *Cell* **136**, 926–938 (2009).

[145] Rybak, A. *et al.* The let-7 target gene mouse lin-41 is a stem cell specific E3 ubiquitin ligase for the miRNA pathway protein Ago2. *Nat. Cell Biol.* **11**, 1411–1420 (2009).

[146] Reinhart, B. J. *et al.* The 21-nucleotide let-7 RNA regulates developmental timing in Caenorhabditis elegans. *Nature* **403**, 901–906 (2000).

[147] Slack, F. J. *et al.* The lin-41 RBCC gene acts in the C. elegans heterochronic pathway between the let-7 regulatory RNA and the LIN-29 transcription factor. *Mol. Cell* **5**, 659–669 (2000).

[148] Ambros, V. & Horvitz, H. R. Heterochronic Mutants of the Nematode Caenorhabditis elegans. *Science* **226**, 409–416 (1984).

[149] Lin, Y.-C. *et al.* Human TRIM71 and its nematode homologue are targets of let-7 microRNA and its zebrafish orthologue is essential for development. *Mol. Biol. Evol.* **24**, 2525–2534 (2005).

[150] Löer, B. *et al.* The NHL-domain protein Wech is crucial for the integrin-cytoskeleton link. *Nat. Cell Biol.* **10**, 422–428 (2008).

[151] Chen, J., Lai, F. & Niswander, L. The ubiquitin ligase mLin41 temporally promotes neural progenitor cell maintenance through FGF signaling. *Genes Dev.* **26**, 803–815 (2012).

[152] Loedige, I., Gaidatzis, D., Sack, R., Meister, G. & Filipowicz, W. The mammalian TRIM-NHL protein TRIM71/LIN-41 is a repressor of mRNA function. *Nucleic Acids Res.* **41**, 518–532 (2012).

[153] Chang, H.-M. *et al.* Trim71 cooperates with microRNAs to repress Cdkn1a expression and promote embryonic stem cell proliferation. *Nat. Commun.* **3**, 910–923 (2012). URL `http://dx.doi.org/10.1038/ncomms1909`.

[154] Zou, Y. *et al.* Developmental decline in neuronal regeneration by the progressive change of two intrinsic timers. *Science* **340**, 372–376 (2013).

[155] Lee, S. H. *et al.* The ubiquitin ligase human TRIM71 regulates let-7 microRNA biogenesis via modulation of Lin28B protein. *Biochim. Biophys. Acta* **1839**, 374–86 (2014).

[156] Worringer, K. A. *et al.* The let-7/LIN-41 pathway regulates reprogramming to human induced pluripotent stem cells by controlling expression of prodifferentiation genes. *Cell Stem Cell* **14**, 40–52 (2014).

[157] Buchholz, F., Angrand, P. O. & Stewart, A. F. Improved properties of FLP recombinase evolved by cycling mutagenesis. *Nat. Biotechnol.* **16**, 657–62 (1998).

[158] Lallemand, Y., Luria, V., Haffner-Krausz, R. & Lonai, P. Maternally expressed PGK-Cre transgene as a tool for early and uniform activation of the Cre site-specific recombinase. *Transgenic Res.* **7**, 105–112 (1998).

[159] Suzuki, H., Tsuda, M., Kiso, M. & Saga, Y. Nanos3 maintains the germ cell lineage in the mouse by suppressing both Bax-dependent and -independent apoptotic pathways. *Dev. Biol.* **318**, 133–142 (2008).

[160] Hameyer, D. *et al.* Toxicity of ligand-dependent Cre recombinases and generation of a conditional Cre deleter mouse allowing mosaic recombination in peripheral tissues. *Physiol. Genomics* **31**, 32–41 (2007).

[161] Ogawa, T., Aréchaga, J. M., Avarbock, M. R. & Brinster, R. L. Transplantation of testis germinal cells into mouse seminiferous tubules. *Int. J. Dev. Biol.* **41**, 111–22 (1997). URL `http://www.ncbi.nlm.nih.gov/pubmed/9074943`.

[162] Glisin, V., Crkvenjakov, R. & Byus, C. Ribonucleic acid isolated by cesium chloride centrifugation. *Biochemistry* **13**, 2633–7 (1974).

[163] Wilkinson, D. G. In Situ Hybridization: A Practical Approach. *IRL Press. Oxford* 75–83 (1992).

[164] Boch, J. *et al.* Breaking the code of DNA binding specificity of TAL-type III effectors. *Science* **326**, 1509–1512 (2009).

[165] Pavletich, N. P. & Pabo, C. O. Zinc Finger DNA Recognition - Crystal-Structure of a Zif268-DNA Complex at 2.1-A. *Science* **252**, 809–817 (1991).

[166] Klug, A. The discovery of zinc fingers and their development for practical applications in gene regulation and genome manipulation. *Q. Rev. Biophys.* **43**, 1–21 (2010).

[167] Morbitzer, R., Römer, P., Boch, J. & Lahaye, T. Regulation of selected genome loci using de novo-engineered transcription activator-like effector (TALE)-type transcription factors. *Proc. Natl. Acad. Sci. U. S. A.* **107**, 21617–21622 (2010).

[168] Zhang, F. *et al.* Efficient construction of sequence-specific TAL effectors for modulating mammalian transcription. *Nat. Biotechnol.* **29**, 149–153 (2011).

[169] Miller, J. C. *et al.* A TALE nuclease architecture for efficient genome editing. *Nat. Biotechnol.* **29**, 143–148 (2011). 5.

[170] Sanjana, N. E. *et al.* A transcription activator-like effector toolbox for genome engineering. *Nat. Protoc.* **7**, 171–192 (2012).

[171] Aslanidis, C. & de Jong, P. J. Ligation-independent cloning of PCR products (LIC-PCR). *Nucleic Acids Res.* **18**, 6069–74 (1990).

[172] Mitschka, S. *et al.* Co-existence of intact stemness and priming of neural differentiation programs in mES cells lacking Trim71. *Sci. Rep.* **5**, 11126 (2015).

[173] Love, M. I., Huber, W. & Anders, S. Moderated estimation of fold change and dispersion for RNA-Seq data with DESeq2. *bioRxiv* 1–50 (2014).

[174] Maere, S., Heymans, K. & Kuiper, M. BiNGO: a Cytoscape plugin to assess overrepresentation of gene ontology categories in biological networks. *Bioinformatics* **21**, 3448–3449 (2005).

[175] Merico, D., Isserlin, R., Stueker, O., Emili, A. & Bader, G. D. Enrichment Map: A Network-Based Method for Gene-Set Enrichment Visualization and Interpretation. *PLoS One* **5**, e13984 (2010).

[176] Oesper, L., Merico, D., Isserlin, R. & Bader, G. D. WordCloud: a Cytoscape plugin to create a visual semantic summary of networks. *Source Code Biol. Med.* **6**, 7 (2011).

[177] Cline, M. S. *et al.* Integration of biological networks and gene expression data using Cytoscape. *Nat. Protoc.* **2**, 2366–82 (2007).

[178] Chiang, H. R. *et al.* Mammalian microRNAs: experimental evaluation of novel and previously annotated genes. *Genes Dev.* **24**, 992–1009 (2010).

[179] Jouneau, A. *et al.* Naive and primed murine pluripotent stem cells have distinct miRNA expression profiles. *RNA* **18**, 253–264 (2012).

[180] Pollard, S. M., Conti, L., Sun, Y. & Smith, A. Adherent neural stem (NS) cells from fetal and adult forebrain. *Cereb. Cortex* **16**, i112–120 (2006).

[181] Chen, C. & Okayama, H. High-Efficiency Transformation of Mammalian Cells by Plasmid DNA. *Mol. Cell. Biol.* **7**, 2745–2752 (1987).

[182] Reddel, R. R., Murphy, L. C. & Sutherland, R. L. Effects of biobiogically active metabolites of tamoxifen on the proliferation kinetics of MCF-7 human breast cancer cells in vitro. *Cancer Res.* **43**, 4618–4624 (1983).

[183] Iwasaki, S., Kawamata, T. & Tomari, Y. Drosophila Argonaute1 and Argonaute2 Employ Distinct Mechanisms for Translational Repression. *Mol. Cell* **34**, 58–67 (2009).

[184] Pevny, L. H., Sockanathan, S., Placzek, M. & Lovell-Badge, R. A role for SOX1 in neural determination. *Development* **125**, 1967–78 (1998).

[185] Suter, D. M., Tirefort, D., Julien, S. & Krause, K.-H. A Sox1 to Pax6 Switch Drives Neuroectoderm to Radial Glia Progression During Differentiation of Mouse Embryonic Stem Cells. *Stem Cells* **27**, 49 –58 (2009).

[186] Zhang, X. *et al.* Pax6 is a human neuroectoderm cell fate determinant. *Cell Stem Cell* **7**, 90–100 (2010).

[187] Vallier, L. *et al.* Early cell fate decisions of human embryonic stem cells and mouse epiblast stem cells are controlled by the same signalling pathways. *PLoS One* **4**, e6082 (2009).

[188] Cimadamore, F., Amador-Arjona, A., Chen, C., Huang, C.-t. & Terskikh, A. V. SOX2 LIN28/let-7 pathway regulates proliferation and neurogenesis in neural precursors. *Proc. Natl. Acad. Sci. U. S. A.* **110**, E3017–3026 (2013).

[189] Friedman, R. C., Farh, K. K.-h., Burge, C. B. & Bartel, D. P. Most mammalian mRNAs are conserved targets of microRNAs. *Genome Res.* **19**, 92–105 (2009).

[190] Wu, G. & Schöler, H. R. Role of Oct4 in the early embryo development. *Cell Regen. (London, England)* **3**, 7 (2014).

[191] Davies, O. R. *et al.* Tcf15 primes pluripotent cells for differentiation. *Cell Rep.* **3**, 472–484 (2013).

[192] Saha, B., Ypsilanti, A. R., Boutin, C., Cremer, H. & Chédotal, A. Plexin-B2 regulates the proliferation and migration of neuroblasts in the postnatal and adult subventricular zone. *J. Neurosci. Off. J. Soc. Neurosci.* **32**, 16892–905 (2012).

[193] Deng, S. *et al.* Plexin-B2, but not Plexin-B1, critically modulates neuronal migration and patterning of the developing nervous system in vivo. *J. Neurosci.* **27**, 6333–6347 (2007).

[194] Yu, X., Ng, C. P., Habacher, H. & Roy, S. Foxj1 transcription factors are master regulators of the motile ciliogenic program. *Nat. Genet.* **40**, 1445–53 (2008).

[195] Vij, S. *et al.* Evolutionarily ancient association of the FoxJ1 transcription factor with the motile ciliogenic program. *PLoS Genet.* **8**, e1003019 (2012).

[196] You, Y. *et al.* Role of f-box factor foxj1 in differentiation of ciliated airway epithelial cells. *Am. J. Physiol.* **286**, L650–7 (2004).

[197] Jacquet, B. V. *et al.* FoxJ1-dependent gene expression is required for differentiation of radial glia into ependymal cells and a subset of astrocytes in the postnatal brain. *Development* **136**, 4021–4031 (2009).

[198] Kretser, D. M. D., Hedger, M. P., Loveland, K. L. & Phillips, D. J. Inhibins, activins and follistatin in reproduction. *Hum. Reprod. Update* **8**, 529–541 (2002).

[199] Matsumoto, K., Asano, T. & Endo, T. Novel small GTPase M-Ras participates in reorganization of actin cytoskeleton. *Oncogene* **15**, 2409–17 (1997).

[200] Kimmelman, A. C., Nun, N., Chan, A. M.-L., Nuñez Rodriguez, N. & Chan, A. M.-L. R-Ras3 / M-Ras induces neuronal differentiation of PC12 Cells through cell-type-specific activation of the mitogen-activated protein kinase cascade. *Mol. Cell. Biol.* **22**, 5946–5961 (2002).

[201] Tsuda, M. *et al.* Conserved role of nanos proteins in germ cell development. *Science* **301**, 1239–41 (2003).

[202] Young, P., Ehler, E. & Gautel, M. Obscurin, a giant sarcomeric Rho guanine nucleotide exchange factor protein involved in sarcomere assembly. *J. Cell Biol.* **154**, 123–36 (2001).

[203] Kontrogianni-Konstantopoulos, A., Jones, E. M., Van Rossum, D. B. & Bloch, R. J. Obscurin is a ligand for small ankyrin 1 in skeletal muscle. *Mol. Biol. Cell* **14**, 1138–48 (2003).

[204] Wu, Y. & Wu, P. Y. CD133 as a marker for cancer stem cells: progresses and concerns. *Stem Cells Dev.* **18**, 1127–34 (2009).

[205] Irollo, E. & Pirozzi, G. CD133: to be or not to be, is this the real question? *Am. J. Transl. Res.* **5**, 563–81 (2013).

[206] Spencer, J. A., Eliazer, S., Ilaria, R. L., Richardson, J. A. & Olson, E. N. Regulation of microtubule dynamics and myogenic differentiation by MURF, a striated muscle RING-finger protein. *J. Cell Biol.* **150**, 771–84 (2000).

[207] Vindry, C., Vo Ngoc, L., Kruys, V. & Gueydan, C. RNA-binding protein-mediated post-transcriptional controls of gene expression: Integration of molecular mechanisms at the 3' end of mRNAs? (2014).

[208] Schulman, B. R. M., Esquela-Kerscher, A. & Slack, F. J. Reciprocal expression of lin-41 and the microRNAs let-7 and mir-125 during mouse embryogenesis. *Dev. Dyn.* **234**, 1046–54 (2005).

[209] Kulkarni, M., Ozgur, S. & Stoecklin, G. On track with P-bodies. *Biochem. Soc. Trans.* **38**, 242–251 (2010).

[210] Cascio, S. *et al.* miR-20b modulates VEGF expression by targeting HIF-1 alpha and STAT3 in MCF-7 breast cancer cells. *J. Cell. Physiol.* **224**, 242–9 (2010).

[211] Zhou, W. *et al.* MicroRNA-20b promotes cell growth of breast cancer cells partly via targeting phosphatase and tensin homologue (PTEN). *Cell Biosci.* **4**, 62 (2014).

[212] Zhu, S. *et al.* Effect of miR-20b on Apoptosis, Differentiation, the BMP Signaling Pathway and Mitochondrial Function in the P19 Cell Model of Cardiac Differentiation In Vitro. *PLoS One* **10**, e0123519 (2015).

[213] Dar, A. A. *et al.* The Role of miR-18b in MDM2-p53 Pathway Signaling and Melanoma Progression. *J. Natl. Cancer Inst.* **105**, 433–442 (2013).

[214] Murakami, Y. *et al.* The expression level of miR-18b in hepatocellular carcinoma is associated with the grade of malignancy and prognosis. *BMC Cancer* **13**, 99 (2013).

[215] Nomura, T. *et al.* MeCP2-dependent repression of an imprinted miR-184 released by depolarization. *Hum. Mol. Genet.* **17**, 1192–9 (2008).

[216] Liu, C. *et al.* Epigenetic regulation of miR-184 by MBD1 governs neural stem cell proliferation and differentiation. *Cell Stem Cell* **6**, 433–44 (2010).

[217] Shi, Q. & Gibson, G. E. Up-regulation of the mitochondrial malate dehydrogenase by oxidative stress is mediated by miR-743a. *J. Neurochem.* **118**, 440–448 (2011).

[218] Chen, L. *et al.* MiR-410 regulates MET to influence the proliferation and invasion of glioma. *Int. J. Biochem. Cell Biol.* **44**, 1711–7 (2012).

[219] Gattolliat, C.-H. *et al.* Expression of miR-487b and miR-410 encoded by 14q32.31 locus is a prognostic marker in neuroblastoma. *Br. J. Cancer* **105**, 1352–61 (2011).

[220] Yang, Y. *et al.* MiR-136 promotes apoptosis of glioma cells by targeting AEG-1 and Bcl-2. *FEBS Lett.* **586**, 3608–12 (2012).

[221] Shen, S. *et al.* Upregulation of miR-136 in human non-small cell lung cancer cells promotes Erk1/2 activation by targeting PPP2R2A. *Tumour Biol.* 631–640 (2013).

[222] Zhang, D. *et al.* miR-136 modulates TGF-β1-induced proliferation arrest by targeting PPP2R2A in keratinocytes. *Biomed Res. Int.* **2015**, 453518 (2015).

[223] Chen, J., Wang, M., Guo, M., Xie, Y. & Cong, Y.-S. miR-127 Regulates Cell Proliferation and Senescence by Targeting BCL6. *PLoS One* **8**, e80266 (2013).

[224] Bhaskaran, M. *et al.* MicroRNA-127 modulates fetal lung development. *Physiol. Genomics* **37**, 268–278 (2009).

[225] Delaloy, C. *et al.* MicroRNA-9 coordinates proliferation and migration of human embryonic stem cell-derived neural progenitors. *Cell Stem Cell* **6**, 323–35 (2010).

[226] Lehmann, U. *et al.* Epigenetic inactivation of microRNA gene hsa-mir-9-1 in human breast cancer. *J. Pathol.* **214**, 17–24 (2008).

[227] Hildebrandt, M. A. T. *et al.* Hsa-miR-9 methylation status is associated with cancer development and metastatic recurrence in patients with clear cell renal cell carcinoma. *Oncogene* **29**, 5724–8 (2010).

[228] Park, S. M., Gaur, A. B., Lengyel, E. & Peter, M. E. The miR-200 family determines the epithelial phenotype of cancer cells by targeting the E-cadherin repressors ZEB1 and ZEB2. *Genes Dev.* **22**, 894–907 (2008).

[229] Peng, C. *et al.* A unilateral negative feedback loop between miR-200 microRNAs and Sox2/E2F3 controls neural progenitor cell-cycle exit and differentiation. *J. Neurosci.* **32**, 13292–13308 (2012).

[230] Li, X. *et al.* MiR-200 can repress breast cancer metastasis through ZEB1-independent but moesin-dependent pathways. *Oncogene* **33**, 4077–88 (2014).

[231] Smirnova, L. *et al.* Regulation of miRNA expression during neural cell specification. *Eur. J. Neurosci.* **21**, 1469–77 (2005).

[232] Vo, N. *et al.* A cAMP-response element binding protein-induced microRNA regulates neuronal morphogenesis. *Proc. Natl. Acad. Sci. U. S. A.* **102**, 16426–16431 (2005).

[233] Klein, M. E. *et al.* Homeostatic regulation of MeCP2 expression by a CREB-induced microRNA. *Nat. Neurosci.* **10**, 1513–1514 (2007).

[234] Thompson, T. B., Cook, R. W., Chapman, S. C., Jardetzky, T. S. & Woodruff, T. K. Beta A versus beta B: is it merely a matter of expression? *Mol. Cell. Endocrinol.* **225**, 9–17 (2004).

[235] Matranga, C., Tomari, Y., Shin, C., Bartel, D. P. & Zamore, P. D. Passenger-strand cleavage facilitates assembly of siRNA into Ago2-containing RNAi enzyme complexes. *Cell* **123**, 607–620 (2005).

[236] Viswanathan, S. R., Daley, G. Q. & Gregory, R. I. Selective blockade of microRNA processing by Lin28. *Science* **320**, 97–100 (2008).

[237] Yang, D. H. & Moss, E. G. Temporally regulated expression of Lin-28 in diverse tissues of the developing mouse. *Gene Expr. Patterns* **3**, 719–26 (2003).

[238] Thornton, J. E., Chang, H.-M., Piskounova, E. & Gregory, R. I. Lin28-mediated control of let-7 microRNA expression by alternative TUTases Zcchc11 (TUT4) and Zcchc6 (TUT7). *RNA* **18**, 1875–1885 (2012).

[239] Nam, Y., Chen, C., Gregory, R. I., Chou, J. J. & Sliz, P. Molecular basis for interaction of let-7 MicroRNAs with Lin28. *Cell* **147**, 1080–1091 (2011). NIHMS150003.

[240] Mayr, F. & Heinemann, U. Mechanisms of Lin28-mediated miRNA and mRNA regulation - A structural and functional perspective. *Int. J. Mol. Sci.* **14**, 16532–16553 (2013).

[241] Viswanathan, S. R. *et al.* Lin28 promotes transformation and is associated with advanced human malignancies. *Nat. Genet.* **41**, 843–848 (2009).

[242] Chang, H.-M., Triboulet, R., Thornton, J. E. & Gregory, R. I. A role for the Perlman syndrome exonuclease Dis3l2 in the Lin28-let-7 pathway. *Nature* **497**, 730–0748 (2013).

[243] Loughlin, F. E. *et al.* Structural basis of pre-let-7 miRNA recognition by the zinc knuckles of pluripotency factor Lin28. *Nat. Struct. Mol. Biol.* **19**, 84–9 (2012). URL `http://www.ncbi.nlm.nih.gov/pubmed/22157959`.

[244] Zwaka, T. P. & Thomson, J. a. A germ cell origin of embryonic stem cells? *Development* **132**, 227–233 (2005).

[245] Bao, S. *et al.* The germ cell determinant Blimp1 is not required for derivation of pluripotent stem cells. *Cell Stem Cell* **11**, 110–7 (2012).

[246] Gassei, K. & Orwig, K. E. SALL4 Expression in Gonocytes and Spermatogonial Clones of Postnatal Mouse Testes. *PLoS One* **8** (2013).

[247] Zheng, K., Wu, X., Kaestner, K. H. & Wang, P. J. The pluripotency factor LIN28 marks undifferentiated spermatogonia in mouse. *BMC Dev. Biol.* **9**, 38 (2009).

[248] Gaytan, F. *et al.* Distinct expression patterns predict differential roles of the miRNA-binding proteins, Lin28 and Lin28b, in the mouse testis: studies during postnatal development and in a model of hypogonadotropic hypogonadism. *Endocrinology* **154**, 1321–1336 (2013).

[249] Culty, M. Gonocytes, the forgotten cells of the germ cell lineage. *Birth Defects Res.* **87**, 1–26 (2009).

[250] Yamaji, M. *et al.* Functional reconstruction of NANOS3 expression in the germ cell lineage by a novel transgenic reporter reveals distinct subcellular localizations of NANOS3. *Reproduction* **139**, 381–393 (2010).

[251] Hunt, S. E. & Mittwoch, U. Y-chromosomal and other factors in the development of testis size in mice. *Genet. Res.* **50**, 205–11 (1987).

[252] Chubb, C. Genes regulating testis size. *Biol. Reprod.* **47**, 29–36 (1992).

[253] Kalinka, A. T. & Tomancak, P. The evolution of early animal embryos: Conservation or divergence? (2012).

[254] Geer, L. Y. *et al.* The NCBI BioSystems database. *Nucleic Acids Res.* **38** (2009).

[255] Cuevas, E., Rybak-Wolf, A., Rohde, A. M., Nguyen, D. T. T. & Wulczyn, F. G. Lin41/Trim71 is essential for mouse development and specifically expressed in postnatal ependymal cells of the brain. *Front. cell Dev. Biol.* **3**, 20 (2015).

[256] Dang, V. T., Kassahn, K. S., Marcos, A. E. & Ragan, M. A. Identification of human haploinsufficient genes and their genomic proximity to segmental duplications. *Eur. J. Hum. Genet.* **16**, 1350–1357 (2008).

[257] Huang, N., Lee, I., Marcotte, E. M. & Hurles, M. E. Characterising and predicting haploinsufficiency in the human genome. *PLoS Genet.* **6**, 1–11 (2010).

[258] Allegrucci, C. & Young, L. E. Differences between human embryonic stem cell lines. *Hum. Reprod. Update* **13**, 103–20 (2007).

[259] Osafune, K. *et al.* Marked differences in differentiation propensity among human embryonic stem cell lines. *Nat. Biotechnol.* **26**, 313–315 (2008).

[260] MacKay, D. R., Hu, M., Li, B., Rhéaume, C. & Dai, X. The mouse Ovol2 gene is required for cranial neural tube development. *Dev. Biol.* **291**, 38–52 (2006).

[261] Zhang, T. *et al.* The zinc finger transcription factor Ovol2 acts downstream of the bone morphogenetic protein pathway to regulate the cell fate decision between neuroectoderm and mesendoderm. *J. Biol. Chem.* **288**, 6166–77 (2013).

[262] Balmer, N. V. *et al.* Epigenetic changes and disturbed neural development in a human embryonic stem cell-based model relating to the fetal valproate syndrome. *Hum. Mol. Genet.* **21**, 4104–4114 (2012).

[263] Krichevsky, A. M., Sonntag, K.-C., Isacson, O. & Kosik, K. S. Specific microRNAs modulate embryonic stem cell-derived neurogenesis. *Stem Cells* **24**, 857–864 (2006).

[264] Yang, L. *et al.* Involvement of miR-9/MCPIP1 axis in PDGF-BB-mediated neurogenesis in neuronal progenitor cells. *Cell Death Dis.* **4**, e960 (2013).

[265] Tan, S. L., Ohtsuka, T., González, A. & Kageyama, R. MicroRNA9 regulates neural stem cell differentiation by controlling Hes1 expression dynamics in the developing brain. *Genes to Cells* **17**, 952–961 (2012).

[266] Leucht, C. *et al.* MicroRNA-9 directs late organizer activity of the midbrain-hindbrain boundary. *Nat. Neurosci.* **11**, 641–648 (2008).

[267] Yoo, A. S. *et al.* MicroRNA-mediated conversion of human fibroblasts to neurons. *Nature* **476**, 228–231 (2011). NIHMS150003.

[268] Zhao, C., Sun, G., Li, S. & Shi, Y. A feedback regulatory loop involving microRNA-9 and nuclear receptor TLX in neural stem cell fate determination. *Nat. Struct. Mol. Biol.* **16**, 365–371 (2009).

[269] Lim, L. P. *et al.* Microarray analysis shows that some microRNAs downregulate large numbers of target mRNAs. *Nature* **433**, 769–773 (2005).

[270] Cruz, C. *et al.* Foxj1 regulates floor plate cilia architecture and modifies the response of cells to sonic hedgehog signalling. *Development* **137**, 4271–4282 (2010).

[271] Jacquet, B. V. *et al.* Specification of a Foxj1-dependent lineage in the forebrain is required for embryonic-to-postnatal transition of neurogenesis in the olfactory bulb. *J. Neurosci.* **31**, 9368 –9382 (2011).

[272] Chen, H.-W. *et al.* Expression of FOXJ1 in hepatocellular carcinoma: correlation with patients' prognosis and tumor cell proliferation. *Mol. Carcinog.* **52**, 647–59 (2013).

[273] Wang, J. *et al.* Decreased expression of FOXJ1 is a potential prognostic predictor for progression and poor survival of gastric cancer. *Ann. Surg. Oncol.* (2014).

[274] Zielonka, M., Xia, J., Friedel, R. H., Offermanns, S. & Worzfeld, T. A systematic expression analysis implicates Plexin-B2 and its ligand Sema4C in the regulation of the vascular and endocrine system. *Exp. Cell Res.* **316**, 2477–86 (2010).

[275] Ichimura, T. *et al.* 14-3-3 proteins sequester a pool of soluble TRIM32 ubiquitin ligase to repress autoubiquitylation and cytoplasmic body formation. *J. Cell Sci.* **126**, 2014–2026 (2014).

[276] Hornbeck, P. V., Chabra, I., Kornhauser, J. M., Skrzypek, E. & Zhang, B. PhosphoSite: A bioinformatics resource dedicated to physiological protein phosphorylation. *Proteomics* **4**, 1551–1561 (2004).

[277] Zhong, X., Li, N., Liang, S., Coukos, G. & Zhang, L. Identification of microRNAs regulating reprogramming factor LIN28 in embryonic stem cells and cancer cells. *J. Biol. Chem.* **285**, 41961–41971 (2010).

[278] The UniProt Consortium. UniProt: a hub for protein information. *Nucleic Acids Res.* **43**, D204–212 (2014).

[279] Rybak, A. *et al.* A feedback loop comprising lin-28 and let-7 controls pre-let-7 maturation during neural stem-cell commitment. *Nat. Cell Biol.* **10**, 987–993 (2008).

[280] Chen, Y.-L., Yuan, R.-H., Yang, W.-C., Hsu, H.-C. & Jeng, Y.-M. The stem cell E3-ligase Lin-41 promotes liver cancer progression through inhibition of microRNA-mediated gene silencing. *J. Pathol.* **229**, 486–496 (2013).

[281] Chang, T.-C. *et al.* Lin-28B transactivation is necessary for Myc-mediated let-7 repression and proliferation. *Proc. Natl. Acad. Sci. U. S. A.* **106**, 3384–3389 (2009).

[282] Moss, E. G. & Tang, L. Conservation of the heterochronic regulator Lin-28, its developmental expression and microRNA complementary sites. *Dev. Biol.* **258**, 432– 442 (2003).

[283] Yokoyama, S. *et al.* Dynamic gene expression of Lin-28 during embryonic development in mouse and chicken. *Gene Expr. Patterns* **8**, 155–160 (2008).

[284] Shinoda, G. *et al.* Lin28a regulates germ cell pool size and fertility. *Stem Cells* **31**, 1001–1009 (2013).

[285] Yang, M. *et al.* Lin28 promotes the proliferative capacity of neural progenitor cells in brain development. *Development* **142**, 1616–1627 (2015).

[286] Newman, M. A., Thomson, J. M. & Hammond, S. M. Lin-28 interaction with the Let-7 precursor loop mediates regulated microRNA processing. *RNA* **14**, 1539–1549 (2008).

[287] Takamizawa, J. *et al.* Reduced Expression of the let-7 MicroRNAs in Human Lung Cancers in Association with Shortened Postoperative Survival. *Cancer Res.* **64**, 3753–3756 (2004).

[288] Yu, F. *et al.* let-7 regulates self renewal and tumorigenicity of breast cancer cells. *Cell* **131**, 1109–1123 (2007).

[289] Anglesio, M. S. *et al.* Deregulation of MYCN, LIN28B and LET-7 in a molecular subtype of aggressive high-grade serous ovarian cancers. *PLoS One* **6**, e18064 (2011).

[290] Resnick, J. L., Bixler, L. S., Cheng, L. & Donovan, P. J. Long-term proliferation of mouse primordial germ cells in culture. *Nature* **359**, 550–551 (1992).

[291] Durcova-Hills, G., Ainscough, J. & McLaren, A. Pluripotential stem cells derived from migrating primordial germ cells. *Differentiation.* **68**, 220–226 (2001).

[292] Donovan, P. J. & de Miguel, M. P. Turning germ cells into stem cells. *Curr. Opin. Genet. Dev.* **13**, 463–471 (2003).

[293] Pesce, M. & Schöler, H. R. Oct-4: gatekeeper in the beginnings of mammalian development. *Stem Cells* **19**, 271–278 (2001).

[294] Chambers, I. *et al.* Functional expression cloning of Nanog, a pluripotency sustaining factor in embryonic stem cells. *Cell* **113**, 643–655 (2003).

[295] Hobbs, R. M. *et al.* Functional antagonism between Sall4 and Plzf defines germline progenitors. *Cell Stem Cell* **10**, 284–298 (2012).

[296] Saitou, M., Barton, S. C. & Surani, M. A. A molecular programme for the specification of germ cell fate in mice. *Nature* **418**, 293–300 (2002).

[297] Kocer, A., Reichmann, J., Best, D. & Adams, I. R. Germ cell sex determination in mammals. *Mol. Hum. Reprod.* **15**, 205–213 (2009).

[298] Tam, P. P. L. & Snow, M. H. L. Proliferation and migration of primordial germ cells during compensatory growth in mouse embryos (1981).

[299] Hayashi, K. *et al.* MicroRNA biogenesis is required for mouse primordial germ cell development and spermatogenesis. *PLoS One* **3** (2008).

[300] Kurimoto, K. *et al.* Complex genome-wide transcription dynamics orchestrated by Blimp1 for the specification of the germ cell lineage in mice. *Genes Dev.* **22**, 1617–1635 (2008).

[301] Forbes, A. & Lehmann, R. Nanos and Pumilio have critical roles in the development and function of Drosophila germline stem cells. *Development* **125**, 679–90 (1998).

[302] Juliano, C. E., Swartz, S. Z. & Wessel, G. M. A conserved germline multipotency program. *Development* **137**, 4113–26 (2010).

[303] Joly, W., Chartier, A., Rojas-Rios, P., Busseau, I. & Simonelig, M. The CCR4 deadenylase acts with Nanos and Pumilio in the fine-tuning of Mei-P26 expression to promote germline stem cell self-renewal. *Stem Cell Reports* **1**, 411–424 (2013).

[304] Beck, A. R., Miller, I. J., Anderson, P. & Streuli, M. RNA-binding protein TIAR is essential for primordial germ cell development. *Proc. Natl. Acad. Sci. U. S. A.* **95**, 2331–6 (1998).

[305] Youngren, K. K. *et al.* The Ter mutation in the dead end gene causes germ cell loss and testicular germ cell tumours. *Nature* **435**, 360–4 (2005).

[306] Tocchini, C. *et al.* The TRIM-NHL protein LIN-41 controls the onset of developmental plasticity in Caenorhabditis elegans. *PLoS Genet.* **10**, e1004533 (2014).

[307] Spike, C. A. *et al.* The TRIM-NHL protein LIN-41 and the OMA RNA-binding proteins antagonistically control the prophase-to-metaphase transition and growth of Caenorhabditis elegans oocytes. *Genetics* **198**, 1535–58 (2014).

[308] Hayes-Lattin, B. & Nichols, C. R. Testicular cancer: a prototypic tumor of young adults. *Semin. Oncol.* **36**, 432–8 (2009).

[309] Bray, F. *et al.* Trends in testicular cancer incidence and mortality in 22 European countries: Continuing increases in incidence and declines in mortality. *Int. J. Cancer* **118**, 3099–3111 (2006).

[310] Rosen, A., Jayram, G., Drazer, M. & Eggener, S. E. Global trends in testicular cancer incidence and mortality. *Eur. Urol.* **60**, 374–379 (2011).

[311] World Health Organization. Report of the Meeting on the Prevention of Infertility at the Primary Health Care Level (1983).

[312] Baird, D. T. *et al.* Diagnosis and management of the infertile couple: Missing information (2004).

Acknowledgment

I would like to thank Prof. Waldemar Kolanus who has assigned this research topic to me and who allowed the exploration of the subject off the beaten track.

For helpful advice and support, I am deeply grateful to Karin Schneider, who worked together with me on the Trim71 project. Furthermore, I am indebted to Dr. Tobias Goller who has helped with the analysis of the Trim71 knockout phenotype and performed the dissection of mouse embryos. Lucia Torres has majorly supported the "TRIM-team" with scientific competence and her unique positive energy. I would like to thank Michael Rieck for the opportunity to have numerous stimulating scientific and non-scientific discussions. My special thanks also to Felix Eppler and Bettina Jux who contributed to the nice atmosphere in our lab and helped proofreading this manuscript. With Felix Tolksdorf I spent very enjoyable time inside and outside of the lab. I would like to express my gratitude to Christa Mandel who helped to do maxi-preparations and prepared buffer solutions as well as to Susanne Weese who performed the genotyping of mouse tail tips for me. Barbara Reichwein was invaluable for the general organization of the lab. Gertrud Mierzwa and Katharina Klein who were always infectiously good-humored kept the lab running by both working in the scullery and bringing delicious cakes. I also want to thank Thomas Quast, Angrit Namislo, Henriette Peter, Johanna Kolanus, Katrin Heße, Helga Ueing, Eloho Etemire and Donald Guu for the really nice atmosphere in the lab and the encouragement.

I would like to express my gratitude to Prof. Hubert Schorle and Angela Egert who provided the technical expertise for the derivation of the conditional Trim71 mESCs and supervised the breeding of the germline-specific Trim71 knockout mice. Jérôme Mertens from the group of Prof. Oliver Brüstle has helped to establish the RG-like neural stem cell cultures from Trim71 conditional mice. Additionally, my work has greatly benefited from the bioinformatic team of the group of Prof. Joachim Schultze who contributed new interesting aspects to the project. Special thanks to Thomas Ulas, Kevin Bassler, Patrick Günther and Kathrin Klee who have

performed the analysis of the mRNA and miRNA expression data from the different knockout mESC lines.

Furthermore, Marc Beyer, Ann-Kathrin Baumgart and Annika Peters provided valuable help for the planning of the Lin28a knockout strategy and gave technical advice for the cloning.

Appendix

Upregulated genes in Trim71$^{-/-}$ mESCs							
Rank	**Gene**	**FC**	**p-value**	**Rank**	**Gene**	**FC**	**p-value**
1	Gm364	6,01	0,0016	31	2610528J11Rik	2,31	0,0176
2	**Foxj1**	**4,50**	**0,0364**	32	Bend5	2,27	0,0334
3	Rsad2	4,30	0,0093	33	Rapgef3	2,24	0,0268
4	Ccr4	4,15	0,0012	34	Slco4a1	2,23	0,0004
5	Slc6a1	4,09	0,0095	35	Zbtb7c	2,20	0,0088
6	Nfia	4,03	0,0223	36	Hopx	2,15	0,0093
7	Nrg2	3,72	0,0290	37	Wdr78	2,14	0,0474
8	Adrb1	3,65	0,0287	38	E030030I06Rik	2,13	0,0280
9	Vsig2	3,53	0,0118	**39**	**Tcf15**	**2,11**	**0,0171**
10	Pifo	3,37	0,0037	40	Kifc3	2,08	0,0559
11	Nkx6-3	3,30	0,0280	41	Gbx2	2,07	0,0448
12	Pglyrp1	3,29	0,0147	42	Gpx2	2,07	0,0001
13	Esam	3,16	0,0365	43	Cdkl4	2,06	0,0452
14	9030617O03Rik	3,03	0,0037	44	Zc3h12a	2,02	0,0024
15	Ntn1	2,99	0,0029	45	Plek2	2,00	0,0064
16	Ndufb2	2,98	0,0145	**46**	**Plxnb2**	**2,00**	**0,0243**
17	Id1	2,95	0,0426	47	Vwa1	2,00	0,0140
18	Emp1	2,91	0,0127	48	Trim7	2,00	0,0305
19	Tex13	2,90	0,0091	49	Urah	1,99	0,0162
20	Insc	2,83	0,0393	50	Ankrd34a	1,99	0,0204
21	Hist3h2ba	2,63	0,0083	51	Krt17	1,97	0,0283
22	Pdzd3	2,61	0,0385	52	Rsg1	1,96	0,0589
23	**Inhbb**	**2,57**	**0,0004**	53	Il34	1,96	0,0231
24	**Mras**	**2,47**	**0,0002**	54	Ndufab1	1,96	0,0517
25	Tsix	2,47	0,0433	55	Lmna	1,96	0,0281
26	Cdx2	2,45	0,0411	56	Efna3	1,95	0,0546
27	Slc52a3	2,42	0,0095	57	Ccdc28b	1,95	0,0403
28	Fah	2,35	0,0018	58	H2afj	1,95	0,0229
29	Cdh4	2,31	0,0180	59	Pqlc1	1,93	0,0005
30	Robo4	2,31	0,0112	60	Epha2	1,92	0,0241

Table 5.2: **List of upregulated genes in Trim71$^{-/-}$ mESCs.** Genes with a higher sequence count than 20 and a p-value $\leq$0.05 were listed in decreasing order of the their respective mean fold change. Genes that were selected for further analysis are marked in bold.

Downregulated genes in Trim71$^{-/-}$ mESCs							
Rank	**Gene**	**FC**	**p-value**	**Rank**	**Gene**	**FC**	**p-value**
1	Trim71	-4.44	0.0006	31	Myl9	-2.15	0.0257
2	Aurkc	-4.04	0.0110	32	Saa2	-2.14	0.0492
3	Gm13139	-3.99	0.0027	33	Obox6	-2.14	0.0235
4	Lrrc15	-3.43	0.0104	**34**	**Trim54**	**-2.13**	**0.0050**
5	Ctrb1	-3.19	0.0181	35	Letm2	-2.12	0.0341
6	Gm21293	-2.93	0.0138	36	AU041133	-2.11	0.0196
7	Gm21304	-2.93	0.0138	37	Parp10	-2.11	0.0113
8	Gm6763	-2.93	0.0138	38	Nrsn1	-2.10	0.0283
9	Gm8764	-2.93	0.0138	39	Ccdc170	-2.08	0.0111
10	Col26a1	-2.87	0.0060	40	Nuggc	-2.07	0.0391
11	Ror1	-2.87	0.0335	41	Usp29	-2.06	0.0086
12	Ceacam10	-2.85	0.0005	42	Clgn	-2.05	0.0088
13	Myh13	-2.77	0.0177	43	Itih5	-2.04	0.0377
14	Zscan4b	-2.76	0.0335	44	Hrc	-2.03	0.0032
15	**Obscn**	**-2.75**	**0.0008**	45	Nlrp4c	-2.01	0.0249
16	Epx	-2.60	0.0119	46	Hdac9	-2.01	0,0002
17	Gm13152	-2.60	0.0249	47	Lrrn1	-2.01	0.0155
18	Atp10a	-2.55	0.0150	48	Tsga10	-2.00	0.0127
19	Gm5662	-2.50	0.0067	49	Adcyap1r1	-1.99	0.0110
20	Dcdc2a	-2.40	0.0099	50	Pm20d2	-1.99	0.0060
21	**Prom1**	**-2.31**	**0.0303**	51	Thbd	-1.97	0.0443
22	Serpina3m	-2.30	0.0482	52	Tnnc2	-1.95	0.0129
23	Spic	-2.26	0.0356	53	Klhl13	-1.95	0.0045
24	Peril	-2.23	0.0346	54	Cep85l	-1.95	0.0012
25	Slc11a1	-2.23	0.0225	55	Nexn	-1.94	0.0364
26	Sema3e	-2.21	0.0064	56	Pla2g5	-1.93	0.0157
27	Slco4c1	-2.21	0.0402	57	Pcdh19	-1.92	0.0074
28	Wnk3	-2.21	0.0265	58	Lrmp	-1.92	0.0324
29	Meg3	-2.19	0.0273	59	Igtp	-1.92	0.0312
30	Igsf10	-2.19	0.0407	60	Fam13c	-1.92	0.0045

Table 5.3: **List of downregulated genes in Trim71$^{-/-}$ mESCs.** Genes with a higher sequence count than 20 and a p-value $\leq$0.05 were listed in increasing order of the their respective mean fold change. Genes that were selected for further analysis are marked in bold.

Upregulated miRNAs in Trim71$^{-/-}$ mESCs			
Rank	**Gene**	**FC**	**p-value**
1	mmu-miR-743a-3p	2,35	0,0078
2	mmu-let-7e-5p	2,27	0,0130
3	mmu-miR-132-5p	1,88	0,0088
4	mmu-miR-378a-5p	1,72	0,0065
5	mmu-miR-200c-3p	1,60	0,0019
6	mmu-miR-145a-3p	1,55	0,0248
7	mmu-miR-24-2-5p	1,51	0,0185

Downregulated miRNAs in Trim71$^{-/-}$ mESCs			
Rank	**mmu-miR-378a-5p**	**FC**	**p-value**
1	mmu-miR-377-3p	-3,78	0,0202
2	mmu-miR-410-3p	-3,71	0,0433
3	mmu-miR-410-5p	-3,51	0,0090
4	mmu-miR-323-3p	-3,26	0,0113
5	mmu-miR-136-3p	-3,20	0,0284
6	mmu-miR-376b-3p	-3,19	0,0064
7	mmu-miR-300-3p	-2,82	0,0486
8	mmu-miR-127-3p	-2,63	0,0482
9	mmu-miR-127-5p	-2,58	0,0448
10	mmu-miR-485-3p	-2,53	0,0140
11	mmu-miR-433-3p	-2,36	0,0129
12	mmu-miR-434-3p	-2,29	0,0318
13	mmu-miR-466d-5p	-2,26	0,0196
14	mmu-miR-409-3p	-2,26	0,0385
15	mmu-miR-369-5p	-2,26	0,0156
16	mmu-miR-3475-3p	-2,24	0,0359
17	mmu-miR-1934-5p	-2,19	0,0488
18	mmu-miR-6240	-2,01	0,0036
19	mmu-miR-673-3p	-1,99	0,0371
20	mmu-miR-466a-5p	-1,79	0,0165
21	mmu-miR-129-1-3p	-1,69	0,0486
22	mmu-miR-669-3p	-1,62	0,0313
23	mmu-miR-155-3p	-1,60	0,0221
24	mmu-miR-3068-5p	-1,57	0,0373

Table 5.4: **List of significantly up- and downregulated miRNAs in Trim71$^{-/-}$ mESCs.** miRNAs with a higher sequence count than 10 and a p-value $\leq$0.05 were listed according to their respective mean fold change.